Mechanisms underlying cell-fate determination in the mammary gland development

THÈSE N^{O} 6431 (2015)

PRÉSENTÉE LE 13 MARS 2015

À LA FACULTÉ DES SCIENCES DE LA VIE

UNITÉ DU PROF. BRISKEN

PROGRAMME DOCTORAL EN APPROCHES MOLÉCULAIRES DU VIVANT

ÉCOLE POLYTECHNIQUE FÉDÉRALE DE LAUSANNE

POUR L'OBTENTION DU GRADE DE DOCTEUR ÈS SCIENCES

PAR

Duje BURIC

acceptée sur proposition du jury:

Prof. O. Hantschel, président du jury
Prof. C. Brisken, directrice de thèse
Prof. K. Brennan, rapporteur
Prof. D. Constam, rapporteur
Prof. G.-P. Dotto, rapporteur

ÉCOLE POLYTECHNIQUE
FÉDÉRALE DE LAUSANNE

Suisse
2015

TABLE OF CONTENTS

ABSTRACT

Notch signaling pathway is an important developmental pathway and has been implicated in both mammary gland development and tumorigenesis. Several studies investigating Notch signaling in mouse mammary gland implied that Notch signaling is an important factor in the determination of the luminal cell type. Clinical studies on breast tumors as well as studies in transgenic mouse models overexpressing active Notch receptors suggested an oncogenic function of Notch in the mammary gland connecting it to the poor breast cancer prognosis. However the physiological role of Notch signaling and its downstream mechanisms remain unclear.

Analysis of Transgenic-EGFP Notch reporter mouse mammary epithelium revealed that Notch signaling is active specifically in a subset of hormone receptor positive cells. More sensitive FACS analysis consistently shows EGFP expression in HR+ luminal cells and reveals a weaker signal in a subset of basal ($CD24^{lo}$) cells. Additionally mRNA analysis revealed that Notch active luminal cells are expressing Wnt4 ligand.

To unveil the role of the Notch signaling in the Wnt4 expressing HR+ cells, we conditionally deleted RBP-Jκ, Notch signaling mediator, in Wnt4 expressing subpopulation of hormone receptor positive cells via Wnt4Cre. Abrogation of RBP-Jκ resulted in loss of progesterone receptor expression in 90% of cells bearing the RBP-Jκ deletion while estrogen receptor expression remained intact, implicating RBP-Jκ in regulation of progesterone receptor expression.

To test whether Notch signaling regulates PR expression in the entire HR+ population, we analyzed mammary epithelium in which RBP-Jκ has been conditionally deleted via MMTV-Cre in progenitor cells revealing the presence of a subpopulation of luminal hormone receptor positive cells that differentiate independently of Notch signaling.

Time directed deletion of RBP-Jκ via intraductally injected Adeno-Cre virus into the adult mouse mammary ductal system through the nipple additionally confirmed that RBP-Jκ is required for progesterone receptor expression.

Chromatin immunoprecipitation assay showed that RBP-Jκ binds two out of four putative RBP-Jκ binding sites in the progesterone receptor promoter. Inhibition of Notch signaling *in vivo* via intraductal injection of γ-secretase inhibitor, DAPT, resulted in reduced progesterone receptor expression strongly suggesting that Notch-related RBP-Jκ signaling is responsible for PR expression.

In this project we are proposing that there are two different populations of HR+ cells: one defined as Wnt4 expressing subpopulation of HR+ cells in which PR expression is dependent of Notch signaling, and another one defined as Wnt4 non expressing subpopulation of HR+ cells which is independent of Notch signaling. Since Notch signaling is able to replace ER signaling and activate ER target genes in the endocrine therapy resistant cell lines, Wnt4 expressing population of HR+ luminal cells might play a crucial role in the acquiring of the resistance.

Keywords:

Mammary gland, breast cancer, Notch signaling, RBP-Jκ, hormone receptor, progesterone receptor, estrogen receptor, cell fate, differentiation

RÉSUMÉ

La voie de signalisation Notch est une voie développementale importante et a été impliquée à la fois dans le développement et la tumorigenèse de la glande mammaire. Plusieurs études portant sur la signalisation Notch dans la glande mammaire murine a laissé entendre que la signalisation Notch joue un rôle important dans la détermination du destin cellulaire luminal. Des études cliniques sur des tumeurs du sein ainsi que des études menées sur des modèles de souris transgéniques surexprimant des récepteurs Notch constitutivement actifs ont suggéré une fonction oncogénique de Notch dans la glande mammaire permettant de la relier avec un mauvais pronostic du cancer du sein. Toutefois, le rôle physiologique de la voie de signalisation Notch et ses mécanismes en aval restent inconnus.

L'analyse des épithéliums mammaires des différentes souris transgéniques EGFP-Notch a révélé que la signalisation Notch est spécifiquement active dans un sous-ensemble de cellules exprimant les récepteurs hormonaux. Une analyse fine par cytométrie en flux a révélé l'expression de EGFP dans les cellules luminales HR + ainsi qu'un signal plus faible dans un sous-groupe de cellules basales (cellules CD24lo). En outre l'analyse de l'ARNm a révélé que les cellules luminales Notch actives expriment le ligand Wnt4.

Pour dévoiler le rôle de la signalisation Notch dans les cellules HR+ exprimant Wnt4, nous avons supprimé conditionnellement RBP-Jκ, un médiateur de la signalisation Notch, dans les cellules HR+ exprimant Wnt4 via Wnt4Cre. L'abrogation de RBP-Jκ a entraîné la perte d'expression du récepteur de la progestérone dans 90% des cellules portant la deletion RBP-Jκ tandis que l'expression du récepteur des oestrogènes est restée intacte, impliquant RBP-Jκ dans la régulation de l'expression du récepteur de la progestérone.

Pour tester si la signalisation Notch régule l'expression de PR dans l'ensemble de la population HR+, nous avons analysé l'épithélium mammaire où RBP-Jκ a été conditionnellement supprimé via MMTV-Cre dans les cellules progénitrices révélant la présence d'une sous-population de cellules luminales HR+ qui se différencient indépendamment de la signalisation Notch.

La suppression à des temps déterminés de RBP-Jκ via l'injection intraductale d'un virus adéno-Cre dans le système canalaire mammaire de souris adulte par le mamelon a confirmé que RBP-Jκ est nécessaire pour l'expression du récepteur de la progestérone.

Les expériences d'immunoprécipitation de la chromatine a montré que RBP-Jk lie deux sites putatifs sur quatre de liaison de RBP-Jκ dans le promoteur du récepteur de la progestérone. L'inhibition de la signalisation Notch *in vivo* par injection intraductale d'un inhibiteur de la γ-secrétase, DAPT, a provoqué une baisse de l'expression du récepteur de la progestérone suggérant que la signalisation Notch-RBPJκ est responsable de l'expression de PR.

Dans ce projet, nous proposons qu'il existe deux populations différentes de cellules HR+: une définie comme exprimant Wnt4 dans laquelle l'expression de PR est dépendante de la signalisation Notch, et une autre définie comme n'exprimant pas Wnt4 et qui est indépendant de la signalisation Notch. La signalisation Notch est en mesure de remplacer la signalisation ER et d'activer la transcription des gènes cibles de ER dans les lignées cellulaires résistantes à la thérapie endocrinienne, les cellules luminales HR+ exprimant Wnt4 pourraient ainsi jouer un rôle crucial dans l'acquisition de la résistance.

Mots clés:

glande mammaire, cancer du sein, voie de signalisation Notch, RBP-Jκ, récepteur aux hormones, récepteur à la progestérone, récepteur aux estrogènes, destinée cellulaire, différentiation.

ACKNOWLEDGMENTS

First of all, I would like to thank my supervisor Cathrin Brisken for her unconditional support and guidance during my PhD. Your enthusiasm and dedication to science and teaching younger generations of scientists were a beautiful inspiration and a great encouragement to continue pursuing my dream career as a scientist.

Endless thanks to my dear colleagues,

Renuga Devi Rajaram who helped me settle in to the lab and start my project, transferred all her knowledge to me, pushed me forward and constantly supported me and my ideas.

Tamara Tanos, my colleague, my mentor and my friend.

Cécile Lebrand, an exquisite scientist and a very special person to me, for all the long discussions, both scientific and personal, for encouragement and kind words during the toughest times and for relentlessly reminding me that I am a good scientist at the times when I was losing faith in myself.

Melanie Wirth, a brilliant and diligent technician of the lab and a dear friend. Her help with the experiment and support were essential for my project.

Stephanie Cagnet and Valerian Dormoy who invested an enormous effort in helping me while writing my thesis.

Rachel Jeitziner for always being there for me and for her great help with all the statistics.

And to all current and past lab members.

I would like to thank Prof. Gian-Paolo Dotto and members of his lab for all the help with experiments. A special thanks to Clare for her great effort and free time invested in my project.

I would also like to thank Sara Brodarić for carefully proofreading my thesis.

A big big big thanks to my flatmates, Sanja Blaskovic, Brigida Rusconi and Eric Savioz for all the love, care, friendship and good times. Because of them our apartment always felt like home.

I would also like to thank Maša Milošević and Kasia Šturlan, my sisters from another mother. You taught me how to respect and accept myself. Without you, I would never have become the proud and self-confident person I am today.

A special thanks to Blandine Capelo, my beautiful tango partner and a very dear and very special friend. We literally danced through these years. You will always have a very special place in my heart.

And finally, an enormous thank you to my parents Ivo and Mirjana, my brother Marin and his wife Jelena for their unconditional love and timeless support, and to my niece Ena for being the greatest love of my life.

ABBREVIATIONS

TDLU	terminal ductal lobular unit
ADH	atypical ductal hyperplasia
DCIS	ductal carcinoma in situ
IBC	invasive breast carcinoma
HER2	epidermal growth factor receptor 2
ER	estrogen receptor
GRB7	growth factor receptor bound protein 7
Wnt	wingless-related
FGF	fibroblast growth factor
Tbx3	T-box protein 3
BMP4	bone morphogenesis protein 4
LEF1	lymphoid enhancer binding factor 1
PTHLH	parathyroid hormone-like hormone
RASGRF1	Ras protein-specific guanine nucleotide-releasing factor 1
IGF-1/p190-B	insulin growth factor 1/Rho GTPase activating protein 5
P	progesterone
PRL	prolactin
SGP2	serum gp70 production 2
STAT3	signal transducer and activator of transcription 3
LIF	leukemia inhibitory factor
OSM	oncostatin M
p53	tumor suppressor p53
C-myc	myelocytomatosis oncogene
TGF-ß	transforming growth factor ß
TEBs	terminal end buds
SMA	smooth muscle actin
Prlr	prolactin receptor
ERE	estrogen responsive elements
FACS	fluorescence activated cell sorting
Aldh1	aldehyde dehydrogenase isoform 1
AP1	activator protein 1
GATA-3	GATA binding protein 3
Elf-5	E74-like factor 5
PML	promyelocytic leukemia protein
NECD	Notch extracellular domain
NTMS	Notch transmembrane subunit
HD	heterodimerization domain
NICD	Notch intracellular domain
RAM	RBP-Jκ-associated module
PEST	proline-glutamine-serine-threonine
RBP-Jκ	Recombination signal binding protein for immunoglobulin kappa J
Dll1	Delta-like-1
Dll3	Delta-like-3
Dll4	Delta-like-4
Jag1	Jagged1

Jag2	Jagged2
DSL	Delta/Serrate/Lag-2 motif
vWF	von Willebrand factor
ICL	intracellular cytoplasmic part
APH1	anterior pharynix-defective 1
TACE	TNFα-converting enzyme
PEN2	presenilin enhancer protein-2
NCoR2	nuclear receptor co-repressor 2
SHARP	SMART/HDAC1 associated repressor protein
SKIP	Ski-interacting protein
MAML	mastermind-like
CBP	CREB-binding protein
PCAF	p300/CBP associated factor
HIF1α	hypoxia induced factor 1α
Fbw7	F-box/WD repeat domain-containing protein 7
Itch	E3 ubiquitin-protein ligase Itchy homolog
CDK8	cyclin dependent kinase 8
Hes	hairy/enhancer-of-split genes
Hey	hairy/enhancer-of-split related with YPRW motif
bHLH	basic-helix-loop-helix protein
MSI1	RNA binding protein Musashi homolog 1
T-ALL	T-cell acute lymphoblastic leukemia
HNSCC	head and neck squamous cell carcinomas
CMML	chronic myelomonocytic leukemia
TNR	transgenic Notch reporter
EGFP	enhanced green fluorescent protein
MaSCs	mammary stem cells
MMTV	mouse mammary tumor virus
WAP	whey acidic protein
LTR	long terminal repeat
MAST	microtubule associated serine-threonine kinase
PIN1	peptidyl-prolyl cis-trans isomerase NIMA-interacting 1
Gli1	zinc finger protein Gli1
p53REs	p53 response elements
ChIP	chromatin immunoprecipitation
TA	transactivation domain
SAM	sterile alpha motif
DBD	DNA-binding domain
OD	oligomerization domain
TA2	second transactivation domain
TID	transinhibitory domain
ECM	extracellular matrix
HR+	hormone receptor positive
HR-	hormone receptor negative
DAPT	N-[N-(3,5-Difluorophenacetyl)-L-alanyl]-S-phenylglycine t-butyl ester
DNNM	dominant negative Mastermind
GSI	γ-secretase inhibitor
PMSF	phenylmethylsulfonyl fluoride

CHAPTER I: **INTRODUCTION**

BREAST CANCER

BREAST CANCER: AN OVERVIEW

Breast cancer is the leading form of cancer among women. It is estimated that 1 in 8 women will develop breast cancer in their lifetime in "Western countries". Almost 30% of all cancers diagnosed in women are breast cancer. Although the number of diagnosed cases of cancers is on the rise, in part due to increased mammography screening, the breast cancer death rate has been decreasing since year 2000 onward. The improvement in death rate probably results from treatment advances, earlier detection through screening, and increased awareness. Although many factors arose recently, mainly from changes in the lifestyle, the most significant risk factors for breast cancer are still gender (being a woman) and age. Breast cancer is present in male population at the rate of 1 in 1000 which is significantly less than in women. The fact that 95% of diagnosed breast cancers and 97% of breast cancer deaths is in women older than 40 postulates age as an important breast risk factor (www.breastcancer.org).

Standard practice to manage early-stage breast cancer involves usually surgery followed by radiotherapy to destroy residual cancer cells in the breast. Radiotherapy reduces the 20-year local recurrence from 39% to 14% (Fisher et al., 2002). Additionally, based on the genetic nature of the disease and risk of relapse, adjuvant therapies are prescribed to reduce risk of cancer recurrence and to improve survival. These therapies include chemotherapy, hormone therapy (aromatase inhibitors, selective estrogen receptor modulators and estrogen receptor down regulators) and targeted therapies (Herceptin) (Jatoi and Miller, 2003).

To identify the prognostic and predictive markers for early detection and the development of novel, more effective targeted treatments are two basic approaches in breast cancer field. These will hopefully lead to better cancer care and offer new, more effective and more targeted drugs.

BREAST CANCER DEVELOPMENT AND STAGES

The accumulation of epigenetic and genetic changes that will cause a cell to acquire characteristics defined as "hallmarks of cancer" (Hanahan and Weinberg, 2011) generates the malignant cells of breast cancer. These cells are able to preserve proliferative signaling, bypass growth suppressors, resist cell death and induce angiogenesis and metastasis. They can also reprogram energy metabolism and avoid immune response. The gain of these "hallmarks" is probably promoted by genomic instability and inflammation.

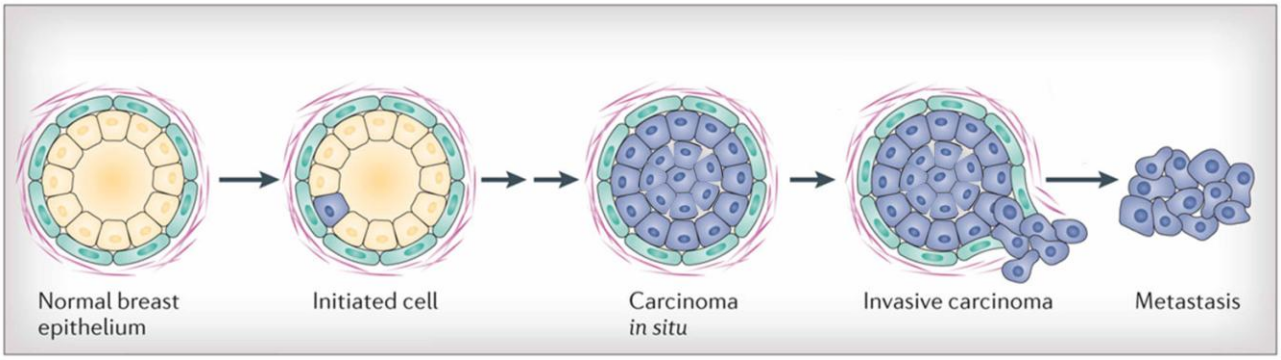

Figure 1. Breast tumorigenesis*. Illustration of a milk duct with luminal (beige) and basal (green) layer surrounded by basal lamina (pink). The tumorigenic event happens in the cell called initiated cell developing ductal carcinoma in situ which can eventually rise into an invasive carcinoma with metastatic properties. Adapted from Brisken, 2014*

From a clinical point of view, the development of breast cancer is a long process that is held to progress through defined stages. The majority of lesions start in the terminal ductal lobular unit (TDLU), a structure comprised of lobules and ducts of mammary epithelium. It starts as an atypical ductal hyperplasia (ADH), which is a premalignant state characterized by anomalous cell layers within the lobules or ducts. ADH can then progress into the preinvasive stage called ductal carcinoma in situ (DCIS). DCIS can develop into invasive breast cancer (IBC), but not necessarily has to. The Danish pathologist Maja Nielsen performed a study on breast tissue of women in their 40s who had died of causes other than cancer and noticed that 30% of them had DCIS (Nielsen et al., 1987) as opposed to 12% that developed a clinically relevant disease. In DCIS extensive genetic alterations similar to those in nearby invasive lesion were found by comparative hybridization and therefore it is considered to be a direct precursor of the invasive carcinoma (Buerger et al., 1999, reviewed in Brisken, 2013). Additionally, transcriptome analysis of both DCIS and associated invasive cancer showed that their molecular profiles are highly similar and that an aberrant expression of genes is present also in pre-invasive stages (Ma et al., 2003).

The risk of metastatic progression increases significantly when the cells become invasive, forming an invasive breast cancer. All three stages, ADH, DCIS, and IBC, are histologically different. Surprisingly, an analysis of their molecular profiles unveiled their strong resemblance at the transcriptome level, which suggests that genome aberrancies that carry invasive properties are present much before invasive stages (Ma et al., 2003).

BREAST CANCER SUBTYPES

Breast cancer is a heterogeneous disease. In clinics, the prognosis of a patient and therapy are determined by factors like tumor size, lymph node status, hormone receptor status, proliferation index and presence of epidermal growth factor receptor 2 (HER2) amplification/overexpression. This approach of classifying breast cancer is limited since there is a high degree of variability both in terms

of overall patient survival and response to therapy within the same histological subtype or within the same histological grade and stage (reviewed in Rakha EA 2010.)

Recently, the molecular characterization of breast cancer by gene expression profiling established an improved classification of breast cancers, due to technical advances in methodology. Gene expression profiling led to identification of five breast cancer subtypes: luminal A, luminal B, HER2+, basal-like and normal breast-like (Perou et al., 2000; Sorlie et al., 2001).

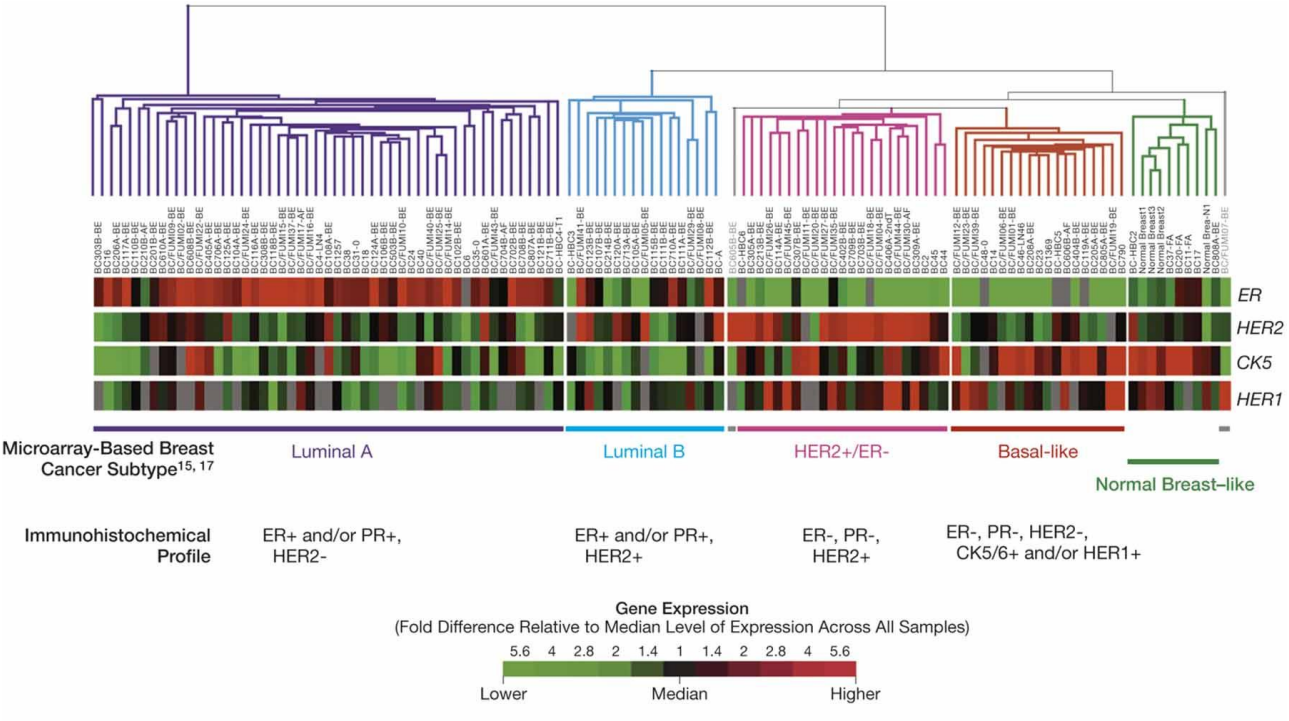

Figure 2 Molecular subtypes of breast cancer*. Gene expression analysis based classification of breast cancer into five different subtypes. Adapted from Carey et al., 2006*

ER-positive cancers express ER and ER-responsive genes, and luminal epithelial cells markers (keratin 8/18). ER-positive subtypes are Luminal A (40% of breast cancers) and Luminal B (20% of breast cancers). Luminal A subtype has lower proliferative index but a higher expression of ER-related genes than luminal B (Sorlie et al., 2003). The best overall prognosis is associated with luminal tumors. However, Luminal B subtype does have a significantly worse clinical profile than Luminal A, as well as a higher grading and proportion of p53 mutations, and larger genomic instability (Calza et al., 2006). In luminal tumors, the mitogenic activity of estrogen can be neutralized by selective estrogen receptor modifiers (i.e. tamoxifen) or by inhibition of estrogen production (i.e. aromatase inhibitors). Such hormonal therapies significantly improve the outcome of both localized and advanced ERα positive breast cancer (reviewed in Pritchard 2005 and Tobias 2004)

Other four subtypes are ER-negative cancers. HER2+ tumors overexpress genes located in the HER2 amplicon on 17q22.24, including HER2 and growth factor receptor bound protein 7 (GRB7) (Sorelie et al., 2001). They are aggressive cancers and usually elicit poor patient prognosis (Salmon et al., 1987 and Sorelie et al., 2001). However, the overexpression of HER2 makes them sensitive to HER2

inhibition by the humanized monoclonal antibody Trustuzumab which has been shown to significantly improve the clinical outcome of the patients with this type of breast cancer (Nahta et al., 2007)

The basal-like breast cancers express high levels of genes associated with basal epithelial cells such as keratin 5/6 and 17, P-cadherin, laminin and fatty acid binding protein 7 (Perou et al., 2000, Sorelie et al., 2001, Livasy et al., 2006, Sotiriou et al., 2003, Moyano et al., 2006, Shien et al., 2005, Abd El-Rehim et al., 2004). This type of cancer is reported to have the worst clinical outcome. It is characterized by an aggressive phenotype with high histological grade, high mitotic count, invasive borders, the presence of central necrotic zones, and stromal lymphocytic response (Livasy et al., 2006, Dabbs et al., 2006, Shin et al., 2008, Jones et al ., 2004). The majority of basal-like breast cancers do not express hormone receptors nor HER2 receptor which classifies them as triple negative cancers that are especially hard to treat because they fail to respond to targeted therapies (hormonal therapy and Trustuzumab) leaving conventional chemotherapies as the only therapeutic option (Rouzier et al., 2005).

Normal-like breast tumors are not yet well characterized and their clinical and pathological significance is yet to be determined. This subtype is enriched in genes normally expressed in adipose cells and non-epithelial cells (Perou et al., 2000).

MAMMARY GLAND

MAMMARY GLAND: AN OVERVIEW

Mammary glands are specific anatomical structures in female mammals that are responsible for the production and secretion of milk which contains proteins and fat for the nourishment of the newborn offspring. The mammary gland is an epidermal appendage which evolved from an ancestral apocrine gland that was associated with the hair follicles (Oftedal et al., 2002). Mammary glands provide an effective strategy for fostering the young, increasing the success of breeding and allowing further development outside the egg or uterus, which some authors link to the evolution of a large-sized human brain (Widelitz et al., 2007). The mammary gland comprises the epithelial ductal tree, randomly branched in order to increase milk producing area, and the surrounding stroma containing mostly adipocytes but also fibroblasts, endothelial and different immune cells.

Mammary glands are bilateral glands, specialized to provide nourishment for the young progeny. They are dynamic organs which undergo dramatic changes during their development. Mammary gland epithelium is present in rudimentary form in both sexes until the age of puberty when, in response to ovarian steroid hormones, they start to grow rapidly.

Additionally, mammary gland epithelium is the source of the most frequent cancer in the female population (Jemal et al., 2003) and therefore, extensive studies have been conducted in order to understand the effect of different signaling molecules involved in the mammary gland development and carcinogenesis.

MAMMARY GLAND AS A MODEL ORGAN

As the only organ to undergo most of its development postnatally, the mouse mammary gland is a particularly attractive experimental system for studying developmental processes. It is easily accessed as it is localized under the ventral skin. Mammary tissue is abundant as there are 5 pairs of mammary glands in mice, which allows the isolation of a large number of cells from a single animal. The transplantation of mammary tissue is a powerful mouse genetic tool to study differentiation processes, particularly cell fate determination in vivo.

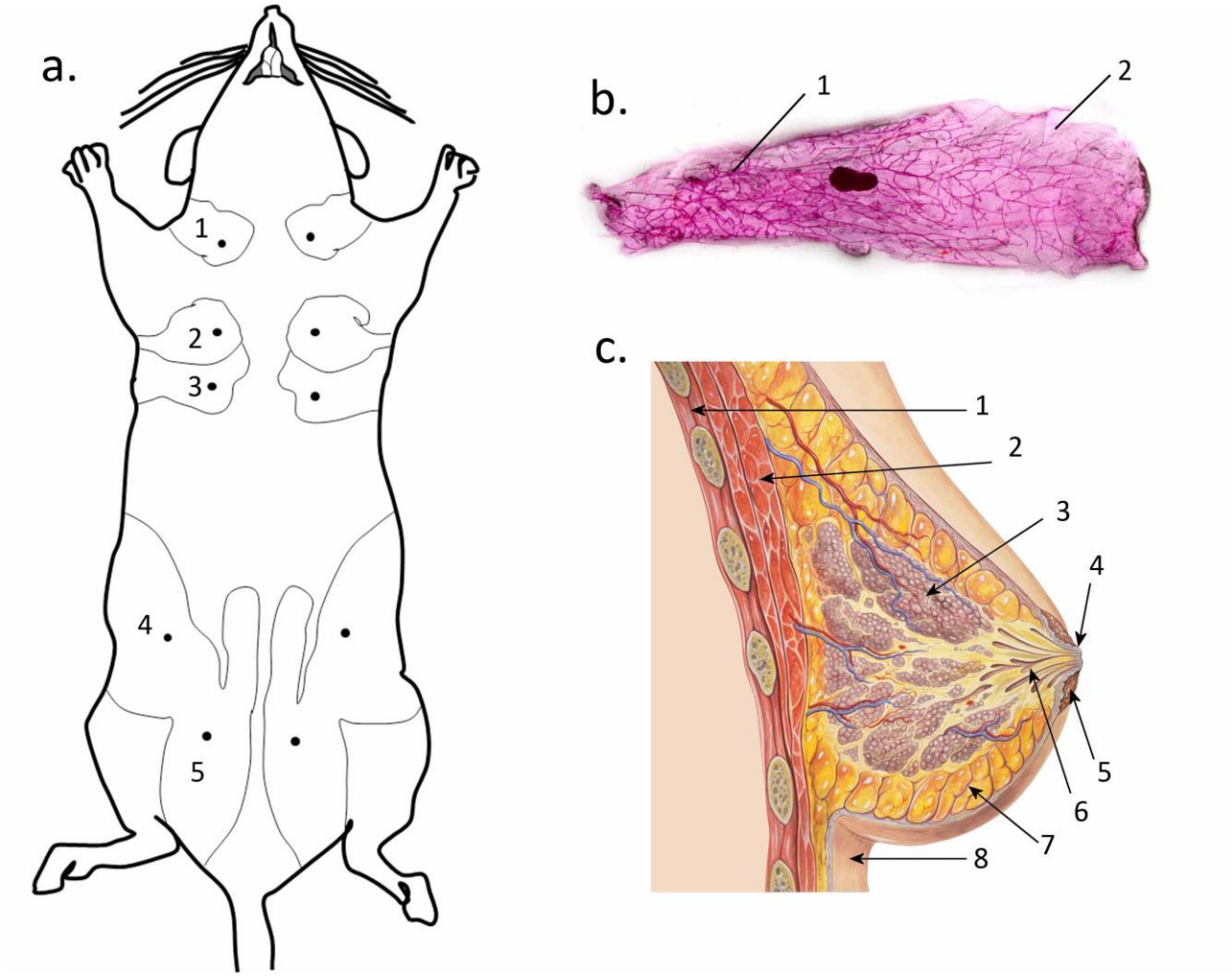

Figure 3. The mammary gland as an experimental model*. a) Scheme showing a female mouse with five pairs of mammary glands (depicted with thin lines) b) A carmine alum stained whole mount of a mouse mammary gland demonstrating epithelium (1) presented with dark pink emerged into light pink stroma (2) c) Scheme of a cross section of a human breast structure demonstrating chest wall (1), pectoralis muscles (2), lobules (3), nipple (4), areola (5), milk duct (6), fatty stroma (7) and skin (8). Illustration c) taken from www.wikipedia.org*

MAMMARY GLAND DEVELOPMENT

Mammary gland development can be divided into 2 stages: embryonic development, which is hormone independent and postnatal development, which can be divided into three stages: prepubertal, which is hormone independent, and pubertal and adult development which are orchestrated by hormones. In adulthood the mammary gland can be in a non-pregnant, pregnant, lactating and involuting state both of which show characteristic physiology.

EMBRYONIC DEVELOPMENT

Mammary gland development begins at E10 with the formation of the mammary/milk lines. Milk lines arise from ectoderm and stretch between the anterior and posterior limb buds, on the ventral side of the embryo. At E11.5 the mammary lines resolve into mammary placodes – lens-shaped epidermal structures consisting of several layers of large columnar cells (Veltmaat et al., 2004). Five pairs of mammary placodes form at symmetrically positioned reproducible locations.

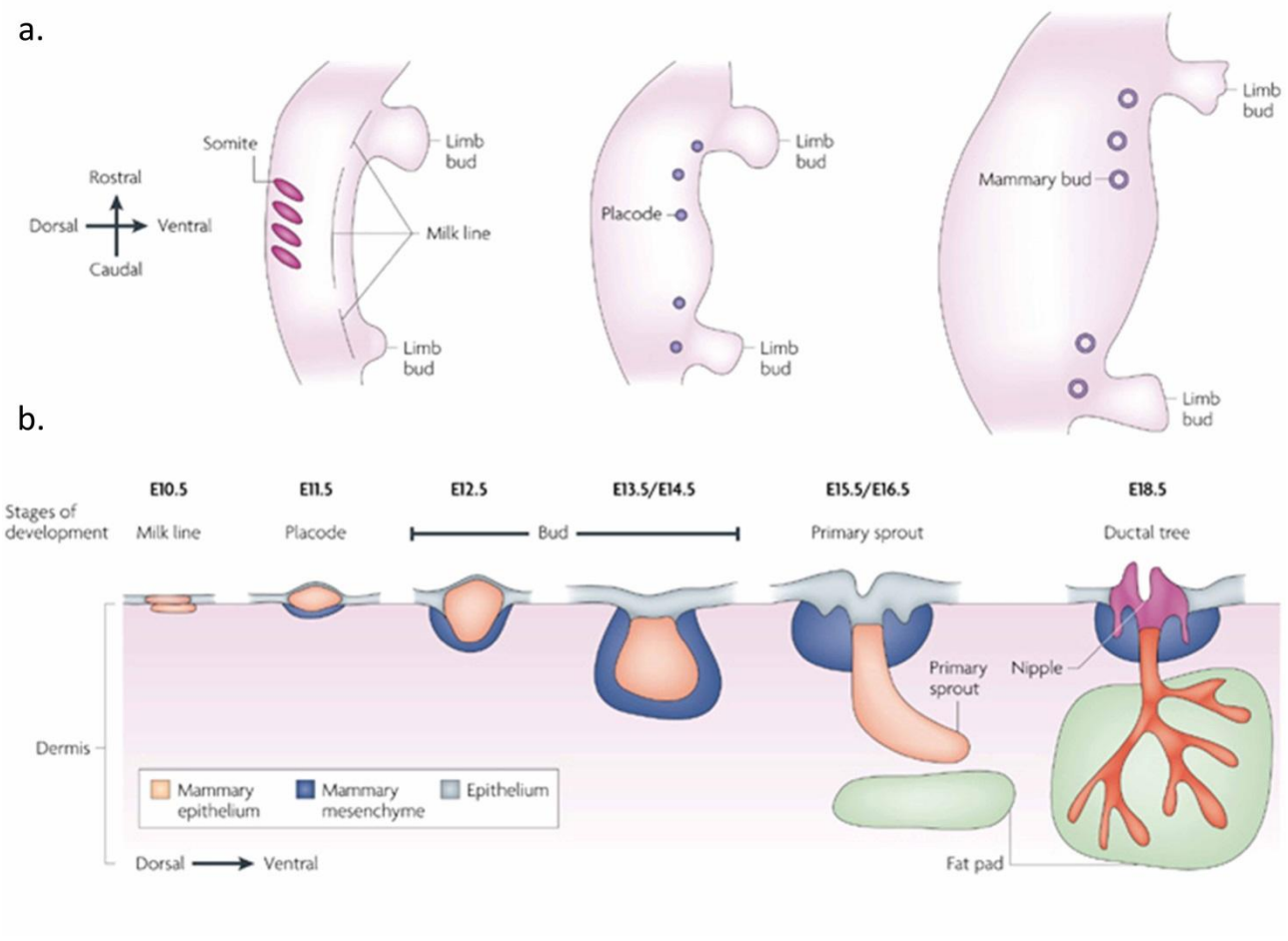

Figure 4. Embryonic mouse mammary gland development*. a) Formation of milk lines and positioning of mammary placodes and buds. b) Development of mammary gland starting from a milk line over mammary placode, bud and sprout to the rudimentary ductal tree. Adapted from Robinson, 2007.*

They are not identically determined since different signals are required for the formation of each pair. The development of the individual pair is not simultaneous and occurs at distinct order: Firstly number 3 followed by number 4, the number 1 and 5 appear simultaneously and finally number 2 (Veltmaat et al., 2004, Balinsky et al., 1950, Veltmaat et al., 2003). In the next step of the development, placodes invaginate into the underlying mesenchyme to form bulb shaped buds (Sakakura et al., 1987). Finally at E16, buds elongate to form mammary sprouts with a lumen that forms an opening to the skin (Veltmaat et al., 2003, Foley et al., 2001). By E18,5 a rudimentary ductal system is constituted of one short primary duct and about 10-15 initial branches. At this stage further development is arrested until puberty (Watson and Khaled, 2008).

The embryonic mammary gland development is coordinated by several signaling pathways and involves communication between the epidermis and mesenchyme. Several regulators have been identified to orchestrate the early stage of mammary gland development.

Canonical Wnt signaling is involved both in the specification of the mammary line and in mammary bud formation (Veltmaat et al., 2004). The experiments on FGF10 and FGFR2b mutants showed that fibroblast growth factor (FGF) signaling is also responsible for initiation of mammary

gland development, suggesting that FGF signaling functions in parallel with Wnt signaling in specifying the mammary line (Mailleux et al., 2002). FGF and Wnt signaling cooperate in placode formation by regulating the expression of T-box protein 3 (Tbx3) (Eblaghie et al., 2004). Tbx3 protein together with bone morphogenesis protein 4 (BMP4) can regulate the expression of lymphoid enhancer binding factor 1 (LEF1), a Wnt signaling mediator, in order to define dorso-ventral positioning of mammary placodes (Cho et al., 2006). Once the initial placode is formed, the mammary epithelium signals to the mesenchymal cells in its vicinity to transcribe several genes that are not expressed in the more distant dermal mesenchyme. The mesenchymal cells become arranged in concentric layers around the epithelial bud. They represent the primary mammary mesenchyme, specialized cells that carry out important functions in the further development of the bud: they maintain mammary epithelial cell identity, support ductal morphogenesis and growth, cause destruction of the epithelial bud in the presence of testosterone and participate in the formation of the nipple. The formation of primary mammary mesenchyme is regulated by a parathyroid hormone-like hormone (PTHLH) (Wyslomerski et al., 1998).

PTHLH has dual role in the mammary bud formation. Together with BMP4 it directs ductal outgrowth and mediates nipple formation by inhibiting the formation of hair follicles (Hens et al., 2007, Foley et al., 2001).

Experiments on *Rasgrf*$^{-/-}$ and *Igf1*$^{-/-}$ embryos suggested that insulin-like growth factor 1 (IGF1) signaling through Ras protein-specific guanine nucleotide-releasing factor 1 (RASGRF1) is important for the formation of a normal sized mammary bud and the induction of mammary mesenchyme cell identity.

POSTNATAL DEVELOPMENT

During the first 3 weeks of life, the mammary gland displays isometric growth with the rest of the body (reviewed by Knight and Parker, 1982). Further development of the mammary gland is orchestrated by the steroid hormones, estrogens and progesterone, and the polypeptide hormone prolactin. A hormonally controlled mammary gland development can be further divided in three main stages: ductal elongation, which takes place during puberty, ductal side branching that occurs during adulthood, and alveologenesis starting with pregnancy.

PUBERTY

Ductal elongation starts with puberty. It is triggered by estrogens signaling through estrogen receptor α (Mallepel et al. 2006). Structures called terminal end buds (TEBs) are formed during this stage (Silberstein, 2001). TEBs are club-shaped structures comprising an outer layer of cap cells and multilayer inner core of cells called body cells which are both highly proliferative and give rise to the

subtending ducts. Proliferation within the TEBs results in ductal elongation and their splitting in dichotomous branching to generate a simple ductal tree which fills an entire fat pad of the gland.

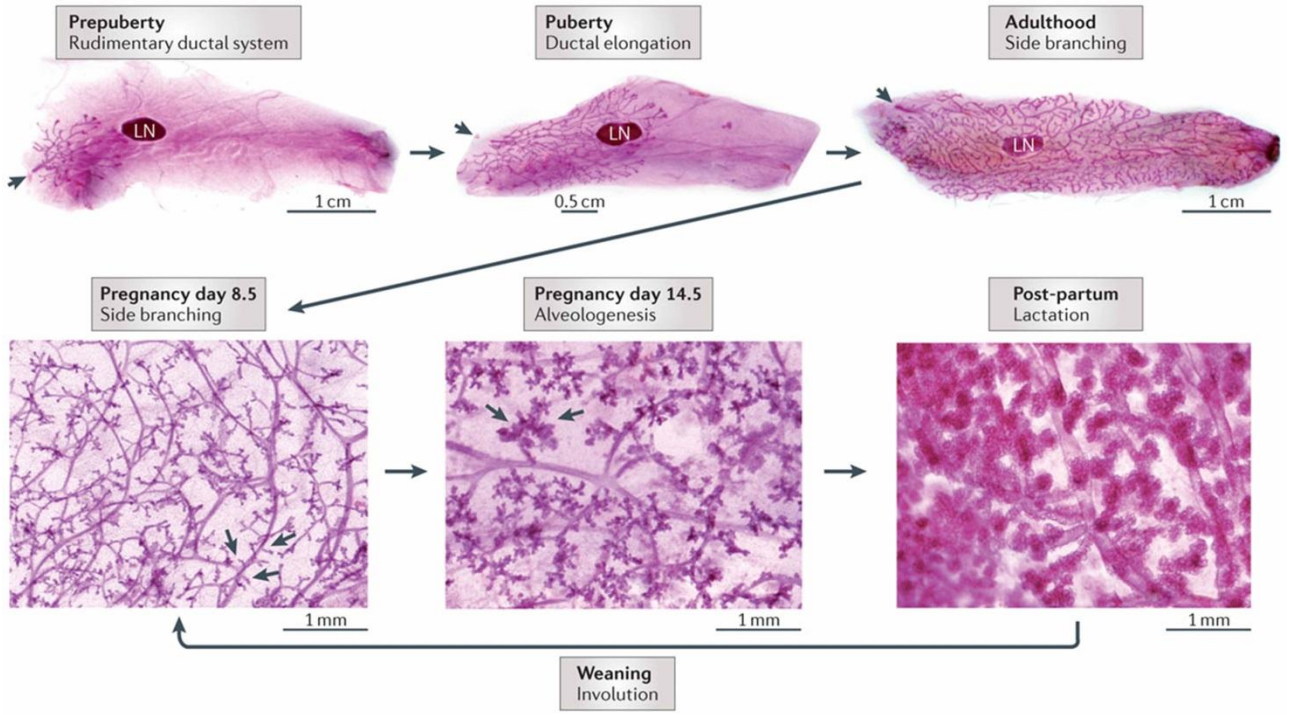

Figure 5. Postnatal development of the mouse mammary gland. *The mouse mammary glands consist of a rudimentary ductal tree in the prepubertal stage (nipple position depicted by arrow) which grows extensively in a bifurcational manner during puberty. In adulthood and early pregnancy through the process of side branching the ductal system increases its complexity (side branches shown by arrows). During late pregnancy and post-partum the functional surface of the epithelium enlarges in the process of alveologenesis forming alveoli, which will produce milk. After weaning, the mammary gland involutes and undergoes the process of reorganization of epithelium to return to a pre-pregnant state. (LN, subiliacal lymph node)*

VIRGIN ADULTHOOD

The ductal elongation is followed by ductal side-branching which takes place after puberty. This type of branching is triggered by cyclic changes in estrogens (E) and progesterone (P) secretion during adulthood and it increases the complexity of milk duct system. These morphogenetic and cellular responses are controlled by signaling cascades initiated by elevated serum levels during diestrus (Fata et al. 2001). The side branches that are formed during this process contribute to the complexity of the ductal tree and bud perpendicularly to the previously existing duct. Different molecules have been established as downstream mediators, such as Cyclin D1, Wnt4, receptor activator of nuclear factor kappa-B ligand (RANKL) and calcitonin (Brisken et al., 2000, Beleut et al., 2010). Side-branching continues to be enhanced during early pregnancy.

PREGNANCY

Finally, during mid/late pregnancy, prolactin (PRL) triggers a process called alveologenesis during which round saccular structures called alveoli are formed all over the ducts (Brisken et al., 2002, Brisken 2002, Brisken et al., 1999). Alveoli synthesize and secrete milk from late pregnancy

throughout lactation. In the alveoli myoepithelial cells are less continuous enabling luminal cells contact with basement membrane, which is a critical event for complete differentiation and milk secretion (Lee et al., 1985). The main regulators of the mammary developmental processes during gestation are P and PRL (Brisken et al. 1999).

INVOLUTION

After pups are removed from the mother, in response to milk stasis, the mammary gland enters the process of involution, a phase of extensive cell death and tissue remodeling. The expression of milk proteins decreases to basal levels and the expression of genes associated with apoptosis (serum gp70 production 2 (SGP-2), the signal transducer and activator of transcription 3 (STAT3) mediated by leukemia inhibitory factor (LIF), oncostatin M (OSM)) regulation of proliferation and differentiation (e.g. tumor suppressor p53 (p53), myelocytomatosis oncogene (C-myc), transforming growth factor ß (TGF-ß)) increases (Strange et al., 1992, Kritikou et al., 2003, Tiffen et al., 2008).

The involution of the secretory luminal cells starts few hours after weaning and 3 days after it becomes irreversible (Li et al., 1997). An early reversible phase does not involve apoptosis while the later irreversible phase exhibits hallmarks of classical apoptosis. A recent study showed that the physiological process of post-lactational regression of the mammary gland is accomplished through a non-classical, lysosomal-mediated pathway of cell death. During involution, lysosomes in the mammary epithelium undergo a widespread lysosomal membrane permeabilisation causing lysosome mediated programmed cell death regulated by STAT3 (Kreuzaler et al., 2011).

By day 4 of involution, apoptotic cells are cleared and the rearrangement of epithelium, stroma and basement membrane occurs (Monks et al., 2008, Strange et al., 1992). Involution lasts 14-21 days, subsequently the mammary gland resembles an adult virgin gland again but it can contain occasional remaining alveoli (Richert et al., 2000).

Therefore, the development of the mammary gland is a complex process where a number of signaling molecules are directly or indirectly involved in forming a large network, which drives differentiation and growth within mammary epithelium.

MAMMARY EPITHELIUM STRUCTURE

The mammary gland, as a complex secretory organ, comprises several different cell types: Epithelial cells that compose a ductal system of the gland; adipocytes, that form a fat pad in which the ductal tissue is embedded; stromal fibroblasts; endothelial cells, forming the vascular tissue; and an array of different immune cells.

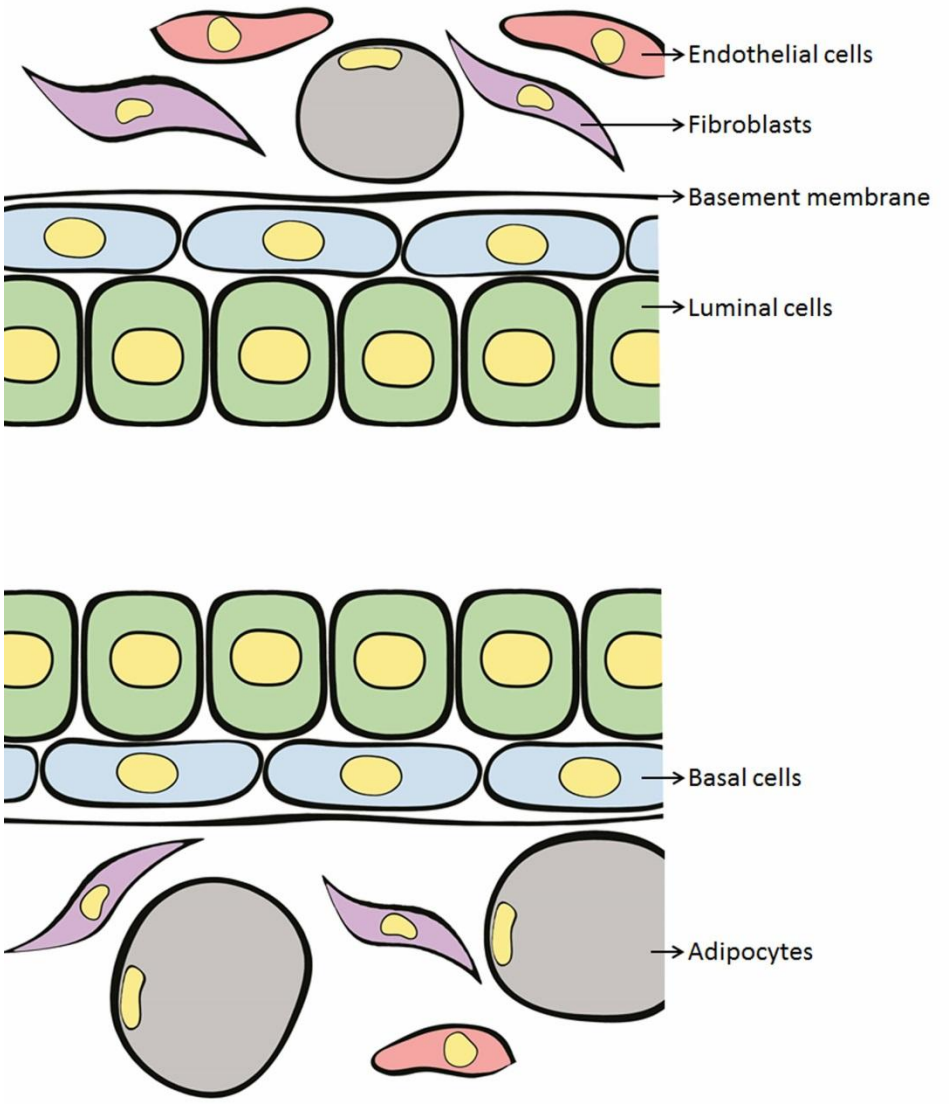

Figure 6. A simplified scheme representing the cellular components of mammary epithelium

Mammary epithelium is a simple bi-layered structure surrounded by basement membrane formed of an inner luminal layer considered to contain all the cells that are in direct contact with the lumen and an outer basal layer containing all the cells that are in close contact with the basement membrane. Luminal cells can be either hormone receptor positive or hormone receptor negative while basal cells are mostly myoepithelial. The mammary epithelium is embedded within the fatty stroma consisted of mainly adipocytes and keratinocytes (Watson and Khaled, 2008).

LUMINAL CELLS

The inner epithelial layer is called luminal layer and is composed of luminal epithelial cells. It comprises two populations of cells: hormone receptor positive, and hormone receptor negative cells that can produce milk during the lactation period. Furthermore, they are polarized cells that exhibit short, blunt microvilli on their apical surface and display well-developed cell-cell junctions (Mikaelian et al., 2006). During puberty, while TEBs are still present, the luminal layer of cells exhibits a higher apoptosis rate than the basal one which is consistent with an increased cell proliferation in this cell

layer (Humphreys et al., 1999, Humphreys et al., 1996) In an adult virgin mouse approximately 30% of luminal cells express hormone receptors (Shyamala et al., 1999; Zeps et al., 1998) which through binding to their cognate ligands, steroid hormones estrogens and progesterone, regulate proliferation of epithelial cells in both layers and also some in stroma (Brisken et al., 1998, Mallepell et al., 2006)

BASAL CELLS

Myoepithelial cells are spindle-shaped and cytologically characterized by desmosomes, hemidesmosomes, myofilaments, irregular nuclei with marked heterochromatin, peripheral cytoplasmic caveoli and ragged basal borders (Mikaelian et al., 2006). They form a basally arranged smooth muscle actin (SMA) expressing thin monolayer that possibly has a role in oxytocin-triggered milk ejection. Myoepithelial cells are surrounded by basal membrane which exposes them to the morphogenetic and differentiation signals from extracellular matrix and stroma. Therefore, basally located myoepithelial cells might transmit the signal from stroma to the luminal layer through desmosomes, adherens and gap-junctions (Teuiliere et al., 2005), playing an important role in mammary growth and differentiation (Faraldo et al., 2006).

Luminal and myoepithelial cells can be discriminated as they express specific markers (Faraldo et al., 2005). In particular murine myoepithelial cells specifically express cytokeratins K5 and K14, SMA, p63 and P-cadherin, while luminal cells express K8 and K18. With the development of the fluorescence activated flow cytometry techniques it has become possible to sort luminal and myoepithelial cells based on the surface markers characteristic for each population. Luminal cells are characterized by a high expression of CD24 while low expression marks the myoepithelial layer of cells (Sleeman et al., 2006). Furthermore, they can be distinguished based on the differential expression of epithelilal cell adhesion molecule (EpCam) and CD49f where luminal cells are defined by a high expression of EpCam and low expression of CD49f and myoepithelial cells by low expression of EpCam and high expression of CD49f markers (Shehata et al., 2012).

HORMONAL REGULATION

Mammary morphogenesis is orchestrated by sex hormones estrogens, progesterone and prolactin which were defined as the main regulators of mammary gland development. Minimal hormonal requirements were established by hormone ablation and replacement studies in mice (Nandy et al., 1958) and rats (Lyons et al., 1958). The generation of mice lacking the genes for either ERα (Dupont et al., 2000), PR (Lydon et al., 1995) or prolactin receptor (Prlr) (Ormandy et al., 1997) enabled through tissue recombination experiment unveiled that ERα is required for mammary epithelial ductal elongation during puberty (Mallepell et al., 2006), whereas PR signaling is responsible for the process of side-branching (Brisken et al., 1998). Further to this, the processes of alveologenesis and lactogenic differentiation during late pregnancy were completely inhibited upon deletion of Prlr and therefore implicating prolactin as an important regulator of these events (Brisken et al. 1999.).

Steroid hormones estrogens and progesterone elicit their function through binding to respective intracellular receptors. This leads to dimerization of the receptor-hormone complex which finally binds DNA via estrogen responsive elements (ERE). EREs are short sequences of DNA, located in the promoter regions of the target genes which are recognized by the hormone-receptor complex. The binding of the complex to these sequences regulates the expression of target genes. Estrogen can also exert genomic actions in an ERE-independent manner, whether it is through the interaction with Fos and Jun at AP1 binding site, genes containing STAT5 binding sites, or the interaction with NF-κB where it inhibits the transcription of interleukin 6 (IL-6) (reviewed in Nilsson et al., 2001).

Both in humans (Clarke et al., 2006, Clarke et al., 1997) and in mice (Seagroves et al., 2000) mammary tissue has shown that ER and PR are mostly expressed in the same mammary epithelial cells, which are rarely proliferating. However in human breast epithelium this is not entirely the case because it has been shown that PR and ER can segregate into different cell subpopulations. Furthermore, PR expression was detected also in the basal compartment in putative bipotent progenitor cells (Hilton et al., 2012); however, *in vivo* evidence for this was provided only from the experiments with FACS sorted cells.

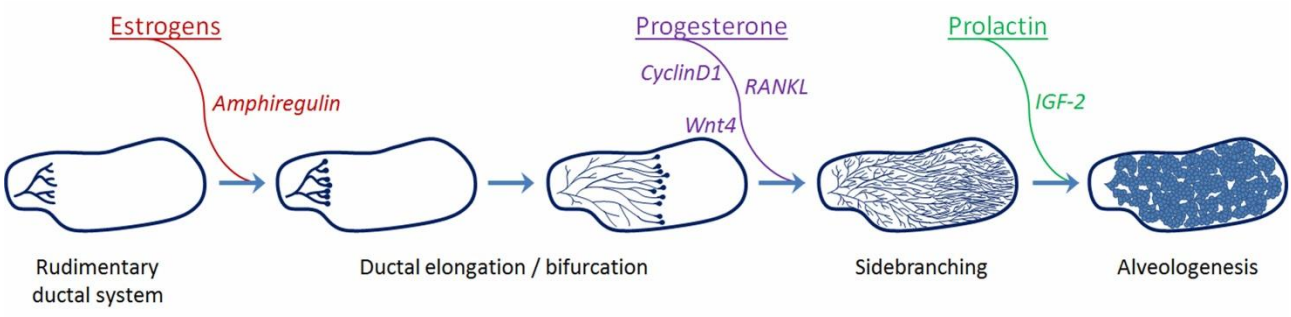

Figure 7. A simplified scheme of hormonal regulation of the post-natal development*. Hormones are orchestrating the post-natal development of the mammary gland: Estrogens drive ductal elongation through the mediator amphiregulin. Progesterone regulates side branching through Cyclin D1, RANKL and Wnt4. Alveologenesis is driven by prolactin with IGF-2 as mediator.*

Several players of different signaling pathways were identified as hormone targets and shown to be important for the different steps of the mammary gland development. The epidermal growth factor receptor ligand, amphiregulin was shown to be a major paracrine mediator of ERα induced cell proliferation orchestrating ductal elongation process (Ciarloni et al., 2007). PR signaling was shown to cause two distinct waves of proliferation of mammary epithelial cells, where HR+ cells proliferate in the first one regulated by Cyclin D1, and HR- cells in the second one run by tumor necrosis factor superfamily member RANKL (Beleut et al., 2010). Additionally, Wnt4 has been shown as PR target that regulates directly and/or indirectly stem cells by activating the myoepithelial compartment (Brisken et al 2000, Rajaram et al., 2015). Prolactin signaling paracrine regulation of alveologenesis and lactogenic differentiation is mediated by IGF-2. (Brisken et al., 2002)

STEM CELLS AND EPITHELIAL CELL HIERARCHY

The discovery that tissues in higher organisms are not only heterogeneous but composed of a cellular hierarchy has brought up numerous new insights into both how the organism functions as well as how diseases occur within them. Therefore, a concept of stem cells has provided new means to address many developmental questions.

The mammary gland is a highly dynamic organ, undergoing constant remodeling after birth. Its complex development can be explained through the concept of the "adult stem cell", explaining how different cell types emerge throughout all the developmental stages. This concept has been argued by a concept of stem cell plasticity insisting on the fact that bipotent cells are present only during embryonic development. Postnatally in physiological conditions only luminally and basally restricted progenitors are present which will give rise to luminal and basal cell types (Van Keymeulen et al. 2011).

The current model suggests that from mammary stem cells differentiation can undergo either myoepithelial or luminal path. The myoepithelial path to fully differentiated myoepithelial cell goes from the stem cell through the putative basally located stem cell and myoepithelial restricted progenitor, both of unknown phenotype, to the myoepithelial cell ($CD29^{hi}CD49f^{hi}CD24^{lo}EpCAM^{lo/med}$). The luminal path is more complex containing more final products. From a putative stem cells differentiation process arises a putative common luminal progenitor of unknown phenotype that can give a ductal ($CD49f^{+}CD29^{lo}CD24^{+/hi}EpCAM^{hi}CD61^{+}c\text{-}Kit^{+}Sca\text{-}1^{+}CD49b^{+}CD14^{+}$) and alveolar progenitor ($CD49f^{+}CD29^{lo}CD24^{+/hi}EpCAM^{hi}CD61^{+}c\text{-}Kit^{+}Sca\text{-}1^{-}CD49b^{+}CD14^{+}Aldh1^{+}$). The ductal progenitor will give rise to the fully differentiated luminal cell either ER^{+} or ER^{-}. Alveolar progenitors can be characterized as $c\text{-}Kit^{hi}$ early or $c\text{-}Kit^{lo}$ late and they will give rise to fully differentiated alveolar cells which are ER-.

Although single cells assays are more often used, serial transplantation, considered to be a "golden standard" in mammary stem cell research (reviewed by Visvader and Stingl 2014), was published for the first time in 1968 (Daniel et al., 1968). However, the stem cell enriched population has not been successfully isolated until recently. Two publications showed that the expression of CD24 (Heat stable antigen) and integrin α6 (CD49f) or β1 (CD29) can be used to enrich mammary stem cells. Furthermore, a single cell from stem cell enriched population defined as $CD24^{lo}CD49f^{hi}$ (Stingl et al., 2006) or $CD24^{lo}CD29^{hi}$ (Shackleton et al., 2006) can regenerate the complete mammary ductal system in the cleared fat pad.

The luminal compartment is thought to elicit higher complexity in terms of cellular hierarchy, where multiple distinct subsets have been identified at morphological and functional levels. Various cell surface markers have recently been used to discriminate luminal progenitors from differentiated luminal cells: CD61 (Asselin Labat et al., 2007), CD49b (Shehata et al., 2012), CD14 (Asselin Labat et al., 2011, Shehata et al., 2012) and c-Kit (Asselin Labat et al., 2011, Regan et al., 2012). Some of these

markers, such as CD14 and CD49b, are expressed by all luminal progenitors while others (CD61 and c-Kit) are expressed in more restrictive pattern. CD61 and c-Kit expression markers are mouse strain dependent and can be used for FVB/N strain of mice (Asselin Labat et al., 2011, Regan et al., 2012) but not for mice of C57Bl6/J origin (Shehata et al., 2012). Furthermore, CD61 marks a population of progenitors comprising a large subset of HR- and smaller subset of HR+ cells but only in non-pregnant mice since it is down-regulated during pregnancy (Asselin Labat et al., 2007). Hormone receptor positive luminal cells are successfully enriched with Sca1 marker and show a high expression of ER, K8 and K18. Aldehyde dehydrogenase isoform 1 (Aldh1) has been reported to mark human stem cells in the human breast (Ginestier et al., 2007), but recently it has also been used in mouse cells (Shehata et al., 2012).

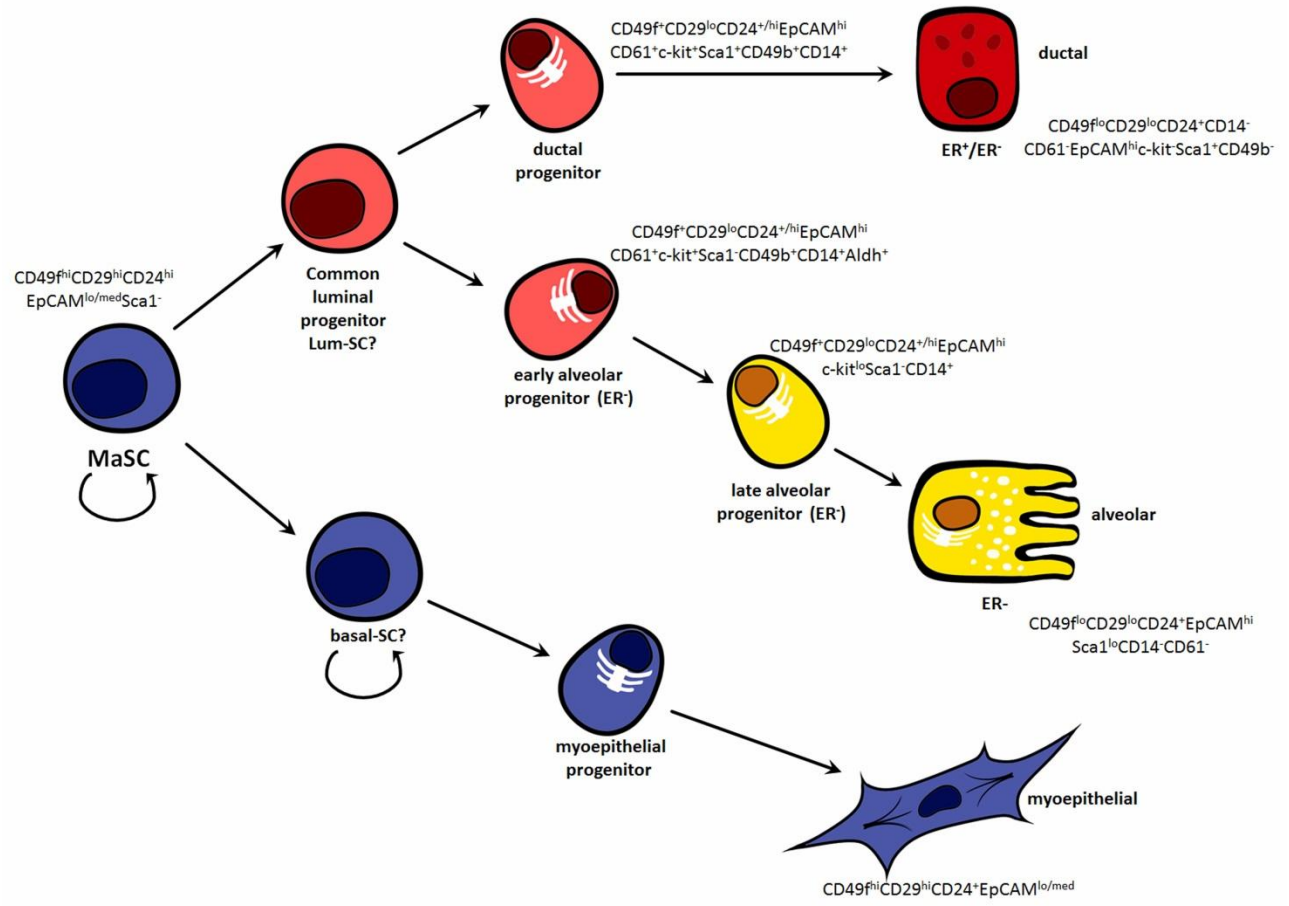

Figure 8. Model of the mammary epithelial hierarchy*. A multipotent mammary stem cell gives rise to basally and luminally restricted stem cell. The luminally restricted stem cell can give rise to a ductal lineage through a ductal progenitor, or alveolar lineage through alveolar progenitor. The basally restricted stem cell gives rise to myoepithelial cells through the myoepithelial progenitor. Characteristic markers used for isolation of epithelial cell subsets are summarized next to each cell type. Illustration based on Visvader and Stingl, 2014.*

Different combinations of these markers can reveal a subpopulation of cells with distinct characteristics. $CD49b^{+}CD14^{+}Sca1^{-}Aldh1^{+}$ has been shown to be enriched for undifferentiated colony-forming cells suggesting their regenerative potential (Shehata et al., 2012). This population can be further divided based on the marker c-Kit where $c\text{-}Kit^{hi}$ subset would correspond to more primitive alveolar progenitors. Progenitor cells mostly show HR- phenotype, however , a rare ER+ population of

progenitor cells was detected in adult mice expressing CD49b^{+}c-Kit^{+}Sca-1^{+} combination of surface markers (Regan et al., 2012, Shehata et al., 2012). On the other hand a non-clonogenic population that corresponds to mature luminal cells was defined by CD49b^{-} c-Kit^{-} Sca-1^{+} phenotype.

Recent studies provided evidence for such a hierarchical model. However, precise genetic mechanisms that regulate stem/progenitor differentiation and lineage commitment during mammary gland development are incompletely understood. Yet, a number of factors have been implicated.

DIFFERENTIATION OF MAMMARY EPITHELIAL CELLS

GATA binding protein 3 (GATA-3) is a transcription factor that has been shown to promote differentiation of lineage-restricted progenitor cells. Loss of GATA-3 factor blocks luminal progenitor cell differentiation and leads to expansion of undifferentiated luminal cells (Kouros-Mehr et al., 2006, Asselin-Labat et al., 2007, Asselin-Labat., 2011).

E74 like factor 5 (Elf-5) is a transcription factor and a component of the prolactin signaling pathway that has recently been proposed to play a key role in alveolar cell-fate specification (Oakes et al., 2008). Elf-5 is required to establish the secretory alveolar lineage during pregnancy (Zhou et al., 2005).

Recently, promyelocytic leukemia protein (PML) has emerged as a factor possibly involved in chromatin remodeling during lineage commitment in the mammary gland. Furthermore, its interaction with STATs and relative concentration of STAT/PML complexes has been proposed to drive cell-fate (Li et al., 2009).

Notch signaling is also implicated in cell-fate determination and commitment. Its physiological role in the mammary gland is still controversial; literature suggests different functions of its activity.

NOTCH SIGNALING

DISCOVERY OF NOTCH SIGNALING AND ITS IMPLICATIONS IN DEVELOPMENT

Notch was first discovered by Thomas Hunt Morgan and his colleagues in a strain of Drosophila melanogaster when they noticed notches at the margins of the wing blades (Morgan et al., 1917). They noticed that this Notch phenotype was inherited in a Mendelian fashion. However, the significance of the pathway in development was described later in the classical embryonic analysis of lethal homozygous loss-of-function mutations (Poulson et al., 1937). Poulson showed that loss of section within the X-chromosome resulted in abrogation of segregation of the early ectoderm into neural and epidermal cell lineages and the consequence of this was “neurogenic” phenotype where neural tissue was hypertrophic at the expense of epidermal structures. Notch locus was cloned in 1983 which has been a starting point of several genetic and molecular interaction studies which proved that mutated

Notch locus was, indeed, cause of the neurogenic phenotype. Several studies followed identifying the product of the Drosophila Notch gene as a single-pass type 1 transmembrane receptor (Wharton et al., 1985, Kidd et al., 1986, Artavanis-Tsakonas et al., 1983). Further to this it was revealed that Notch signaling played an important part in various developmental processes in Drosophila melanogaster, such as bristle formation (Heitzler et al., 1991), maintenance of muscular founder cell (Bate et al., 1993) and regulation of cell-fate decision of stem cells in the intestines (Ohlstein and Spradling, 2007). Since it has been discovered in Drosophila, Notch signaling has been shown to play an important role in a wide variety of cellular processes, such as cell proliferation, apoptosis, maintenance of stem cells, and specification of cell fates in all metazoan organisms.

Further to this, Notch signaling was reported as an important factor in binary cell-fate decisions via lateral or inductive signaling which could explain the neurogenic phenotype, previously observed (Poulson et al., 1937). Here, Notch signaling operates in a population of equipotent cells with the capacity to differentiate into neural precursors or epidermal cells. In this population cells will express either Notch ligand or receptor, exclusively. Ligand expressing cells acquire a neuron progenitor fate and send inhibitory signals to the receptor expressing cells, directing them into different developmental pathways (reviewed in Bolos et al., 2007). In the neurogenic phenotype, ligand expressing neuron progenitor cells predominate as they lack functional Notch receptor.

Developmental studies of the murine central nervous system (CNS) unveiled Notch's signaling influence on the equilibrium between the progenitor cell pool and differentiated progeny (Lutolf et al., 2002, Yang et al., 2004, Yoon et al., 2004, Yun et al., 2002, Hitoshi et al., 2002, Ohtsuka et al., 1999). These studies revealed that Notch signaling is an important player in the maintenance of the neural progenitor pool by abrogating premature neuron differentiation and by triggering proliferation and apoptosis among neural progenitor cells.

Notch signaling has been implicated in regulation of several other developmental processes in mammals, including cardiovascular and mammary gland development. In cardiovascular development, Notch signaling is indispensable to establish arterial endothelial specification (Krebs et al., 2004, Duarte et al., 2004, Wang et al., 1998), mediate angiogenesis (Krebs et al., 2000), and regulate proper vascular remodeling (Timmerman et al., 2004, Lincoln et al., 2004). Communication between the endocardial and myocardial layers to from the valves and ventricles is mediated by Notch signaling (Grego Bessa et al., 2007, Jenni et al., 2001).

In the mammary gland Notch has been implicated in mammary stem cells renewal (Dontu et al., 2003, Dontu et al., 2004) and contrarily, promotion of the expansion of the luminal progenitor populations (Bouras et al., 2008). This topic will be addressed in more details in further reading.

NOTCH RECEPTORS

In mammals, the Notch receptor family consists of four homologs (Notch1-4) with a highly conserved structure, which display both redundant and unique functions. Extracellular domain (NECD) consists of 29-36 epidermal growth factor (EGF)-like repeats responsible for ligand binding (Uyttendaele et al., 1996), followed by 3 negative regulatory LIN repeats. LIN repeats contain Ca2+binding sites which are important for heterodimerization (Rand et al., 2000) and prevention of signaling in the absence of ligand. The hydrophobic C' terminal region of NECS binds to the N'-terminal region of the transmembrane subunit (NTMS) which contains a pair of conserved cysteine residues which putatively assist in the formation of a non-covalent bond sensitive to reducing conditions responsible for heterodimerization of the receptor (Blaumueller et al., 1997).

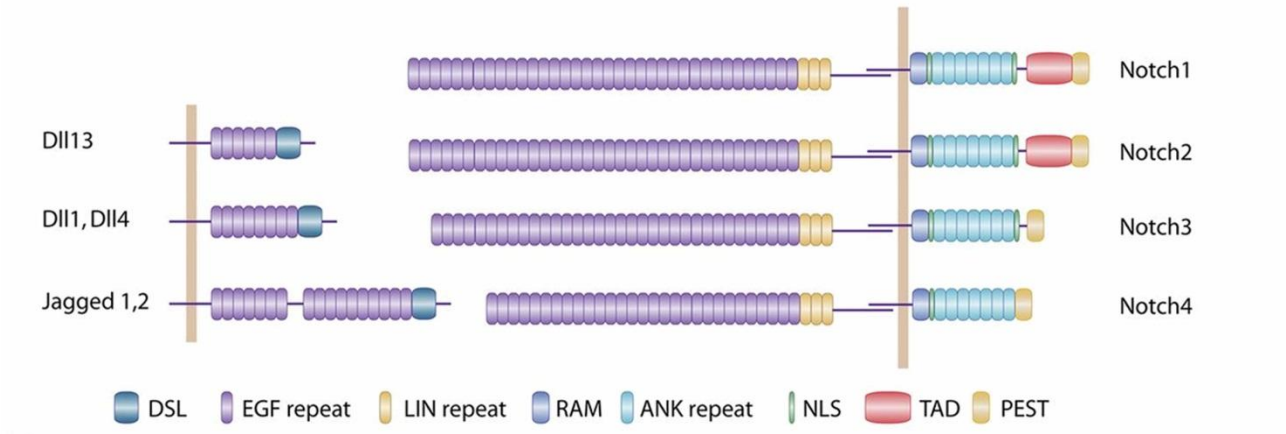

Figure 9. Mammalian Notch ligands and receptors. *5 Notch ligands (on the left) are known in mammals: Delta-like1 (Dll1), Delta-like3 (Dll3), Delta-like4 (Dll4), Jagged1 (Jag1) and Jagged2 (Jag2). All the ligands have a DSL (Delta, Serrate, and Lag2) domain responsible for binding to receptors, followed by EGF repeats. There are 4 Notch receptors (on the right): Notch1 to Notch4. Extracellular domain has 3 negative regulatory LIN repeats and variable number of EGF repeats. Intracellular part comprises RAM domain, nuclear localization signal (NLS), ankyrin repeats (ANK) and PEST domain regulating protein stability. Adapted from Lobry et al., 2014.*

The cytoplasmic portion of the receptor (NICD) contains, sequentially, a RBP-Jκ-associated module (RAM) domain, seven tandem copies of CDC10/ankyrin repeats that are flanked by nuclear localization signals, and a C'-terminal proline-glutamine-serine-threonine (PEST) sequence involved in ubiquitination and receptor turnover and protein stability. Notch1 and Notch2 receptors have a transactivation domain just before PEST domain, however it is absent in the Notch3 and Notch4 influencing promoter selectivity at least in vitro (Ong et al., 2006). Experimental evidence indicates that a high-affinity interaction between NICD and Recombination signali binding protein for immunoglobulin kappa J region (RBP-Jκ) occurs through the ankyrin repeats which are essential for the formation of the transcriptional activation complex (Zweifel et al., 2003).

POSTTRANSLATIONAL MODIFICATION OF NOTCH RECEPTORS

Notch receptors are synthesized as single precursor proteins in the endoplasmic reticulum. Notch receptors are cleaved by a furin-like convertase at the S1 site (Logeat et al., 1998) in the trans-

Golgi network to give two subunits: the N'-terminal subunit contains most of NECD, and the C'-terminal subunit comprises approximately 70 amino acids of NECD domain, NTMS and NICD. The two Notch subunits are then transported to the membrane where they associate through a Ca2+-dependent, non-covalent bond (Rand et al., 2000).

Drosophila studies showed that in the Golgi apparatus, Notch receptors undergo various posttranslational modifications that play an important role in modulating receptor-ligand interactions. Extracellular EGF-like repeats are fucosylated by protein O-fucosyltransferase 1 (Pofut1 in mammals), followed by subsequent modifications by Fringe proteins (Panin et al., 1997).

In mammals, the Fringe family comprises three N-acetylglucosaminyl transferases, lunatic fringe, radical fringe and manic fringe. They glycosylate Notch receptors in order to potentiate their activation by DSL ligands. Contrarily, they act antagonistically on Jagged ligands due to the specific pulling mechanism of activation explained in detail later (Yang et al., 2005).

NOTCH LIGANDS

There are five Notch ligands in mammals: Delta-like-1, -3 and -4 (Dll1, Dll3 and Dll4) and Jagged1 and Jagged2 (Jag1 and Jag2). Notch ligands are also membrane tethered proteins (Mumm and Kopan, 2000) with an extracellular region that comprises a DSL (Delta/Serrate/Lag-2) motif involved in receptor binding and an altering number of EGF-like repeats followed by a transmembrane region and a short intracellular cytoplasmic part (ICL). Proximally to the trans-membrane segment, Jagged ligands additionally have a cysteine-rich region which controls Notch receptor binding specificity, and a von Willebrand factor (vWF) motif involved in ligand oligomerization (Fleming et al., 1998).

The intracellular regions of Jag1, Dll1, and Dll4, but not Jag2 and Dll3, are predicted to contain PDZ binding motifs that could independently couple the ligands to PDZ-containing, membrane-associated molecules that might play a role in the cell-cell junctions organization (Pintar et al., 2007). The role of ICL domain of Notch ligands is poorly investigated. However, it is known that it is highly important for ligand-mediated Notch signaling. In fact, truncated ligands lacking the ICL part of ligand showed dominant-negative effects on Notch signaling (Sun and Artavanis-Tsakonas, 1996).

BASIC MECHANISM OF NOTCH SIGNALING PATHWAYS

Unlike most of the signaling pathways, Notch signaling does not have any enzymatic amplification steps and therefore Notch receptor by itself is directly involved in the transduction of the signal from membrane to the nucleus.

ACTIVATION OF NOTCH

When ligand is not bound, Notch receptors are present at the cell surface as heterodimers (Blaumueller et al., 1997). A small motif between LIN repeats and transmembrane region is preventing receptors from spontaneous activation of the pathway (Kimble et al., 1998).

Upon recognition on an adjacent cell and due to the pulling force caused by internalization of the bound ligand, the Notch receptor undergoes a conformational change that disrupts its heterodimeric structure and the exposure of the proteolytic cleavage site, S2. Cleavage at S2 is mediated by the metalloprotease ADAM10 (Brou et al., 2000) in human and Kuzbanian in Drosophila (Lieber et al., 2001). The released extracellular portion of the receptor is then trans-endocytosed by the ligand-expressing cell (Parks et al., 2000).

ADAM17 has also been reported to cleave Notch to facilitate NICD release by γ-secretase. However, it has been shown that ADAM 17 is the main effector of the S2 cleavage site only if the Notch receptor is destabilized in a ligand independent fashion by mutation or addition of the reducing agent such as EDTA (Bozkulak and Weinmaster, 2009, van Tetering et al., 2009).

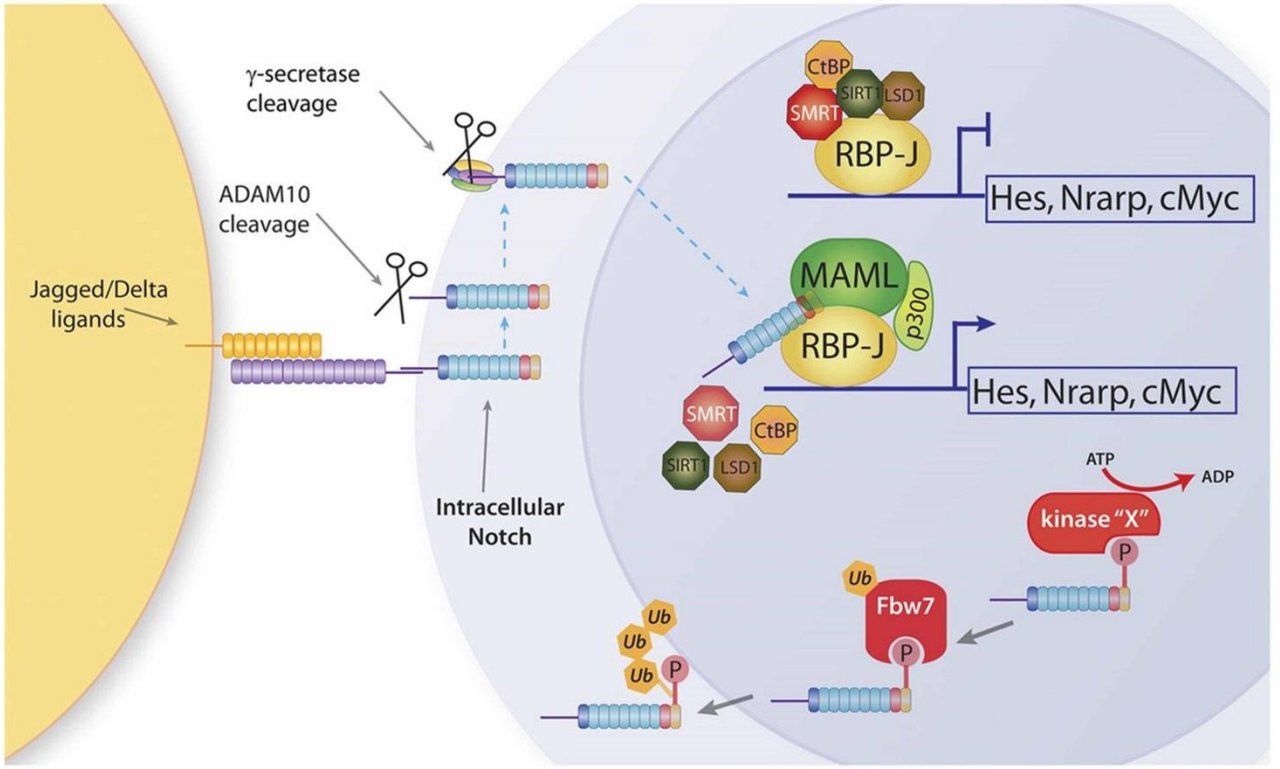

Figure 10. Notch signaling activation. *Interaction between ligand and receptor triggers 2 consecutive proteolytic cleavages resulting in release of receptors intracellular domain and its translocation to the nucleus where, together with coactivator MAML, it activates transcription of target genes through transcription factor RBP-Jκ. Activating complex is short-lived as the PEST domain gets phosphorylated, ubiquitinated and subsequently degraded by proteasome. Adapted from Lobry et al., 2014.*

In the receptor expressing cell, consequence of this cleavage is the cleavage within the transmembrane region, catalyzed by a complex of Presenilin-1/2, nicastrin, anterior pharynx-defective

1 (Aph1) and presenilin enhancer protein-2, PEN2 protein complex called γ-secretase, which releases NICD from the membrane and allowing it to translocate into the nucleus (Saxena et al., 2001). Monoubiquitination and clathrin-dependent endocytosis of Notch predispose for cleavage by γ-secretase, probably because ubiquitination targets Notch to a compartment where it can be activated (Gupta-Rossi et al., 2004). At the same time, internalization of the ligand and trans-endocytosis of the NECD by the ligand-expressing cell are required for effective Notch activation (Itoh et al., 2003). Upon endocytosis a mechanical pulling force is created on the receptor, which can either cause a conformational change and expose the juxta membrane region of the receptor to S3 cleavage, or physically dissociate the Notch heterodimer therefore directly promoting activation (Nichols et al., 2007). Hence, it is crucial to understand the mechanism of ligand-NECD endocytosis as a putative target to inhibit Notch signaling. In flies and vertebrates, Neuralized and Mindbomb, E3-ubiquitin ligases are key components which mediate ubiquitination of the Notch ligands (Song et al., 2006).

RBP-Jκ -DEPENDENT TRANSCRIPTIONAL ACTIVITY

The main feature of canonical Notch signaling is the transactivation of target genes through the conversion of RBP-Jκ (RBP-Jκ is a mouse homolog of CSL protein: CSL stands for CBF1 in mammals, Su(H) in *Drosophila*, and Lag-1 in *C.Elegans*) from a transcriptional repressor state to an activator state. RBP-Jκ is a constitutively expressed transcription factor that can recognize a consensus DNA sequence 5'-TGGGAA-3' (Brou et al., 1994). When NICD is absent from the nucleus, RBP-Jκ binds to promoter of the target genes forming a repressive complex with co-repressors nuclear receptor co-repressor (NCoR), SMART/HDAC1 associated repressor protein (SHARP) and Ski-interacting protein (SKIP), histone deacetylases by function (Oswald et al., 2002). Upon translocation to the nucleus, NICD competes with the co-repressors for RBP-Jκ, interaction firstly through RAM domain (Nam et al., 2006) and later associating with CDC10/ankyrin repeats. Further to association to ankyrin, NICD forms a ternary complex with Mastermind-like (MAML-1, -2, -3) that is directly in interaction with NICD (Wu and Griffin, 2004). MAML recruits acetyltransferases CREB-binding protein (CBP)/p300 (Oswald et al., 2001; Wallberg et al., 2002) or p300/CBP associated factor (PCAF)/GCN5 (Kurooka and Honjo, 2000) responsible for altering the structure of chromatin making it susceptible for transcription.

RBP-Jκ -INDEPENDENT SIGNALING

All 4 Notch receptors exert their function through RBP-Jκ; however, a non-canonical signaling independent of RBP-Jκ has been reported in multiple contexts. Among examples there is interaction of NICD with NF-κB in B-cells (Shin et al., 2006), β-catenin (Hayward et al., 2005), and hypoxia-induced factor-1α (HIF-1α) (Zheng et al., 2008). It can also act through Deltex, a RING finger E3 ligase which is also canonical Notch target. It can, bound to NICD (Fuwa et al., 2006), mediate (Yamamoto et al., 2001) and inhibit (Izon et al., 2002) Notch signaling, depending on context.

Notch intracellular domain can also activate LEF1 transcription factor. However, LEF-1 is likely to be activated only in those cells where NICD levels are high (with transfection experiments or transduced cell lines in vitro). However, hi nuclear localization of NICD has been found in nuclei of various cell types, including cortical neurons and certain cancers, leaving a possibility that in these cells LEF1 is activated by non-canonical Notch signaling.

TERMINATION OF NOTCH SIGNAL

Several E3 ubiquitin ligases control Notch signaling by different negative regulatory mechanisms: F-box/WD repeat domain-comtaining protein 7 (Fbw7)/Sel10, promotes PEST-dependent NICD degradation in the nucleus; E3 ubiquitin-protein ligase Itchy homolog (Itch), regulates PEST-independent degradation of cytoplasmic Notch proteins; and Deltex (Lai et al., 2002). MAML, a Notch coactivator, can trigger proteasome degradation by recruiting Cyclin dependent kinase 8 (CDK8), which in turn is responsible for phosphorylation of activated nuclear Notch within the PEST domain that leads to recognition by Fbw7/Sel-10 and subsequent degradation (Fryer et al., 2004).

Itch can also negatively regulate cytoplasmic Notch by promoting NICD ubiquitination and endocytosis in cooperation with cytoplasmic protein Numb (McGill et al., 2009; McGill and McGlade, 2003). Numb, when overexpressed, antagonizes NICD activity by sorting of Notch1 through the late endosomes to lysosomes where it is degraded and its absence facilitates recycling of Notch1. Therefore it is suggested to be a regulator of Notch trafficking and degradation in a post-endocytic compartment (McGill et al., 2009).

Deltex, a transcriptional target of Notch, is a RING-finger E3 ligase. It leads Notch to ubiquitination by forming a ternary complex with Notch and β-arrestin homolog Kurz (Mukherjee et al., 2005). Deltex has also been shown to mediate Notch signaling. However, it is still not known what determines which function it will perform.

TARGET GENES

HES AND HEY

Hes and Hey genes are the primary targets of RBP-Jκ-dependent Notch signaling. Ubiquitously expressed, they are mammalian homologs of the hairy and enhancer-of-split (Hes) genes and hairy-related transcription factors (Iso et al., 2003). Out of seven Hes genes, Notch directly induces Hes1, Hes5 and Hes7 (Bessho et al., 2001; Ohtsuka et al., 1999). Hes family members have distinct patterns of expression in mice; Hes1 and Hes2 are expressed in various embryonic and adult tissues; Hes3 is expressed solely by cerebellar Purkinje cells; Hes5 is characteristic for nervous system; Hes6 regulates development of limbs in embryos.

Hey genes in mammals (Hey1, Hey2 and HeyL) are also direct targets of Notch signaling. They encode a subclass of hairy-related bHLH transcription factors (Maier and Gessler, 2000). They are

dynamically expressed throughout mouse development, specifically in processes as somitogenesis, neurogenesis, and cardiovascular development (Leimeister et al., 1999; Leimeister et al., 2000). Loss of Hey2 or Hey1/L combination is lethal causing a congenital disorder in the heart leading to cardiac failure shortly after birth (Fischer et al., 2007; Gessler et al., 2002).

OTHER GENES

Notch signaling is additionally inducing cell cycle regulatory genes (Myc, Cyclin D1 and p21) in a cell-type and context specific manner.

Cyclin D1 has been shown to be a Notch1 and Notch3 target in a triple-negative tumor cell line (Cohen et al., 2010) and to mediate the development of Notch1-induced mammary tumors (Ling et al., 2010).

NOTCH IN HUMAN CANCERS

Notch signaling has been implicated in several human cancers. Whether its ligands or receptors are deregulated it has shown an oncogenic role in numerous solid tumors: colorectal, renal, lung, pancreatic, endometrial cervical, mesothelioma, melanoma, prostate cancers, ovarian, osteosarcomas, gliomas and medulloblastomas (reviewed in Ranganathan et al., 2011).

Contrarily, a tumor suppressor function of Notch has been observed in several studies, firstly in skin (Rangarajan et al., 2001) and later in head and neck squamous cancers (Agrawal et al., 2011; Stransky et al., 2011) and in a subset of leukemias (Klinakis et al., 2011).

ONCOGENIC NOTCH SIGNALING

Altered Notch1 expression has been shown to cause a development of T-cell acute lymphoblastic leukemia (T-ALL) in humans (Ellisen et al., 1991; Pear and Aster, 2004). 56% of all T-ALL cases contained an activating Notch mutation. However less than 1% had the chromosomal translocation t(7:9)(q34;q34.3) which gives a constitutively active truncated form of the receptor thanks to which Notch 1 was discovered (Weng et al., 2004).

TUMOR SUPPRESSIVE NOTCH SIGNALING

NOTCH IN SKIN CANCER

Although considered oncogene, Notch1 has a tumor suppressor role in the epidermis. It prevents cell proliferation and differentiation in primary mouse keratinocytes by inducing p21WAF1/Cip1 expression, and deregulating expression of several differentiation markers (Rangarajan et al., 2001). Importantly, mice with a skin-specific ablation of Notch1 developed hyperplasia and had corneal epithelial proliferation, and eventually developed spontaneous basal cell carcinoma-like tumors. Notch1 deficiency also facilitated chemical-induced carcinogenesis in these

mice (Nicolas et al., 2003). Activated Notch was also shown to be important for *in vitro* maturation of human epidermis (Nickoloff et al., 2002).

Notch does behave differently in keratinocytes from other cell types, but it is unclear why. Possible explanation might lay in a dose-dependent action of Notch shown in the cervical cancer where moderate expression of activated Notch1 receptor caused transformation of cells and growth in soft agar, while high overexpression led the cells to growth arrest (Lathion et al., 2003). Applied to the skin, lower activation might be responsible for the transformation of keratinocytes together with other oncogenes, while higher levels would cause growth arrest by inducing a different transcriptional program involving p21 WAF1/Cip1.

NOTCH IN HEAD AND NECK SQUAMOUS CELL CARCINOMAS (HNSCC)

Head and neck squamous carcinoma is another example where Notch showed a tumor suppressive role. Notch1 is the second most mutated gene after p53 in these tumors, frequently both alleles are inactivated (Agrawal et al., 2011). Other genes involved in the keratinocytes differentiation were also reported mutated, such as Notch2, Notch3, and p63 (Stransky et al., 2011).

NOTCH IN CHRONIC MYELOMONOCYTIC LEUKEMIA (CMML)

Recently, it has been shown that several genes involved in signaling were targets of somatic inactivating mutations in myeloid leukemia, including nicastrin, MAML1 and Notch2. This supported the observation that inactivation of Notch signaling in mouse hematopoietic stem cells indeed induces a CMML-like disease (Klinakis et al., 2011).

NOTCH IN MAMMARY GLAND

NOTCH IN MAMMARY GLAND DEVELOPMENT

Role of Notch signaling in mammary gland has long been a subject of research since a Notch4 receptor was identified as an insertion site 3 (*int3*) of the mouse mammary tumor virus causing the development of mammary adenocarcinomas. However, different possible roles emerged from studies depending on whether they were performed in human or mouse tissue, *in vivo* or *in vitro*.

Notch activity in the mouse mammary gland was examined in two different Notch reporter mice (Yalcin Ozuysal et al., 2010, Lafkas et al., 2013); transgenic Notch reporter (TNR) mouse expressing EGFP downstream of SV40 promoter containing RBP-Jκ responsive element containing 4 tandem copies of RBP-Jκ binding sites, generated by N. Gaiano (Mizutani et al., 2007) and Hes1 reporter where EGFP gene was knocked-in downstream of endogenous Hes1 promoter (Fre et al., 2011)

From previous studies it is known that TNR mice show EGFP signal during puberty, the estrogen-driven part of a gland development. Signal was the highest in TEBs but also present in the

subtending duct. After puberty, GFP signal in mammary gland of the TNR mice was not detectable (Yalcin Ozuysal et al., 2010).

Hes1-EGFP mouse model showed Notch activity in ≈52% of the luminal and ≈4% of the myoepithelial cells, but also a stronger signal than the TNR mouse model (Šale et al., 2012). Reason for this discrepancy can be looked for in the fact that TNR promoter is artificial and therefore can show lower activity than the HES1 promoter which is one of the most prominent Notch target genes. Also, a higher number of cells and stronger expression of GFP might cause higher residual signal since half-life of GFP protein is ≈26 hours (Corish and Tyler-Smith, 1999).

Extensive study of putative mammary stem cells led to the discovery of the a sub-population of mouse mammary epithelial cells defined by its ability to efflux the dye Hoechst 33342 and called the side population (Goodell et al., 1997, Welm et al., 2002). Study by Clarke and colleagues showed that side population cells are able to form branching epithelial structures in 3D culture and are 30-fold enriched for mammosphere formation in suspension culture which is predicted to be a measure of stem cell self-renewal activity (Dontu et al., 2003). They also showed that these cells are enriched in ER and express Notch positive regulator Musashi1 (Msi1), suggesting active Notch signaling in the putative stem cell population but also in ER+ background (Clarke et al., 2004).

In human breast, Notch has been linked to self-renewal of human mammary stem cells (MaSCs) in the study by Dontu et al. where the link was assessed by mammosphere assay, an in vitro culture system that enriches for MaSCs based on their capability to proliferate in suspension as spherical cultures (Dontu et al., 2003). They showed that activated Notch signaling significantly enhances human mammosphere formation while abrogation of Notch via Notch4 antibody inhibits them. This suggested that activation of Notch via Notch4 receptor promotes MaSC self-renewal (Dontu et al., 2003, Dontu et al., 2004). Also, it has been shown that mammospheres have increased expression of Notch3 and Notch4. In an independent study Notch3 was additionally implicated in self-renewal and hypoxia survival in mammospheres (Sansone et al., 2007).

In the mouse mammary gland, early studies suggested that Notch suppresses ductal elongation and branching, as well as promotes development and differentiation of alveoli (Uyttendeale et al., 1998, Soriano et al., 2000, Smith et al., 1995).

Bouras et al. looked at the effect of Notch signaling MaSC in mouse ($CD24^{lo}CD29^{hi}$ (Shackleton et al., 2006)). In a short-term in vitro culture system, MaSC cells were genetically manipulated to overexpress activated NICD1 and engrafted into the mammary fat pad to observe repopulation potential. Results showed a formation of aberrant epithelial nodules that lack normal architecture and ability to differentiate into milk producing cells during pregnancy. Therefore, they proposed that constitutive Notch signaling promotes commitment of MaSCs to the luminal lineage but maintains these cells in an undifferentiated state. Given that Notch1 expression appears to be restricted to the

luminal populations, it is possible that this receptor is the primary mediator of luminal cell commitment in vivo (Bouras et al., 2008).

Transcriptome analysis of sorted populations from human mammary glands revealed differences in expression of particular Notch components, in particular cell types. Notch4 gene expression was highest in undifferentiated human clonogenic mammary progenitors and was then significantly down regulated when these cells became committed to the luminal lineage. Opposite pattern has been shown for Notch3 and to a lesser extent Notch1 and Notch2. Furthermore, blocking of Notch signaling in bipotent progenitors selectively prevented them from generating mature luminal progeny without affecting their ability to proliferate and generate mature myoepithelial cells, confirming that Notch activation can directly stimulate luminal cell fate specification (Raouf et al., 2008). Interestingly, the mammary gland appeared grossly normal in Notch3 and Notch4 knockout mice, suggesting that Notch1 and Notch2, or multiple Notch genes function redundantly to control cell fate specification, proliferation, and differentiation in this tissue (Raafat et al., 2010).

Targeted disruption of Notch expression or Notch signaling in the mouse mammary gland during pregnancy has also revealed that Notch signaling regulates alveolar cell maintenance (Buono et al., 2006, Raafat et al., 2009). As mentioned before, Elf-5 has been shown to play an important role in alveologenesis since. Elf-5 knockout mice exhibit complete failure of the alveologenesis (Zhou et al., 2005, Oakes et al., 2008) and biochemical study suggested that loss of Elf-5 leads to hyperactivation of the Notch signaling pathway, explaining in part the underlying molecular mechanism for the altered cell lineage decisions in Elf-5-null mammary epithelial cells.

NOTCH IN BREAST CANCER

NOTCH IN MOUSE MAMMARY TUMOR MODELS

Notch1 and Notch4 were originally identified through mouse mammary tumor virus insertion mutagenesis, as inserts that, constitutively active, cause development of mammary tumors. Further to this, several transgenic mouse models were generated to study the influence of Notch on the mammary gland tumorigenesis.

MMTV/Notch4IC and WAP/Notch4IC Models

Mouse transgenic model in which Notch4 was expressed via MMTV long termina repeats (LTR) or by the whey acidic protein (WAP) gene promoter was generated by Callahan and colleagues (Gallahan et al., 1996; Jhappan et al., 1992). MMTV/Notch4IC virgin mice showed hindered ductal growth while pregnant ones showed suppression of lobular development and lactation.

WAP/Notch4IC virgin mice developed normally, since WAP promoter is active only in secretory mammary epithelium (Burdon et al., 1991). Therefore, the lobular development and lactation in these mice was impaired.

Both models developed mammary adenocarcinomas that were poorly differentiated with 100% penetrance and lung metastasis in 100% of parous and ≈50% of virgin tumor bearing females (Gallahan et al., 1996).

MMTV/hNotch1IC (human) Model

Virgin mice bearing human NICD1 driven by MMTV LTR develop different mammary hyperplasia however DCIS was observed very rarely (Kiaris et al., 2004). Pregnant mice developed lactation dependent papillary tumors. These tumors were not invasive and also regressed with involution process, however tumors appeared in subsequent pregnancies were invasive and did not regress (Kiaris et al., 2004). To explain this, Efstratiadis suggested in his review the cause of regressing tumor might be accumulation of milk in the extralobular ducts obstructed by development of neoplasms (reviewed by Efstratiadis et al., 2007).

MMTV/Notch1ICD and MMTV/Notch3ICD Models

A mouse with Notch1ICD overexpressed by MMTV LTR (Hu et al., 2006) suffered from ductal hyperplasia and had impaired lobuloalveolar development as well as lactation impairment. Furthermore, mice developed invasive tumors at 7 to 10 months of age.

In the same laboratory, a mouse overexpressing Notch3ICD by MMTV LTR was developed. I exhibited similar phenotype and developed tumor with 9 months latency (Hu et al., 2006)

Tumor types in both mouse models were diverse and represented the full spectrum of differentiation from hyperplasia, in situ ductal carcinoma, glandular adenocarcinoma, to poorly differentiated adenocarcinoma. Their long latency and stochastic formation suggested that NICD1 and NICD3 overexpression is not sufficient to promote transformation and requires the action of other oncogenes or the inactivation of tumor suppressor genes.

RBP-Jκ Knockout Model

RBP-Jκ knock-out model was examined by different groups in different conditions. Buono et al. examined straight RBP-Jκ knock-out model concluding that there is no effect on the mammary gland during virginity, but in pregnancy, mammary epithelium thickens losing the luminal layer of cells and obtaining several layers of p63 positive basal cells (Buono et al. 2006). Analysis of the conditionally deleted RBP-Jκ via MMTV-Cre where deleted cells were followed by the expression of the EGFP reporter of Cre activity showed that during puberty and virgin adult stage epithelium overtly looks normal. However, its cellular composition is severely affected. Only myoepithelial cells with deletion

are able to stay in the epithelium, while luminal layer is repopulated with wild type cells (Yalcin Ozuysal et al., 2011)

Rafaat et al crossed RBP-Jκ conditional knockout model with WAP/*Int3* mouse. Their data suggests that deletion of RBP-Jκ has little or no effect to WAP/*Int3* tumorigenesis since the only effect was a slightly longer latency. The longer latency of primary and secondary tumor development in the Wap-Int3/Rbpj knockout mice could be due to the fact that these glands fully develop and are more differentiated than the Wap-Int3/Rbpj control mammary glands. They have also shown that sh-RNA mediated knockdown of RBP-Jκ in Hc11-*Int3* did not affect their growth in soft agar, confirming the previous *in vivo* results (Raafat et al., 2007).

NOTCH IN BREAST CANCER CLINICAL STUDIES

Generally, oncogenic activity of Notch in breast can be exerted either by overexpression of ligands and/or receptors, or by loss of negative regulator Numb while chromosomal aberrations involving Notch components in breast tumorigenesis have been rarely found.

Chromosomal Aberrations

Until recently, chromosomal translocations involving Notch were not identified in breast cancer except a single occurrence containing Notch2 locus. In a study involving 48 breast cancer samples Notch2 receptor was truncated due to the nonsense mutation in a PEST domain. Truncation was suggested to enhance Notch2 signaling (Lee et al., 2007). Robinson and colleagues reported a number of fusion gene transcripts caused by chromosomal rearrangements that they found in a panel of breast cancer cell lines and tumors. By transcriptome sequencing they identified 384 fusion proteins from 87 different cancers. Only 24 genes were found to be recurrent fusion partners and among them most often were members of the Notch family genes and microtubule associated serine-threonine kinase (MAST) family (Robinson et al., 2011).

Aberrant expression of Notch ligands and/or receptors

Overexpression of Notch receptors and/or ligands is the most often way in which Notch signaling is involved in the breast carcinogenesis.

Reedijk et al. examined levels of RNA in 50 breast cancer samples and found that high expression of Jag1, Notch1 or Notch3 correlated with increased mortality at 10 years. Additionally, they examined 192 patient samples to see how 5-years survival is correlated with the expression of ligands and receptors showing that higher expression of Jag1, Notch1 and Notch3 correlated with lower survival (Reedijk et al., 2005). The same group performed a study on 887 breast cancers which were lymph node negative to show that Jag1 expression was associated with reduced disease-free survival and basal breast cancer markers (Reedijk et al., 2008).

A study by Parr et al showed that Notch 1 and Notch2, when overexpressed could have different effects, meaning that Notch1 overexpression was associated with less differentiated cancers with poor prognosis while Notch2 expression correlated with good outcome suggesting a tumor suppressive role (Parr et al., 2004). Further studies supported this showing that ectopically expressed Notch2 in breast cancer cells induced apoptosis and inhibited growth (O'Neill et al., 2007) while Notch1 shown to be activated in a cohort of 9 patients with basal breast cancer (Lee et al., 2008b). Moreover, Notch 1 mRNA expression segregated with the basal cancer patients in a hierarchical database clustering of microarray database, and patients expressing Notch1 had drastically lower overall survival.

A connection between Notch and Ras was suggested in a study involving 7 DCIS samples analyzed by immunohistochemistry, where all 7 samples showed elevated Notch1 expression whereas adjacent ducts were reported negative. 4 samples additionally showed expression of Hras1. Further experiments showed that Notch1 expression up regulated by oncogenic Ras was necessary for transformation by Ras. Ras also showed to up regulate Notch ligand Dll1 and presenilin-1 (Weijzen et al., 2002).

An oncogene Myc has been implicated in the development of many human cancers including breast cancer (Escot et al., 1986; Scorilas et al., 1999). C-myc has been shown to be an important player of tumorigenesis induction in the NICD1 overexpressing mice, and is also a direct transcriptional target of Notch (Kinaki et al., 2006). Notch has also been shown to be linked with Myc in human breast cancers. A study on 125 primary breast cancer samples showed that 93% of NICD1 expressing carcinomas are also positive for Myc, suggesting cooperation in carcinogenesis (Efstratiadis et al., 2007).

Numerous additional targets of Notch linked to mammary tumorigenesis have been described such as a Notch activator peptidyl-prolyl cis-trans isomerase NIMA interacting 1 (Pin1) (Rustighi et al., 2009), and survivin (Lee et al., 2008a).

Aberrant expression of Notch modulators

Numb, an antagonist of Notch signaling has also been implicated in breast cancer (Guo et al., 1996). It is expressed in normal breast parenchyma. On the other hand, breast cancers had heterogeneous expression of this protein, and in almost 50% of the cases it was completely lost due to its polyubiquitinantion-mediated proteosomal degradation (Pece et al., 2004). Together with Notch1 accumulation, Numb loss was confirmed in ductal and lobular carcinomas (Stylianou et al., 2006).

However, loss of Numb should not be solely connected to Notch alterations since it has been shown that it inhibits degradation of p53 (Colaluca et al., 2008) and degrades zinc finger protein Gli1 (Gli1), a Hedgehog transcriptional target (Di Marcotullio et al., 2006).

Nicastrin is a component of the γ-secretase complex, and it has been shown to be elevated in 50% of breast cancers suggesting its role in the aberrant activation of Notch signaling in breast cancer (Filipovic et al., 2011).

P63

P63 is a homolog of the well-known tumor suppressor protein p53. Recently, it has become a subject of interest in the developmental biology and cancer biology field. Sequence and structural homology of p63 and p53 is remarkable, especially in the DNA binding domain which would suggest overlaps in target recognition specificity. For this reason p63 can bind to p53 response elements (p53REs) *in vitro* and *in vivo* (147). There are several p53 targets that are also regulated by p63 such as p21Waf2/Cip1, 14-3-3σ, MDM2, Bax, PERP, NOXA (reviewed in Westfall and Pietenpol, 2004). Furthermore, p63 can regulate transcription of genes p53 does not regulate. These genes are mostly involved in the DNA repair like *Rad51*, *BRCA2*, *mre11* and *Rad50* (Lin et al., 2009). P63 indeed targets a large number of genes identified by chromatin immunoprecipitation (ChIP) on chip analysis placing p63 in a key role of a broad transcription regulatory network involved in many biological processes (Pozzi et al., 2009).

GENE STRUCTURE

TP63 gene produces two groups of isoforms as a result of two promoters: the full length TAp63 group that has full-length transactivation (TA) domains and the ΔNp63 group with truncated N-terminal domains. Both groups comprise three different isoforms, named α, β and γ as a result of the alternative splicing at the C termini. Sterile alpha motif (SAM) domain, which is absent in p53, is present only in the α isoforms of p63 and it is responsible for protein-protein interactions in different processes such as transcriptional activation, focal adhesion and chromatin remodeling (reviewed in Westfall and Pietenpol, 2004). The TAp63 group, with TA domains homologous to the TA domain of p53, can activate multiple p53 target genes. ΔNp63, without the TA domain, was considered to function as a dominant negative molecule toward TAp63 (Yang et al., 1998). However, ΔNp63 isoforms contain a transactivation domain on their N-termini allowing them to transactivate p53 targets (Helton et al., 2006, Dohn et al., 2001). Therefore, these six isoforms create a complex transcriptional network of independent and/or overlapping target genes that are either activated or antagonized by the p63 activity.

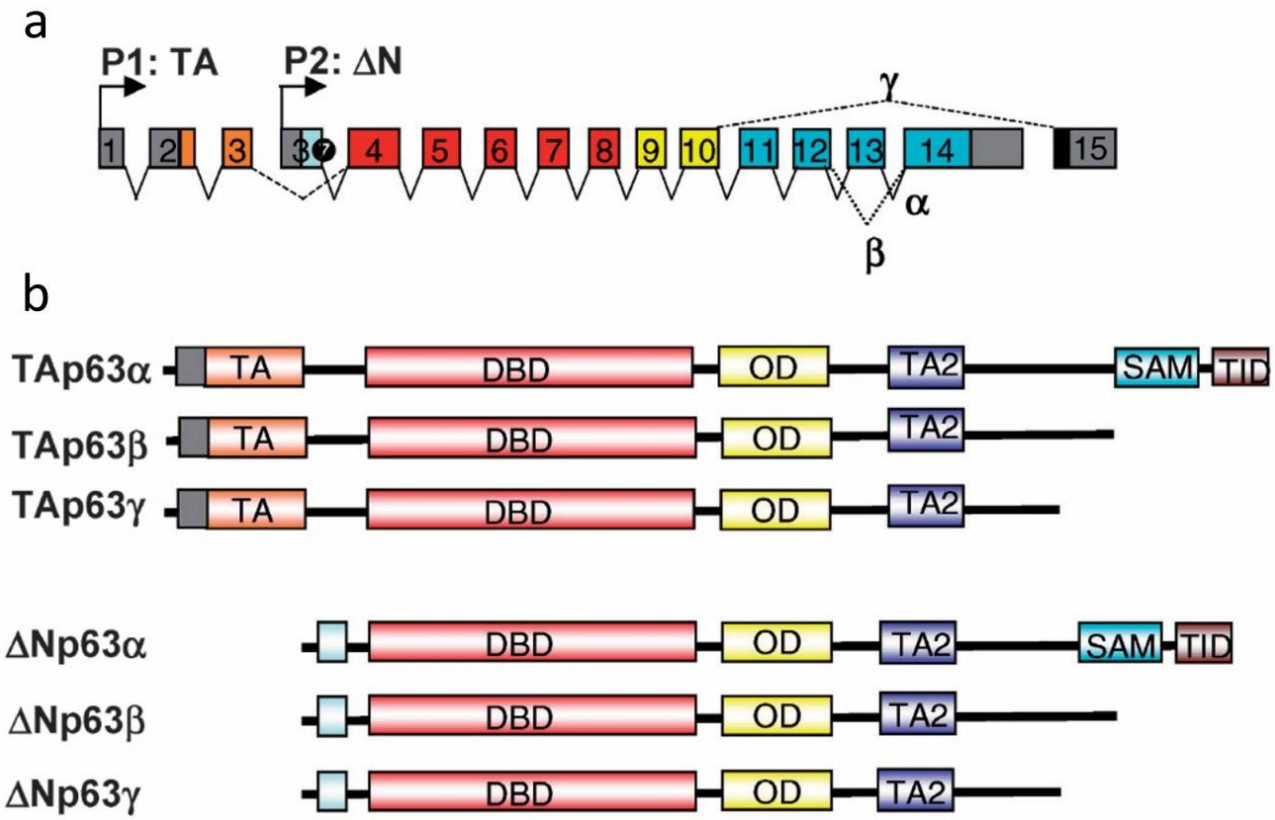

Figure 11. p63 gene structure and transcripts*. a) Scheme of the intron- exon structure, showing two transcription initiation sites (P1 and P2) and alternative splicing route. b) Structure of p63 gene: P1 and P2 alternative promoters drive transcription of transactivating (TA) and N-terminally truncated (ΔN) isoforms. Variants α, β and γ arise from the alternative splicing at the 3' end of the gene. Present domains are transactivation domain (TA), DNA-binding domain (DBD), oligomerization domain (OD), second transactivation domain (TA2), sterile α motif (SAM) and transinhibitory domain (TID). Adapted from Candi et al., (2008)*

P63 IN DEVELOPMENT

First interest for p63 was raised for its indispensable role in epithelial development. Two knockout mice were produced by two independent groups; however, the different targeting construct caused different effects on p63 expression resulting in quite different phenotypes. Developmental aberrancies were identical in both cases but the interpretation of the function of p63 differed significantly.

P63 deficient mice died one day after birth exerting severe effects in epithelial, craniofacial and limb development. Epithelial tissues affected severely were skin, prostate, mammary gland and urothelium (Mills et al., 1999, Yang et al., 1999). Mills et al concluded p63 is essential for lineage commitment and differentiation because their mouse had an unstratified single cell layer epithelium that covered the body surface, tongue, and oral cavity lacking differentiation markers (Mills et al., 1999). On the other hand, a mouse produced by Yang et al had clumps of differentiated cells in the epidermis, suggesting that p63 has a crucial role in the maintenance of the stem/progenitor cells in the epithelium (Yang et al., 1999)

Later, transgenic mice expressing only ΔNp63α or TAp63α via K5 promoter were crossed into p63 deficient background to generate mice expressing ΔNp63α and/or TAp63α in the epidermis. $p63^{-/-}$; ΔNp63α mice developed an epidermal basal layer as a rescued phenotype, while the $p63^{-/-}$; TAp63α's mice were not able to revert deleterious effect of the p63 deficiency. Co-expression of ΔNp63α and TAp63α had a rescue effect on the tissue suggesting that ΔNp63α is indispensable for retaining the progenitor cell population in the basal layer whereas TAp63α acts synergistically or subsequently to control epithelial development. The same study showed that while ΔNp63α was responsible for regulation of expression of basal epidermal genes such as K14, TAp63α affected the expression of differentiation markers Ets1, keratin 1, transglutaminases, and involucrin (Candi et al., 2006).

A study on *ΔNp63*-null mice further demonstrated the important role of ΔNp63 in epithelial development and differentiation (Romano et al., 2012). *ΔNp63*-null mice exhibited a developmental defective phenotype similar to the phenotype of *p63*-null mice, some keratinocytes managed to form a basal cell layer and patches of stratified epithelium prematurely expressing terminal differentiation markers. Therefore, ΔNp63 is indispensable in epithelial development, specifically in embryonic epidermis. Contrarily, TAp63 is not since *TAp63*$^{-/-}$ mice survived after birth and had median lifespans of 333 days. But they exhibited multiple signs of premature aging such as ulcerated wounds and blisters in the skin suggesting a role of TAp63 isoforms in regulation of proliferation of epidermal and dermal precursor cells after embryogenesis (Su et al., 2009)

In normal tissue, it has been shown that p63 is highly expressed in the basal and suprabasal cells of stratified and glandular epithelia in foreskin, tonsil, breast, cervix, vaginal epithelium, esophagus, prostate, and urothelium. Expression of p63 decreases with differentiation, and disappears once the cells are terminally differentiated (Yang et al., 1998, Nylander et al., 2002, Reis-Filho et al., 2002).

P63 IN MAMMARY GLAND

p63 knockout mice exhibited a phenotype of a complete absence of mammary gland in embryo (Yang et al., 1999, Mills et al., 1999). This point raised an interest for the p63 in the mammary gland field. In the mammary gland, the basal/myoepithelial cells express high levels of p63. Already in the embryonic stage p63 is strongly expressed in the outer layer of the mammary bud and less in the inner mass, while in the adulthood it is restricted only to basal layer of mammary epithelial bilayer. The function of basal/myoepithelial cells and their role in cancer and development are still not well understood. They mediate the interaction between luminal cells and the extracellular matrix, providing primarily structural support and contractility during lactation. In addition, they have been shown to contribute to the suppression of breast cancer cell growth, invasion and angiogenesis (Deugnier et al., 2002, Sternlicht et al., 1997);

Basal/myoepithelial cells are characterized by high levels of expression of integrins and extracellular matrix (ECM) proteins absent in the luminal cell population, further supporting a fundamental role for p63 in the biology of this cell type.

Furthermore, p63 is selectively expressed in a subset of highly aggressive breast cancers (15%) that exhibit a basal phenotype and have a poor clinical outcome (Sorlie et al., 2003, Sorlie et al., 2001, Perou et al., 2000). p63 expression can affect expression of many of the genes characteristics of this tumor type. These include cell adhesion proteins and ECM components such as laminin γ2 and α3 chains, fibronectin and β4- and α6-integrin as well as EGFR (Nielsen et al., 2004).

Yalcin Ozuysal study showed a clear link between loss of p63 and loss of basal phenotype in CD10+ sorted primary human mammary epithelial cells. Human basal cells in culture proliferate faster and tend to retract and scatter. Luminal cells, on the other hand form sheets with indistinct cell boundaries and are able to proliferate for significantly less passages. Depletion of ΔNp63 in basal cells resulted in lower density of growth of the cells, and decreased proliferation. Furthermore, basal markers (CK14 and ITGα6) decreased while luminal ones (CD24 and CK18) increased. Ectopic expression of ΔNp63 in luminal cells resulted in change of phenotype of cells in culture, resembling more to basal ones. Additionally, proliferation increased as well as CK14 and ITGα6 while luminal markers CD24 and CK18 decreased. Therefore, ΔNp63 has shown to be essential for the maintenance of the basal cell fate, and as discussed previously, it is negatively regulated by Notch signaling. Mammary gland reconstitution experiments *in vivo* showed that MMECs ectopically expressing ΔNp63 were unable to participate in the luminal layer of the reconstituted mammary ductal system confirming incompatibility of the ΔNp63expression with luminal cell fate (Yalcin Ozuysal et al., 2010).

p63 AND CELL ADHESION IN MAMMARY EPITHELIAL CELLS

Beyond a critical function in the epidermis, p63 is essential for the development of other stratified epithelia, such as mammary gland epithelium. In order to find the endogenous functions and biological activities regulated by p63, the effects of loss or gain of p63 expression have been examined in a study from Caroll et al.2006. Down regulation of ΔNp63 isoforms in the MCF10A immortalized myoepithelial/basal-like epithelial cell line, or in mouse primary mammary epithelial cells, led to cell detachment and subsequent apoptosis, while reduction of the TAp63 had no or very little effect on the cells. Additionally, up regulated expression of both isoforms protected cells from death induced by detachment of cells from matrix, suggesting that ΔNp63 isoforms are key players for normal cell-matrix adhesion and survival in epithelial cells *in vitro* (Carroll et al., 2006).

Transcriptional profiling showed that many of the adhesion genes that were reduced when p63 was down regulated using short hairpin RNAs (shRNAs) displayed reciprocal up regulation upon p63 overexpression (Carroll et al., 2006). These included integrins α6 and β6, laminin α3, γ2, γ3, several collagens, fibronectin, two cadherins, the collagen receptor DDR1, MCAM and NCAM, plakoglobin and δ

catenin suggesting that cell adhesion is indeed regulated by ΔNp63. Furthermore, α3 integrin, a component of the laminin receptor, is a p63 target gene suggesting a novel crucial role for p63 as a critical regulator of epithelial cell adhesion (Kurata et al., 2004).

CHAPTER II: **AIM OF THE THESIS AND RESULTS**

AIM OF THE PROJECT

Notch signaling via RBPjκ has been implicated as an important player in the development of the mammary gland, in particular in luminal cell fate determination, but also in breast carcinogenesis. Increased expression of Notch signaling components has been linked to poor prognosis and its aberrant activation has been connected to triple negative breast cancer, a subtype that presents the worst prognosis for patient survival because of its aggressiveness and lack of available targeted therapy. Recent work from our laboratory demonstrated the importance of Notch signaling during differentiation processes in the mammary gland (Yalcin Ozuysal et al., 2010). Specifically, the transgenic Notch reporter mouse model (RBPjκ-Cre reporter mouse) indicated that Notch signaling was only activated during pubertal development in the subpopulation of PR-expressing luminal cells, suggesting the importance of Notch signaling in the differentiation of HR positive cells. In addition, the expression of p63, factor important for the maintenance of the basal characteristics of the mammary epithelial cells, was antagonized by activation of Notch signaling. Since a recent report suggested that mammary stem cells also have basal cell properties (Prater et al., 2014), we hypothesized that p63 expression might be important for the maintenance of stem cell properties in the basal compartment.

The role of Notch signaling in the luminal cell fate determination *in vivo* still remains poorly understood. Therefore my thesis project aimed to elucidate the role of Notch signaling during mammary gland development.

My project is constituted of two specific aims.

Specific aim 1: To investigate the role of Notch signaling in the regulation of HR+ population of luminal mammary epithelial cells.

To dissect the role of Notch signaling in HR+ luminal mammary epithelial cells, I will use the following models:

1. The transgenic Notch reporter mouse (TNR) to determine the localization of Notch active cells within the epithelium and track its progeny during mammary gland development thanks to GFP expression. Using this model, I will check the preliminary results obtained by Ozden Yalcin Ozuysal during puberty and additionally include adult virgin and pregnant stages into the analysis. The Notch active population will be defined by immuno-fluorescent co-staining for GFP and both ER and PR as well as basal marker p63.
2. RBP floxed WNT4Cre mTmG model (Han et al., 2002; Shan et al., 2010; Muzumdar et al., 2007) to analyse the effect of the conditional deletion of RBP, a Notch signaling mediator, in WNT4 expressing subpopulation of HR positive cells in the mammary gland. Expression of WNT4Cre-reporter gene with mTmG can be detected 3 days after birth when mTomato-expressing cells will be recombined to express GFP.

3. RBP floxed MMTVCre mTmG model (Han et al., 2002; Wagner et al., 2001; Muzumdar et al., 2007) to delete RBP in the entire mammary gland epithelium soon after birth and analyse the effect of RBP deletion in the entire mammary gland. This model was used by Ozden Yalcin Ozuysal in her study on antagonistic role of Notch on p63 expression (Yalcin Ozuysal et al. 2010).

4. RBP floxed AdenoCre mTmG mouse model to abrogate Notch signaling in the mammary epithelium at a specific time point. In this model, an adenovirus expressing Cre-recombinase (AdenoCre virus) is directly injected into the mammary gland lumen via cleaved nipple to induce recombination of floxed cells.

5. T47D and MCF7 HR+ breast cancer cell lines to test the hypothesis that Notch signaling inhibition and activation can influence expression of hormone receptors as downstream targets.

Specific aim 2: To interrogate the involvement of p63 in stem cell activity in mammary gland epithelium.

To test p63 involvement in mammary stem cell activity, I would have perform serial transplantation of p63 heterozygous knock-out mammary epithelium. .I couldn't use homozygous knock-out mice for p63 as these mice develop severe developmental defects such as lack of stratified skin, lack of epidermal appendages including mammary gland, severe craniofacial defects and they die immediately after birth (Yang et al., 1999, Mills et al., 1999). However, during the course of my studies, this hypothesis was addressed by the Kang laboratory (Chakrabarti et al., 2014) and therefore the project was discontinued after the experiments presented in the result section.

AIM1: ROLE OF NOTCH SIGNALING IN THE MOUSE MAMMARY GLAND

ENDOGENOUS NOTCH ACTIVITY IN THE MOUSE MAMMARY GLAND (TRANSGENIC NOTCH REPORTER MOUSE MODEL)

INTRODUCTION AND WORKING HYPOTHESIS

Notch signaling via RBP-Jκ has been implicated in luminal cell fate determination in several studies described in the introduction (Bouras et al., 2008; Raouf et al., 2008; Yalcin Ozuysal et al., 2010).

To follow Notch activity in mouse mammary gland, I used the TNR mouse model that has an EGFP transgene downstream of a basal SV40 promoter containing four Rbp-Jκ responsive elements and. Therefore, EGFP expression faithfully reflects Rbp-Jκ activity as previously shown in the nervous system (Mizutani et al., 2007) and mammary gland (Yalcin Ozuysal et al., 2010). The expression of EGFP reporter of Notch activity in TNR mammary glands has been correlated with increased expression of the Notch targets Hes1, 5 and Hey 1 in these epithelial cells expressing EGFP reporter of Notch activity. In the study conducted by Ozden Yalcin Ozuysal, she showed that in pubertal mammary glands, EGFP is mostly expressed in the terminal end buds (TEBs), the highly proliferative enlarged ductal tips, as well as in the subtending ducts. In adult virgin glands and during puberty, not any EGFP signal was detected. Flow cytometry analysis of pubertal TNR mammary glands showed EGFP expression in luminal compartment of the mammary epithelium (Yalcin-Ozuysal et al., 2010). Coimmuno-staining of EGFP and PR on pubertal glands showed that EGFP is widely colocalizing with PR expression suggesting that EGFP expressing cells represent a subpopulation of PR expressing cells.

Therefore we hypothesize that Notch signaling is activated in a subpopulation of luminal hormone receptor positive cells.

Using this mouse model, I firstly confirmed the results of Ozden Yalcin Ozuysal and then I expanded the analysis on both adult virgin and pregnant stages of mammary gland development using a novel tissue clarification technique for wholemount analysis and more accurate combination of surface markers for flow cytometry analysis (CD24 and CD49f). Furthermore, Ozden Yalcin Ozuysal distinguished 4 different subpopulations of mammary epithelial cells by FACS (using the CD24 cell surface marker) separated by type (luminal and basal) and Notch activity (Notch+ and Notch-). We analyzed and validated by RT-qPCR the microarray analysis data from the global gene expression performed on these 4 cell groups.

RESULTS

Notch signaling activity in the mammary epithelium of TNR mice.

Ozden Yalcin Ozuysal showed that Notch signaling activity, reported by expression of EGFP in TNR mice, is present during puberty while during adult virgin stage, she couldn't register any signal (Yalcin-Ozuysal et al., 2010).

The impossibility to detect a possible low signal in adult and pregnant gland could be due to the auto-fluorescence of the fatty stroma shown in the green channel (488 nm). For this reason, I used a new tissue clarification technique: TNR mouse mammary glands from 3 pubertal (6 weeks of age), 3 adult virgin (13 weeks of age) and 3 pregnant (P8.5) mice were firstly clarified in 50% glycerol (Landua et al., 2009) and then reanalyzed by fluorescent stereomicroscope. As previously shown, in the pubertal mammary epithelium, a strong EGFP signal was localized in the TEBs and a weaker one in the subtending ducts (Figure 12.a, b). However now, in adult virgin (Figure 12.c, d) and pregnant mammary glands (Figure 12.e, f), I was able to detect a weak signal throughout the whole ductal system.

By epifluorescence, the intensity of EGFP signal in TEBs of pubertal mammary glands was stronger than in mature ducts of pubertal, adult virgin and pregnant mammary glands. Unlike bilayered mature ducts, TEBs are multilayered structures; hence the stronger EGFP intensity might be due to a higher number of EGFP positive cells per area or stronger EGFP expression per cell. To distinguish between the two possibilities, we performed FACS analysis of pubertal (Figure 13.d,e,f), adult virgin (Figure 13.g,h,i) and pregnant (Figure 13.j,k,l) mammary epithelium. Luminal and basal mammary epithelial cells have been distinguished by flow cytometry according to the expression of the cell surface markers CD24 and CD49f (Stingl et al., 2006) in which I analyzed the expression of EGFP. The presence of EGFP positive population was detected in both in luminal and basal compartment of mammary epithelium in all examined stages of mammary development. The number of Notch active cells was constant in the basal compartment throughout the stages of development (Figure 13.m). In the luminal compartment, as expected, the highest number of EGFP positive cells was present during pubertal development (11,2%±2,7) while during adulthood (1,6%±0,2%) and pregnancy (2,5%±0,2%), the levels were significantly lower (Figure 13.m).

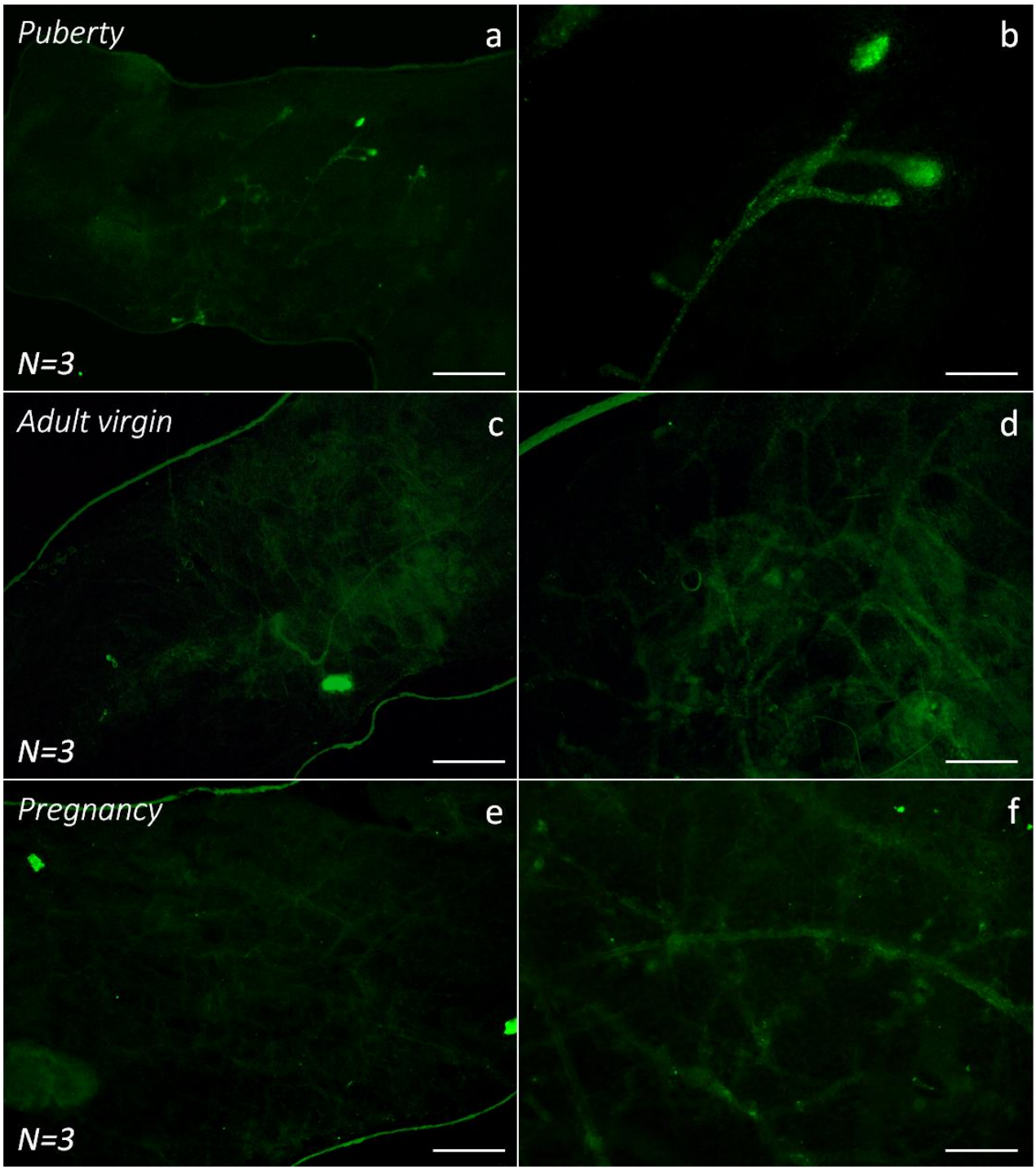

Figure 12. Notch activity in mammary gland. *Fluorescence whole mount analysis of the mammary glands from Transgenic Notch Reporter mice in a) and b) pubertal 6-weeks-old mouse; c) and d) adult virgin 13-weeks-old mouse; e) and f) P8.5 day pregnant mouse. Scale bars: In a), c) and e) scale bar represents 2,5mm and in b), d) and f) 500 µm.*

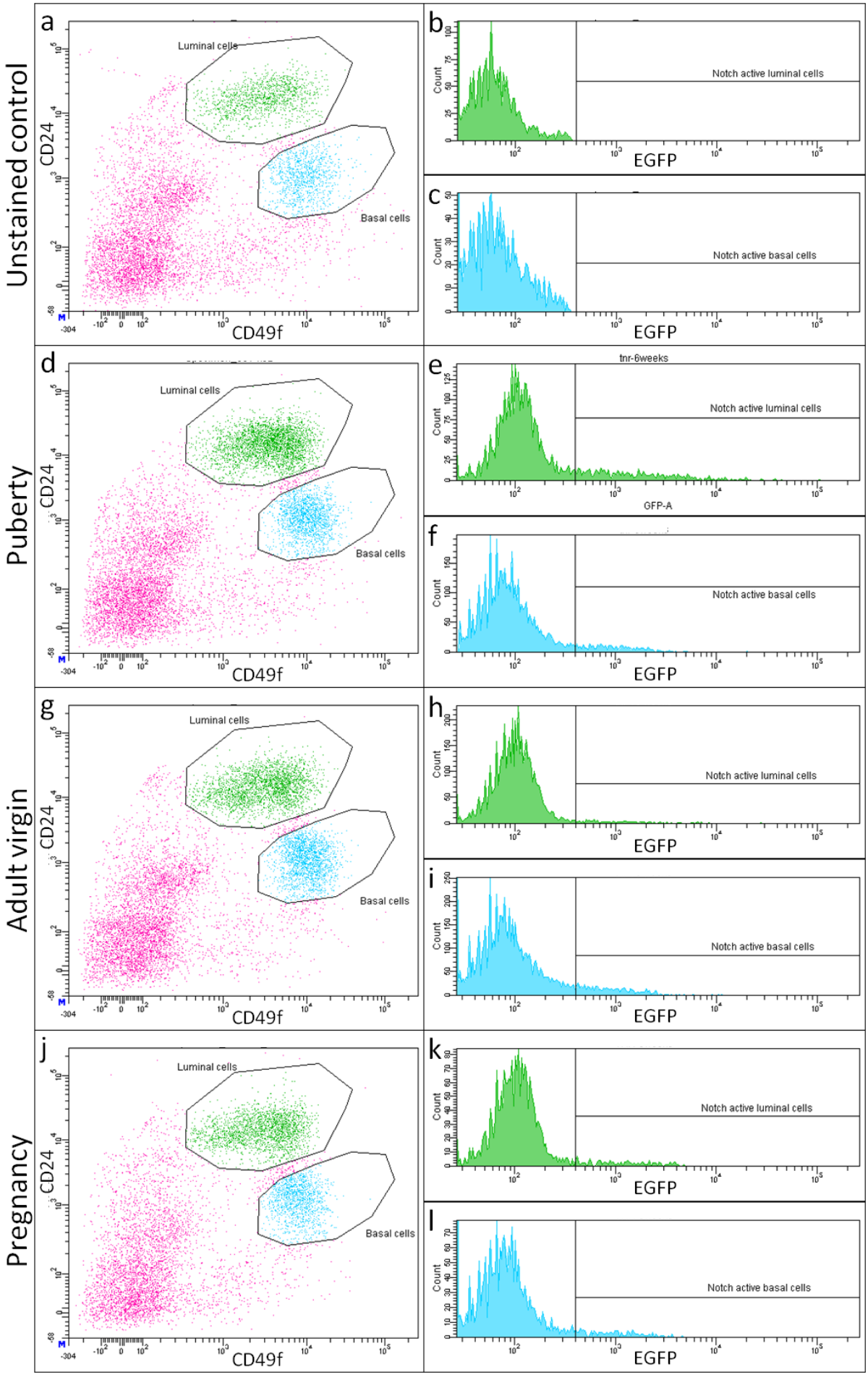
Unstained control
Puberty
Adult virgin
Pregnancy
a
b
c
d
e
f
g
h
i
j
k
l
Luminal cells
Basal cells
CD24
CD49f
Count
EGFP
GFP-A
Notch active luminal cells
Notch active basal cells
tnr-6weeks

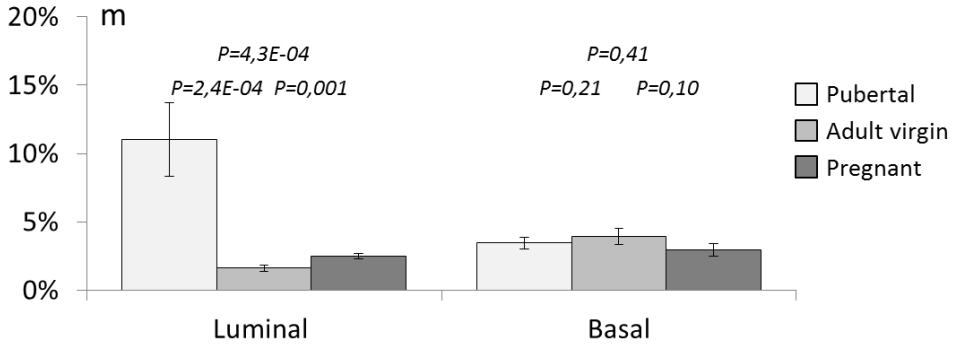

Figure 13. EGFP levels in the basal and luminal epithelial cells. *FACS analysis of the mammary epithelium from TNR mice. a, b, c) EGFP negative mammary epithelium; d, e, f) pubertal TNR mammary epithelium (N=3); g, h, i) adult virgin mammary epithelium (N=3); j, k, l) pregnant (P8,5) mammary epithelium. Panels a, d, g and j represent dot plots showing signal from the CD24 marker on the x-axis and signal from the CD49f marker on the y-axis. Luminal cells are gated, marked in green and plotted for EGFP signal in panels b, e, h and l. Basal cells are gated, marked in blue and plotted for EGFP in panels c, f, I and l. m) Bar graph showing percentage of Notch active cells within luminal and basal population in pubertal (N=3), adult virgin (N=3) and pregnant (N=3) TNR females.*

In order to confirm the hypothesis that Notch signaling is active in the portion of HR positive cells, Immunofluorescent co-staining with anti-EGFP, anti-ER and anti-PR antibodies of paraffin sections from pubertal (Figure 14), adult virgin (Figure 15) and pregnant mammary glands (Figure 16) was performed on. The quantification was done according to the following parameters: one gland from 3 age-matched mice per developmental stage group was used; mice from the same developmental stage were from different litters; 2 sections from each gland were entirely scanned; and all the ducts present on a section were taken into account.

Quantification of the sections from pubertal mammary glands showed that the portion of HR+ cells in the entire epithelium, was comparable with 33,5%±3,3% of the cells positive for ER and 35,4%±1,1% of the cells positive for PR (Figure 14.m). 93,7%±3,8% of the Notch active (EGFP positive) cells expressed the ER and 96,4%±1,8% the PR (Figure 14.n). 21,7%±7,4% of the ER+ cells and 30,6%±7,4% of the PR+ cells were detected GFP+ (Figure 14.o)

The portion of HR+ cells in the epithelium of pubertal mammary glands, defined by ER or PR stainings, was comparable (33,5%±3,3 for ER; 35,4%±1,1 for PR). The vast majority of Notch active (EGFP positive) cells was expressing both ER (93,7%±3,8) and PR (96,4%±1,8) and roughly one quarter of all HR positive cells were Notch active (21,7%±7,4 by ER; 30,6%±7,4 by PR) (Figure 14. m,n,o).

To determine if Notch activity was restrained to the luminal compartment, immunofluorescent co-staining with EGFP and p63 (a basal marker) antibodies was performed on pubertal mammary gland sections. None of the p63 positive glands showed EGFP expression (Figure 14.i-l).

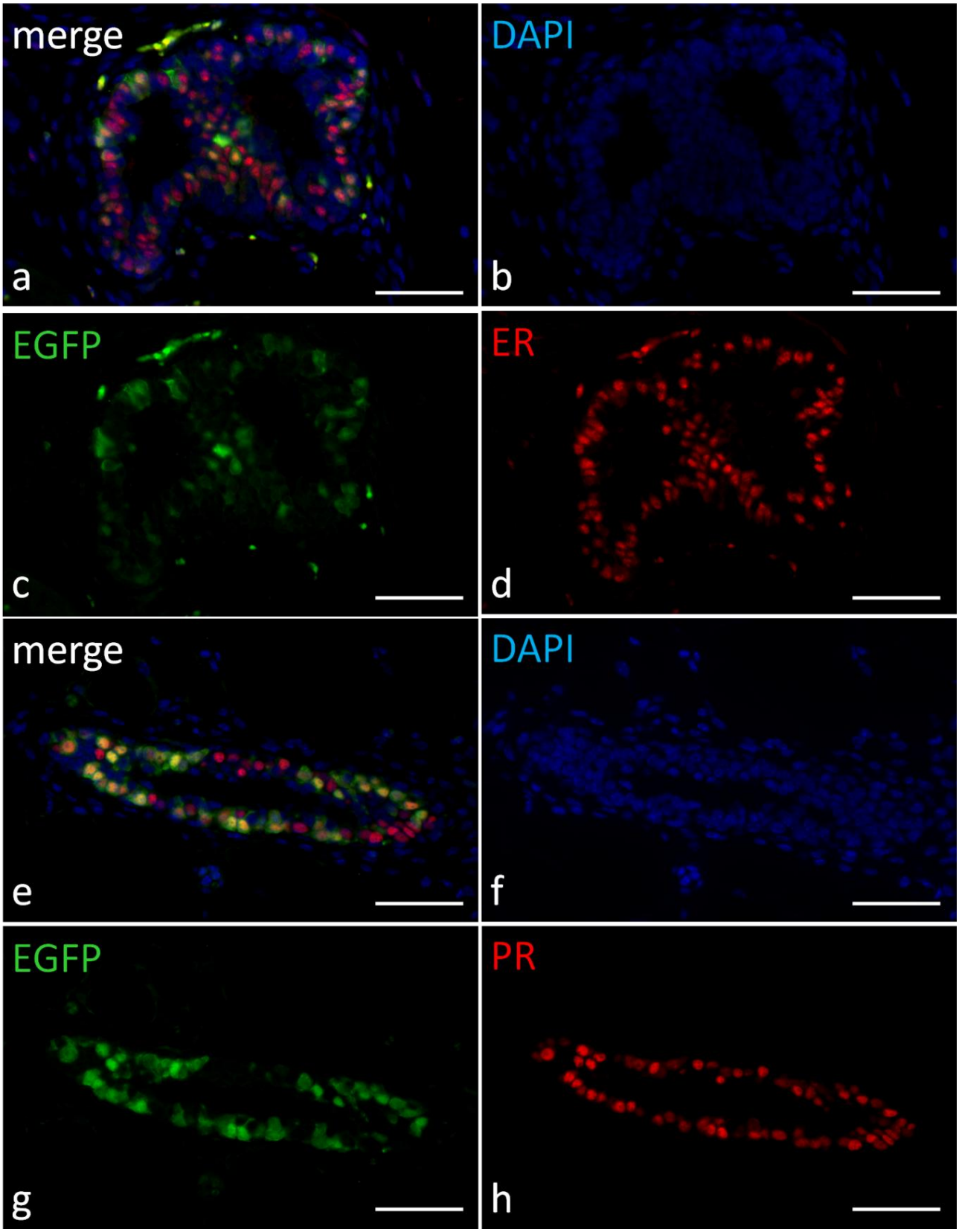
merge
a
DAPI
b
EGFP
c
ER
d
merge
e
DAPI
f
EGFP
g
PR
h

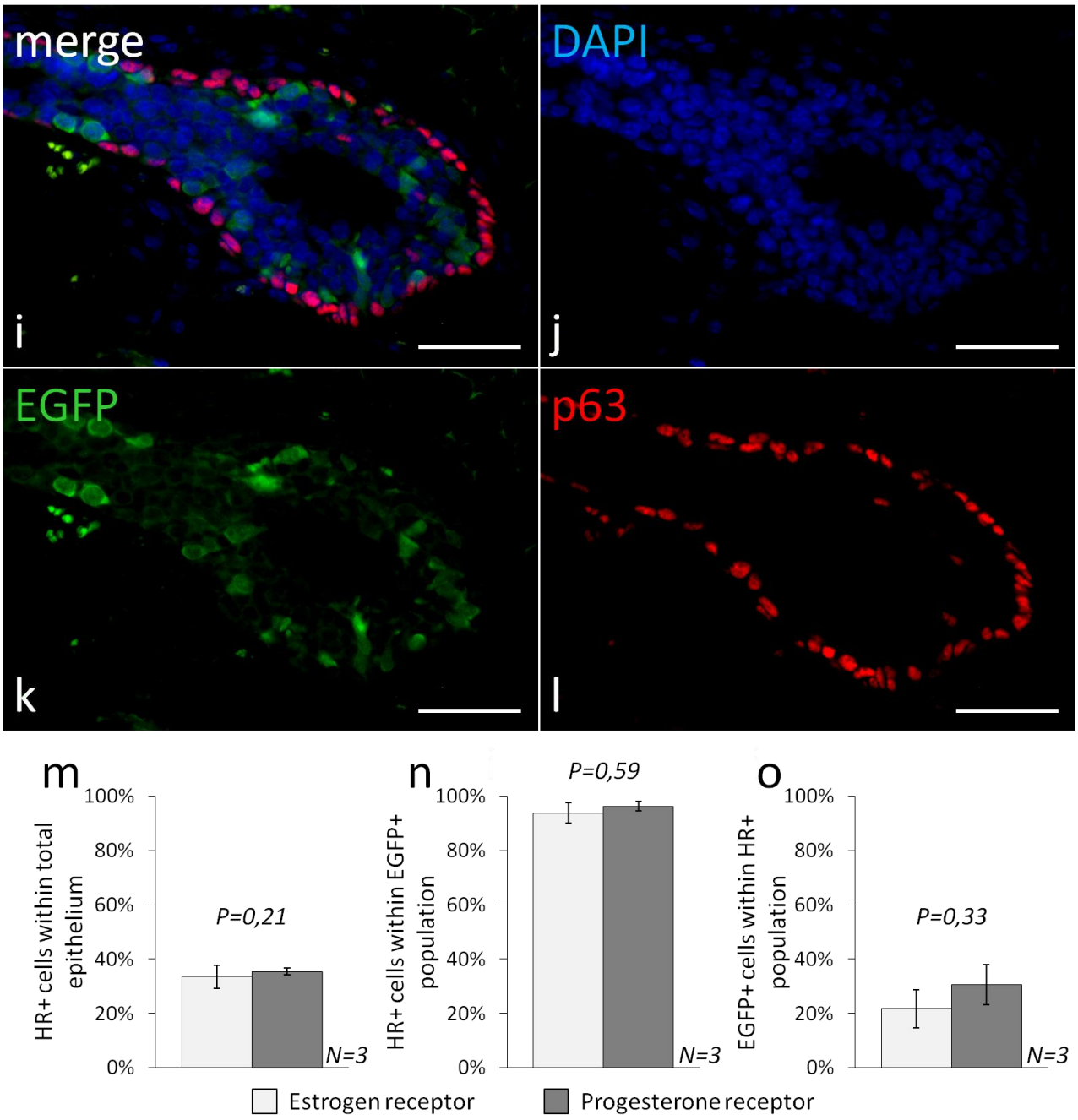

Figure 14. Colocalization of ER/PR/p63 and EGFP reporter of Notch activity in 6-weeks-old mouse mammary gland*: a) – d) Co-staining for EGFP and ER protein; e) – h) Co-staining for EGFP and PR protein; i) - j) Co-staining for EGFP and p63 protein; a) –l) scale bar represents 50µm; m) Bar graph showing portion of HR positive cells in mammary epithelial cells (N=3); j) Bar graph showing portion of Notch active (EGFP positive) expressing ER or PR (N=3); k) Bar graph showing portion of HR positive cells that are Notch active (EGFP positive)(N=3). Scale bars in a-l) represent 50 µm*

Immunostaining of adult virgin (Figure 15) and pregnant glands (Figure 16) did not show any Notch active cells in these glands.

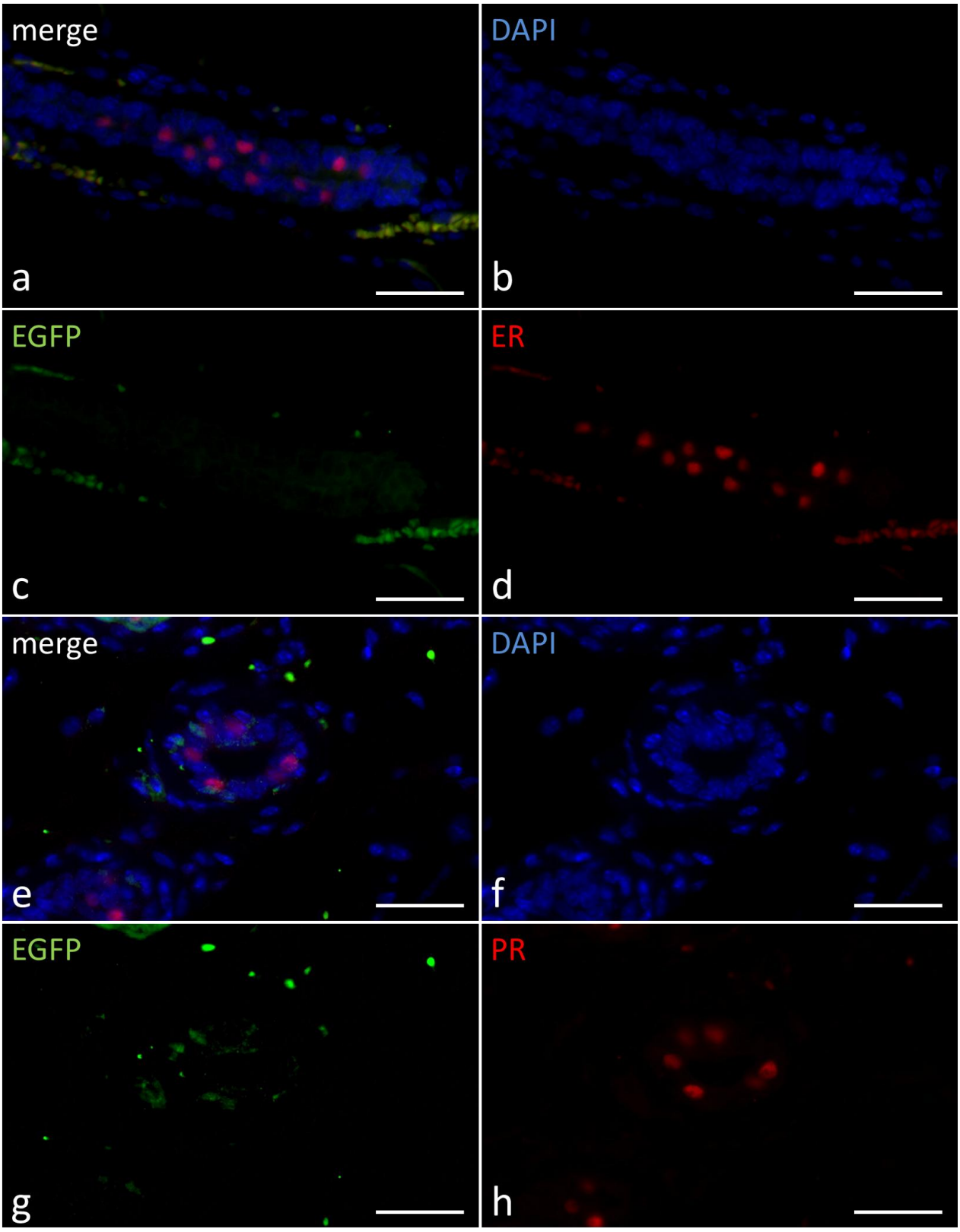

Figure 15. Colocalization of ER/PR and EGFP reporter of Notch activity in 13-weeks-old mouse mammary gland*: a) – d) Co-staining for EGFP and ER protein (N=3); e) – h) Co-staining for EGFP and PR protein (N=3); Scale bar represents 50µm.*

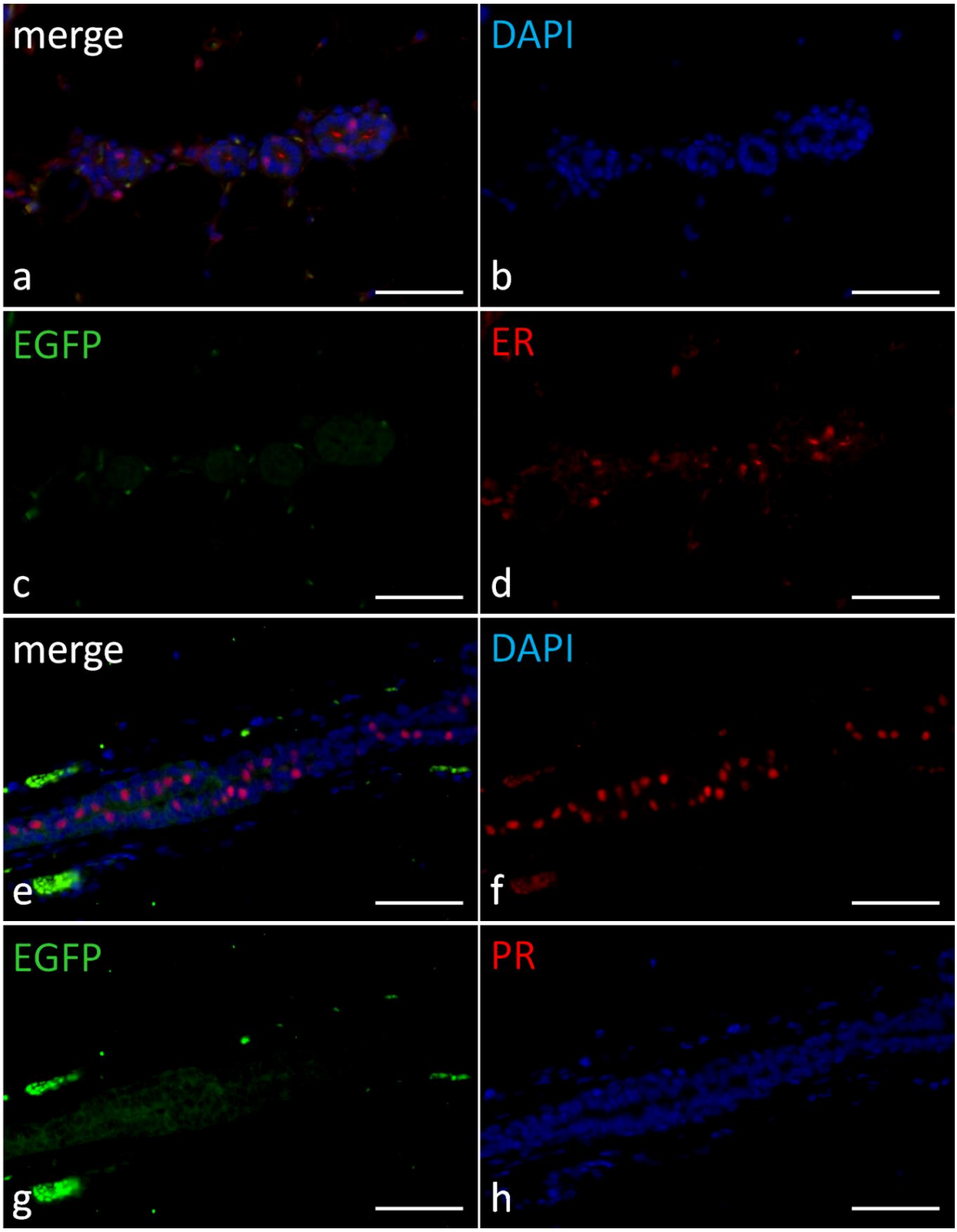

Figure 16. Colocalization of ER/PR and EGFP reporter of Notch activity in mouse mammary gland from 8,5 day of pregnancy: *a) – d) Co-staining for EGFP and ER protein (N=3); e) – h) Co-staining for EGFP and PR protein; Scale bars in a-h) represent 50 μm*

Gene expression profiles of the 4 epithelial subpopulations: luminal Notch active, luminal Notch inactive, basal Notch active and basal Notch inactive.

To further characterize which genes are differentially expressed in Notch active cells, a global gene expression was recorded in pubertal Notch active mammary epithelial cells. Technical part of this experiment was performed by Ozden Yalcin Ozuysal. For the global gene expression microarray Ozden prepared 3 groups of 18 TNR mice. 4 glands per mouse were collected and single epithelial cells were prepared. Epithelial cells were sorted by type (based on the expression of the CD24 marker) and by Notch activity (based on EGFP expression). From 4 populations of sorted cells (luminal Notch$^-$, luminal Notch$^+$, basal Notch$^-$, basal Notch$^+$) RNA was extracted, reversely transcribed to cDNA and used for the global gene expression microarray by Affymetrix GeneChip technology.

Microarray data were analyzed by hierarchical clustering using all differentially expressed genes (P<0,05). Luminal Notch active (EGFP+) population from two samples clustered with luminal Notch inactive (EGFP-) population from the same two samples. Basal Notch active (EGFP+) population from two samples clustered with basal Notch inactive (EGFP-) population from the same, suggesting that one of the samples was not sorted properly (Figure 17).

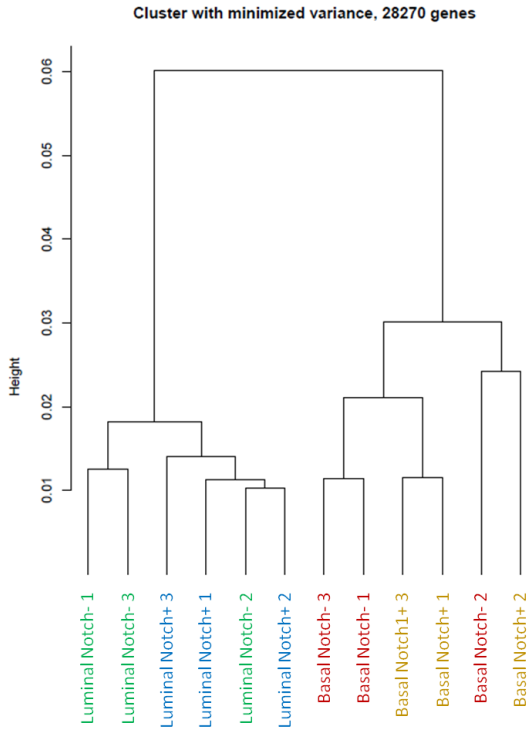

Figure 17. Analysis of the microarray gene expression data by hierarchical clustering. *Dendogram obtained by hierarchical clustering analysis of the 4 populations of mammary epithelial cells (luminal (CD24hi) Notch active, luminal Notch inactive, basal (CD24lo) Notch active and basal Notch inactive) sorted from 3 independent groups of mice, taking only the all the significant genes according to the adjusted p-value, among all annotated genes. This aims to illustrated samples that are close by Ward's minimum variance method.*

RNA from valid two samples used for microarray completed with the third new sample sorted under the same conditions were used for quantitative PCR to test for the expression only of genes characteristic for different cell types in the mammary epithelium, Notch target gene HEY1 and EGFP, Notch activity reporter.

To validate the purity of the sorted populations (luminal vs. basal), we first tested the expression of basal markers (Smooth muscle actin (SMA), p63 and keratin 14) in all 4 populations. The analysis confirmed that SMA (Figure 18.a) and keratin 14 (Figure 18.c) are significantly enriched in both basal Notch active (SMA:159,3±50,2; K14: 7,86±1,85) and basal Notch inactive populations (SMA:275,6±107,7; K14: 6,5±1,13). The transcription factor p63 (Figure 18.b) was significantly enriched in the basal Notch inactive (p63: 336,5±188,6) population but not in the basal Notch active one (p63:55,3±36,5). This result is in line with previous results published by Yalcin Ozuysal et al that showed that Notch signaling is antagonizing the expression of p63 and reducing basal cell characteristics. In line with this is also the observation that the amount of smooth muscle actin is significantly reduced in basal Notch active population when compared to basal Notch inactive population.

To check that the EGFP expression really reflect the activation of the Notch signaling pathway, we analyzed the expression of EGFP and of the Notch target gene HEY1 in all 4 populations. EGFP (Figure 18.d) and HEY1 (Figure 18.e) were both significantly enriched in Notch active populations when compared to Notch inactive populations. Comparison between basal Notch active and luminal Notch active population showed that both EGFP and HEY1 were significantly more expressed in the luminal Notch active population (Luminal Notch active - EGFP:115,8±49,0; HEY1:7,08±1.164) (Basal Notch active - EGFP:33,5±18,9; HEY1:2,87±0,49). This observation is in line with our FACS analysis of the pubertal TNR mice that showed presence of higher intensity EGFP signal indicating higher Notch activity in the luminal Notch active population.

Since data from immunofluorescent staining showed that more than 90% of luminal Notch active population expresses hormone receptors (Figure 14), we tested the expression of ER, PR and FoxA1, an important mediator of ER endocrine response (Hurtado et al., 2011), in all 4 populations. As expected, ER (Figure 18.f) and PR (Figure 18.g) were significantly enriched in both luminal Notch active (ER:12,8±3,7; PR:10,0±2,8) and luminal Notch inactive population (ER:4,1±1,1; PR:3,9±0,5) when compared to basal populations. We also observed that the expression of ER and PR in luminal Notch active population is roughly 3 fold higher than in luminal Notch inactive population probably because luminal Notch active population contains mostly HR positive cells, while luminal Notch inactive populations contains both HR+ and HR- cells. Additionally, the expression of FoxA1 was also restricted to HR+ cells and more specifically enriched in the luminal Notch active population (Figure 18.h) (FoxA1: 10,6±1,9) confirming that luminal Notch active population of mammary epithelial cells is predominantly HR+.

Casein α and Elf 5 are proteins expressed in milk secreting cells which are HR-. Therefore we tested their expression in all 4 populations (Figure 18.i,j) to find that they are strongly enriched in the luminal Notch inactive population (Cas α:20,5±8,3; Elf5:7,0±1,5) which is predominantly HR.

Recent work from Devi Rajaram (Rajaram et al., 2015) showed that a subpopulation of HR+ cells expresses Wnt4 downstream of PR. In the microarray results, Wnt4 also appeared slightly enriched in the luminal Notch active population. Therefore, we tested expression of Wnt4 in all 4 populations by quantitative PCR and observed a 7-fold enrichment in luminal Notch active population when compared to the basal populations, and a 4-fold enrichment when compared to luminal Notch inactive population (Figure 18.k).

Recent work from Dr. Renuga Devi Rajaram (Rajaram et al., 2015) showed that a subpopulation of HR+ cells expresses Wnt4 downstream of PR. Therefore, we tested expression of Wnt4 in all 4 populations by quantitative PCR and observed 7-fold enrichment in luminal Notch active population when compared to the basal populations, and 4-fold enrichment when compared to luminal Notch inactive population.

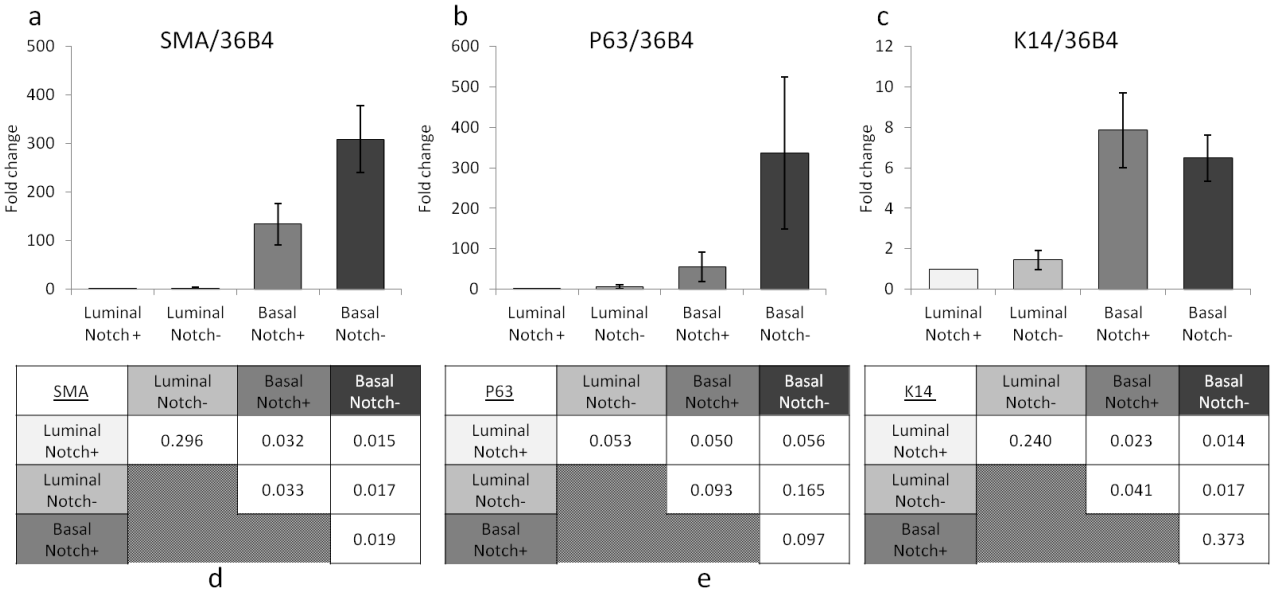

SMA	Luminal Notch-	Basal Notch+	Basal Notch-
Luminal Notch+	0.296	0.032	0.015
Luminal Notch-		0.033	0.017
Basal Notch+			0.019

P63	Luminal Notch-	Basal Notch+	Basal Notch-
Luminal Notch+	0.053	0.050	0.056
Luminal Notch-		0.093	0.165
Basal Notch+			0.097

K14	Luminal Notch-	Basal Notch+	Basal Notch-
Luminal Notch+	0.240	0.023	0.014
Luminal Notch-		0.041	0.017
Basal Notch+			0.373

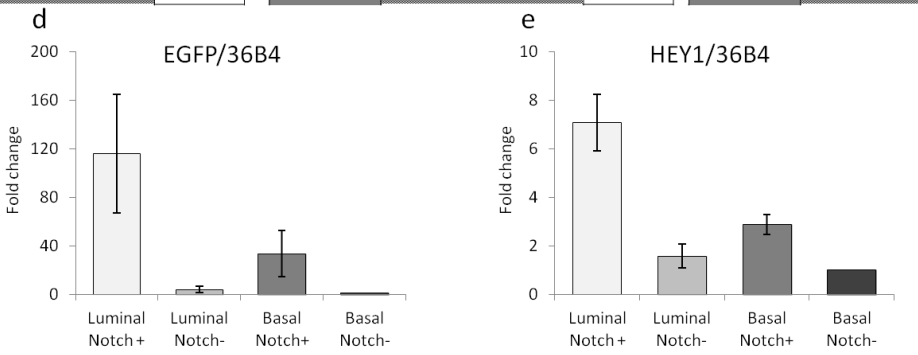

GFP	Luminal Notch-	Basal Notch+	Basal Notch-
Luminal Notch+	0.053	0.050	0.056
Luminal Notch-		0.093	0.165
Basal Notch+			0.057

HEY1	Luminal Notch-	Basal Notch+	Basal Notch-
Luminal Notch+	0.011	0.012	0.012
Luminal Notch-		0.015	0.185
Basal Notch+			0.015

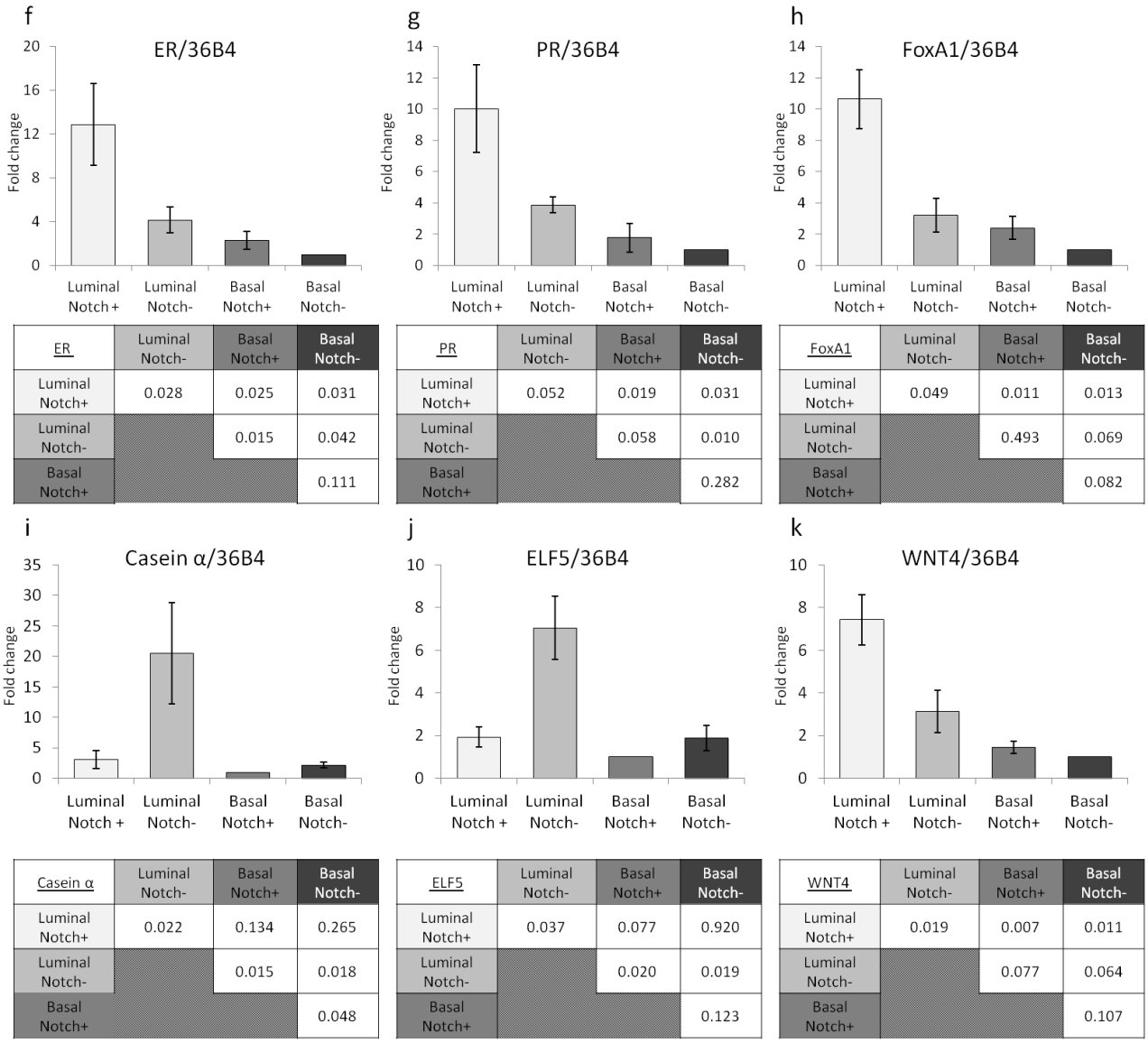

ER	Luminal Notch-	Basal Notch+	Basal Notch-
Luminal Notch+	0.028	0.025	0.031
Luminal Notch-		0.015	0.042
Basal Notch+			0.111

PR	Luminal Notch-	Basal Notch+	Basal Notch-
Luminal Notch+	0.052	0.019	0.031
Luminal Notch-		0.058	0.010
Basal Notch+			0.282

FoxA1	Luminal Notch-	Basal Notch+	Basal Notch-
Luminal Notch+	0.049	0.011	0.013
Luminal Notch-		0.493	0.069
Basal Notch+			0.082

Casein α	Luminal Notch-	Basal Notch+	Basal Notch-
Luminal Notch+	0.022	0.134	0.265
Luminal Notch-		0.015	0.018
Basal Notch+			0.048

ELF5	Luminal Notch-	Basal Notch+	Basal Notch-
Luminal Notch+	0.037	0.077	0.920
Luminal Notch-		0.020	0.019
Basal Notch+			0.123

WNT4	Luminal Notch-	Basal Notch+	Basal Notch-
Luminal Notch+	0.019	0.007	0.011
Luminal Notch-		0.077	0.064
Basal Notch+			0.107

Figure 18. Validation of the expression levels of the proteins of interest selected from microarray analysis in the 4 sorted populations from mammary epithelium. *Real-time PCR analysis of mRNA levels of Smooth muscle actin (a), p63 (b), keratin 14 (c), EGFP (d), Hey1 (e), er (f), PR (g), FoxA1 (h), Casein α (i), Elf 5 (j) and Wnt4 (k) in 4 populations of mammary epithelial cells sorted by type (luminal and basal) and by Notch activity (Notch+ and Notch-). p values between the different populations are presented in the tables bellow the graphs and standard deviations are calculated from 3 different samples per population originating from 3 independent groups of mice. Statistical significance was calculated by paired Student's T-test.*

CONCLUSION

Experiments from TNR mouse model showed that Notch signaling activity, reported by the expression of EGFP reporter gene, shows strongest activity during puberty where Notch signaling as detected by FACS through the TNR reporter is active in ≈11% of luminal and ≈3% of basal cells.

Furthermore we confirmed that luminal Notch active population predominantly expresses HR. Also, Notch active luminal population expresses higher levels of Wnt4 ligand which led us to hypothesize that this population is a subpopulation of Wnt4 expressing HR+ population of mammary epithelial cells.

CONDITIONAL DELETION OF RBP-JK GENE IN THE WNT4 EXPRESSING SUBPOPULATION OF HR+ CELLS (RBP^{floxed} WNT4-CRE MTMG MOUSE MODEL).

INTRODUCTION AND WORKING HYPOTHESIS

Recent study from Lucio Miele's group proposed that Notch signaling can replace ER signaling pathway when this latter is not present to activate the transcription of ER target genes in HR+ breast cancer cell lines (Rizzo et al., 2008). This observation, together with our data from TNR mouse model showing that Notch active luminal cells are expressing HR as well as Wnt4 ligand, led us to hypothesize that Notch signaling plays a role in the hormone signaling pathway in the mammary epithelium.

To test this hypothesis, and taking into account that Notch active luminal cells express Wnt4 ligand, we used a conditional deletion mouse model in which Notch signaling is abrogated by deletion of RBP-Jκ (a general Notch mediator) via Cre recombinase expressed under Wnt4 promoter. Therefore, we crossed the RBP^{floxed} mouse (Buono et al., 2006) with the Wnt4-Cre mouse (Shan et al., 2009) to obtain RBP$^{fl/fl}$ Wnt4-Cre. Wnt4-Cre activity was previously characterized in the study by Dr. Renuga Devi Rajaram on which I collaborated (Rajaram et al., 2015). We showed by immunofluorescence that Cre recombinase under the expression of the Wnt4 promoter is active in a subpopulation of HR+ luminal mammary epithelial cells within 3 days after birth.

To analyse Cre expression and to follow Cre targeted cells and their progeny, we crossed RBP$^{fl/fl}$ Wnt4-Cre mice with mice carrying mTmG reporter gene (Muzumdar et al., 2007). mTmG mice are transgenic mice in which a Cre-reporter gene contains both membrane targeted dTomato and membrane targeted EGFP gene driven by ubiquitously active Rosa26 promoter. dTomato gene is flanked by loxP sites and upon Cre activity, it will be deleted by recombination which will bring EGFP gene in frame. Therefore, cells in which Cre recombinase was active will constitutively express EGFP and cells without Cre activity will continue to constitutively express dTomato.

RESULTS

Analysis of Wnt4-Cre expression during mammary development

To characterize the expression of the Wnt4-Cre promoter in frame with the study of Renuga Devi Rajaram, I performed immunofluorescent co-staining for EGFP, p63, and PR on the mammary tissue sections from 5 days, 15 days, 4 weeks and 8 weeks old RBP$^{wt/wt}$ Wnt4-Cre mTmG mice (Rajaram et al., 2015). We observed low Wnt4 activation at day 5 after birth before onset of PR expression (Figure 19.a-e). At 15 days of age, as well as 4 weeks and 8 weeks we noticed, as expected, strong colocalization of EGFP with PR, but never with p63 (Figure 19.f-t). Therefore, we confirmed that Wnt4-Cre is expressed in subpopulation of HR+ luminal cells.

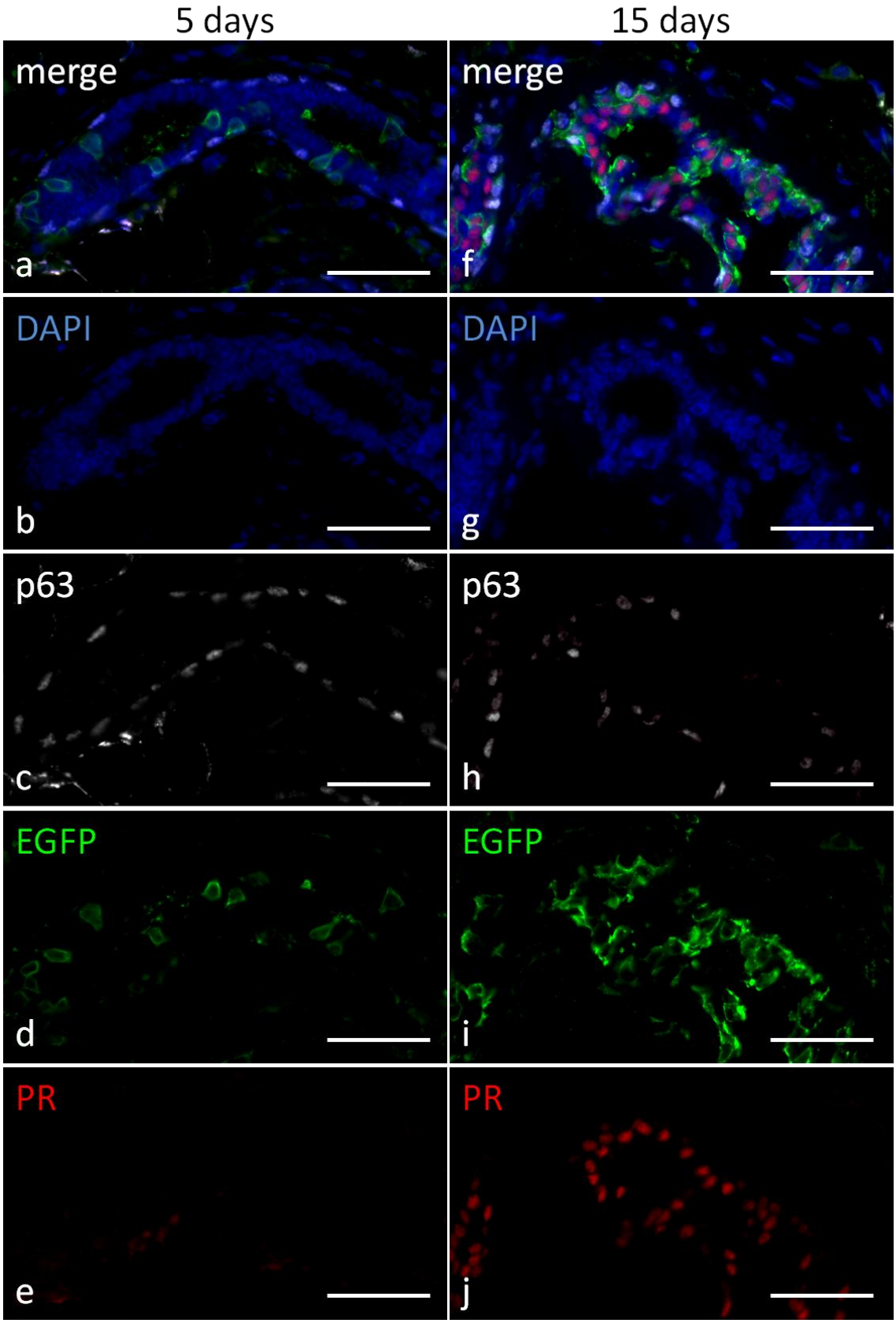
5 days
15 days
merge
a
merge
f
DAPI
b
DAPI
g
p63
c
p63
h
EGFP
d
EGFP
i
PR
e
PR
j

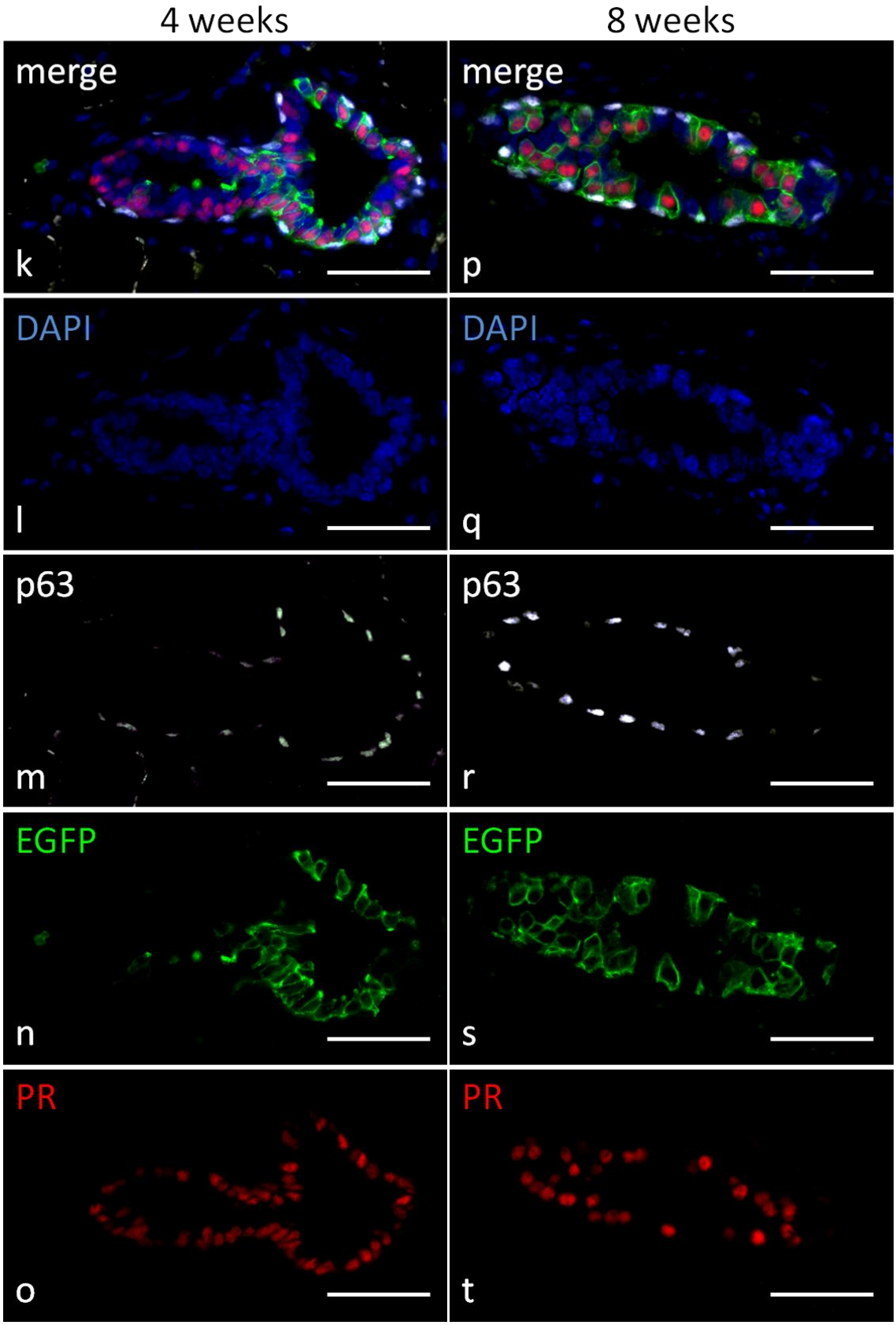

Figure 19. Colocalization of ER/PR, p63 and EGFP reporter in the RBP$^{wt/wt}$ Wnt4-Cre mTmG and RBP $^{fl/fl}$ Wnt4-Cre mTmG mammary epithelium. *a)-e) Co-staining of EGFP with PR and p63 in 5 day old RBP$^{wt/wt}$ Wnt4-Cre mTmG mammary epithelium (N=3); f)-j) Co-staining of EGFP with PR and p63 in 15 day old RBP$^{wt/wt}$ Wnt4-Cre mTmG mammary epithelium (N=3); k)-o) Co-staining of EGFP with PR and p63 in 4-weeks-old RBP$^{wt/wt}$ Wnt4-Cre mTmG mammary epithelium (N=3); p)-t) Co-staining of EGFP with PR and p63 in 8-weeks-old RBP$^{wt/wt}$ Wnt4-Cre mTmG mammary epithelium (N=3). Scale bars in a-t) represent 50μm*

Role of Notch signaling in the Wnt4 expressing epithelial cells during adulthood

To address the question of the role of Notch signaling in hormone signaling pathway in the mouse mammary epithelium, we analyzed adult epithelium from $RBP^{fl/fl}$ Wnt4-Cre mTmG and $RBP^{wt/wt}$ Wnt4-Cre mTmG mice by immunofluorescent co-staining for EGFP with ER, PR, p63, Ki67 and cleaved Caspase 3. However, to analyze $RBP^{fl/fl}$ Wnt4-Cre mTmG epithelium during adulthood, we had to perform tissue transplantation approach where mammary epithelial fragments from mutant and control glands are transplanted into contralateral mammary gland fat pads previously cleared of its endogenous epithelium. This way, we will have $RBP^{fl/fl}$ Wnt4-Cre mTmG and $RBP^{wt/wt}$ Wnt4-Cre mTmG epithelium growing in the same recipient mouse. To avoid possible rejection of the tissue, we used immunocompromised $RAG1^{-/-}$ mice (Mombaerts et al., 1992) as recipients. We had to use this method because Wnt4 gene is expressed in various organs such as kidneys (Itaranta et al., 2006), muscles (Strochlic et al., 2012) and ovaries (Mandel et al., 2008) where RBP-Jκ plays important role. For this reason, RBP-Jκ deletion using Wnt4-Cre promoter is lethal around 2 weeks after birth.

As tissue donors, we used 3 groups of mice containing one $RBP^{fl/fl}$ Wnt4-Cre mTmG and one $RBP^{wt/wt}$ Wnt4-Cre mTmG mice. Mice within the group were littermates, while each group of mice was taken from an independent litter. Mammary tissue from $RBP^{fl/fl}$ Wnt4-Cre mTmG and $RBP^{wt/wt}$ Wnt4-Cre mTmG from the same group was transplanted into 5 recipient mice and analyzed 2 months after the transplantation procedure.

Two months after surgery, the outgrowths were examined by fluorescent stereomicroscopy. Out of 15 grafts, 14 $RBP^{fl/fl}$ Wnt4-Cre mTmG and 14 $RBP^{wt/wt}$ Wnt4-Cre mTmG showed outgrowth. The size of the outgrowths on both sides was comparable (Figure 20.a,b,d) and the amount of branching points did not show any significant difference (Figure 20.c). However, the amount of green fluorescence was much higher in the $RBP^{wt/wt}$ Wnt4-Cre mTmG grafts than in the $RBP^{fl/fl}$ Wnt4-Cre mTmG, indicating that there are more recombined cells in the $RBP^{wt/wt}$ Wnt4-Cre mTmG epithelium. This result suggests that Cre targeted cells in $RBP^{fl/fl}$ Wnt4-Cre mTmG mice survive and/or proliferate less after Cre recombination.

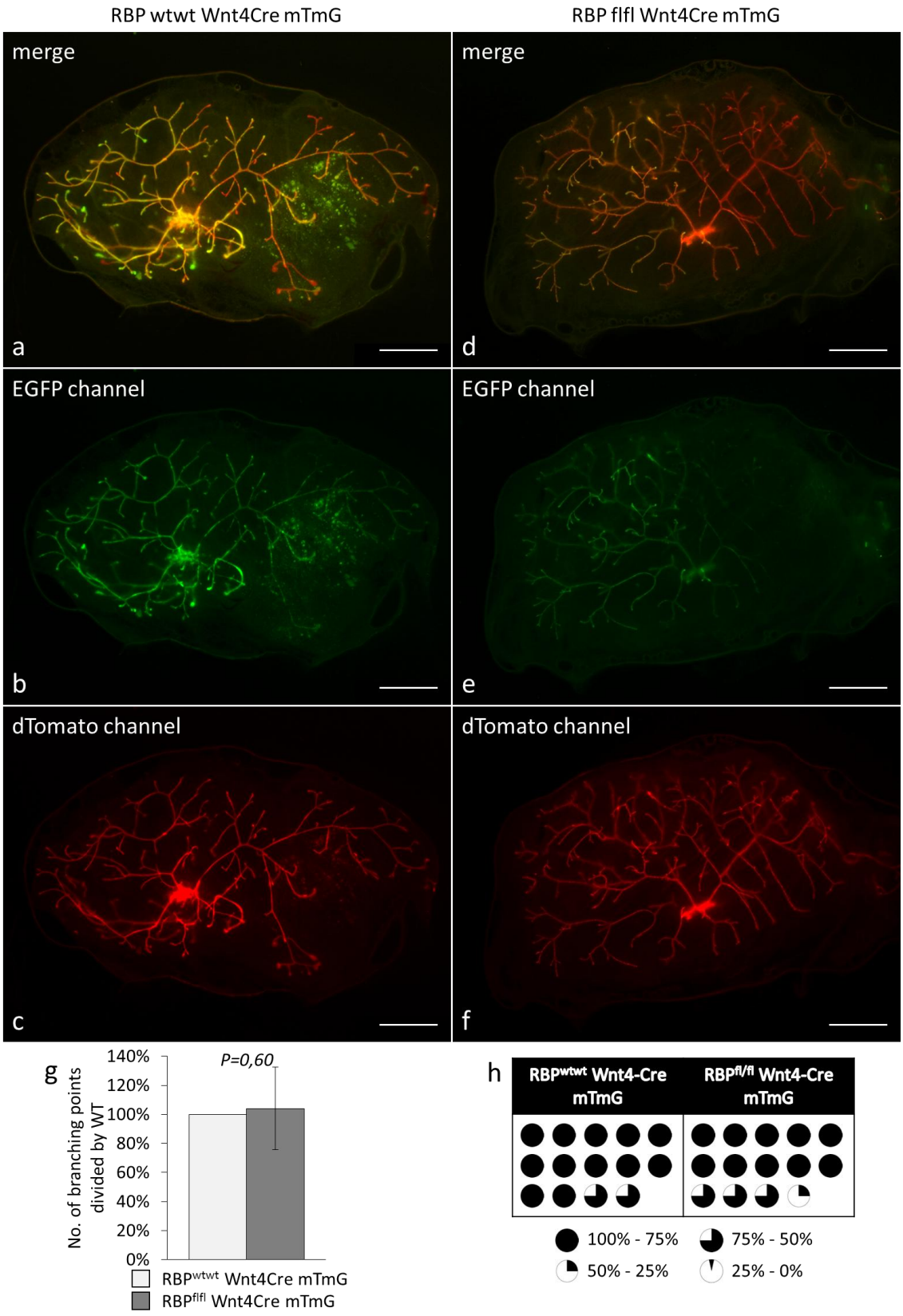

Figure 20.Transplantation of RBP$^{wt/wt}$ Wnt4-Cre mTmG and RBP $^{fl/fl}$ Wnt4-Cre mTmG mammary epithelium. *a-c) Wholemount analysis of the outgrowths of RBP$^{wt/wt}$ Wnt4-Cre mTmG (N=14). d-f) Wholemount analysis of the outgrowths of RBP$^{fl/fl}$ Wnt4-Cre mTmG epithelium (N=14). Scale bars in a-f represent 2,5 mm g) Bar plot showing branching points (N=14). h) Mammary gland reconstitution with RBP$^{wt/wt}$ Wnt4-Cre mTmG and RBP $^{fl/fl}$ Wnt4-Cre mTmG epithelium (N=14). Each circle represents one mammary gland; the blackened region represents the area filled with outgrowth. Statistical significance of the analysis was calculated by paired Students' T-test*

To confirm that Cre recombination deleted RBPjk gene in RBP$^{fl/fl}$ Wnt4-Cre mTmG epithelium, we co-stained sections for EGFP and RBP-Jκ we sectioned and stained couples of gland from 2 recipient mice per donor, having in total 6 samples per genotype for each type of staining. On each section more than 2000 cells were counted.

Stainings revealed that while in RBP$^{wt/wt}$ Wnt4-Cre mTmG tissue EGFP positive cells readily expressed RBP, in RBP$^{fl/fl}$ Wnt4-Cre mTmG tissue EGFP and RBP are not colocalized in the same cells (Figure 21). Therefore, Cre recombinase expression driven by Wnt4 reporter is successfully deleting the RBP-Jκ and RBP deficient mammary epithelial cells are selected against.

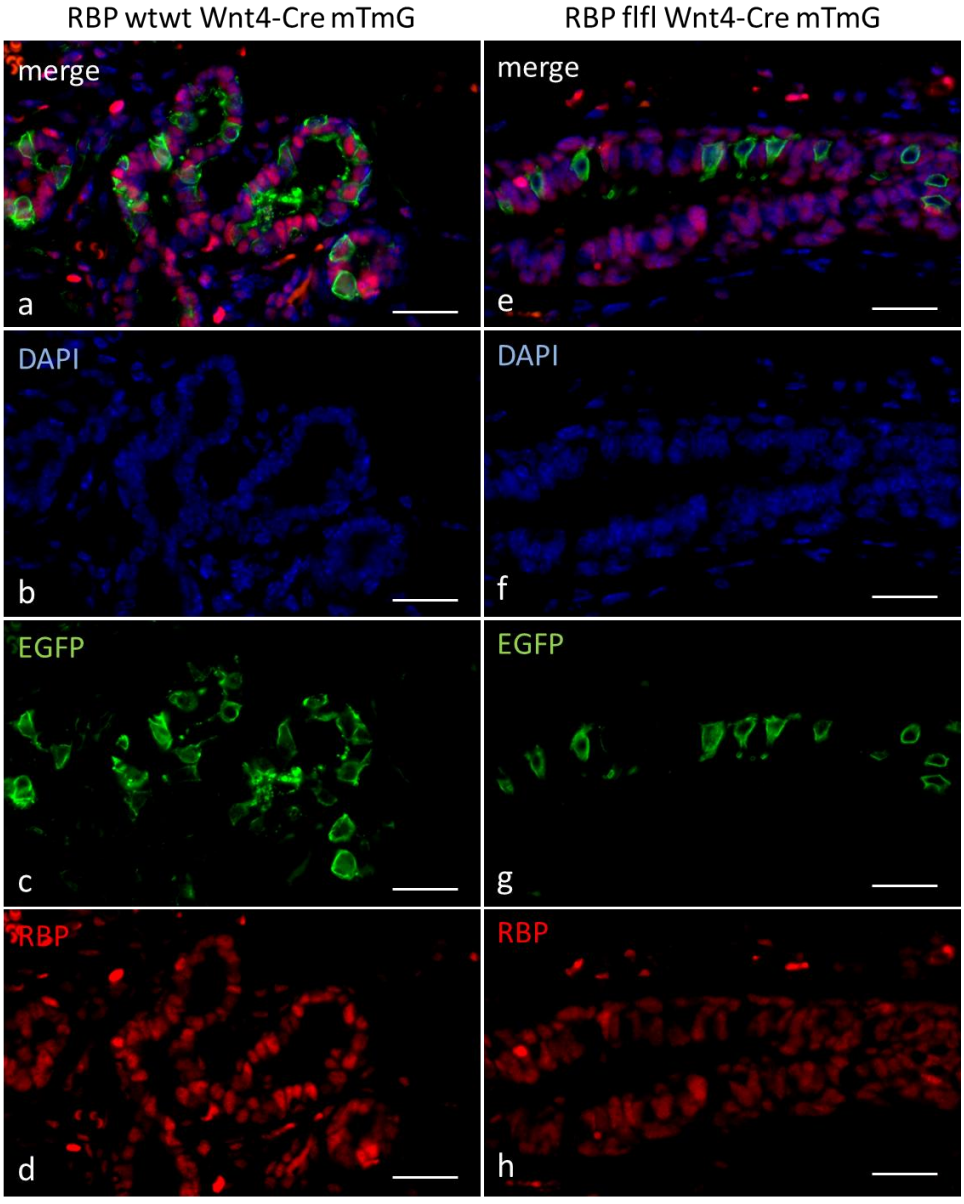

Figure 21: Colocalization of RBP-Jκ and EGFP expressing cells in the RBP^{floxed}Wnt4-Cre mTmG transplanted glands*. Immunofluorescent co-staining of EGFP with RBP-Jκ in RBP$^{wt/wt}$ Wnt4-Cre mTmG and RBP$^{fl/fl}$ Wnt4-Cre mTmG transplanted mammary epithelium: a) - d) Co-staining of EGFP with RBP-Jκ in RBP$^{wt/wt}$ Wnt4-Cre mTmG mammary epithelium (N=3); e)-h) Co-staining of EGFP with RBP-Jκ in RBP$^{wt/wt}$ Wnt4-Cre mTmG mammary epithelium (N=3). Scale bars represent 50 μm*

RBP wtwt Wnt4Cre mTmG

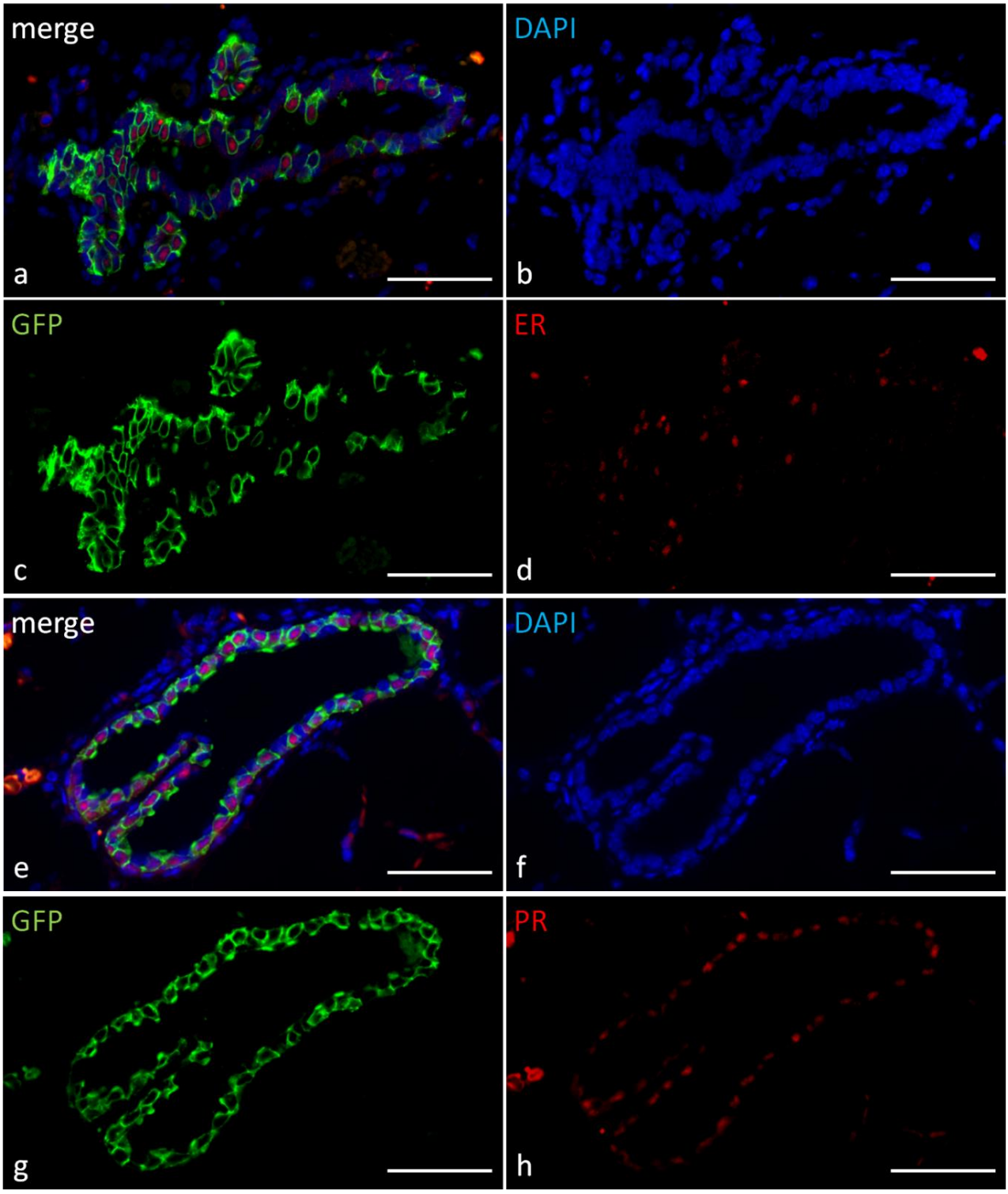

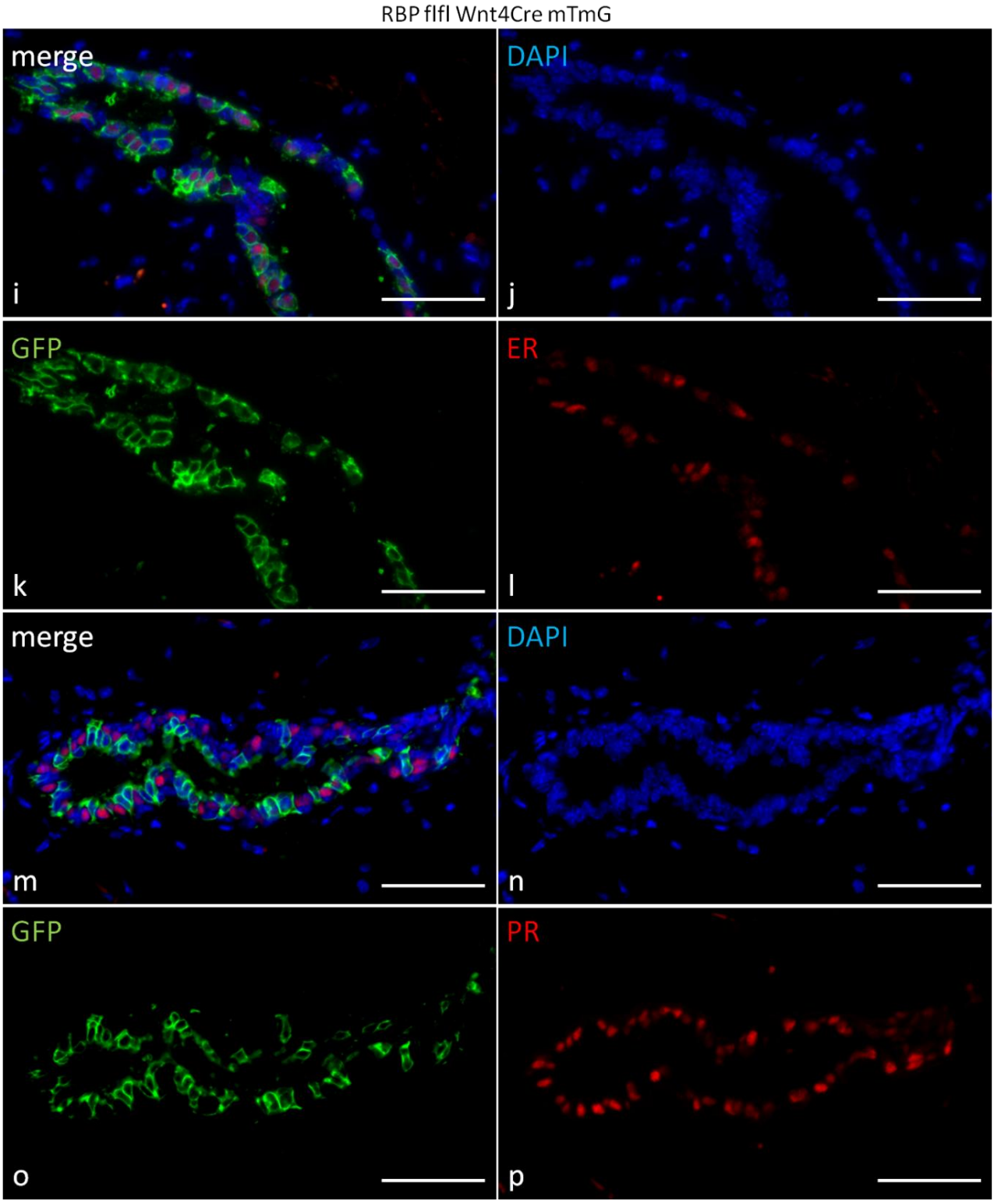

Figure 22. Colocalization of ER/PR and EGFP reporter in the RBP^{floxed}Wnt4-Cre mTmG transplanted glands. *Immunofluorescent co-staining (a-p) of EGFP with ER and PR in RBP$^{wt/wt}$ Wnt4-Cre mTmG and RBP $^{fl/fl}$ Wnt4-Cre mTmG transplanted mammary epithelium: a) – d) Co-staining of EGFP with ER in RBP$^{wt/wt}$ Wnt4-Cre mTmG mammary epithelium (N=6); e)-h) Co-staining of EGFP with PR in RBP$^{wt/wt}$ Wnt4-Cre mTmG mammary epithelium (N=6); i) - l) Co-staining of EGFP with ER in RBP$^{fl/fl}$ Wnt4-Cre mTmG mammary epithelium (N=6); m) - p) Co-staining of EGFP with PR in RBP$^{fl/fl}$ Wnt4-Cre mTmG mammary epithelium (N=6). Scale bars represent 50 µm.*

To analyze the expression of hormone receptors in the Notch abrogated cells, sections from RBP$^{fl/fl}$ Wnt4-Cre mTmG and RBP$^{wt/wt}$ Wnt4-Cre mTmG transplants were co-stained for EGFP and ER or PR (Figure 22). Quantification of 6 sections per genotype showed that in the RBP$^{wt/wt}$ Wnt4-Cre

mTmG epithelium, there were 2-fold more recombined cells identified by EGFP expression in compare to $RBP^{fl/fl}$ Wnt4-Cre mTmG (Figure 25.a). However, there was no significant difference in the number of HR+ cells in the whole epithelium. In both $RBP^{wt/wt}$ Wnt4-Cre mTmG and $RBP^{fl/fl}$ Wnt4-Cre mTmG epithelium, there was roughly one third of cells expressing hormone receptors ER and PR (Figure 25b,c) Within the recombined population, there was no significant difference in the number of EGFP cells expressing ER among the genotypes (Figure 25.d), but the difference in the amount of cells co-expressing EGFP and PR was important. The amount of EGFP and PR colocalization in the $RBP^{wt/wt}$ Wnt4-Cre mTmG epithelium was, as expected, 91,8%±6,3%, but in the $RBP^{fl/fl}$ Wnt4-Cre mTmG only 15,3%±11,3% of EGFP positive cells co-expressed PR, implicating RBP-Jκ into PR expression regulation (Figure 25.e).

To determine if there is less recombined cells expressing EGFP in the $RBP^{fl/fl}$ Wnt4-Cre mTmG epithelium because of differences in cell proliferation or apoptosis, histological sections of both phenotypes were co-stained for EGFP and Ki67 as a proliferation marker (Scholzen et al., 2000) (Figure 23.a-d, i-l) and cleaved Caspase 3 as an apoptosis marker (Nicholson et al., 1995) (Figure 23.e-h, m-o). $RBP^{fl/fl}$ Wnt4-Cre mTmG epithelium did not show altered proliferative activity neither in total cell population nor in recombined population (Figure 25.f,g). Cleaved caspase 3 staining showed very few positive cells both in $RBP^{fl/fl}$ Wnt4-Cre mTmG and $RBP^{wt/wt}$ Wnt4-Cre mTmG indicating that there is no difference in apoptotic activity in both epithelia.

RBP wtwt Wnt4Cre mTmG

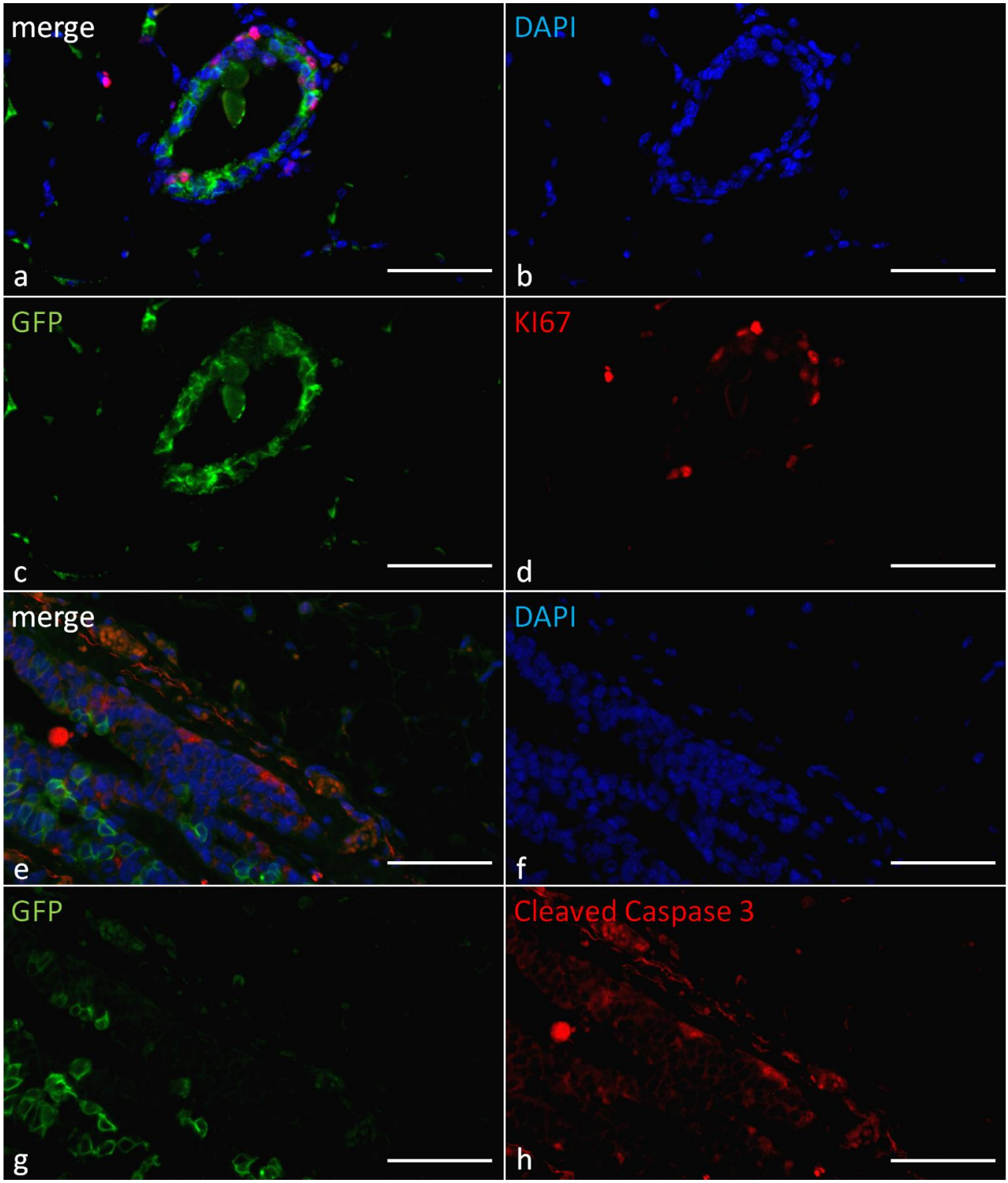

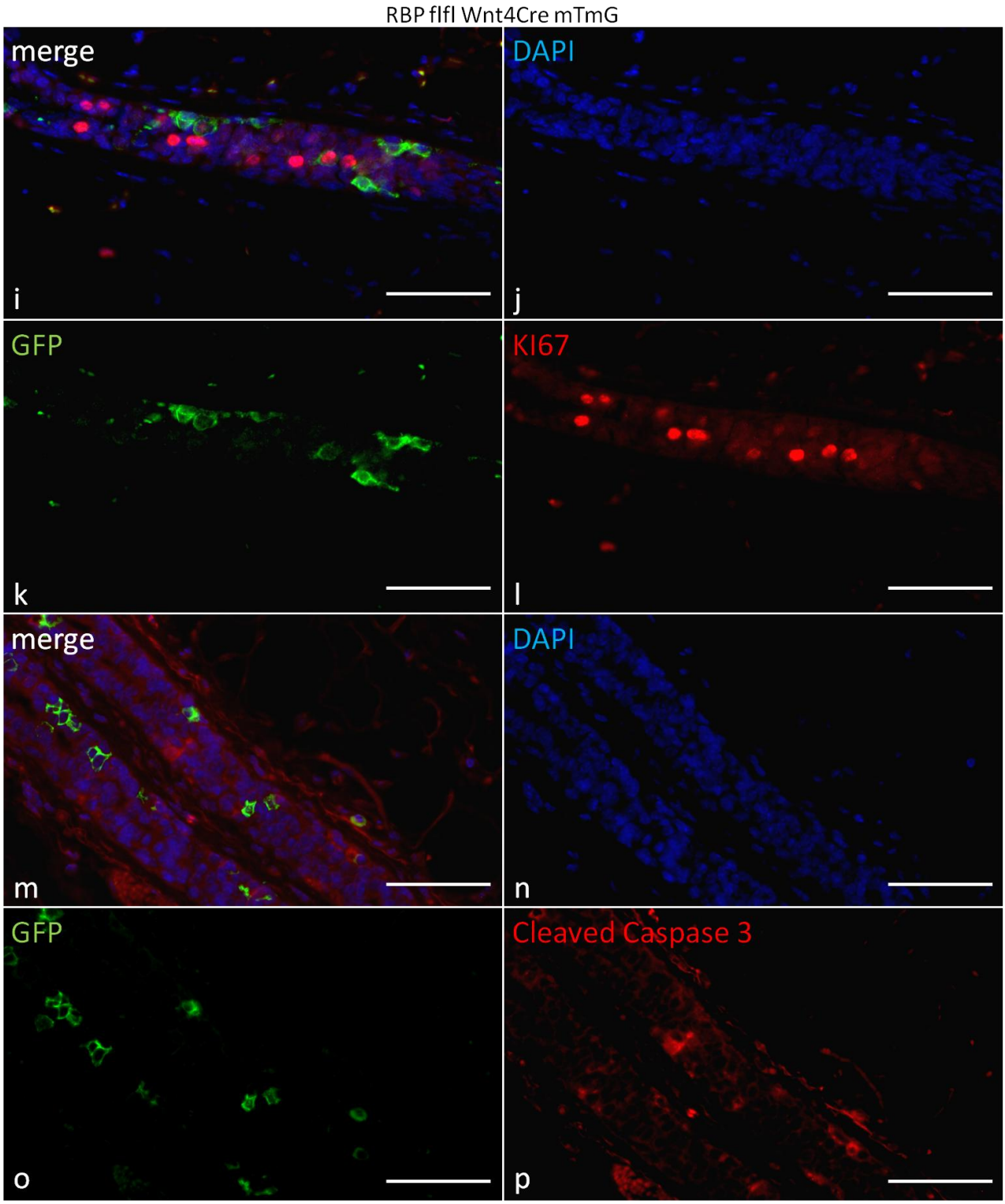

Figure 23: Colocalization of EGFP with KI67 and cleaved Caspase 3 in the RBP^{floxed}Wnt4-Cre mTmG transplanted glands. *a) - d) Co-staining of EGFP and KI67 in RBP$^{wt/wt}$ Wnt4-Cre mTmG mammary epithelium (N=6); e)-h) Co-staining of EGFP and cleaved Caspase 3 in RBP$^{wt/wt}$ Wnt4-Cre mTmG mammary epithelium (N=6); i) - l) Co-staining of EGFP and KI67 in RBP$^{fl/fl}$ Wnt4-Cre mTmG mammary epithelium (N=6); o) - r) Co-staining of EGFP and cleaved Caspase 3 in RBP$^{fl/fl}$ Wnt4-Cre mTmG mammary epithelium (N=6). Scale bars represent 50 µm.*

As previously shown, ER and PR proteins in RBP$^{wt/wt}$ mouse mammary tissue are expressed in the same population of luminal epithelial cells (Seagroves et al., 2000). We did not detect any difference in the overall number of HR+ cells however upon Notch abrogation via RBP-Jκ deletion, PR expression is lost. Therefore, we performed immunostaining with ER and PR antibodies to detect cells expressing only ER and not PR (Figure 24). Quantification of total HR+ cells confirmed presence of small portion of ER+ only cells (11,9%±2,0) in RBP$^{fl/fl}$ Wnt4-Cre mTmG tissue while in the wild type this portion was very small (1,2%±0,4) (Figure 25.h).

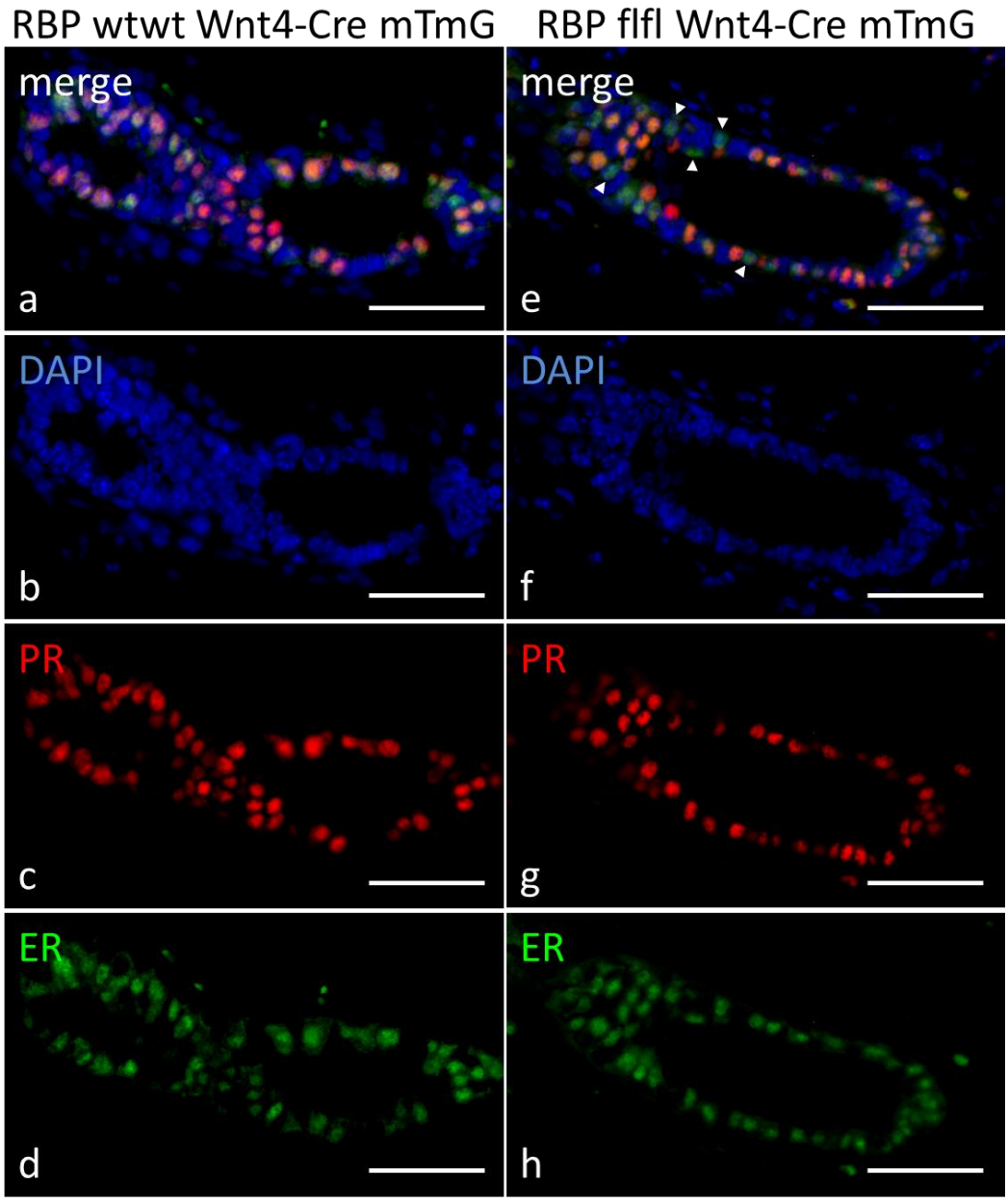

Figure 24. Colocalization of ER and PR in RBP$^{fl/fl}$Wnt4-Cre mTmG transplanted glands*. a) - d) Co-staining of ER and PR in RBP$^{wt/wt}$ Wnt4-Cre mTmG mammary epithelium (N=6). e) - h) Co-staining of ER and PR in RBP$^{fl/fl}$ Wnt4-Cre mTmG mammary epithelium (N=6). Scale bars represent 50 μm.*

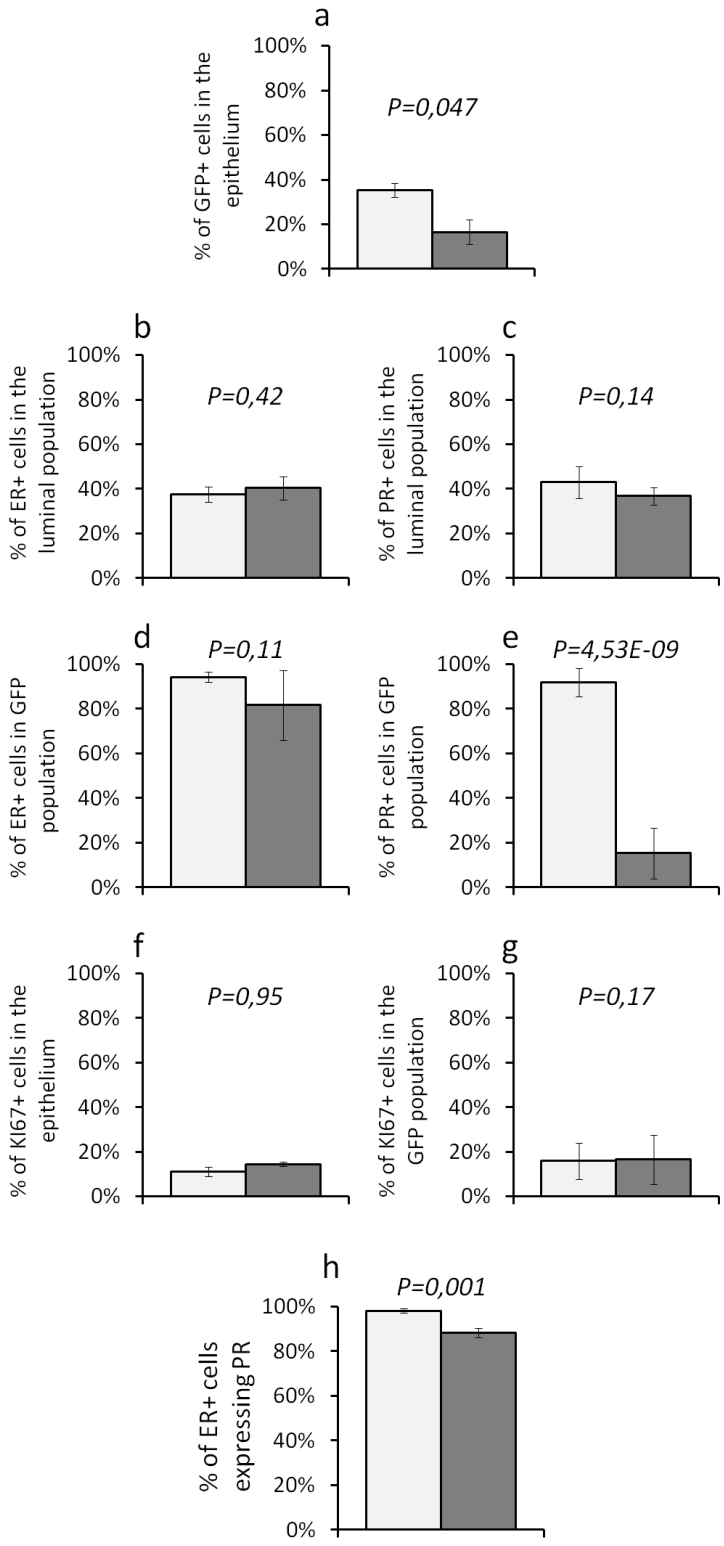

Figure 25: Quantification of colocalization of ER/PR and EGFP reporter in the RBP^{floxed}Wnt4-Cre mTmG transplanted glands*. a) Portion of EGFP positive cells in mammary epithelium (N=6); b) Portion of ER positive cells in the mammary epithelium (N=6); c) Portion of PR positive cells in the mammary epithelium (N=6); d) Portion of ER positive cells in the luminal EGFP positive population of MMECs (N=6); e) Portion of PR positive cells in the luminal EGFP positive population of MMECs (N=6); f) Portion of Ki67 positive cells in the mammary epithelium (N=6); g) Portion of Ki67 positive cells in the luminal EGFP positive population of MMECs (N=6); h) Portion of ER positive luminal MMECs that are co-expressing PR (N=6). Statistical significance of all comparisons was calculated by paired student's T-test.*

CONCLUSION

Experiments performed with the $RBP^{fl/fl}$ Wnt4-Cre mTmG mouse model showed that abrogation of Notch signaling via deletion of RBP-Jκ in Wnt4 expressing HR+ luminal epithelial cells results in strong loss of PR expression. This observation suggests that Notch signaling is implicated in the regulation of PR expression.

CONDITIONAL DELETION OF RBP-JK GENE IN THE WHOLE MAMMARY EPITHELIUM (RBP^{FLOXED} MMTV-CRE MTMG MOUSE MODEL).

INTRODUCTION AND WORKING HYPOTHESIS

Experiments performed with RBP$^{fl/fl}$ Wnt4-Cre mTmG mice led us to hypothesize that Notch signaling is involved in the regulation of PR expression in HR+ mammary epithelial cells. However, the Cre recombinase is expressed and deletes floxed RBP-Jκ only in HR+ cells that are expressing Wnt4 ligand.

To test whether RBP-Jκ regulates PR expression in the entire HR+ population, we recurred to the use of MMTV- Cre a promoter that will affect floxed RBP-Jκ in the entire population of HR+ epithelial cells.

RBP-Jκ conditional deletion via MMTV-Cre had previously been done by Ozden Yalcin Ozuysal. She presented evidences that in the RBP$^{fl/fl}$ MMTV-Cre mouse, Notch deleted cells, traced by presence of a Cre-reporter Z/EG in which , when recombined via Cre recombinase, EGFP is expressed under chicken β actin promoter (Novak et al., 2000), are present only in the basal layer while luminal layer is repopulated with wild-type cells (Yalcin Ozuysal et al.,2010). In agreement with this result, previous studies showed that Notch signaling is implicated in mammary gland development, specifically in the determination of luminal cell-fate, however the molecular and cellular mechanisms underlying this process remained unknown.

Z/EG reporter expressed under chicken β actin promoter (Novak et al., 2000) in the wild type control mouse did not mark the entire mammary epithelium. We decided to cross RBP^{floxed} MMTV-Cre mouse with mTmG reporter that showed overall expression in the mouse mammary epithelial cells.

Therefore, to test the hypothesis that Notch signaling regulates PR expression in the entire population of HR+ mouse mammary epithelial cells, we analyzed RBP$^{fl/fl}$ MMTV-Cre mTmG mouse mammary epithelium.

RESULTS

Analysis of MMTV-Cre deletion of RBPjk gene

To verify if MMTV-Cre is active in the entire mouse epithelium and if it correctly and completely deletes RBP-Jκ floxed gene, we analyzed mammary epithelium from 4, 8, 14 and 21-day old RBP$^{wt/wt}$ MMTV-Cre mTmG by immunofluorescent co-staining for EGFP and PR or p63. EGFP and p63 immunofluorescent co-staining confirmed that MMTV-Cre is expressed in the entire mammary epithelium including luminal and basal cells (Figure 26). EGFP and PR immunofluorescent co-staining showed that MMTV-Cre is active in all the PR+ cells (Figure 27).

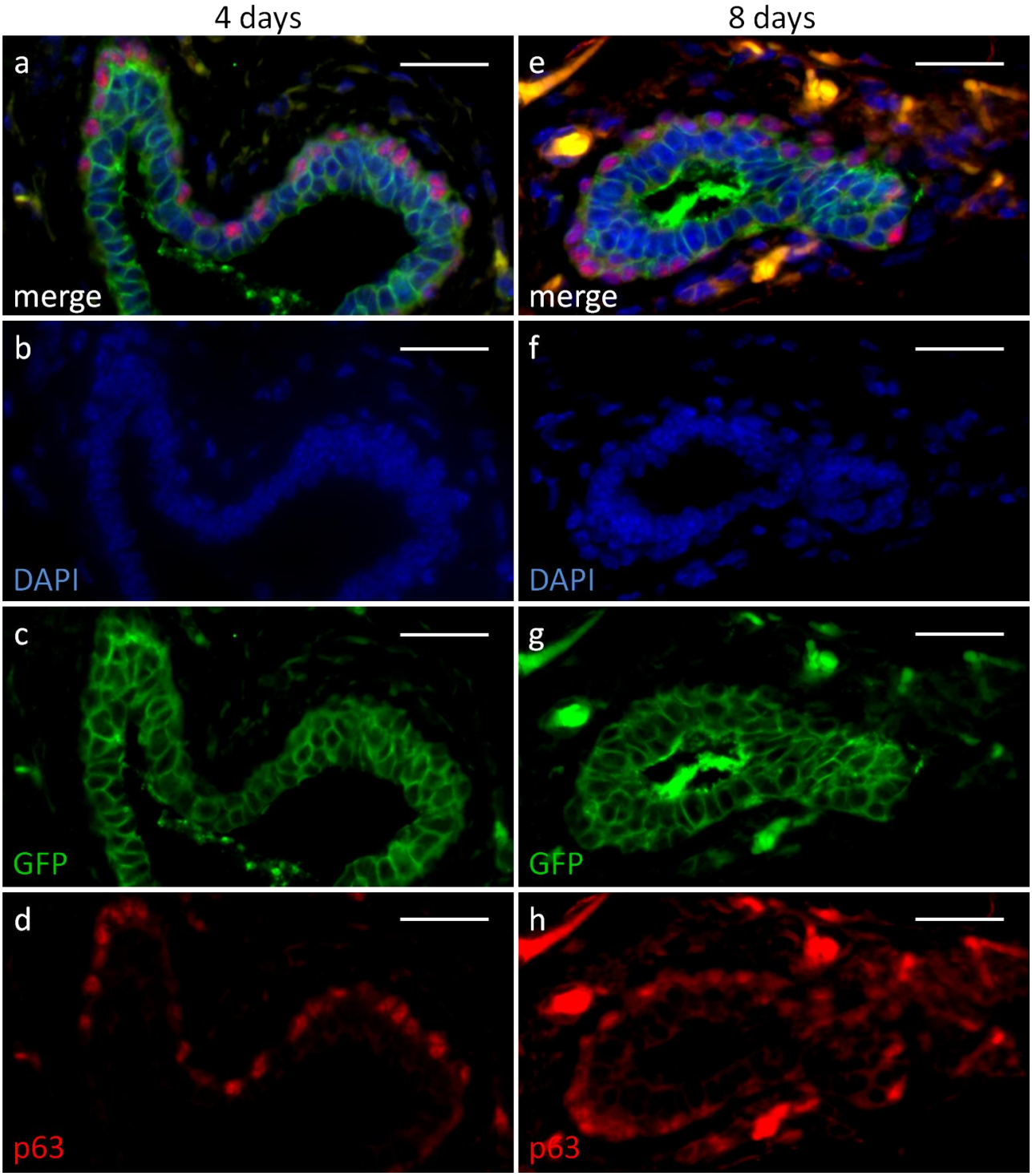
4 days
8 days
a
merge
e
merge
b
DAPI
f
DAPI
c
GFP
g
GFP
d
p63
h
p63

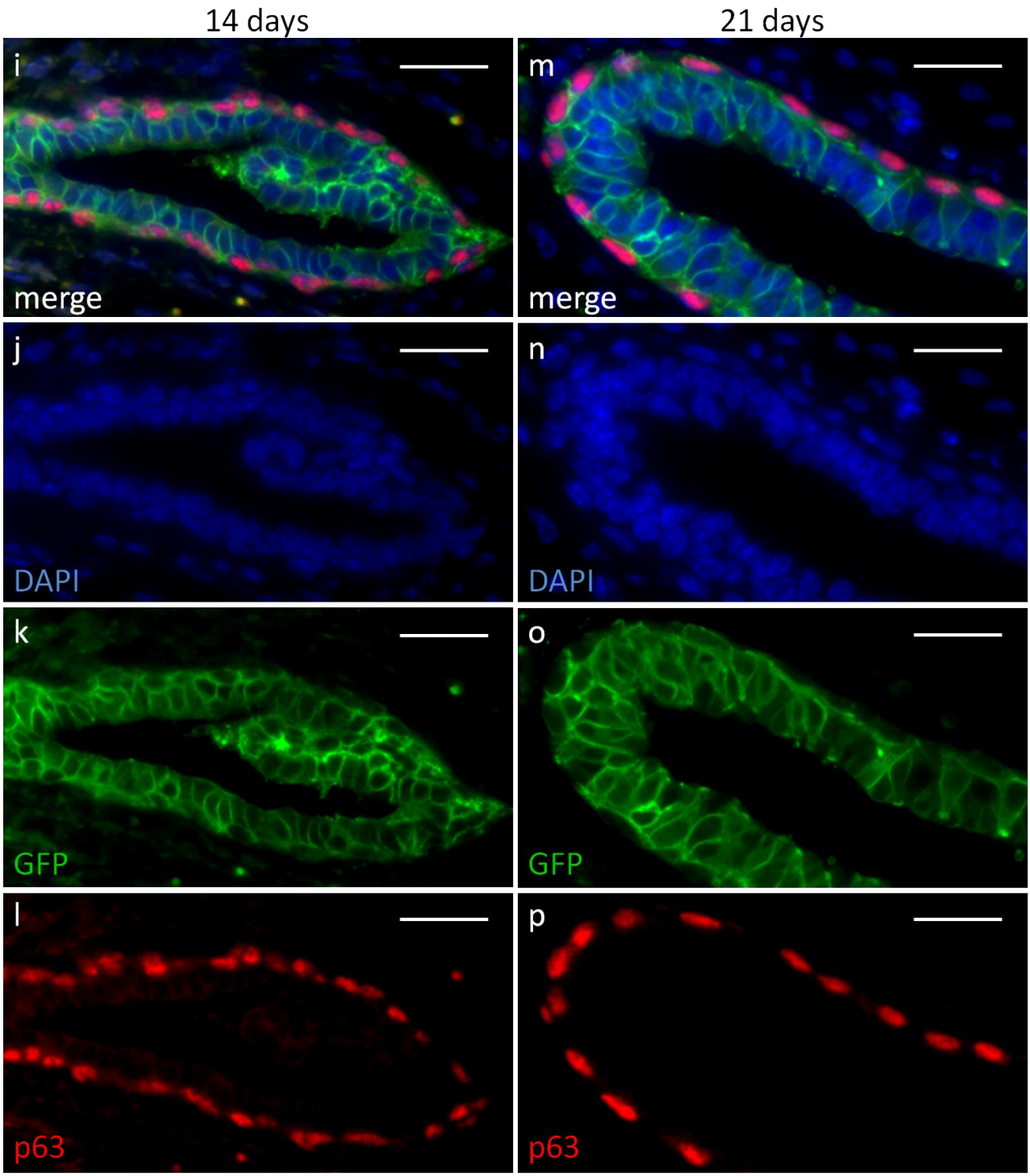

Figure 26. Localization of P63 and EGFP reporter in the MMTV-Cre mTmG mice*. Immunofluorescent co-staining (a-p) of EGFP and PR in MMTV-Cre mTmG mammary epithelium: a) – d) 4-day old (N=2); e)-h) 8-day old (N=2); i) - l) 14-day old (N=2); m) - p) 21-day old (N=2). Scale bars represent 50 µm.*

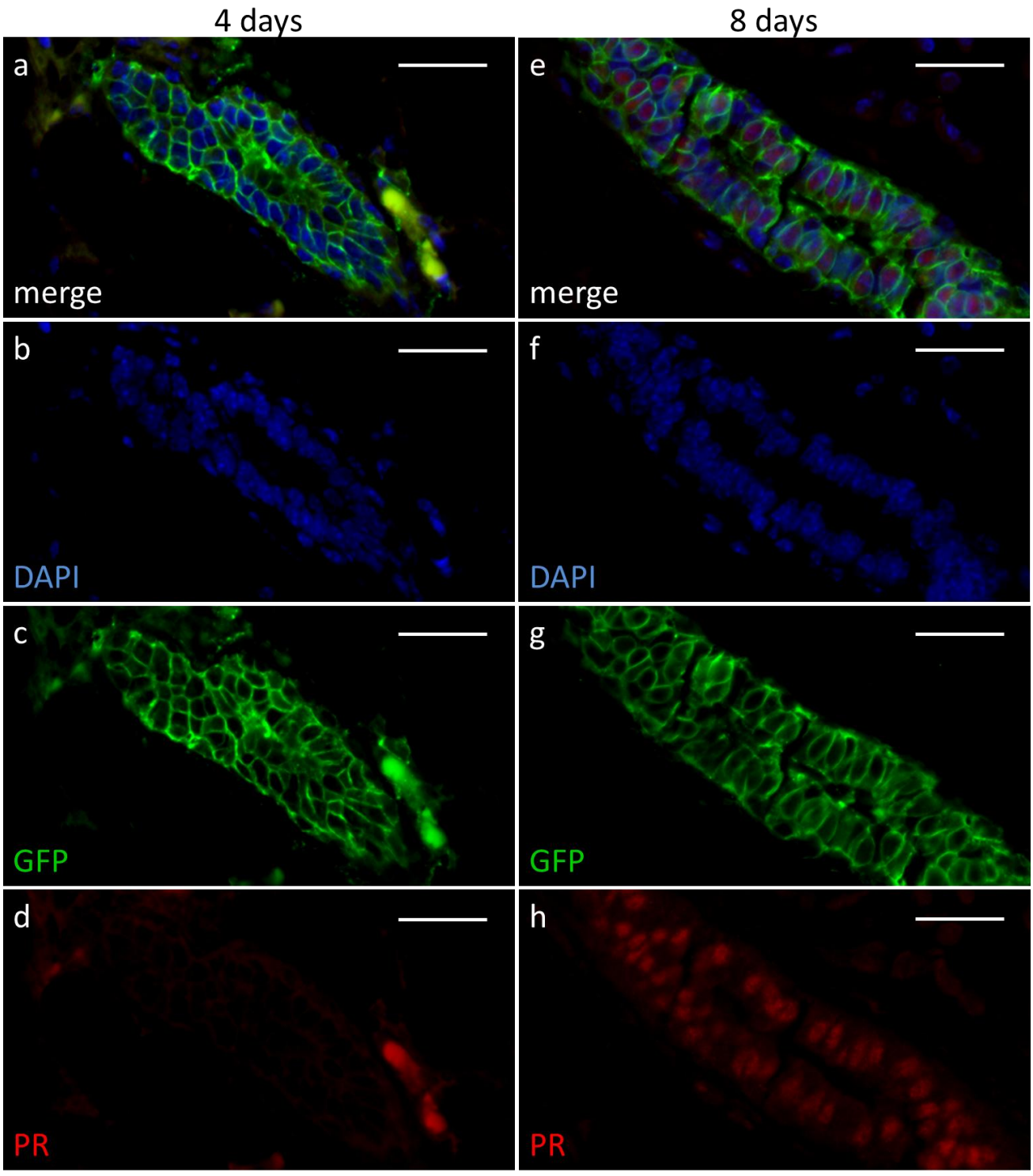
4 days
8 days
a
merge
e
merge
b
DAPI
f
DAPI
c
GFP
g
GFP
d
PR
h
PR

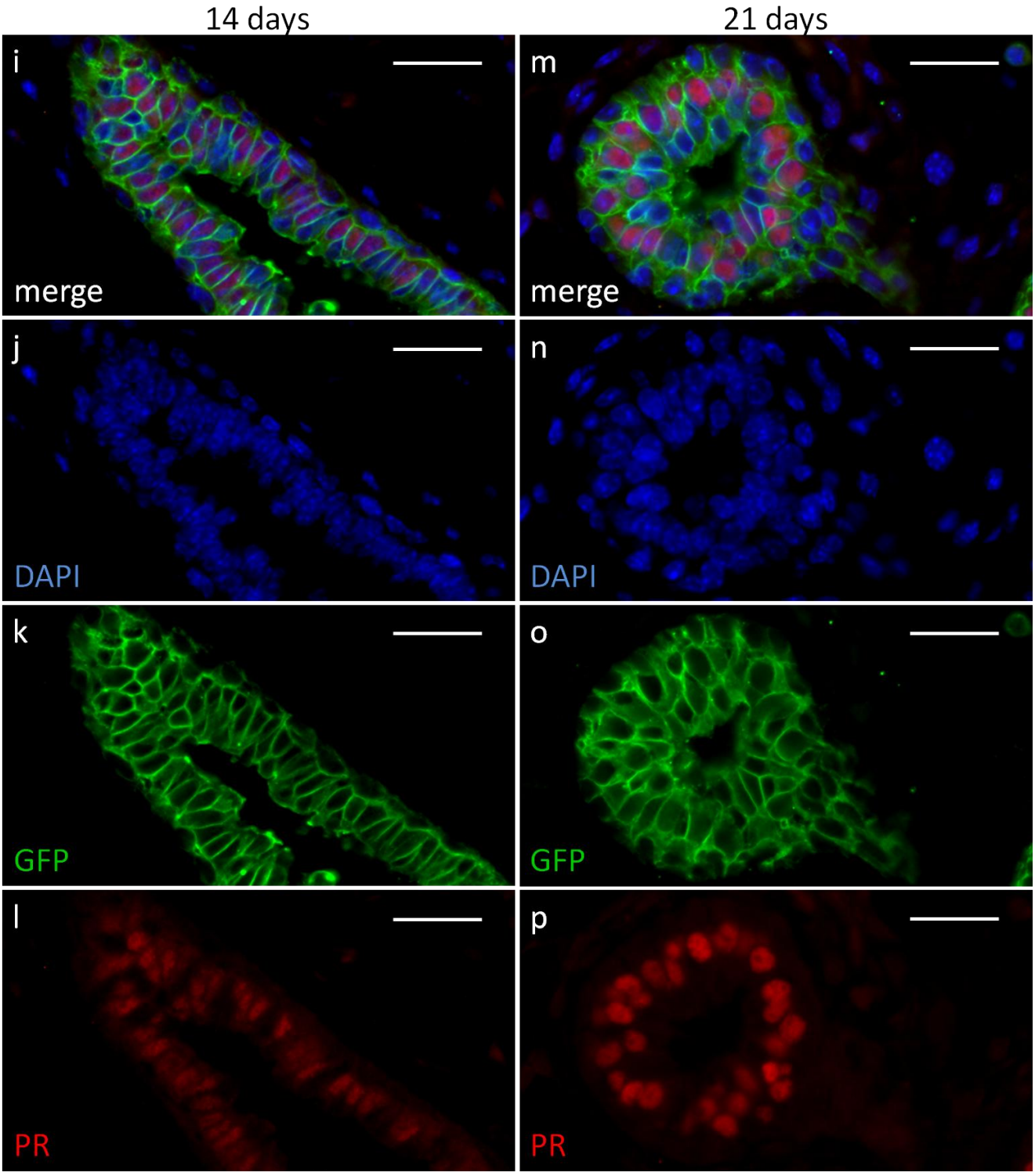

Figure 27. Colocalization of PR and EGFP reporter in the MMTV-Cre mTmG mice. *Immunofluorescent co-staining (a-p) of EGFP and PR in MMTV-Cre mTmG mammary epithelium: a) – d) 4-day old (N=2); e)-h) 8-day old (N=2); i) - l) 14-day old (N=2); m) - p) 21-day old (N=2). Scale bars represent 50 µm.*

Analysis of RBP-Jκ$^{fl/fl}$ MMTV-Cre mammary gland phenotype during adulthood

MMTV promoter is also expressed in the skin. Notch signaling is an important player in skin differentiation (Williams et al., 2011). RBP$^{fl/fl}$MMTV-Cre mTmG mice showed a severe phenotype in the skin (hair loss, skin inflammation and cachexia especially by the end of puberty at 8 weeks). To circumvent the confounding effects of the systemic sequela of the MMTV-driven RBP abrogation, we again recurred to transplantation for the analysis of the mammary epithelial phenotype.

As tissue donors, we used 3 groups of 8-weeks-old mice containing one RBP$^{fl/fl}$ MMTV-Cre mTmG and one RBP$^{wt/wt}$ MMTV-Cre mTmG mice. Mice within the group were littermates, while each group of mice was taken from an independent litter. Mammary tissue from RBP$^{fl/fl}$ MMTV-Cre mTmG and RBP$^{wt/wt}$ MMTV-Cre mTmG from the same group were transplanted into 5 recipient mice and analyzed 2 months after the transplantation procedure.

Two months after transplantation outgrowths of the engrafted epithelia was examined. Out of 14 out of 15 RBP$^{fl/fl}$ MMTV-Cre mTmG grafts and 14 out of 15 RBP$^{wt/wt}$ MMTV-Cre mTmG grafts reconstituted mammary ductal tree (Figure 28). In agreement with the results obtained by Ozden Yalcin Ozuysal (Yalcin Ozuysal et al., 2010), we couldn't observe any significant difference in the extent of fat pad filling or number of branching points (Figure 28.g,h). However, we saw a difference in the color of the epithelium. RBP$^{wt/wt}$ MMTV-Cre mTmG tissue was completely green suggesting that all the cells in the gland were expressing EGFP reporter of Cre activity (Figure 28.a-c). RBP$^{fl/fl}$ MMTV-Cre mTmG were showing signal both in green and red channel (Figure 28.d-f) suggesting that mammary epithelium in these glands is mosaic and comprises both cells expressing EGFP reporter of Cre activity and dTomato marking cells where Cre was not active.

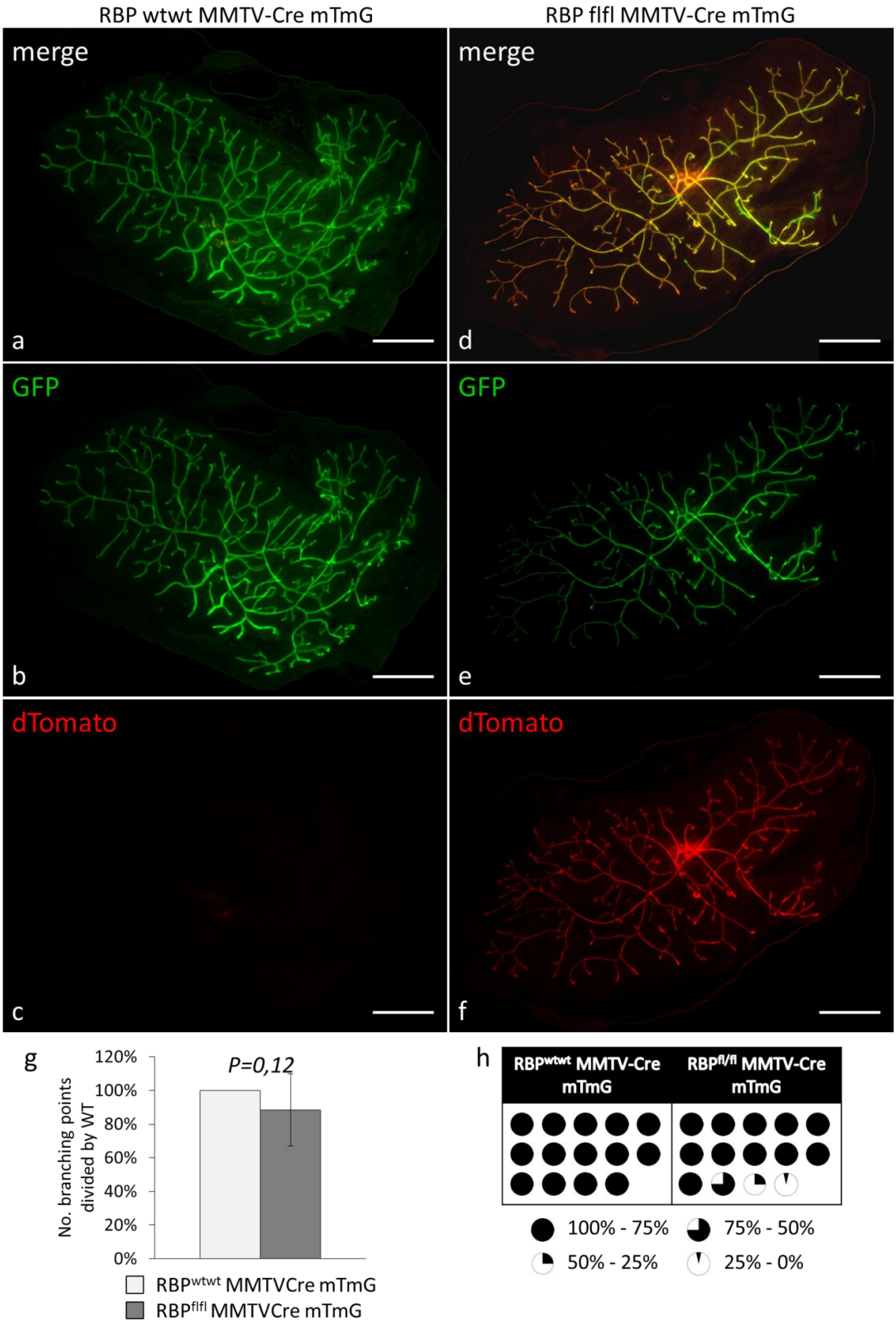

Figure 28. Transplantation of RBP$^{wt/wt}$ MMTV-Cre mTmG and RBP$^{fl/fl}$ MMTV-Cre mTmG epithelium. *Representative wholemounts of transplanted RBP$^{wt/wt}$ MMTV-Cre mTmG (a-c) and RBP$^{fl/fl}$ MMTV-Cre mTmG (d-f) Scale bars represent 2,5 mm; g) Quantification of branching points in RBP$^{wt/wt}$ MMTV-Cre mTmG and RBP$^{fl/fl}$ MMTV-Cre mTmG (N=14) Statistical significance was calculated using paired Student's T-test; h) Quantification of the fatpad filling in RBP$^{wt/wt}$ MMTV-Cre mTmG and RBP$^{fl/fl}$ MMTV-Cre mTmG transplanted glands. Each circle represents one transplanted mammary gland. The blackened region represents the area filled with outgrowth.*

To investigate the expression of both ER and PR in the conditionally knocked out epithelium, we performed immunofluorescent co-staining for EGFP and ER or PR in both $RBP^{wt/wt}$ MMTV-Cre mTmG and $RBP^{fl/fl}$ MMTV-Cre mTmG epithelium. For the quantification of immunofluorescent analysis, we analyzed couples of gland from 2 recipient mice per donor, having in total 6 samples per genotype for each type of staining. More than 2000 cells were counted on each section.

Firstly, we looked at the expression of EGFP in the whole epithelium. As expected, in the $RBP^{wt/wt}$ MMTV-Cre mTmG almost all the cells in both compartments (97,0%±2,0) expressed EGFP confirming that Cre was active in the entire epithelium (Figure 29.a-h) (Figure 30.a). In the $RBP^{fl/fl}$ MMTV-Cre mTmG, we noticed that there are significantly less EGFP expressing cells (37,0%±8,3) (Figure 29.i-p) (Figure 30.a). Previous analysis of $RBP^{fl/fl}$ MMTV-Cre mTmG mammary epithelium showed that cells expressing Cre reporter were present only in the basal compartment and luminal layer was repopulated with EGFP negative cells where Cre was never active and didn't delete RBP-Jκ gene (Yalcin Ozuysal et al., 2010). In our analysis, all the cells in the basal compartment were expressing EGFP, but also there was a significant number of EGFP+ cells in the luminal compartment (figure X). Immunofluorescent co-staining for EGFP with ER or with PR revealed that the vast majority of luminal EGFP positive cells (90,9%±3,8 for ER and 86,9 %±3,8 for PR) in $RBP^{fl/fl}$ MMTV-Cre mTmG mouse tissue are both ER and PR positive (Figure 30.c). Analysis of the number of HR+ cells in total epithelium showed that there are no differences in the number of HR+ cells (analyzed both by ER and PR expression) in $RBP^{wt/wt}$ MMTV-Cre mTmG (31,4%±1,9 for ER and 32,4%±3,6 for PR) and $RBP^{fl/fl}$ MMTV-Cre mTmG (30,1%±6,8 for ER and 33,1%±3,3 for PR) (Figure 30.b). Thus, even in absence of Notch signaling, the proportion of HR+ cells is maintained in the tissue.

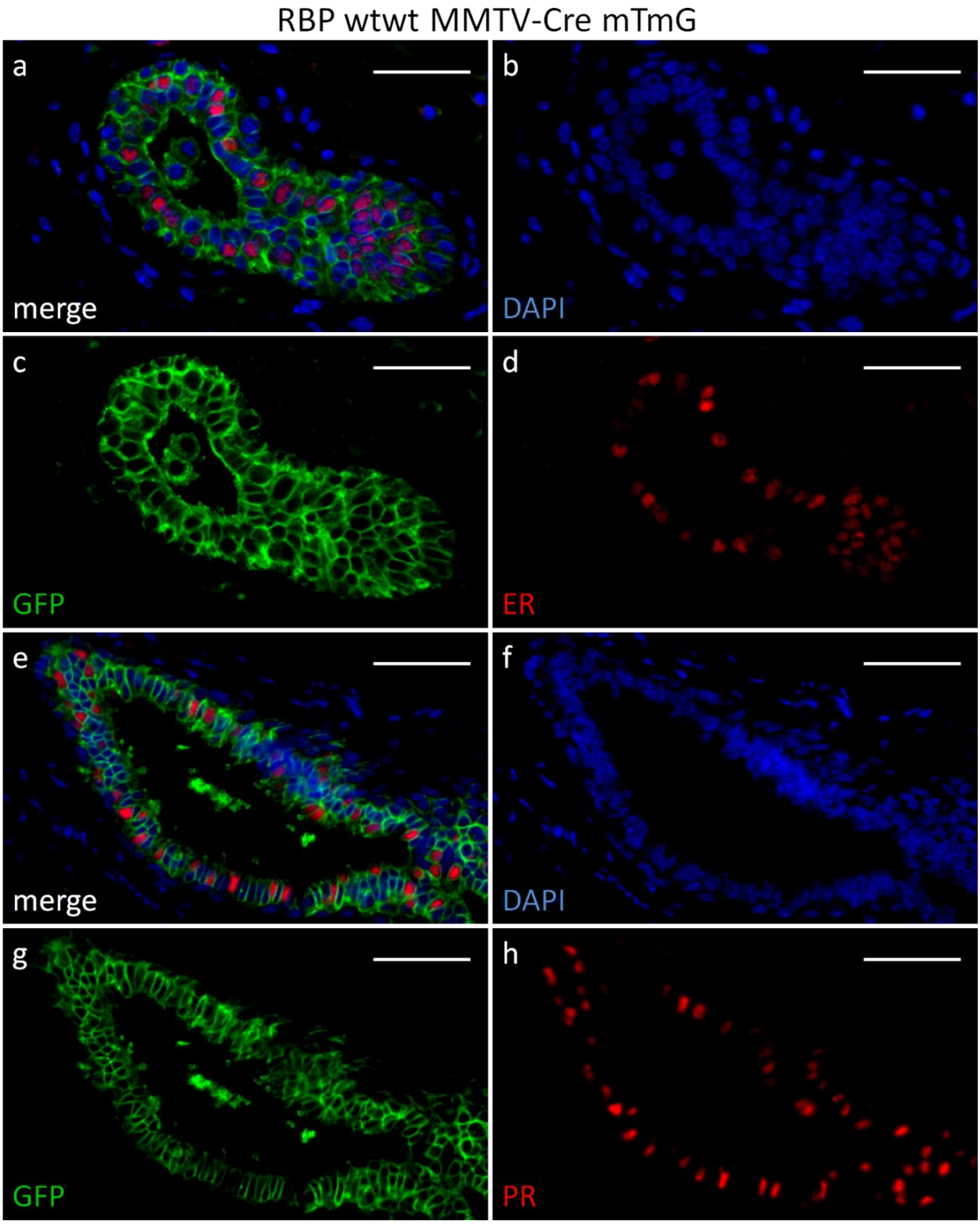
RBP wtwt MMTV-Cre mTmG
a
merge
b
DAPI
c
GFP
d
ER
e
merge
f
DAPI
g
GFP
h
PR

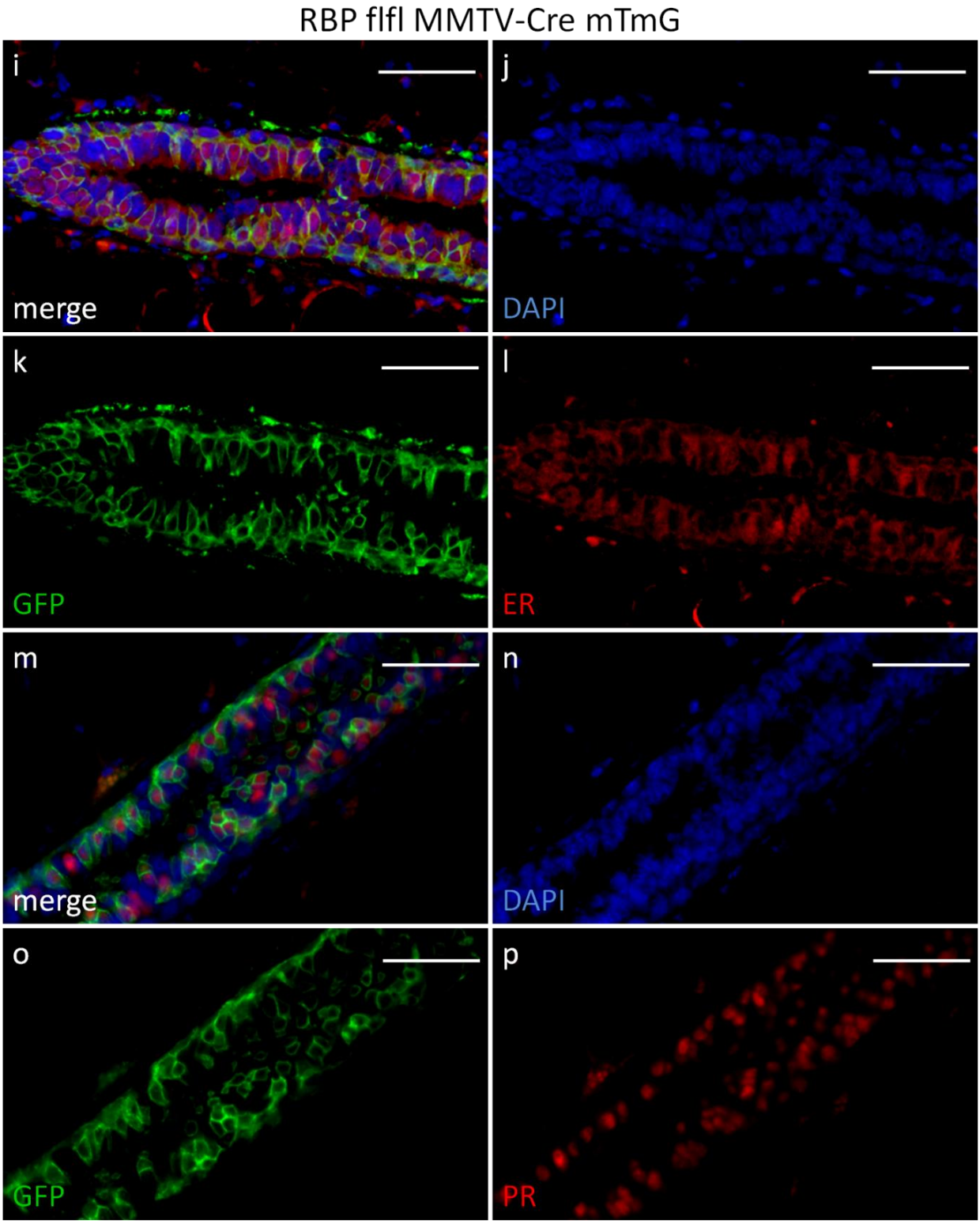

Figure 29. Colocalization of ER/PR and EGFP reporter in the RBP^{floxed}MMTV-Cre mTmG transplanted glands. *Immunofluorescent co-staining (a-p) of EGFP with ER and PR in RBP$^{wt/wt}$ MMTV-Cre mTmG and RBP $^{fl/fl}$ MMTV-Cre mTmG transplanted mammary epithelium: a) – d) Co-staining of EGFP with ER in RBP$^{wt/wt}$ MMTV-Cre mTmG mammary epithelium (N=6); e)-h) Co-staining of EGFP with PR in RBP$^{wt/wt}$ MMTV-Cre mTmG mammary epithelium (N=6); i) - l) Co-staining of EGFP with ER in RBP$^{fl/fl}$ MMTV-Cre mTmG mammary epithelium (N=6); m) - p) Co-staining of EGFP with PR in RBP$^{fl/fl}$ MMTV-Cre mTmG mammary epithelium (N=6). Scale bars represent 50 µm.*

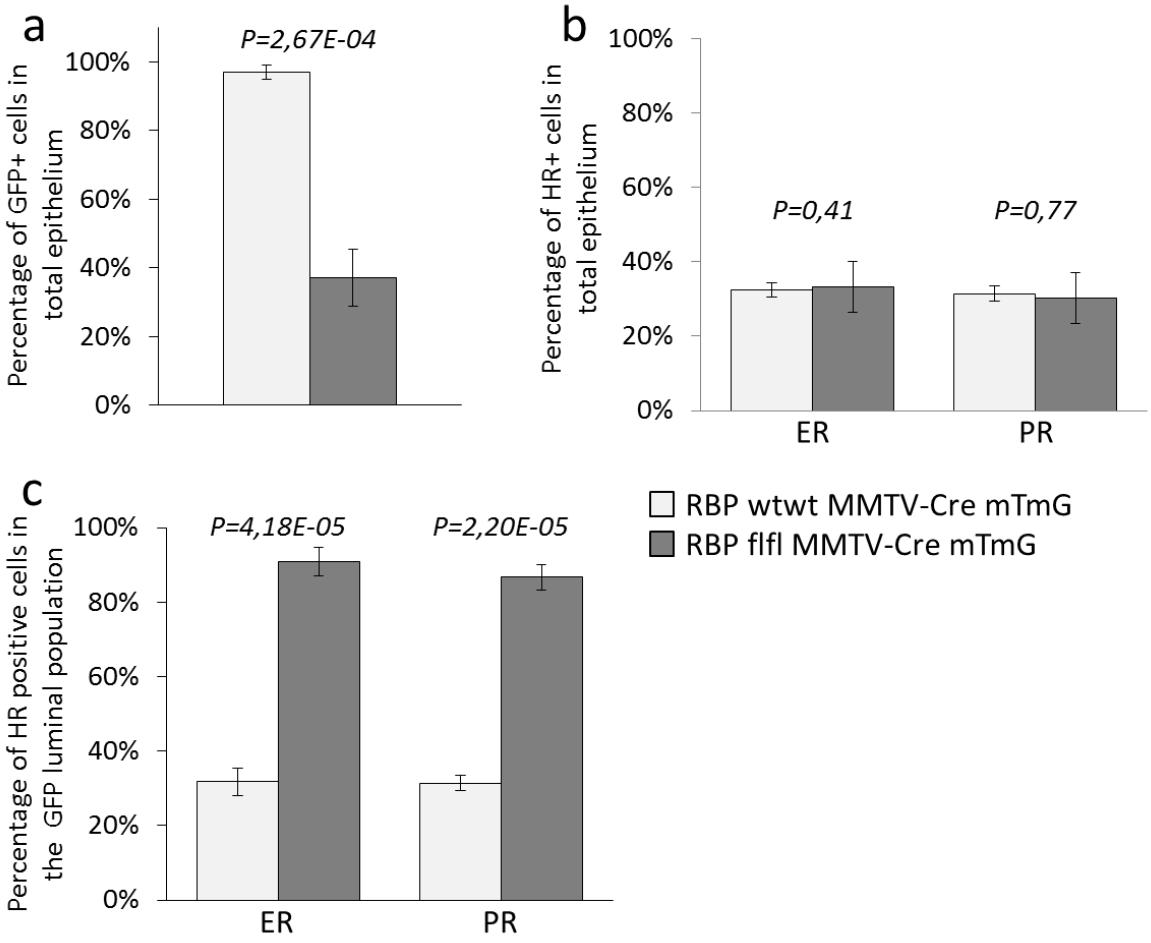

Figure 30: Quantification of colocalization of ER/PR and EGFP reporter in the RBP^{floxed} MMTV-Cre mTmG transplanted glands*. a) Portion of EGFP positive cells in mammary epithelium (N=6); b) Portion of ER and PR positive cells in the mammary epithelium (N=6); c) Portion of ER and PR positive cells in the luminal EGFP positive population of MMECs (N=6). Statistical significance of all comparisons was calculated by paired student's T-test.*

To confirm that in the EGFP positive population of the RBP$^{fl/fl}$ MMTV-Cre mTmG epithelium deletion of RBP-Jκ was fully functional, we performed immunofluorescent co-staining of tissue from both RBP$^{wt/wt}$ MMTV-Cre mTmG and RBP$^{fl/fl}$ MMTV-Cre mTmG transplants with EGFP and RBP-Jκ antibodies. Staining confirmed that in the RBP$^{fl/fl}$ MMTV-Cre mTmG tissue cells expressing EGFP Cre reporter were not expressing RBP-Jκ (Figure 31).

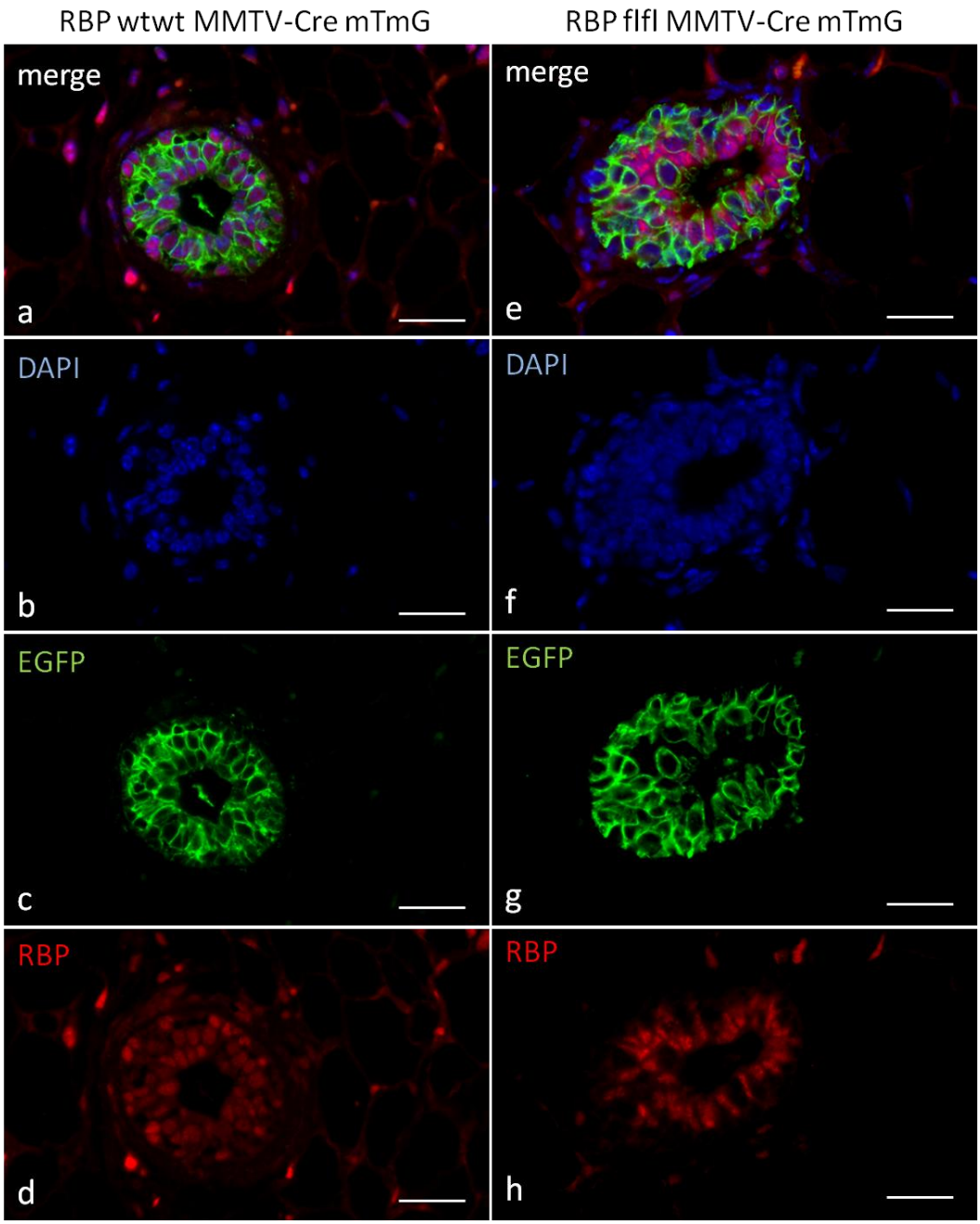

Figure 31. **Colocalization of RBP-Jκ and EGFP reporter in the RBP^{floxed}MMTV-Cre mTmG transplanted glands**. Immunofluorescent co-staining (a-p) of EGFP and RBP-Jκ in RBP$^{wt/wt}$ MMTV-Cre mTmG and RBP $^{fl/fl}$ MMTV-Cre mTmG transplanted mammary epithelium: a) – d) Co-staining of EGFP and RBP-Jκ in RBP$^{wt/wt}$ MMTV-Cre mTmG mammary epithelium (N=6); e)-h) Co-staining of EGFP and RBP-Jκ in RBP$^{fl/fl}$ MMTV-Cre mTmG mammary epithelium (N=6). Scale bars represent 50 μm

CONCLUSION

From the experiments with RBP^{floxed} MMTV-Cre mTmG mouse model we concluded that there is a particular population of HR+ cells that can differentiate independently of Notch signaling. Therefore we are proposing the presence of 2 different populations of HR+ cells in the mouse mammary epithelium: 1) a population that do not rely on Notch signaling and that is detected in RBP$^{fl/fl}$ MMTV-Cre mTmG mouse model. In these cells ER and PR are expressed independently of Notch activation; 2) a population of HR+ cells that is expressing Wnt4 ligand and that is detected by RBP$^{fl/fl}$

Wnt4-Cre mTmG mouse model. In these cells, PR expression is loss upon abrogation of Notch signaling via deletion of RBP-Jκ.

TIME DIRECTED CONDITIONAL DELETION OF RBP-JK IN THE MAMMARY EPITHELIUM (INTRADUCTAL INJECTION OF ADENO-CRE VIRUS INTO RBP-JK^{FLOXED} MTMG MOUSE MODEL)

INTRODUCTION AND WORKING HYPOTHESIS

The results from RBP-Jκ Wnt4-Cre mTmG mouse model led us to propose that in the Wnt4 expressing HR+ cells the expression of PR might be regulated by Notch signaling via RBP-Jκ.

RBP^{floxed} MMTV-Cre mTmG mouse model showed that HR+ cells and PR expression can be established without Notch signaling, therefore we hypothesized that Notch signaling might be important for maintenance of the PR expression in the HR+ luminal cells.

Wnt4 starts to be expressed in the mammary epithelium around day 3 after birth. Therefore, in the RBP-Jκ^{floxed} Wnt4-Cre mTmG mouse model RBP-Jκ is recombined very early in development. Cre activity reporter, mTmG is recombined and expressed EGFP in order to mark the cells in which Cre-recombinase was active but we cannot know the time window of its activity. Hence, the time frame of these events remains undetermined.

Therefore, to test the immediate effect of the Notch abrogation via RBP-Jκ deletion in mammary gland epithelium, we established the protocol of time-directed conditional deletion of floxed RBP-Jκ gene via intraductally injected Adeno-Cre virus which expresses Cre recombinase under the CMV promoter (Russel et al., 2003). The Cre activity is reported by the expression of EGFP from mTmG Cre reporter gene.

The amount of virus injected in each mammary gland was $1*10^7$ PFU in 5 μL of 1% PBS with 0,1% of Trypan blue dye, as reported before (Russel et al., 2003). To validate the model we injected Adeno-CMV-virus into glands of 2 groups of 3 mice per genotype (RBP$^{wt/wt}$ mTmG and RBP$^{fl/fl}$ mTmG). The 2 inguinal glands were injected in each mouse.

Glands from 6 mice per genotype were examined for the expression of EGFP reporter with fluorescent stereomicroscope 7 days after the injection. We were able to see that EGFP from mTmG reporter gene was expressed throughout the whole gland.

Glands from one group of mice were used for flow cytometry showing that both luminal and basal epithelial cells are infected. In addition, comparable amount of cells in both epithelial layers is infected both in RBP$^{wt/wt}$ mTmG and RBP$^{fl/fl}$ mTmG mice (Figure 32).

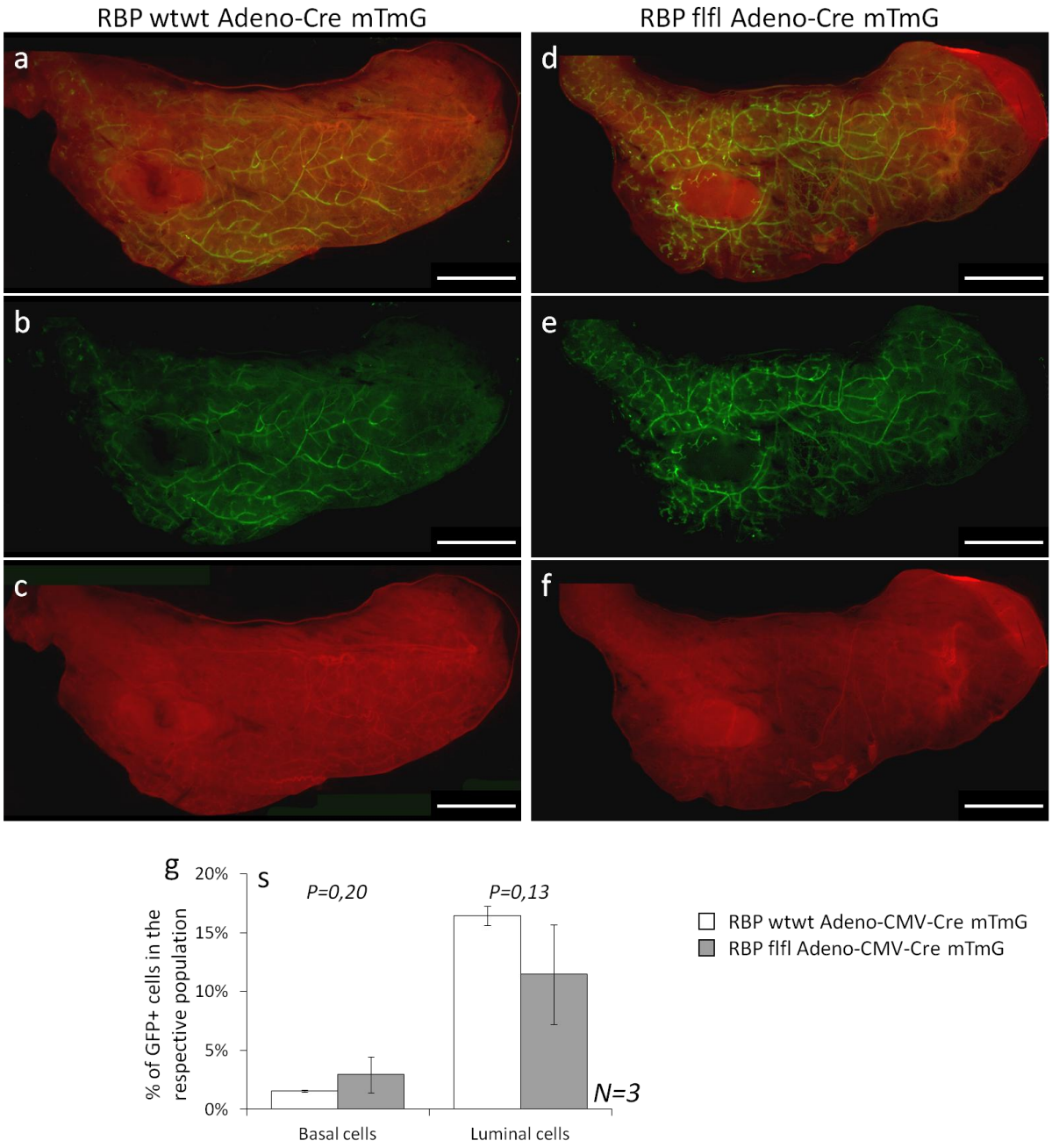

Figure 32. Wholemount and FAC analysis of the glands from the RBP^{floxed} Adeno-CMV-Cre mTmG mouse model. *a-c) Wholemount micrographs of RBP$^{wt/wt}$ Adeno-CMV-Cre mTmG mammary epithelium; d-f) Wholemount micrographs of RBP$^{fl/fl}$ Adeno-CMV-Cre mTmG mammary epithelium; g) Fluorescence activated cell analysis of EGFP expression in basal and luminal mammary epithelial cells in RBP$^{wt/wt}$ Adeno-CMV-Cre mTmG and RBP$^{fl/fl}$ Adeno-CMV-Cre mTmG mice (N=3). Scale bars represent 1 mm*

Glands from the other group of mice were used for the immunofluorescent staining. Analysis of the sections from RBP$^{wt/wt}$ mTmG and RBP$^{fl/fl}$ mTmG mice confirmed data from FAC analysis that both layers of mammary epithelial cells can get infected by Adeno-CMV-Cre virus (Figure 33).

RBP wtwt Adeno-Cre mTmG

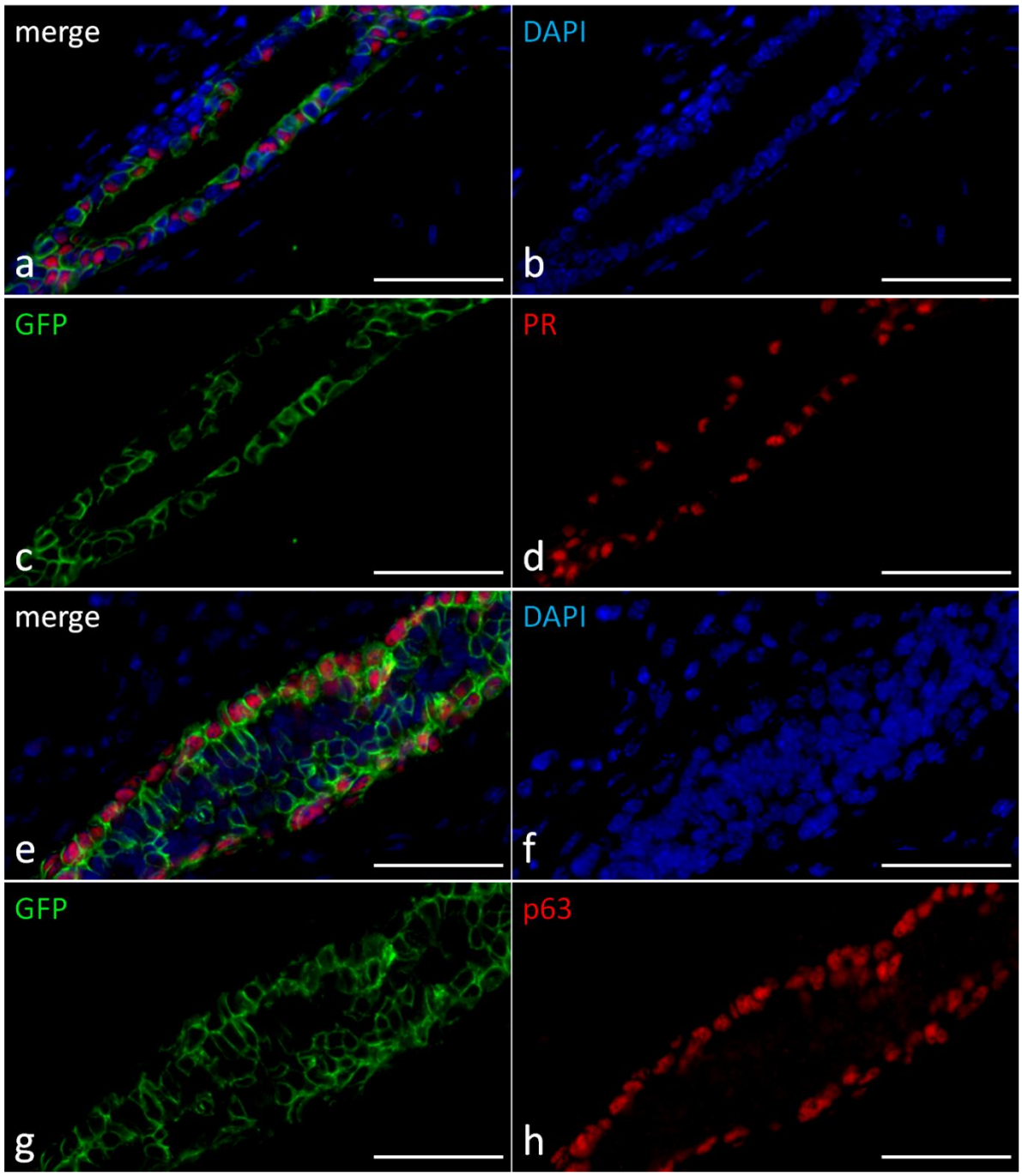

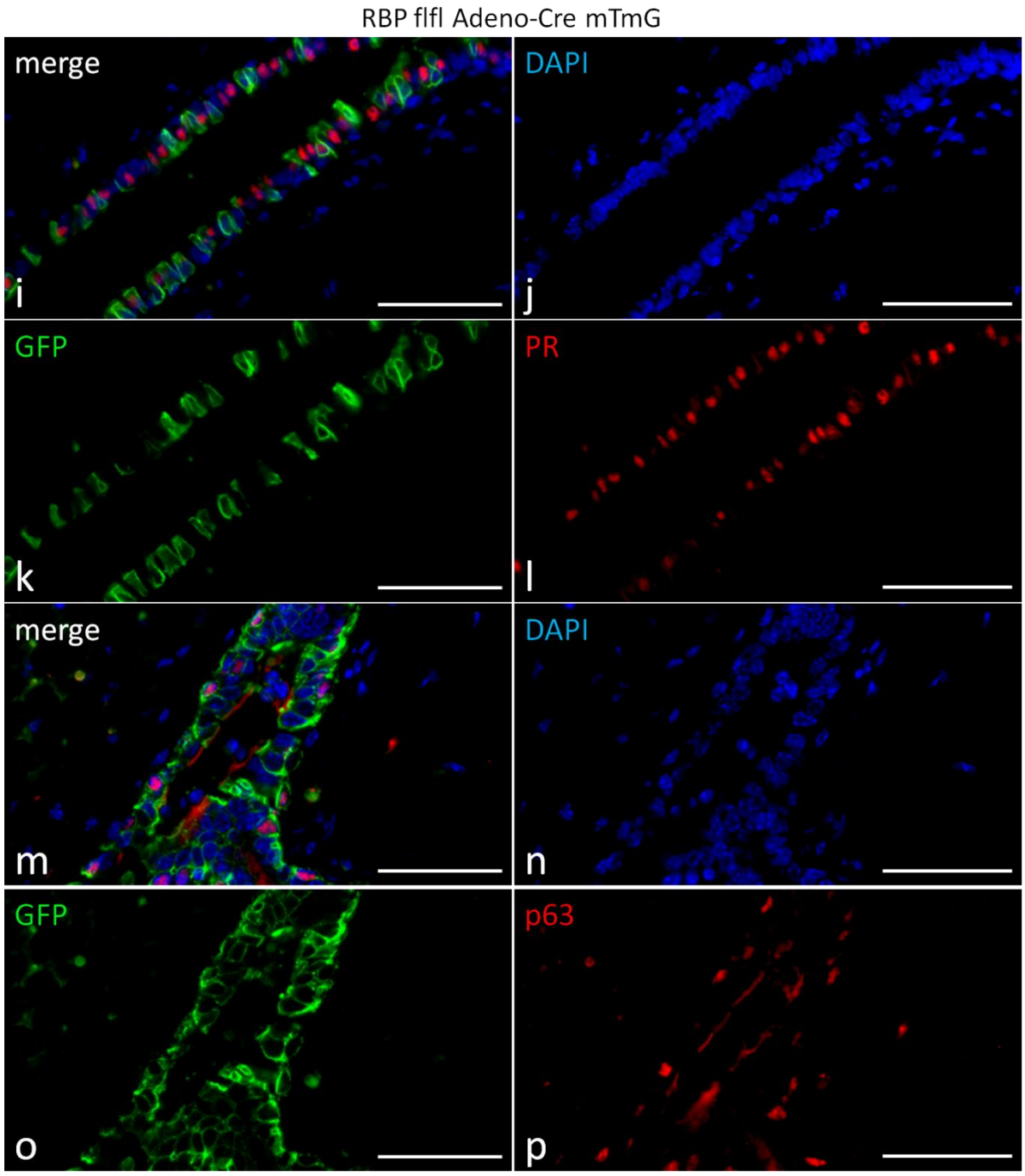

Figure 33. Colocalization of PR/p63 and EGFP reporter in the RBP^{floxed} Adeno-CMV-Cre mTmG transplanted glands*. Immunofluorescent co-staining (a-p) of EGFP with ER and PR in RBP$^{wt/wt}$ Adeno-CMV-Cre mTmG and RBP $^{fl/fl}$ Adeno-CMV-Cre mTmG mammary epithelium: a) – d) Co-staining of EGFP with PR in RBP$^{wt/wt}$ Adeno-CMV-Cre mTmG mammary epithelium (N=3); e) – h) Co-staining of EGFP with p63 in RBP$^{wt/wt}$ Adeno-CMV-Cre mTmG mammary epithelium (N=3); i) – l) Co-staining of EGFP with PR in RBP$^{fl/fl}$ Adeno-CMV-Cre mTmG mammary epithelium (N=3); m) – p) Co-staining of EGFP with p63 in RBP$^{fl/fl}$ Adeno-CMV-Cre mTmG mammary epithelium (N=3). Scale bars represent 50 μm*

Additionally we co-stained both RBP$^{wt/wt}$ mTmG and RBP$^{fl/fl}$ mTmG infected by Adeno-CMV-virus to show that RBP-Jκ gene is deleted and that RBP- jκ protein is absent from the cells expressing EGFP reporter of Cre activity. Co-staining confirmed that RBP-Jκ does not colocalize in the same cells with the EGFP reporter of Cre activity validating that Adeno-CMV-Cre is efficiently deleting RBP-Jκ gene in the RBP$^{fl/fl}$ mTmG mammary epithelium (Figure 34).

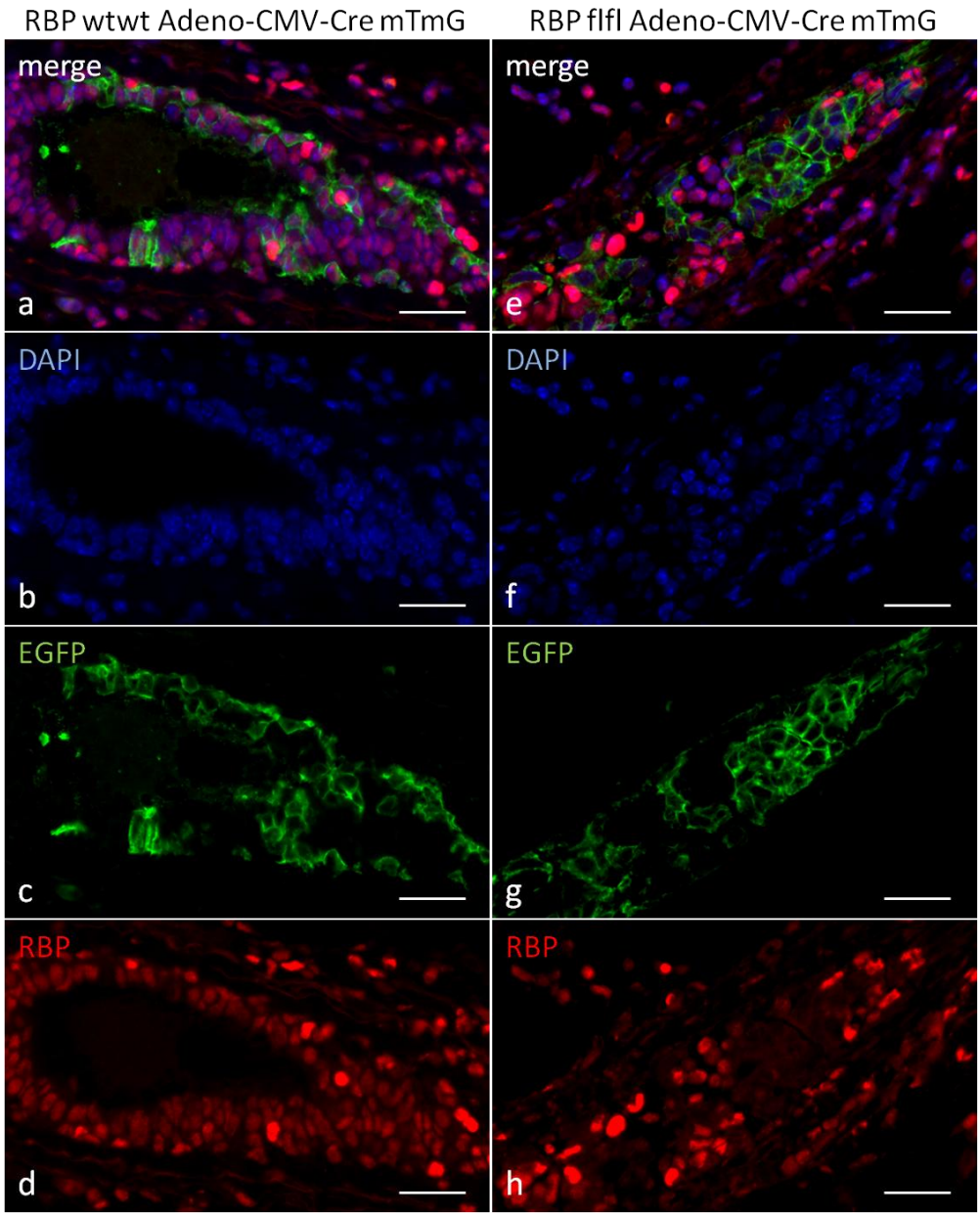

Figure 34. Colocalization of RBP-Jκ and EGFP reporter in the RBP^{floxed}Adeno-CMV-Cre mTmG transplanted glands. *Immunofluorescent co-staining (a-p) of EGFP and RBP-Jκ in RBP$^{wt/wt}$ Adeno-CMV-Cre mTmG and RBP $^{fl/fl}$ Adeno-CMV -Cre mTmG transplanted mammary epithelium: a) – d) Co-staining of EGFP and RBP-Jκ in RBP$^{wt/wt}$ Adeno-CMV-Cre mTmG mammary epithelium (N=6); e)-h) Co-staining of EGFP and RBP-Jκ in RBP$^{fl/fl}$ Adeno-CMV-Cre mTmG mammary epithelium (N=6). Scale bars represent 25 μm*

Following the validation of the model, we tested the hypothesis that Notch signaling via RBP-Jκ is responsible for the maintenance of the PR expression in HR+ mammary epithelial cells.

RESULTS

We injected Adeno-CMV-virus intraductally into 3 groups of 3 mice per genotype (RBP$^{wt/wt}$ mTmG and RBP$^{fl/fl}$ mTmG). The 2 inguinal glands were injected in each mouse. Each group of mice was examined at different time point to monitor overtime the effect of Notch abrogation via RBP-Jκ deletion at 7, 14 and 21 days.

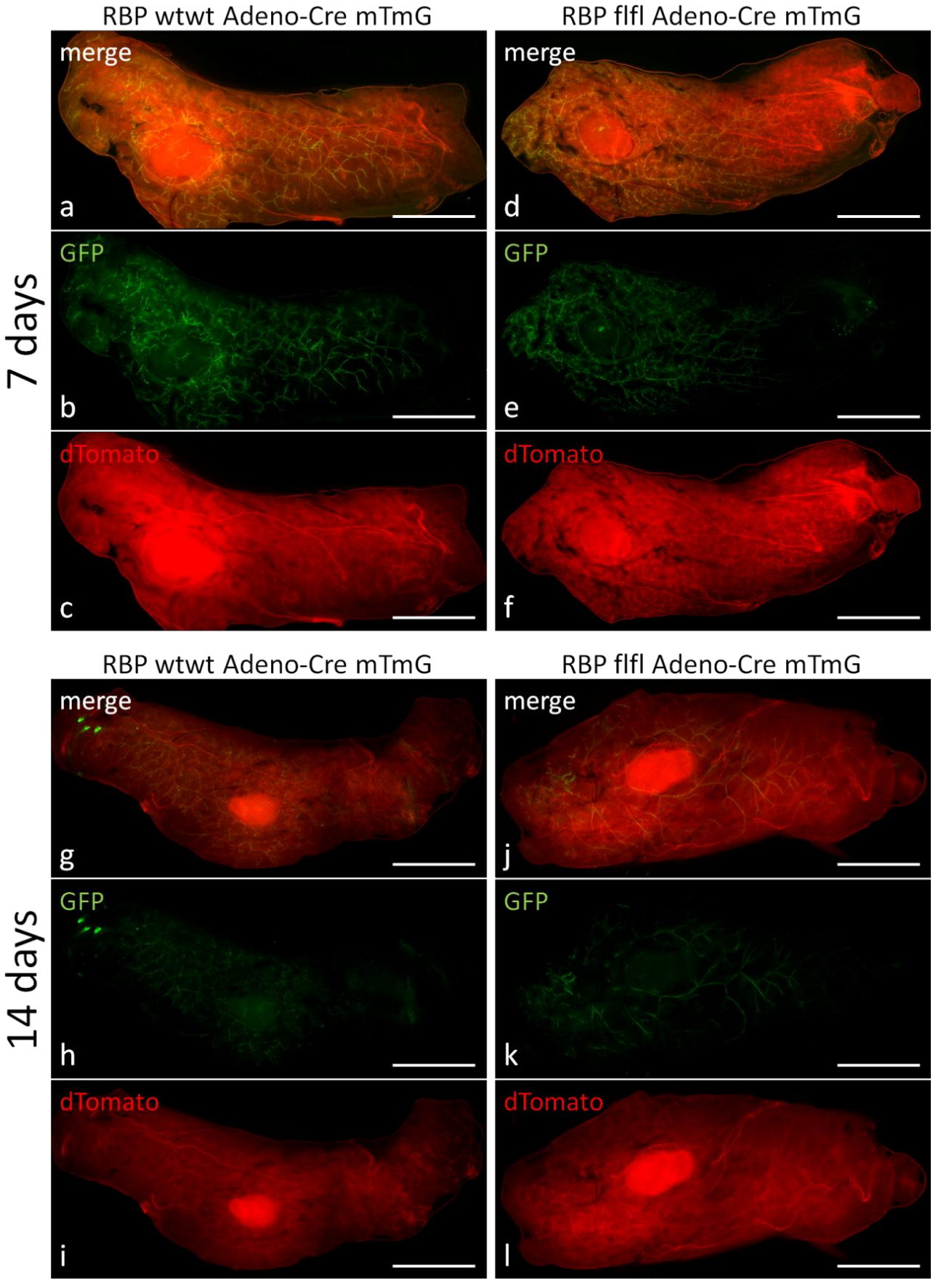
RBP wtwt Adeno-Cre mTmG
RBP flfl Adeno-Cre mTmG
7 days
14 days
merge
GFP
dTomato
a
b
c
d
e
f
g
h
i
j
k
l

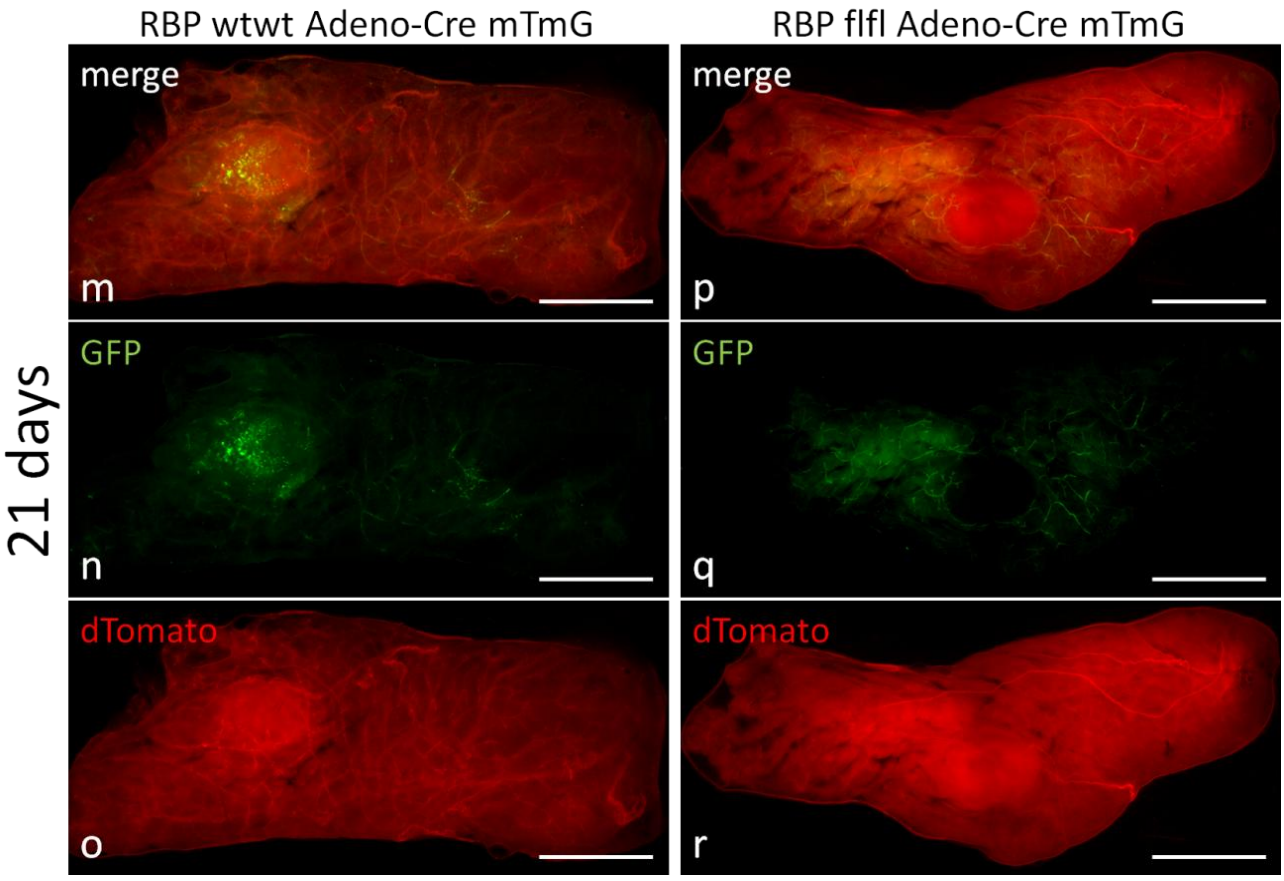

Figure 35. Wholemount analysis of the glands from the RBP^{floxed} Adeno-CMV-Cre mTmG mouse model*. a-c) Wholemount micrographs of RBP$^{wt/wt}$ Adeno-CMV-Cre mTmG and d-f) RBP$^{fl/fl}$ Adeno-CMV-Cre mTmG mammary epithelia 7 days after injection of the virus (N=3); g-i) Wholemount micrographs of RBP$^{wt/wt}$ Adeno-CMV-Cre mTmG and j-l) RBP$^{fl/fl}$ Adeno-CMV-Cre mTmG mammary epithelia 14 days after injection of the virus (N=3); m-o) Wholemount micrographs of RBP$^{wt/wt}$ Adeno-CMV-Cre mTmG and p-r) RBP$^{fl/fl}$ Adeno-CMV-Cre mTmG mammary epithelia 21 days after injection of the virus (N=3); Scale bars represent 2,5 mm*

Wholemount analysis by fluorescent stereomicroscope of the Adeno-CMV-Cre virus infected glands indicated the loss of EGFP post injection overtime (Figure 35). To confirm that less green fluorescence is present due to the lower amount of recombined cells expressing EGFP Cre reporter we quantified the number of green cells in the sections of glands infected by Adeno-CMV-Cre virus from both genotypes by immunofluorescent staining (Figure 36). For the quantification we used sections from 3 mice per genotype and time point. From each mouse an entire section of the gland was scanned and each cross-section of the mammary duct was included for quantification. On average 5000 cells were counted per section of the mammary gland.

RBP wtwt Adeno Cre mTmG

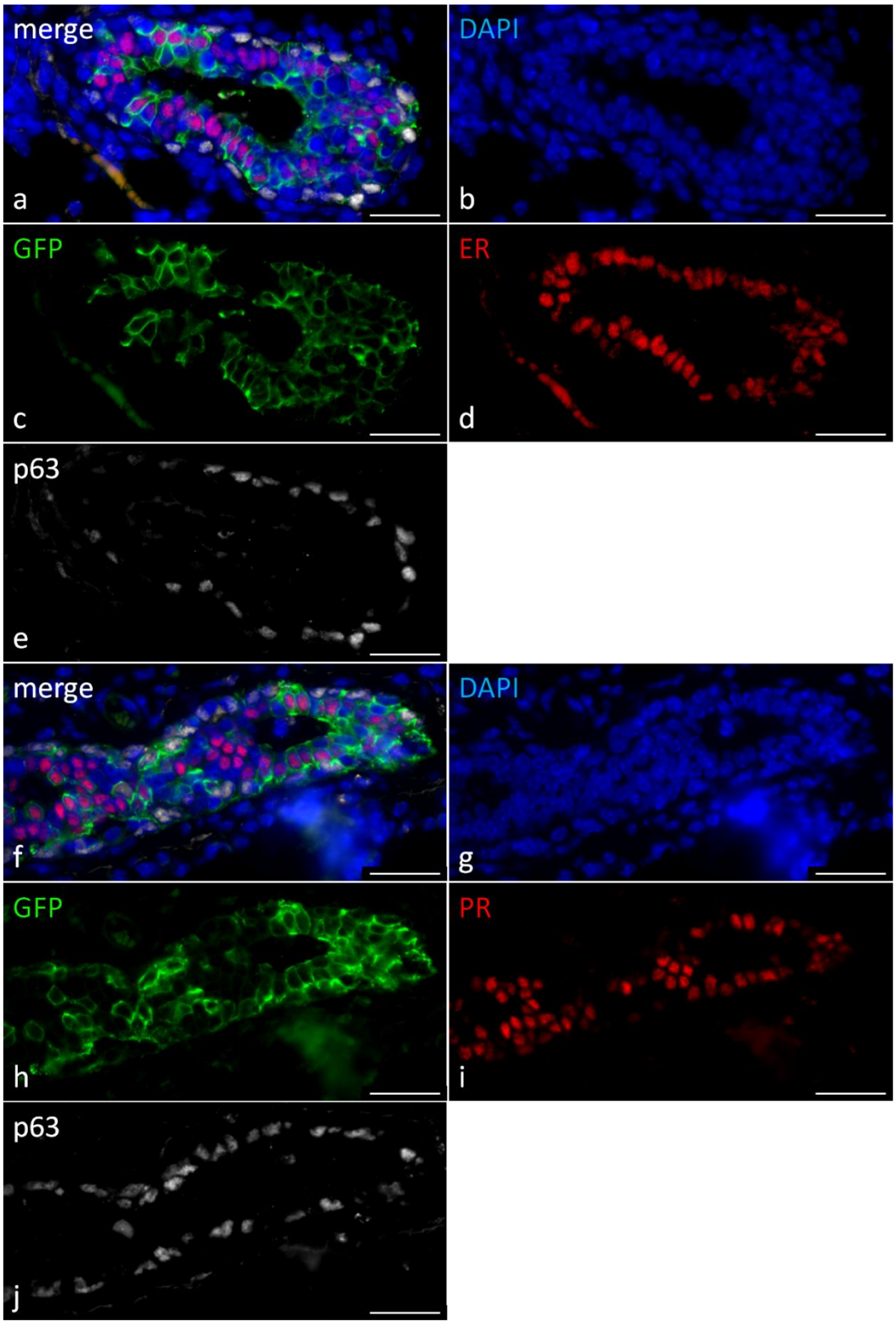

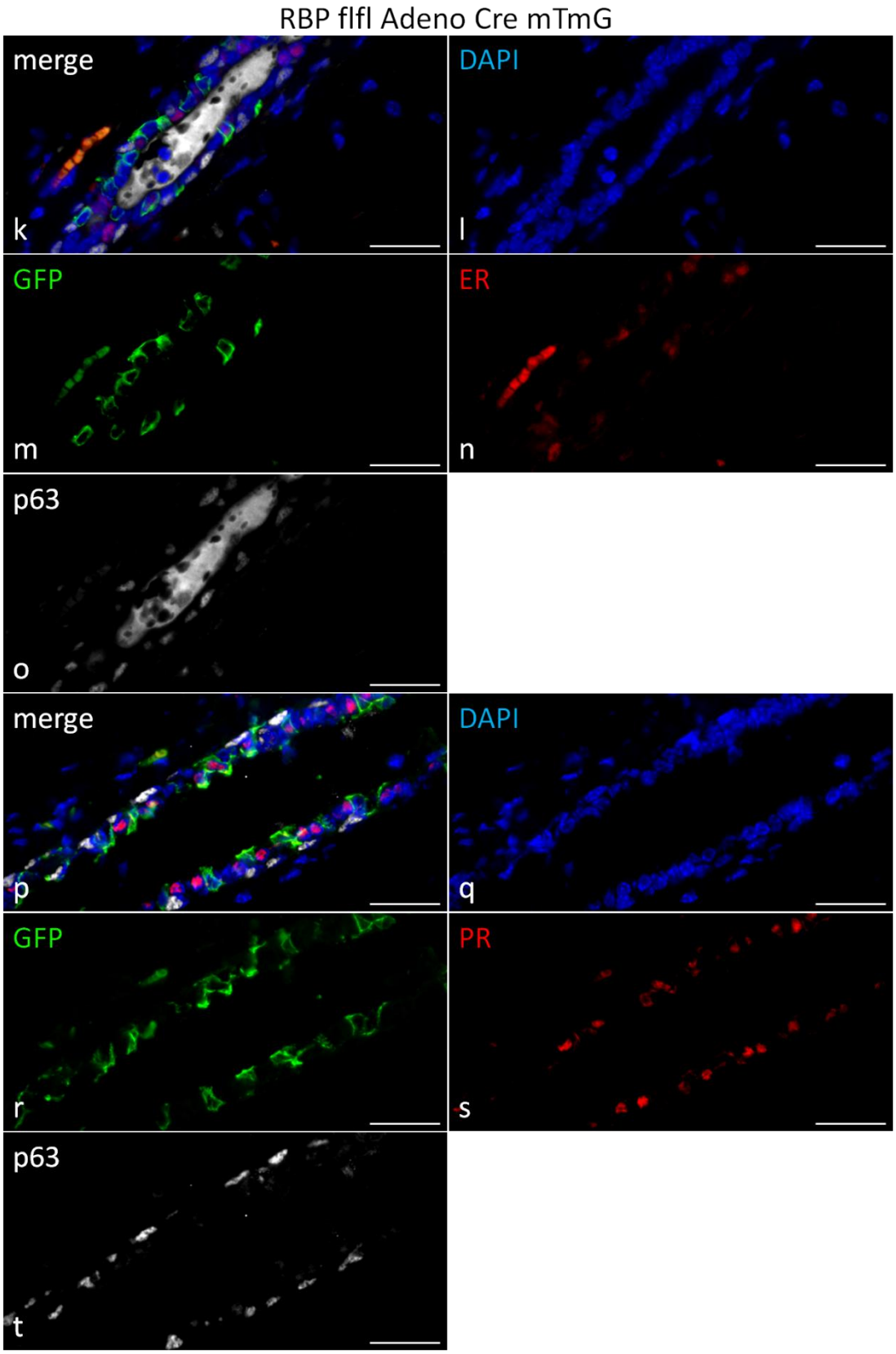

Figure 36. Colocalization of ER, PR and p63 with EGFP reporter in the RBP^{floxed} Adeno-CMV-Cre mTmG glands. *Immunofluorescent co-staining (a-p) of EGFP with ER, PR and p63 in RBP$^{wt/wt}$ Adeno-CMV-Cre mTmG and RBP $^{fl/fl}$ Adeno-CMV-Cre mTmG transplanted mammary epithelium: a) – e) Co-staining of EGFP with ER and p63 in RBP$^{wt/wt}$ Adeno-CMV-Cre mTmG mammary epithelium (N=3); f - j) Co-staining of EGFP with PR in RBP$^{wt/wt}$ Adeno-CMV-Cre mTmG mammary epithelium (N=3); k - o) Co-staining of EGFP with ER in RBP$^{fl/fl}$ Adeno-CMV-Cre mTmG mammary epithelium (N=3); m) - p) Co-staining of EGFP with PR in RBP$^{fl/fl}$ Adeno-CMV-Cre mTmG mammary epithelium (N=3). Scale bars represent 25 µm.*

Quantification of cell types in the infected epithelium showed that there is no significant difference in the amount of basal or luminal cells in the total $RBP^{wt/wt}$ Adeno-CMV-Cre mTmG and $RBP^{fl/fl}$ Adeno-CMV-Cre mTmG epithelia (Figure 37.a,b). Also the ratio of the luminal versus basal cell type was not differing from expected values from an intact epithelium (twice the amount of luminal cells) (37.a,b). Quantification of the portion of ER+ and PR+ cells in the total epithelium showed that there was no significant difference in the number of HR+ cells defined by either ER or PR between $RBP^{wt/wt}$ Adeno-CMV-Cre mTmG and $RBP^{fl/fl}$ Adeno-CMV-Cre mTmG within the time-point and the amount of HR+ cells was not differing from standard values expected in the intact epithelium. Therefore we concluded that the infection does not interfere with the regular proportions of cell types within the mammary epithelium (Figure 37.c,d).

Quantification of the number of cells in the infected glands showed that within the same time-point group there was no difference in the amount of EGFP Cre reporter expressing cells between $RBP^{wt/wt}$ Adeno-CMV-Cre mTmG and $RBP^{fl/fl}$ Adeno-CMV-Cre mTmG epithelia. However, when different time-points were compared we observed a significant loss of EGFP expressing cells with time in both genotypes (7 days - fl:19,4±2,1; wt:21,9±1,8; and 14 days - fl:12,9±1,0; wt:12,7±1,4; 21 days - fl:4,6±0,5; wt:5,8±0,5) (Figure 37.e).

The classical infection pathway of the Adenovirus involves the lysis of a cell by a virus to produce new particles (Reviewed in Leopold and Crystal, 2007). Since we observed a dramatic decrease in the amount of infected cells in both $RBP^{wt/wt}$ Adeno-CMV-Cre mTmG and $RBP^{fl/fl}$ Adeno-CMV-Cre mTmG mammary gland epithelia, we concluded that Adeno-CMV virus had a significant cytotoxic effect 14 and 21 day after the infection.

Quantification of the basal and luminal cells within the EGFP Cre reporter expressing population showed that there was no significant differences in the proportions of infected basal cells per genotype/time-point and infected luminal cells per genotype/time-point (Figure 37.f,g).

Quantification of the number of ER+ cells showed no significant change between $RBP^{wt/wt}$ Adeno-CMV-Cre mTmG and $RBP^{fl/fl}$ Adeno-CMV-Cre mTmG total epithelium overtime (Figure37.h). Contrarily, the amount of PR positive cells was significantly lower in the EGFP expressing population of the $RBP^{fl/fl}$ Adeno-CMV-Cre mTmG epithelium (30,8%±5,4%) compared to $RBP^{wt/wt}$ Adeno-CMV-Cre mTmG (18,7%±4,7%) after 7 days (Figure 37.i). Difference disappeared after 14 and 21 days (Figure 37.i). This observation was even more striking when we compared the portion of PR expressing cells in only luminal EGFP expressing populations of $RBP^{wt/wt}$ Adeno-CMV-Cre mTmG and $RBP^{fl/fl}$ Adeno-CMV-Cre mTmG at the different time points: 7 days (38,3%±3,9% for $RBP^{wt/wt}$ and 20,5%±5,9% for $RBP^{fl/fl}$) and 14 days (57,6%±10,7% for $RBP^{wt/wt}$ and 44,4%±7,9% for $RBP^{fl/fl}$) after injection. The difference was once more lost at 21 day after injection (Figure 37.k).

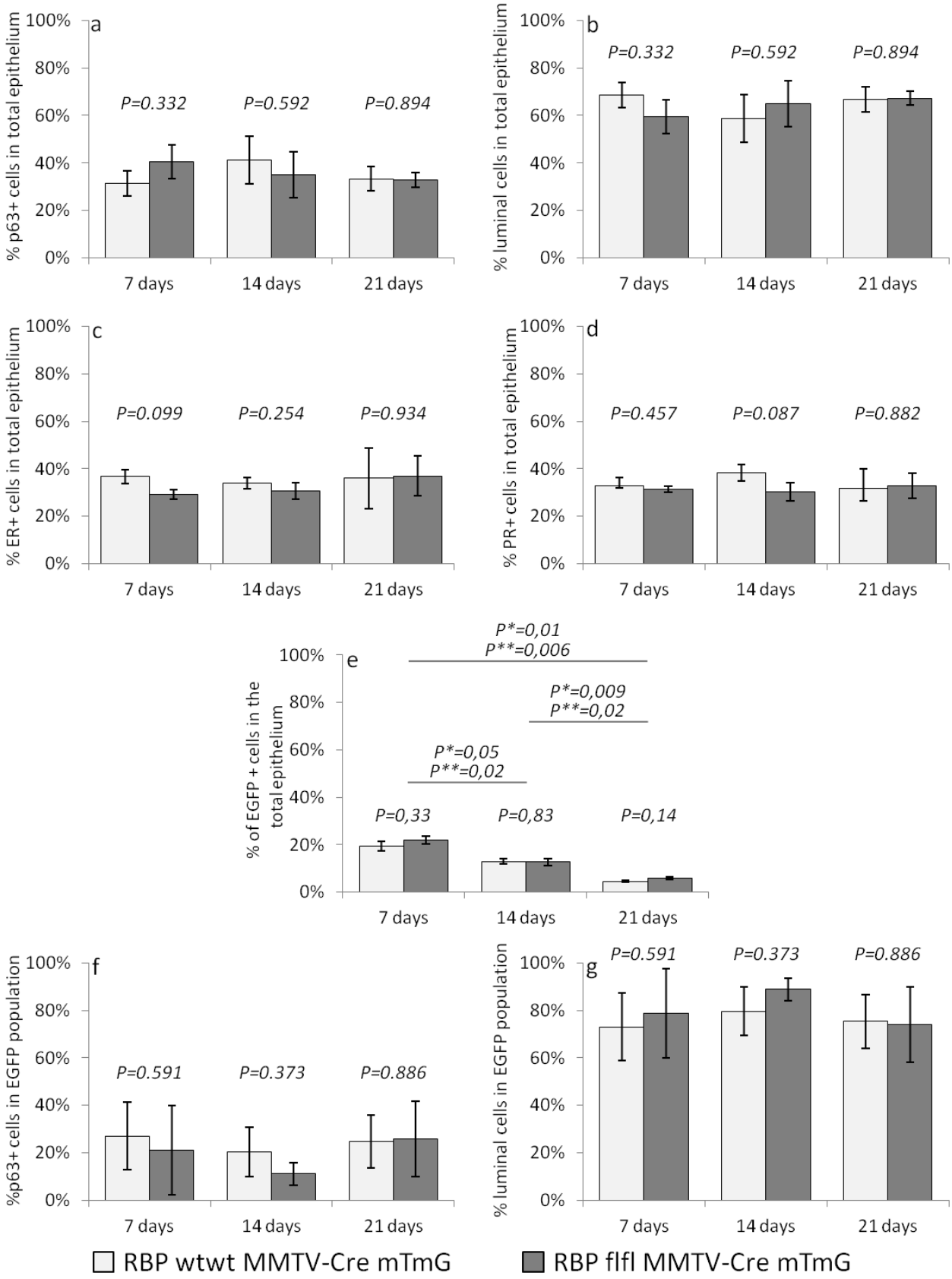
a
% p63+ cells in total epithelium
P=0.332
P=0.592
P=0.894
b
% luminal cells in total epithelium
P=0.332
P=0.592
P=0.894
c
% ER+ cells in total epithelium
P=0.099
P=0.254
P=0.934
d
% PR+ cells in total epithelium
P=0.457
P=0.087
P=0.882
e
% of EGFP + cells in the total epithelium
P*=0,01
P**=0,006
P*=0,009
P**=0,02
P*=0,05
P**=0,02
P=0,33
P=0,83
P=0,14
f
%p63+ cells in EGFP population
P=0.591
P=0.373
P=0.886
g
% luminal cells in EGFP population
P=0.591
P=0.373
P=0.886
100%
80%
60%
40%
20%
0%
7 days
14 days
21 days
RBP wtwt MMTV-Cre mTmG
RBP flfl MMTV-Cre mTmG

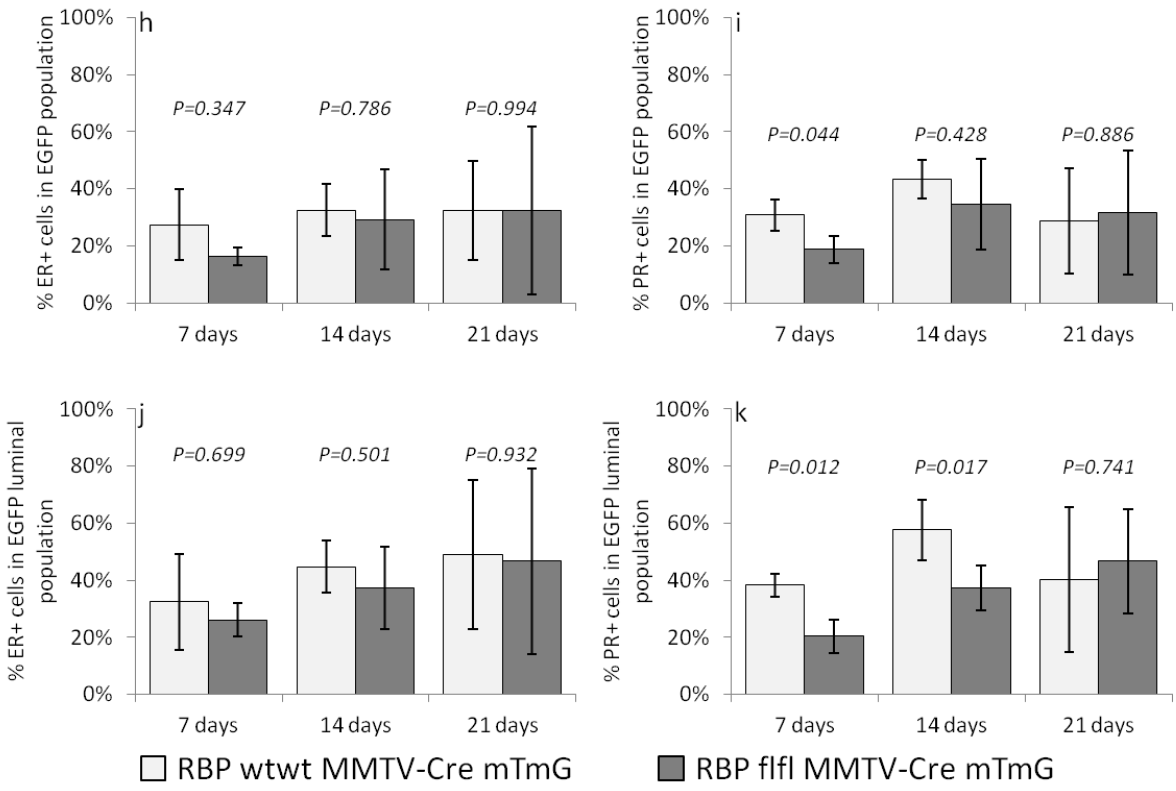

Figure 37. Quantification of colocalization of ER, PR and p63 with EGFP reporter in the RBP^{floxed} Adeno-CMV-Cre mTmG transplanted glands*. a) Portion of basal cells defined by the expression of p63 in the total mammary epithelium (N=3 per genotype); b) Portion of luminal cells defined by position within the duct and by lack of p63 expression in the mammary epithelium (N=3 per genotype); c) Portion of ER positive cells in the total mammary epithelium (N=3 per genotype); d) Portion of PR positive cells in the the total mammary epithelium (N=3 per genotype); e) Portion of EGFP positive cells in the the total mammary epithelium (N=3 per genotype). P values represent comparisons between RBP$^{wt/wt}$ Adeno-CMV-Cre mTmG and RBP$^{fl/fl}$ Adeno-CMV-Cre mTmG epithelium within the same time point. P* values represent comparisons between RBP$^{wt/wt}$ Adeno-CMV-Cre mTmG epithelium between different time points connected with the line. P** values represent comparisons between RBP$^{fl/fl}$ Adeno-CMV-Cre mTmG epithelium between different time points connected with the line ; f) Portion of basal cells in the total EGFP population of mammary epithelium (N=3 per genotype); g) Portion of luminal cells in in the total EGFP population of mammary epithelium (N=3 per genotype); h) Portion of ER positive luminal cells in in the total EGFP population of mammary epithelium (N=3 per genotype); i) Portion of PR positive luminal cells in in the total EGFP population of mammary epithelium (N=3 per genotype); j) Portion of ER positive luminal cells in in the EGFP+ luminal population of mammary epithelium (N=3 per genotype); k) Portion of PR positive luminal cells in in the EGFP+ luminal population of mammary epithelium (N=3 per genotype). Statistical significance of all comparisons was calculated by unpaired student's T-test.*

CONCLUSION

Time directed abrogation of Notch signaling by conditional deletion of floxed RBP-Jκ gene via Adeno-CMV-Cre infection resulted in a significant loss of the PR+ cells shortly after infection (7 days). At the same time point loss of HR+ cells in the entire epithelium or alteration of the ratio luminal/basal cells were not observed. These results are in line with our hypothesis that Notch signaling is responsible for the activation of PR expression in order to maintain the levels of PR in the HR+ mammary epithelial cells.

Adeno-CMV-Cre infection showed strong cytotoxicity in the longer time points (14 days and 21 days) showing 2-fold loss of infected cells after 14 days and 4 fold loss after 21 days. Therefore it is not

possible to distinguish whether the changes in the amount of PR positive cells in infected population at later time points (14 days and 21 days) were caused by the abrogation of Notch signaling or by cytotoxicity of the Adeno-CMV-Cre virus. Hence, we can draw conclusions only from the time point of 7 days.

INHIBITION OF CANONICAL NOTCH SIGNALING IN THE ENDOGENOUS MAMMARY EPITHELIUM VIA INTRADUCTAL INJECTION OF Γ-SECRETASE INHIBITOR DAPT

INTRODUCTION AND WORKING HYPOTHESIS

Canonical Notch signaling activates target genes through activation of RBP-Jκ regulated by Notch receptor intracellular domain. However, RBP-Jκ has been shown to control the expression of target genes without activation by Notch receptor (reviewed in Sanalkumar et al., 2010). To activate Notch target genes, Notch receptor intracellular domain is cleaved by the γ-secretase complex, released from the membrane and translocated to the nucleus where it can bind to RBP-Jκ protein (Saxena et al., 2001). This interaction will activate the recruitment of the activation complex on the RBP-Jκ protein and activate the expression of the targeted genes. N-[N-(3,5-Difluorophenacetyl)-L-alanyl]-S-phenylglycine t-butyl ester (DAPT) is a compound that abrogates γ-secretase cleavage of Notch receptor to efficiently inhibit canonical Notch signaling *in vivo* (Micchelli et al., 2003).

Experiments from 4 different mouse models presented so far showed that the Notch active population is expressing HRs. In addition, abrogation of Notch signaling via RBP-Jκ deletion in this population induces the loss of PR expression. Therefore we hypothesized that Notch signaling is responsible for the regulation of PR expression.

To test whether canonical Notch is responsible for this regulation we injected DAPT intraductally into the 8-weeks-old wild type female mice and analyzed the PR expression by qPCR and immunofluorescent co-staining for ER and PR of the DAPT- and DMSO-treated glands.

RESULTS

To test whether canonical Notch signaling is responsible for PR expression regulation in the Wnt4 expressing population of HR+ mammary epithelial cells we inhibited γ-secretase complex in the mammary epithelium via intraductal injection of DAPT.

For this experiment DAPT dissolved in DMSO and DMSO alone as vehicle were injected contralaterally through the teats in the pair of inguinal glands of 3 mice. Forty eight hours after the injection, glands were isolated and RNA was extracted. Gene expressions of ER and PR were measured by qPCR. As a positive control we used known Notch target Hey1 and for the normalization of the values we used house-keeping gene 36B4.

Quantitative PCR showed that upon Notch inhibition via DAPT treatment the expression of the control gene Hey1 was significantly reduced by 62,1%±5,2% indicating that the drug successfully interfered with Notch signaling (Figure 38.a). Expression of ER was not significantly affected by this treatment unlike the expression of PR which was reduced by 41,2%±11,2% (Figure 38.b,c).

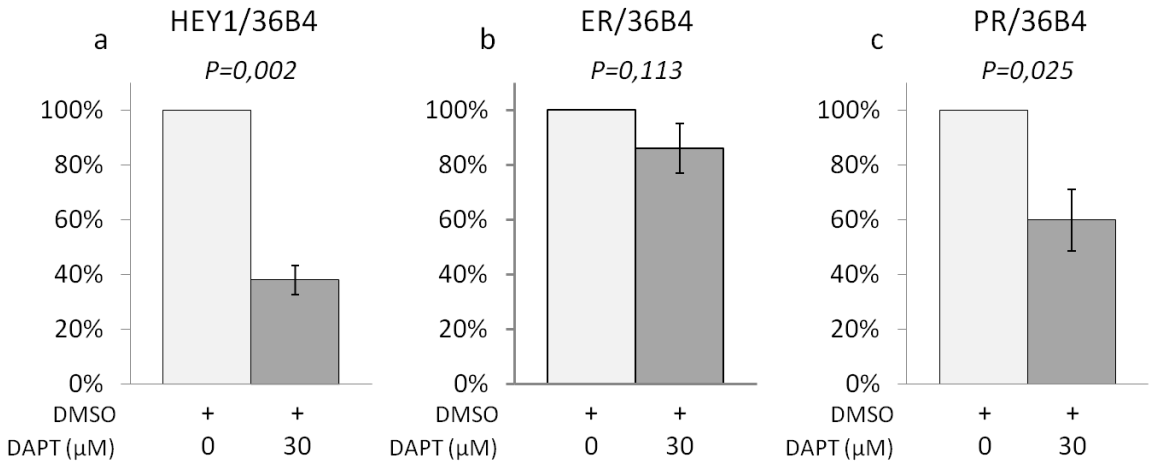

Figure 38. Effects of inhibition of canonical Notch signaling by DAPT in vivo. *Quantitative PCR analysis of mRNA levels in the mouse mammary gland treated with only vehicle (DMSO) and γ-secretase inhibitor DAPT (30μM) injected intraductally to the contralateral glands (N=3). 36B4 was used as a house-keeping gene for normalization. Statistical significance was calculated using paired Student's T-test*

Additionally we stained sections from 3 DAPT treated and 3 DMSO control contralateral mammary glands from 3 different mice to analyze colocalization of ER and PR in the mammary epithelium (Figure 39.a-h). There were minor differences in the number of ER and PR expressing cells in total epithelium when sections from DMSO injected and DAPT injected glands were compared. When we analyzed cells that are expressing both ER and PR we noticed that in the control glands 98,9%±2,6% of ER expressing cells were also expressing PR. However, in the DAPT injected glands, the amount of ER+ cells expressing PR was significantly smaller (85,9%±3,9%) confirming that upon abrogation of Notch signaling via inhibition of γ-secretase complex only a subpopulation of ER expressing cells lost PR expression (Figure 39.i).

CONCLUSION

Abrogation of Notch signaling by inhibition of γ-secretase via intraductal injection of DAPT results in the loss of PR expression analyzed by quantitative PCR. This result confirms our hypothesis that canonical Notch signaling is responsible for the loss of PR expression in the HR+ mammary epithelial cells.

Quantification of the immunofluorescent staining for ER and PR showed that ≈14% of the ER+ cells loses the expression of PR.

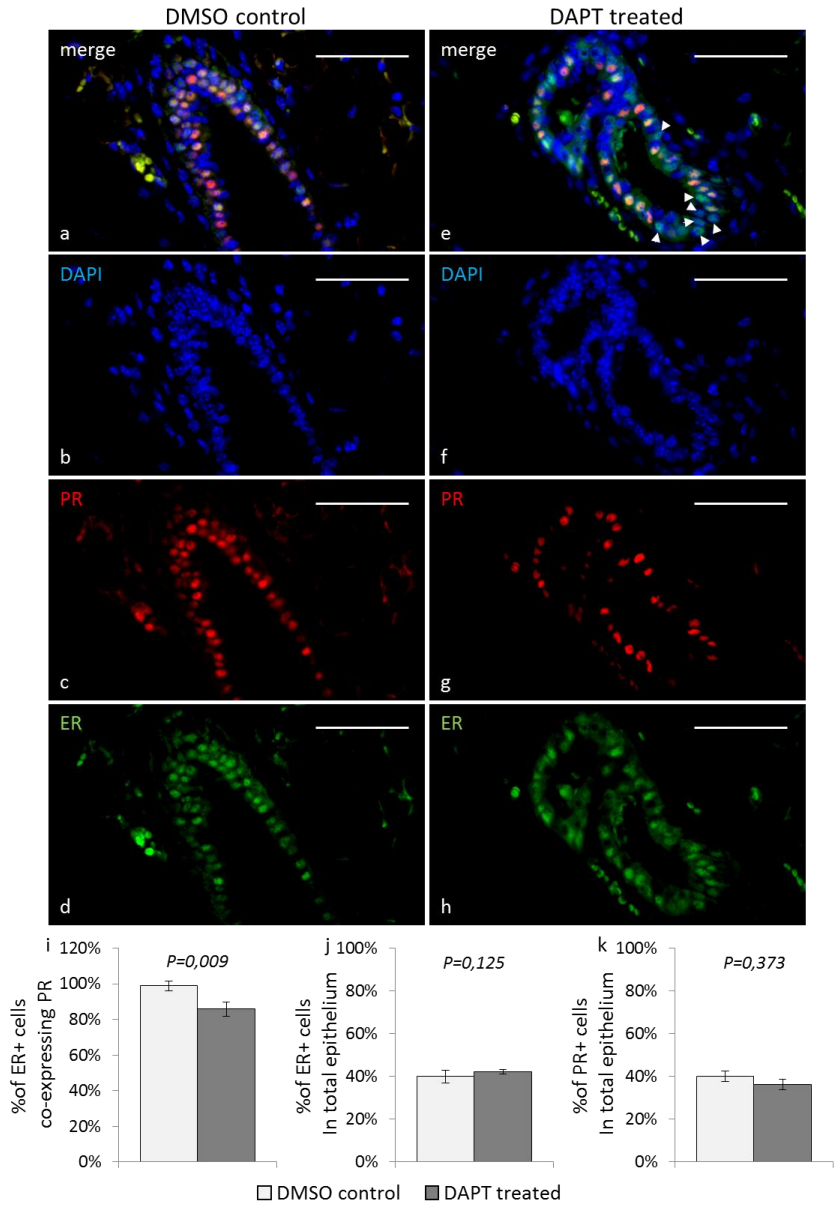

Figure 39: Colocalization and quantification of co-localization of ER and PR in wild type glands inected with wehicle and DAPT contralaterally*. a) - d) Co-staining of ER and PR in in the wild type mammary glands injected with wehicle (DMSO) (N=3) e) - h) Co-staining of ER and PR in wild type mammary glands injected with DAPT in DMSO (N=3) White arrows point cells expressing only PR. Scale bars represent 50 µm; i) Portion of ER+ cells co expressing PR in the DMSO treated vs. DAPT treated mammary gland (N=3); j) Portion of ER+ cells in total epithelium of DMSO treated vs. DAPT treated mammary gland (N=3); k) Portion of ER+ cells in total epithelium of DMSO treated vs. DAPT treated mammary gland (N=3). Statistical significance was calculated using paired Student's T-test.*

BIOINFORMATICAL ANALYSIS OF THE MOUSE PROGESTERONE RECEPTOR PROMOTER

INTRODUCTION AND WORKING HYPOTHESIS

Loss of PR expression upon Notch signaling abrogation via deletion of RBP-Jκ in the Wnt4 expressing HR+ cells led to hypothesize that Notch signaling is regulating the expression of PR gene in these cells. To test whether RBP-Jκ may bind directly to PR promoter, we performed bioinformatical analysis of both mouse and human PR promoter to identify RBP-Jκ binding motifs. Additionally, we performed multiple alignment of PR promoter region from different species to investigate the conservation of RBP-Jκ binding sites.

RESULTS

To analyze PR promoter in order to find RBP-Jκ motifs, we performed an analysis of the PR promoter sequence by short motifs search tool "*Dreg"* in the EMBOSS software (www.emboss.bioinformatics.nl). The tool *"Dreg"* identified 4 putative RBP-Jκ binding sites in the PR promoter region (1st at -2636 to -2631, 2nd at -2077 to 2072, 3rd at -1711 to 1706 and 4th at -1495 to -1490) (Figure 40).

Figure 40. Sequence of the mouse PR promoter. *ATG starting codon is shown in green. Estrogen responsive element is shown in red. RBP-Jκ putative binding sites are marked in yellow.*

Analysis of the human promoter revealed two putative RBP-Jκ motifs (1st at -1890 to 1885 and 2nd at -543 to -537) (Figure 41)

Additional analysis of both mouse and human PR promoters was performed using a tool Pro-Coffee which aligns homologous promoter regions (Erb et al., 2011). In the alignment we additionally included PR promoters of chimpanzee, pig, cat and rat, and checked if putative RBP-Jκ binding sites in the mouse and human PR promoter regions are conserved.

Analysis showed that estrogen binding site is highly conserved showing identity in all the species except pig. In pig only the last nucleotide of the motif was different (Fgure 42.a).

Figure 41. Sequence of the human PR promoter. *ATG starting codon is shown in green. Estrogen responsive element is shown in red. RBP-Jκ putative binding sites are marked in yellow.*

Analysis showed that binding sites 3 and 4 are positioned in highly conserved area (Figure 42.d,e), binding site 1 in conserved area (Figure 42.b) and binding site 2 in averagely conserved area (Figure 42.c). Although mouse RBP-Jκ binding sites 1, 3 and 4 were in the conserved areas of the promoter, they did not show identity with the human promoter, therefore we cannot consider that RBP-Jκ can bind at the exactly same position. RBP-Jκ binding site 3 showed identity with the rat promoter suggesting that it might be conserved in rodents.

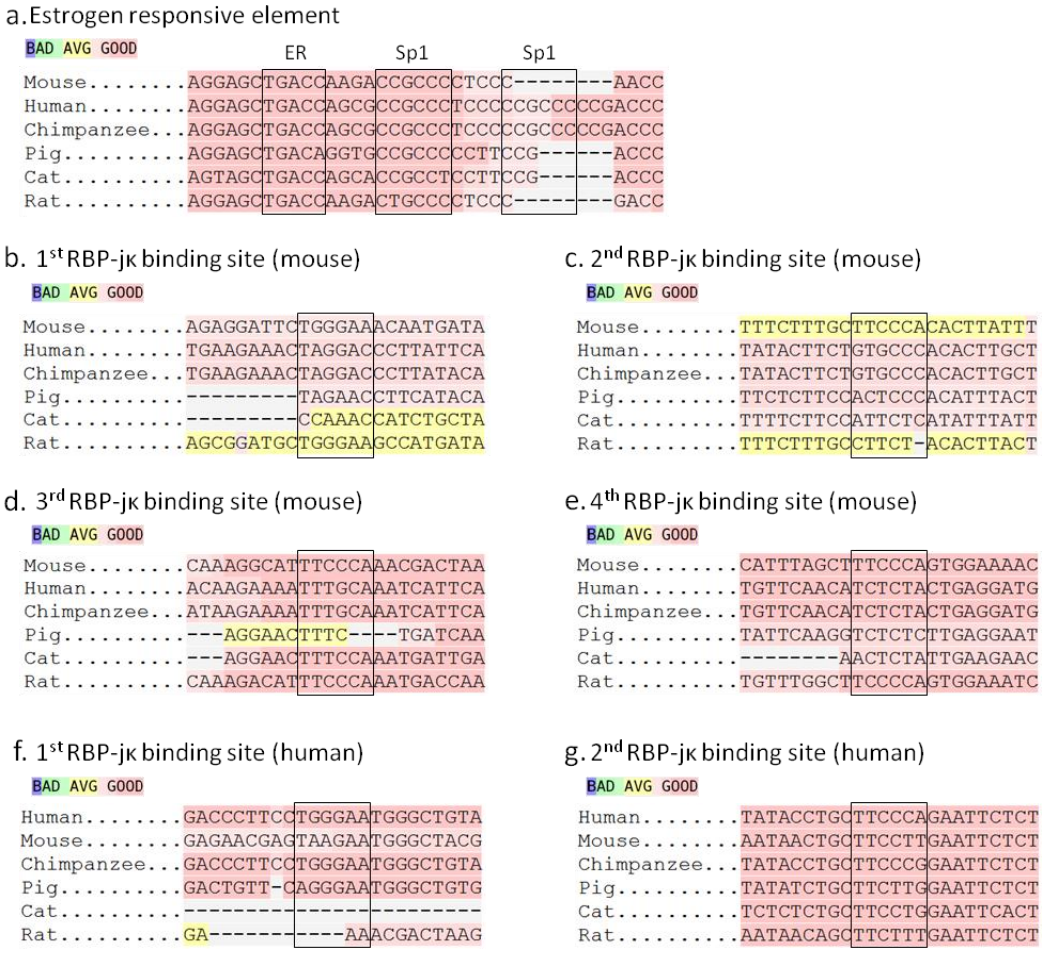

Figure 42. Multiple alignment of the ER responsive element, and RBP-Jκ binding sites in the PR promoter region of human, mouse, chimpanzee, pig, cat and rat. *a) Multiple alignment of the ER responsive element in the PR promoter region; b) Multiple alignment of the 1st RBP-Jκ binding site in the PR promoter region of the mouse; c) Multiple alignment of the 2nd RBP-Jκ binding site in the PR promoter region of the mouse; d) Multiple alignment of the 3rd RBP-Jκ binding site in the PR promoter region of the mouse; e) Multiple alignment of the 4th RBP-Jκ binding site in the PR promoter region of the mouse; f) Multiple alignment of the 1st RBP-Jκ binding site in the PR promoter region of the human; g) Multiple alignment of the 2nd RBP-Jκ binding site in the PR promoter region of the human. Multiple alignment of the PR promoter regions was performed with Pro-Coffee software.*

In the same set of data from the multiple alignment analysis we were able to observe that human RBP-Jκ binding sites are positioned in the highly conserved area but did not show identity with the mouse PR promoter region. However, RBP-Jκ binding site 1 was conserved in the chimpanzee suggesting that it might be conserved in primates (Figure 42.f,g).

CONCLUSION

Bioinformatical analysis of the PR promoter region in mouse and human showed that there are 4 putative RBP-Jκ binding sites in the mouse PR promoter and 2 putative RBP-Jκ binding sites in the human PR promoter. None of the binding sites showed identity between mouse and human.

CHROMATIN IMMUNOPRECIPITATION ASSAY OF PR PROMOTER WITH RBP

INTRODUCTION AND WORKING HYPOTHESIS

Bioinformatical analysis revealed 4 putative RBP-Jκ binding sites in the mouse PR promoter region suggesting that Notch signaling via RBP-Jκ could regulate the expression of the PR via direct binding to the PR promoter.

Therefore to test the hypothesis that RBP-Jκ binds to the PR promoter we performed chromatin immunoprecipitation (ChIP) assay with RBP-Jκ antibody to confirm the interaction.

RESULTS.

We isolated 6 glands per mouse from three groups of three 6-weeks-old mice forming three samples of 18 glands each. Epithelial organoids were isolated from three samples and ChIP was performed using RBP-Jκ antibody.

We examined the binding of RBP-Jκ to all 4 putative binding sites in the promoter region. As a positive control we analyzed binding of RBP-Jκ to the regulatory region of the Notch target gene Hey1 (Maier and Gesler, 2000). As a negative control we used several conditions: 1. IgG instead of antibody for immunoprecipitation; 2. Primers for sequence within the PR gene which does not contain RBP-Jκ binding motif for PCR analysis of the immunoprecipitated DNA; 3. Water instead of immunoprecipitated DNA for each couple of primers in the PCR analysis.

Qualitative analysis of ChIP by PCR confirmed that RBP-Jκ can bind to site 1 and 3 as well as to RBP responsive element of the Hey1 promoter. Importantly, there was no binding to an unrelated internal sequence or to binding sites 2 and 4 (Figure 43.a).

Quantitative analysis of ChIP to the binding sites 1 and 3 as well as to RBP-Jκ responsive element in Hey1 promoter by real-time PCR showed that in 2 out of 3 samples RBP-Jκ significantly binds to all tested sequences. Binding of the RBP-Jκ protein to Hey1 promoter was stronger than binding to RBP-Jκ responsive elements from the PR promoter; ≈5-fold stronger than binding site 1 and ≈35-fold stronger than binding site 3 (Figure 43.b-d).

CONCLUSION.

Chromatin immunoprecipitation assay showed that RBP-Jκ binds to its responsive elements present in the PR promoter, in particular binding site 1 and 3. Binding of RBP-Jκ to sites 1 and 3 is weaker than the binding to the promoter of the Notch target gene Hey1.

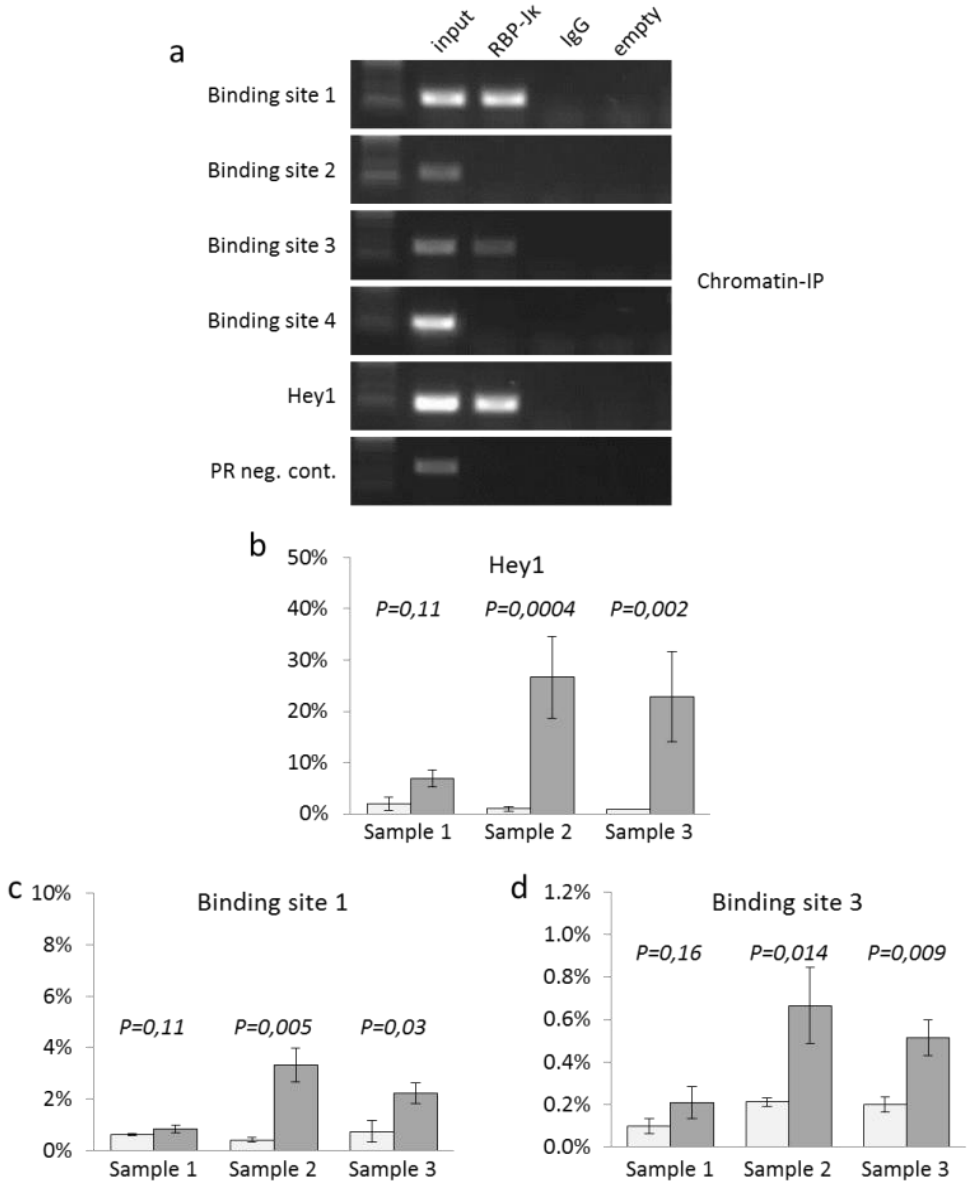

Figure 43. Chromatin immunoprecipitation with RBP-Jκ antibody. *Rbp-Jκ binds to sites 1 and 3 and has no affinity to sites 2 and 4. a) Qualitative analysis of the Chromatin immunoprecipitation assay: First lane is showing input DNA used to perform immunoprecipitation. Second lane is showing immunoprecipitation RBP-Jκ antibody. Third lane is showing immunoprecipitation using IgG as a negative control. Fourth lane is showing negative control using water for the PCR reaction (N=3); b) Quantitative analysis of the chromatin immunoprecipitation with RBP-Jκ antibody to RBP-Jκ responsive element in the Hey1 promoter (N=3); c) Quantitative analysis of the chromatin immunoprecipitation with RBP-Jκ antibody to RBP-Jκ binding site 1 in the PR promoter (N=3); d) Quantitative analysis of the chromatin immunoprecipitation with RBP-Jκ antibody to RBP-Jκ binding site 1 in the PR promoter (N=3).*

ABROGATION OF NOTCH SIGNALING IN HR+ BREAST CANCER CELL LINES

INTRODUCTION AND WORKING HYPOTHESIS

Two thirds of all breast cancers express ER and are treated with anti-estrogens, but resistance to the therapy often occurs (reviewed in Pritchard 2005 and Tobias 2004). Observations on the HR+ breast cancer cell lines suggested a mechanism of resistance via Notch signaling. In the absence of estrogens, Notch signaling can become activated and directly stimulate ER-dependent transcription, overriding the inhibitory effects of anti-estrogens (Rizzo et al., 2008)

Data from mouse models in this project strongly support the hypothesis that Notch signaling is included in the regulation of the expression of PR, an ER target gene. Although RBP-Jκ responsive elements from mouse PR promoter are not showing identity to the human PR promoter, mouse and human PR promoter are showing strong conservation. In addition, the human promoter contains 2 RBP-Jκ responsive elements that could be implicated in the regulation of PR expression.

Therefore, we propose that Notch signaling via RBP-Jκ activation can regulate PR expression in the human breast cancer cell lines.

To test that Notch signaling can regulate PR expression in human breast cancers we inhibited Notch signaling in HR+ human breast cancer cell lines MCF7 and T47D with DAPT, γ-secretase inhibitor (Michelli et al., 2003) and by expression of dominant negative form of Notch coactivator Mastermind (Maillard et al., 2003). Additionally, we overexpressed activated NICD1 in HR negative MCF-10a cell line to induce PR expression by activation of Notch signaling.

RESULTS

To test the hypothesis that Notch signaling can regulate PR expression via RBP-Jκ activation we abrogated Notch signaling via γ-secretase inhibition by DAPT in HR+ cell lines MCF7 and T47D. In 3 independent experiments we treated both MCF7 and T47D cell lines with 10, 20 and 30 μM DAPT dissolved in DMSO (Figure 44). Control cells were treated with the same amount of empty DMSO. Inhibition was performed during 48 hours.

Analysis of the protein levels by Western blotting showed that there was no significant effect on the amount of ER and PR proteins in cells where Notch was inhibited by DAPT (Figure 44). To show that DAPT indeed inhibited Notch signaling we performed Western blot analysis to test the amount of cleaved Notch 1 receptor using Notch1 antibody that detects only cleaved N-terminal intracellular form. Analysis showed concentration-dependent reduction of cleaved Notch1 intracellular domain. As reported in the data sheet of the antibody, 10 μM DAPT had very little effect on the cleavage of the Notch1 receptor by γ-secretase in MCF7 and stronger effect in T47D cell line. 20 μM and 30 μM DAPT showed much stronger effect (Figure 44).

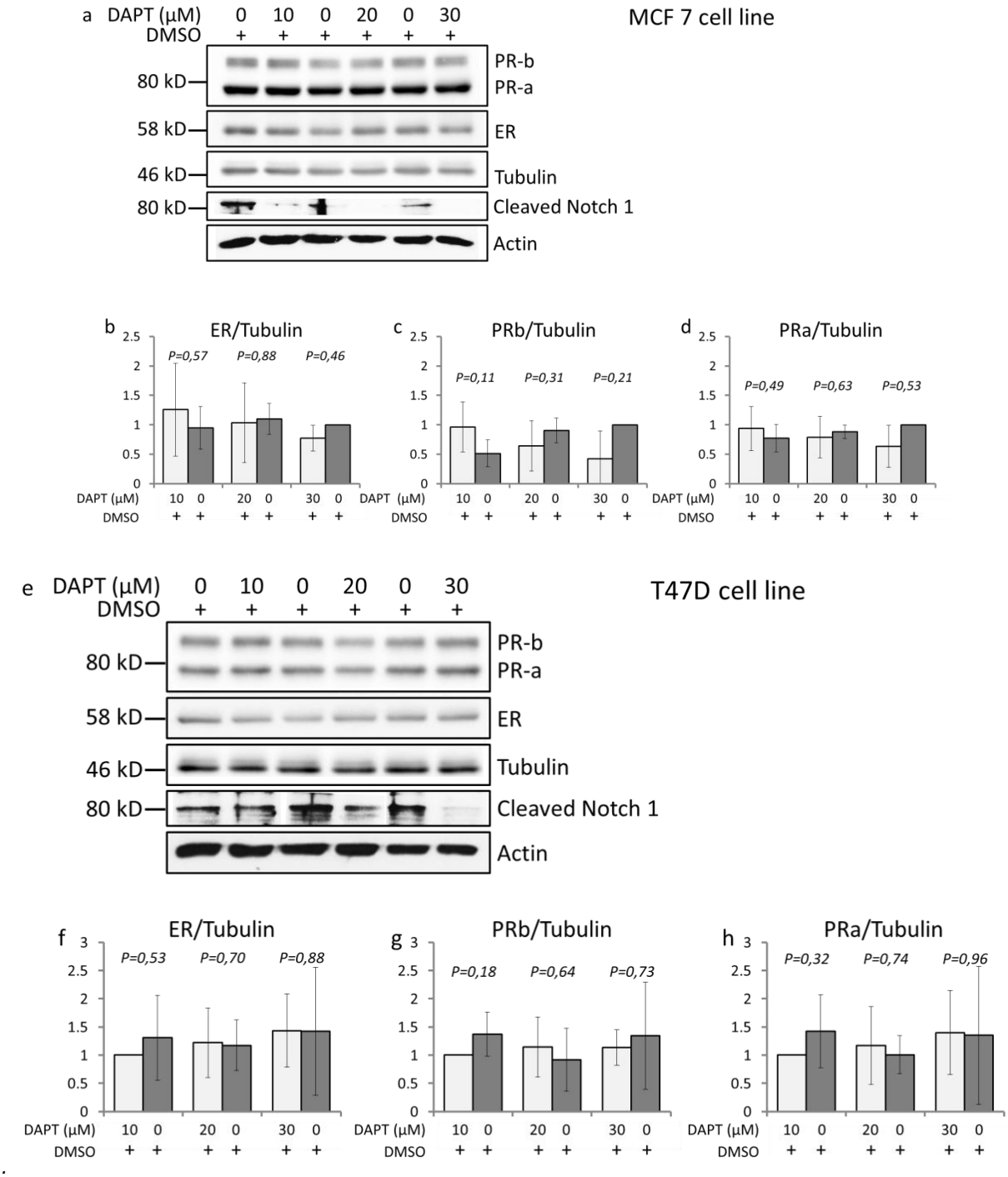

Figure 44. Effect of Notch signaling inhibition by DAPT on the protein expression of HR in MCF7 and T47D cell lines. *Western Blot analysis of protein levels in MCF7 and T47D cell lines upon Notch inhibition by DAPT (γ-secretase inhibitor): a) Western blot analysis of ER, PRa and Prb with tubulin as a loading control and cleaved Notch1 protein with actin as a loading control in MCF7 cell line; b) – d) Quantification of ER, PRa and PRb protein levels in MCF7 cell line normalized to tubulin (N=3); e) Western blot analysis of ER, PRa and PRb with tubulin as a loading control and cleaved Notch1 protein with actin as a loading control in T47D cell line; f) – h) Quantification of ER, PRa and PRb protein levels in T47D cell line normalized to tubulin (N=3).*

Additionally, we analyzed levels of mRNA of ER, PR and Notch target gene Hey1 in the T47D cell line treated with 10, 20 and 30 μM DAPT by quantitative PCR using 36B4 as housekeeping gene. Analysis showed that DAPT inhibited expression of Hey1 confirming the inhibition of Notch signaling

in the cell line. Contrarily, expression of both ER and PR was not affected by γ-secretase inhibition (Figure 45.a-c).

Mastermind is an important Notch coactivator responsible for the formation of activating complex on the RBP-Jκ upon activation by NICD (Wu et al., 2000). To abrogate Notch signaling via the inhibition of the formation of activating complex on RBP-Jκ, we overexpressed dominant negative Mastermind (DNNM) form in T47D cells via retrovirus vector. As a control we used T47D cells infected with empty retroviral vector. Both DNNM expressing and control vector expressed GFP as a reporter of the expression. Expression of genes of interest was analyzed 48 hours after the infection.

Data from 3 independent experiments showed that expression of dominant negative Mastermind did not have any effect on the levels of mRNA of Hey1 and ER. Surprisingly, PR levels were significantly increased by ≈1,5 fold (Figure 45.d). GFP reporter of the vector expression showed similar levels of expression in both DNNM expressing and control T47D cells confirming the validity of the experiment.

According to our working hypothesis, Notch signaling via RBP-Jκ regulates PR expression. In parallel with Notch inhibition experiments we performed experiment where we activated Notch signaling by expression of activated NICD via retroviral infection in HR- cell line MCF10a and analyzed the expression of ER, PR and Notch target gene Hey1.

To test whether activation of Notch signaling can induce expression of PR in HR- MCF10a cell line, in 3 independent experiments we infected MCF10a cell line with retroviruses expressing activated NICD1, and with empty control viruses. Since MCF10a cells do not express hormone receptors, we also analyzed the expressions of ER, PR and Hey1 in MCF7 cell line as positive control to validate the experiment.

Data from 3 independent experiments confirmed activation of Notch signaling via expression of activated NICD1 in MCF10a cells by increase of expression of Notch target gene Hey1. Although notch signaling was clearly activated, neither ER nor PR expression was affected (Figure 45.e).

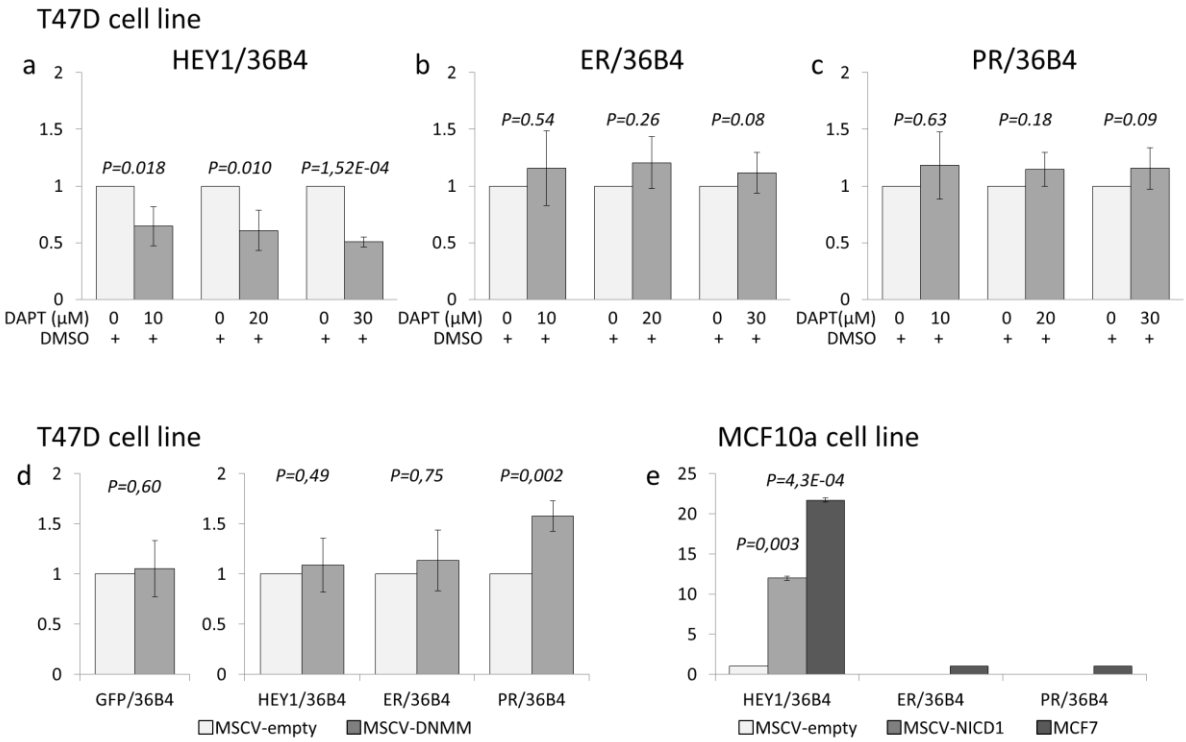

Figure 45. Effect of Notch signaling inhibition on the transcription of HR in T47D cell line and Notch signaling activation in MCF10a cell line*: Quantitative PCR analysis of mRNA levels of Hey1, ER and PR in T47D and MCF10a cell lines upon Notch abrogation or Notch activation: a-c) Analysis of mRNA levels of Hey1, ER and PR in T47D cell line upon abrogation of Notch signaling via γ-secretase inhibition by DAPT (N=3); d) Analysis of mRNA levels of GFP reporter, Hey1, ER and PR in T47D cell line upon abrogation of Notch signaling via expression of dominant negative Mastermind (N=3); e) Analysis of mRNA levels of Hey1, ER and PR in MCF10a cell line upon activation of Notch signaling via expression of activated NICD by retroviral expression. MCF7 cell line used as a positive control for ER and PR expression (N=3). Statistical significance was calculated using unpaired Students' T-test.*

CONCLUSION.

Experiments on HR+ human breast cancer showed that abrogation of Notch signaling via γ-secretase inhibition does not have any effect on the expression of both ER and PR. Abrogation of Notch signaling via expression of DNNM showed unexpected increase of PR expression while Notch target gene Hey1 expression did not change.

Activation of Notch signaling in MCF10a cell line did not induce expression of PR, hence Notch signaling alone cannot activate the expression of PR.

AIM 2: ROLE OF P63 IN MOUSE MAMMARY STEM CELLS

INTRODUCTION AND WORKING HYPOTHESIS

The function of p63 protein has been implicated in plethora of processes from regulating stem cell activity, differentiation, growth and survival to cell adhesion (Carroll et al., 2006) and metastasis (Su et al. 2013). However, the functional role of p63 in regulating MASCs remains unclear.

Notch signaling down-modulates p63 expression in primary human breast epithelial cells and in the mouse mammary epithelium *in vivo* (Yalcin Ozuysal et al., 2010). Down-regulation of p63 in basal cells resulted in loss of basal markers and up regulation of luminal markers *in vitro* and *in vivo*. Therefore loss of p63 via Notch signaling activation promotes differentiation in mouse mammary basal cells.

Therefore, we hypothesized that p63 expression in the basal cells contributes to the maintenance of the stem cell potential.

P63 knock-out mouse has severe developmental defects including lack of stratified skin which causes its death immediately after birth. Furthermore, mice had severe craniofacial defects and were missing skin appendages including mammary gland (Yang et al., 1999, Mills et al., 1999). Therefore, it was not adequate as a mouse model for mammary gland research.

P63 floxed mouse model has been developed (Mills et al., 2002). However, deletion of floxed gene in the entire epithelium via MMTV-Cre was not possible since MMTV promoter is active in skin already around birth and therefore affects epidermal development of the mutant mice.

Therefore, to test this hypothesis we used p63 heterozygous knock-out mouse model ($p63^{+/-}$) and monitored the ability of $p63^{+/-}$ mammary epithelium to repeatedly repopulate mammary fat-pad in the assay of serial transplantation of mammary epithelium.

ROLE OF P63 IN THE ENDOGENOUS MOUSE MAMMARY EPITHELIUM (HETEROZYGOUS P63 KNOCK OUT MOUSE MODEL)

We generated $p63^{+/-}$ expressing EGFP driven by actin promoter by crossing (Okabe et al., 1997).

Firstly, we analyzed endogenous epithelium to detect any growth defects. Six, eight and fourteen week old mice, both wild type and $p63^{+/-}$ were sacrificed; glands were extracted and examined under the fluorescent stereomicroscope. In 6-weeks-old WT mice the extent of the epithelium growth was larger than in $p63^{+/-}$ littermates (Figure 46.a-b). While in the 8-weeks-old WT glands epithelium was almost fully grown and completely filling the fat pad (Figure 46.c-d), in the heterozygous knock out glands, after 8 weeks, epithelium filled only half of the fat pad and reached the

level of the subiliacal lymph node. On the contrary, in the 14-weeks-old glands, there was no difference in the extent of fat pad filling (Figure 46.e-f). Thus, the epithelium of the $p63^{+/-}$ is developing with a delay in compare to the one in WT mice, but it catches up by 14^{th} week of life (Figure 46).

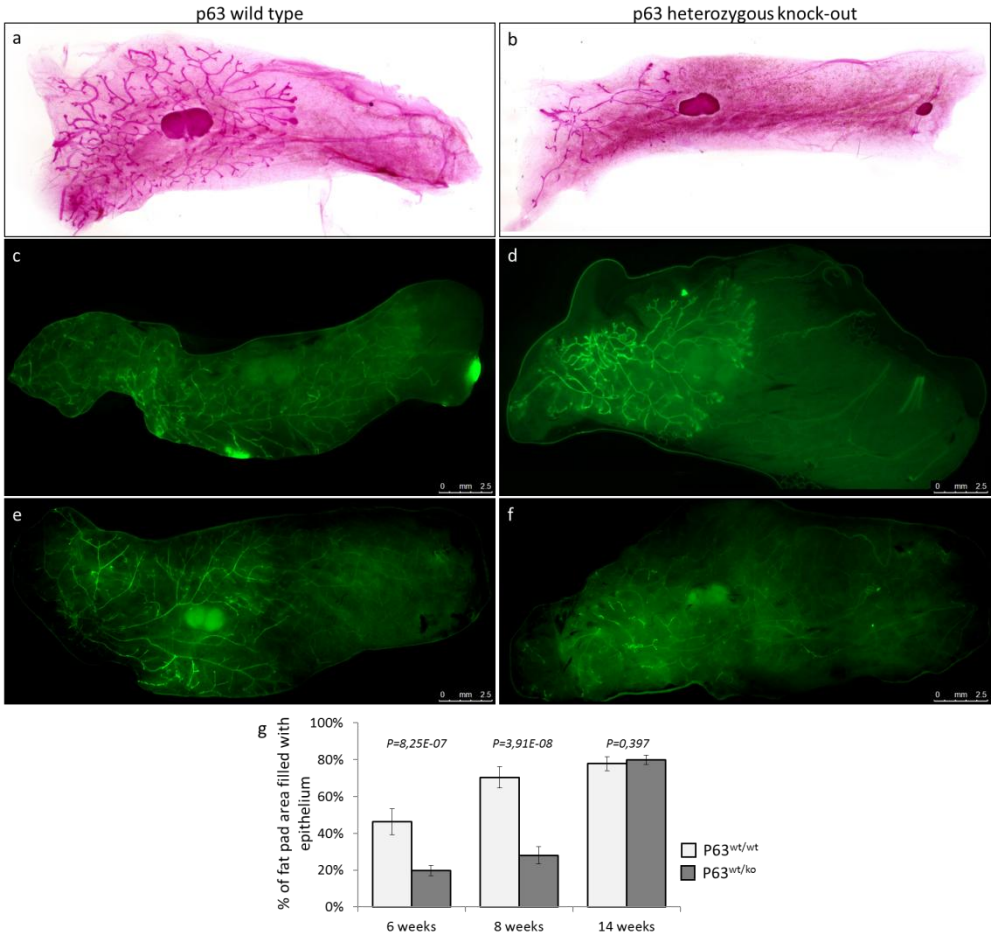

Figure 46: Whole mount of the mammary glands from p63+/+ and p63 +/-: *a) and b) 6-weeks-old glands (pubertal); c) and d) 8-weeks-old glands; e) and f) 14-weeks-old glands; scale bars represent 2,5 mm; g) Quantification of fatpad filling by epithelium in 6-weeks-old, 8-weeks-old and 14-weeks-old mammary gland (N=3). Statistical significance of the analysis was calculated by unpaired Students' T-test.*

SERIAL TRANSPLANTATION OF $P63^{+/-}$ MAMMARY EPITHELIUM

To assess the role of p63 signaling in mammary stem cell function, in a preserved tissue context and microenvironment, pieces of intact mammary epithelium from three different $p63^{+/-}$ and wild-type (WT) donors were serially engrafted into contralateral mammary fat pads of 8 immunocompromised $RAG1^{-/-}$ mice (Mombaerts et al., 1992) surgically divested of their endogenous epithelium per couple of donors and per generation.

Mammary epithelium was expressing EGFP which allowed engrafting comparable amounts of mammary epithelium in all the recipient fat pads. 10 weeks after the engraftment recipient mice were sacrificed, glands extracted and examined under the fluorescent stereomicroscope. Epithelium fragments from contralateral fat pads from 3 different recipients per donor were taken and

retransplanted. Only glands in which we were able to detect outgrowth or piece of transplanted epithelium on both sides were taken into account for the statistical analysis (Figure 47).

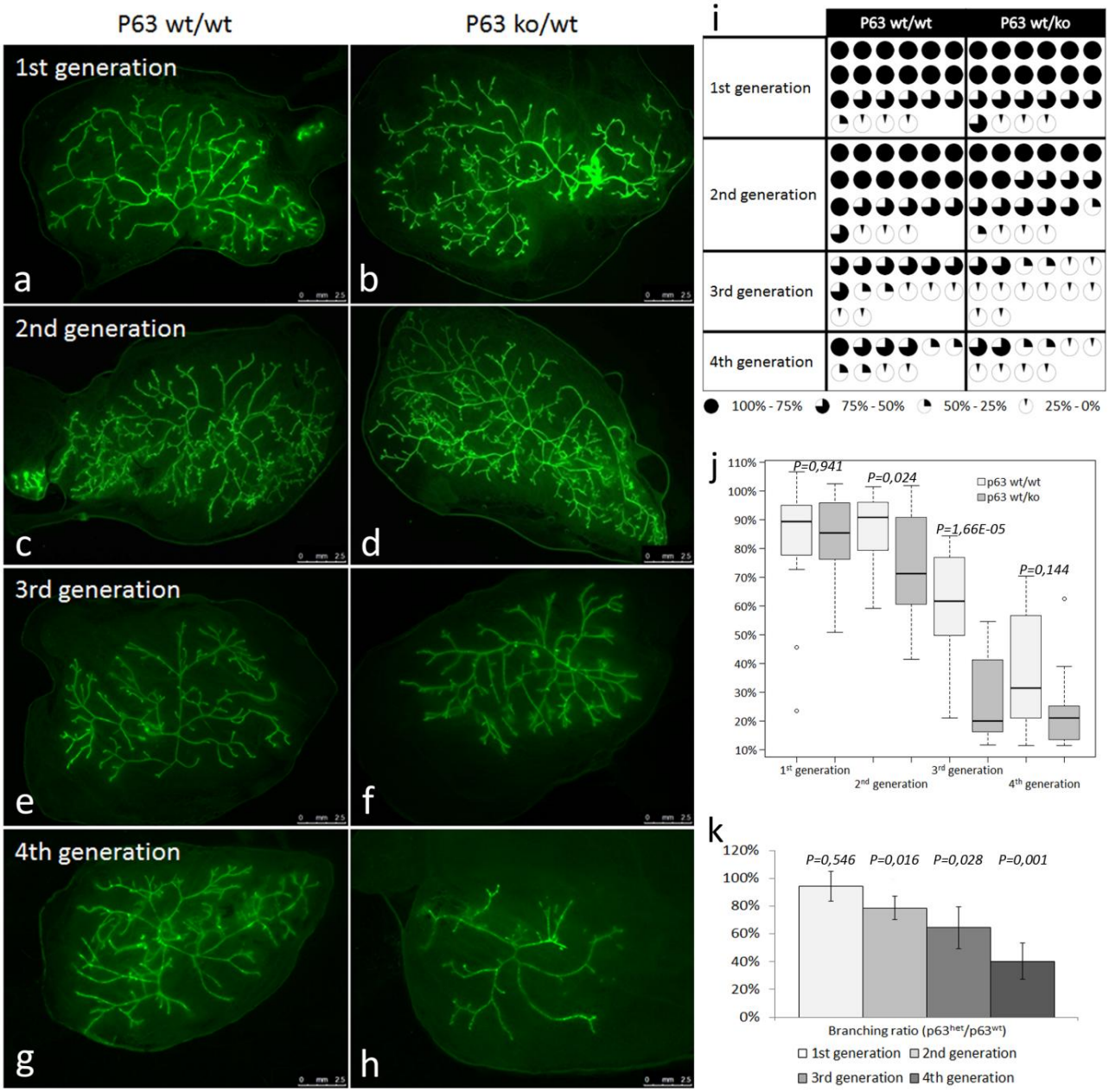

Figure 47. Serial transplantation of p63$^{+/+}$ and p63$^{+/-}$ epithelium into the fat pad of the immunocompromised Rag$^{-/-}$ recipient mice*: a)and b) 1st generation (N=22); c) and d) 2nd generation (N=22); e) and f) 3rd generation (N=14); g) and h) 4th generation (N=10); i) and j) statistical analysis of the fat pad filling of p63$^{+/+}$ and p63$^{+/-}$ serially transplanted epithelium; k) statistical analysis of the amount of branching points of p63$^{+/+}$ and p63$^{+/-}$ serially transplanted epithelium. Statistical significance of the analysis was calculated by paired Students' T-test.*

In the 1st generation p63$^{+/-}$ epithelium did not show any differences in growth or number of branching points in compare to p63$^{+/+}$ epithelium. In the 2nd generation the difference in fat pad filling was significant and in 3rd generation striking: p63$^{+/-}$ epithelium filled less fat pad and had less branching points than p63$^{+/+}$ epithelium. The 4th generation showed no difference in the fat pad filling. However there was significantly less branching points in the p63$^{+/-}$ and the engraftment was less successful (Figure 47).

CONCLUSION

Analysis of endogenous $p63^{+/+}$ and $p63^{+/-}$ epithelium showed a weak but significant defect of growth in the mutant epithelium which is overcome with time. These results implicated p63 in the regulation of MASC activity.

The reduction of branching points in $p63^{+/-}$ epithelium in the 2^{nd}, 3^{rd} and 4^{th} generations additionally confirmed MASC defect.

CHAPTER III: **DISCUSSION AND FUTURE PERSPECTIVES**

Notch signaling is an important player in the development of mammary gland. Conditional knockout of RBP-Jκ in the mammary epithelium via MMTV-Cre revealed that during pregnancy luminal layer is lost leaving multilayered basal cells (Buono et al., 2006). Subsequent reports showed involvement of Notch signaling in the luminal cell fate specification of the putative progenitor cells in the mouse mammary gland by blocking Notch in the progenitor and stem cells (Raouf et al., 2008; Bouras et al., 2008).

Study from our lab showed that abrogation of Notch signaling via conditional deletion of RBP-Jκ by MMTV-Cre in mammary epithelium leads to loss of recombined luminal cells and their substitution by wild type luminal cells (Yalcin Ozuysal et al., 2010). Hence, Notch signaling has been implicated in the mammary gland development, specifically in the determination of luminal cell-fate, however mechanism remained unveiled.

NOTCH SIGNALING IS ACTIVE IN A SUBPOPULATION OF HR+ CELLS IN THE PUBERTAL MICE

Preliminary experiments (Yalcin Ozuysal, unpublished data) suggested that Notch activity presented by expression of EGFP in the TNR mouse is colocalizing with PR.

Detailed analysis of the TNR mouse model performed within this project, showed that in the pubertal mouse 11,2%±2,7% of the luminal cells are expressing EGFP as a result of Notch activity. By immunofluorescence we confirmed that these cells are HR+ in very high percentage and they present one quarter of all HR+ cells.

In the basal compartment we detected lower number of Notch active cells (3,5%±0,4%). However, by immunofluorescence we did not detect any EGFP positive cells in the basal compartment of the pubertal mammary epithelium. Comparison of EGFP intensity in Notch active luminal and basal population by FACS showed presence of 100-fold lower EGFP intensity in the basal Notch active cells. This result suggests that the level of EGFP in the basal cells was too low to be detected by immunofluorescence.

To furthermore characterize luminal Notch+ population an additional FACS sorting experiment could be done. Shehata et al suggested that there is a subpopulation of HR+ cells that is expressing surface marker CD49b. These cells are defined as $EpCam^{hi}CD49f^{lo}Sca1^{+}CD49b^{+}$ and are characterized as ER+ progenitor cells that are rather insensitive to loss of estrogen and progesterone when compared with the other mammary cell populations. This population might be responsible for the development of the endocrine therapy resistance in the breast cancer. It has been reported that Notch signaling can activate ER target genes during anti-estrogen therapy (Rizzo et al., 2008), it is possible that $EpCam^{hi}CD49f^{lo}Sca1^{+}CD49b^{+}$ population is Notch active.

To analyze this, an experiment should be performed where single cells from TNR mice mammary glands would be analyzed by FACS to see if EpCam^{hi}CD49f^{lo}Sca1^{+}CD49b^{+} cells express EGFP reporter gene. During her study Shehata used C57Bl6 and FVB mice. The progenitor marker proved to be tricky so far in a sense that not all strains express these markers on exactly the same cells. Visvader and Stingle reported in their review (Visvader and Stingl, 2014) that CD61, marker of mammary progenitor cells, works only in FVB mice. CD49b has been reported so far only in C57BL6 and FVB mice. Balb-C mice, background in which TNR mice were developed, did not show any sign of expression of CD49b and therefore we were not able to define if luminal Notch active cells are the same HR+ progenitor cells as from the Shehata paper.

Analysis of the microarray data performed by Ozden Yalcin Ozuysal showed that luminal cell populations, whether Notch active or inactive are clustering together as well as basal populations. However in one of the samples sorted populations were not clustering together with same population from other 2 samples. This problem appeared probably because this particular sample was not sorted properly. Reason for this might be usage of only CD24 gene to sort the cells. CD24 expression can show 3 populations of cells (hi-luminal, lo-basal and neg-non epithelial). However, sorting of cells with CD24 in combination with CD49f marker, proposed by Stingl, clearly shows that luminal and basal populations are overlapping if we look only at CD24 expression.

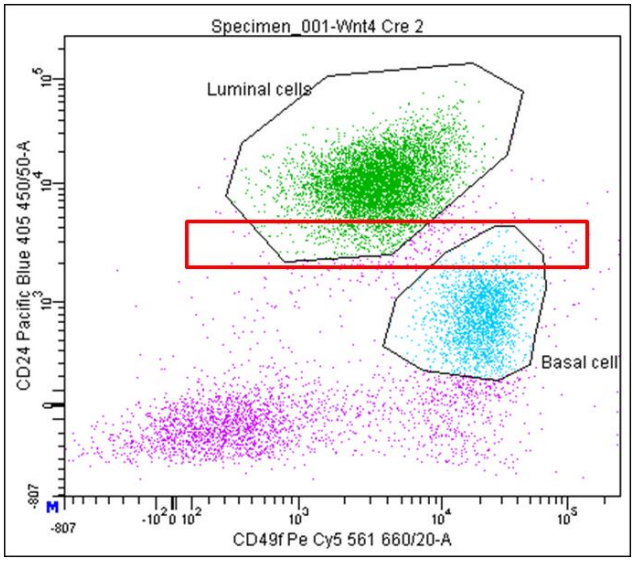

Figure 48. Sorting of mammary epithelial cells based on CD24 and CD49f markers*: black gates represent luminal and basal population of mammary epithelial cells. Red rectangle is highlighting basal and luminal cells that are overlapping if only CD24 marker is used.*

Additional problem might be long half-life of GFP (26 hours). Because of this, low levels of EGFP might represent residual EGFP signal remained in the cells after Notch activity which might also be the reason of the unexpected clustering of the cell populations. To annul this possibility, gates for the sorting EGFP positive and negative cells should be placed more conservatively, with bigger gap between the two populations.

Because of invalid sorting of one out of three samples we were not able to perform further analysis of the microarray data where we would look for differential expression of functionally

selected genes such as regulators of transcription with a role in cell differentiation. To do this, a new experiment should be performed where cells would be sorted by expression of both CD24 and CD49f markers to separate basal and luminal cells, and by expression of EGFP with more strict gating to increase the purity of the populations.

Therefore, to validate lower number of genes associated to different cell types in the mammary epithelium, we set up additional FACS sorting experiment, again using only CD24 marker (to be able to combine it with 2 valid samples), but setting up much more conservative gates between luminal ($CD24^{hi}$) and basal ($CD24^{lo}$) population to avoid sorting of the cells of the different population that are overlapping in CD24 expression.

Quantitative PCR analysis of genes associated to different cell types of mammary epithelium as well as Notch target gene HEY1 and GFP, the reporter gene, in 4 populations sorted by type (luminal and basal) and Notch activity (Notch+ and Notch-) confirmed that Notch active luminal population was indeed HR+ population since it expressed both ER and PR, and FoxA1, an ER mediator.

It is important to have in mind the composition of each population when interpreting the results of the quantitative PCR. Luminal Notch active population represents one quarter of all HR+ cells or roughly 10% of the entire luminal population. Notch inactive luminal population consists of all HR- cells and Notch inactive part of HR+ cells, meaning that in this population we should be able to detect some expression of hormone receptor. Notch inactive basal population contains ≈97% of all basal cells. Notch active basal cells represent only 3,5%±0,4% of basal cells that are expressing EGFP reporter.

Therefore, the expression of HRs as well as FoxA1 in the luminal Notch active population is higher than in the luminal Notch inactive one, because luminal Notch active population is pure population of HR+ cells and Luminal Notch inactive is mostly HR-.

EGFP as a Notch reporter gene and Hey1 as a Notch target gene are expressed in a higher fashion in the luminal Notch active population than in basal Notch active population. These results are consistent with the FACS data saying that EGFP intensity that should be proportional to Notch activity is ≈100–fold lower in the basal Notch active population.

P63 is highest in the basal Notch inactive population. Basal Notch active population shows lower levels of p63 probably because it has been shown that Notch is antagonizing p63 expression in mammary epithelial cells and driving them toward luminal cell fate. Hence, lower expression of SMA in the basal Notch active cells.

Casein α and Elf-5, associated with HR- cells, were strongly enriched in the luminal Notch inactive population mostly comprised of HR- cells.

Finally, Wnt4 showed higher expression in the luminal populations and among them in Notch active one comprised of HR+ cells. This result was encouraging since it suggests that Notch active MMECs are Wnt4 positive cells.

Wnt4 is a known PR target gene and a paracrine mediator of PR signaling. However, lineage tracing experiments in Wnt4-Cre mouse presented in Devi Rajaram (Rajaram et al., 2015) work showed that not all PR+ cells are expressing Wnt4. What triggers this expression is still not known. The fact that Notch active luminal cells are expressing Wnt4 gave us possibility to specifically abrogate Notch signaling by deleting RBP-Jκ in the subpopulation of HR+ cells, and this subpopulation should include Notch active luminal cells.

TWO SUBPOPULATIONS OF HR+CELL BASED ON NOTCH ACTIVITY.

Experiments on RBP^{floxed} Wnt4-Cre mTmG mice showed that upon abrogation of Notch signaling by deleting RBP-Jκ in the Wnt4 expressing cells, expression of PR is lost. MMTV-Cre deletion of the RBP-Jκ which abrogates Notch in the entire epithelium revealed another subpopulation of HR+ cells where PR expression remains intact.

Taken together, these two mouse models give strong base for our working model that suggests presence of the 2 different populations of HR+ cells:

1. Notch dependent population of luminal HR+ cells. This population would be the population that expresses Wnt4 and that upon abrogation of Notch via Wnt4-Cre loses the expression of PR.
2. Notch independent population of luminal HR+ cells. This population would be the population that upon Notch abrogation in the entire epithelium via MMTV-Cre can differentiate to HR+ cells from a progenitor, and can survive in the luminal compartment during the development.

These two populations could be sorted easily from the Wnt4-Cre mTmG mouse. Markers CD24, CD49f and Sca1 can mark for HR+ cells ($CD24^{hi}$ $CD49f^{lo}$ $Sca1^{+}$). In this population from mTmG mouse we would have cells expressing dTomato and EGFP. dTomato+ cells would be the cells where Wnt4 was not expressed. These cells would represent Notch independent HR+ cell population. Cells expressing EGFP would be the cells in which Wnt4 is expressed and therefore, Cre was active. They would represent Notch dependent population of HR+ cells. To analyze the difference between these two populations of cells, global gene expression analysis or RNAseq could be done to find genes of interest that are differentially expressed in each of the populations.

Presence of any luminal cells expressing EGFP in $RBP^{fl/fl}$ MMTV-Cre mTmG model was surprising since it opposes already published data. In the study of Yalcin Ozuysal, $RBP^{fl/fl}$ MMTV-Cre mouse epithelium was analyzed in the presence of the Cre reporter gene Z/EG which upon Cre activation expresses EGFP under chicken actin promoter (Yalcin-Ozuysal). This mouse did not have

any EGFP expressing cells in the luminal compartment suggesting that differentiation towards luminal cell fate following Notch abrogation is impossible. The only difference between hers and our mouse model is the reporter gene. Closer look into the Yalcin Ozuysal's study (Yalcin-Ozuysal et al., 2010, figure 7.g-l) revealed that Z/EG Cre reporter in wild type control mouse did not mark majority of the luminal cells while in mTmG mouse Cre reporter is expressed in all epithelial cells. Therefore, we believe the in RBP^{floxed} MMTV-Cre Z/EG mouse Notch independent population of HR+ luminal cells did not express Z/EG Cre reporter.

TIME DIRECTED NOTCH ABROGATION LEADS TO LOSS OF PR EXPRESSION

Time directed deletion of RBP-Jκ via intraductal Adeno-Cre virus caused loss of PR expression by 2-fold in the luminal EGFP expressing population after 7 days suggesting that Notch signaling is responsible for the expression of PR in the adult glands, at least in the subpopulation of HR+ cells. This subpopulation probably overlaps with Wnt4 expressing HR+ cells which are dependent of Notch signaling. However, after 14 and 21 day this difference was not present anymore.

Problem of working with viruses from the family of *Adenovirdae* is the fact that these viruses have lytic cycle in order to replicate. The lytic cycle results in the destruction of the infected cell and its membrane. Therefore, adenovirus infection shows high cytotoxicity. Analysis of the total number of infected cells in mammary epithelium of both $RBP^{fl/fl}$ and $RBP^{wt/wt}$ mice showed that 14 days after infection with Adeno-virus 2-fold less infected cells were present in compare to 7 day time point. After 21 days more than 4-fold of infected cells disappeared suggesting that Adeno-Cre virus is extremely cytotoxic.

Therefore we cannot distinguish if the loss of difference in the 14 day and 21 day time point is a result of extreme cytotoxicity and severe lysis of the host cells or it is in fact phenotype of the RBP-Jκ deletion via intraductal injection of Adeno-Cre virus.

RBP-JΚ BINDS TO PR PROMOTER.

The results from Adeno-Cre mouse model suggested that Notch signaling regulates expression of PR. However, PR has already been established as a direct target gene of ER signaling (Nardulli et al., 1988). Although PR expression has been shown to be controlled by 17β-estradiol PR promoter does not contain ERE palindromic sequence (Kastner et al., 1990). A study on breast cancer cell lines confirmed existence of ERE half-site whose estrogen responsiveness needs to be mediated by *cis* element. In human PR promoter two adjacent Sp1 sites are present (Petz et al., 2000) and have been shown to regulate PR in humans. In mouse PR promoter only one Sp1 site is present and its function hasn't been examined.

Surprisingly, we found 4 RBP-Jκ binding sites in the promoter region of PR and tested the binding of RBP-Jκ to all of them. Chromatin immunoprecipitation showed that RBP-Jκ can bind 2 of

these binding sites, site No.1 (-2631 bp) and No.3 (-1706 bp). These results confirmed the possibility that these two RBP-Jκ responsive elements might be necessary *cis* element that co-regulates or maybe even regulates PR expression together with ERE half site. In line with this hypothesis goes the study by Rizzo et al., which showed that in the HR+ breast cancer cell lines, upon anti-estrogen treatment Notch signaling can directly stimulate ER target genes (Rizzo et al., 2008). On the other hand, quantitative analysis of ChIP indicates that binding of the RBP-Jκ to mouse PR promoter is much weaker than binding to the regular Notch targets such as Hey1 promoter used as a positive control, leaving the possibility that it might be irrelevant for the PR expression.

ChIP, however, only shows binding of RBP-Jκ and not activation of the transcription by it. To show that PR transcription is, indeed, activated by RBP-Jκ, additional experiments are required where activation of Notch signaling via RBP-Jκ together with Estrogen stimulation would show transcription activation of a reporter gene cloned downstream of PR promoter together with mutated RBP-Jκ sites as negative controls and binding of the ER as a positive control.

Additionally, since RBP-Jκ acts as a repressor of expression outside of the Notch signaling context, it would be necessary to do a ChIP assay on a sorted population of HR+ luminal ($CD24^{hi}$ $CD49^{lo}Sca1^{+}$) and HR- luminal cells ($CD24^{hi}$ $CD49^{lo}Sca1^{-}$) to show that the binding is specific for the HR+ population.

Multiple alignment of the PR promoters from different species showed that RBP-Jκ binding sites are positioned in the highly conserved area of the promoter. The sites did not show identity with the same positions on the human promoter which reduces the significance of these sites in the human promoter. However, we identified 2 binding sites in the human promoter also residing in the highly conserved area. Since it has already been shown that in the endocrine therapy resistant cell lines Notch signaling can substitute ER to activate transcription of ER target genes (Rizzo et al., 2008) it is possible that RBP-Jκ indeed binds these two sites.

LOSS OF PR EXPRESSION VIA RBP-JK DELETION IS AN EFFECT OF CANONICAL NOTCH SIGNALING ABROGATION

RBP-Jκ is a transcription factor that, mediates canonical Notch signaling. Non-canonical RBP-Jκ activation independent of NICD has also been reported in neuroblastoma cells (Stockhausen et al., 2005) and specification of GABAergic neurons specification (Hori et al., 2008). To confirm that loss of PR in RBP-Jκ abrogated cells is caused by Notch dependent RBP-Jκ activation we performed inhibition of Notch signaling *in vivo* by injecting intraductally γ-secretase inhibitor DAPT. Results showed that upon inhibition of γ-secretase, necessary for Notch receptor activation, PR expression is, indeed, reduced together with the Notch target gene Hey1. Consistently with *in vivo* results ER expression did not change significantly.

Immunofluorescence showed that there is 85,6%±3,9% of ER cells that are co-expressing PR in the glands injected with DAPT confirming the hypothesis that ER+ only cells probably lost the PR due to the inhibition of the canonical Notch signaling.

NOTCH SIGNALING AS THERAPEUTIC TARGET

Several studies on the clinical samples connected elevated Notch with the triple negative breast cancer, currently therapeutically the most challenging subtype (Lee et al., 2008; Reedijk et al., 2005; Reedijk et al., 2008). A study in cell lines revealed possibility that inhibition of ER by therapeutics activates Notch signaling that can activate ERα targets (Rizzo et al., 2008) which can be interpreted as a mechanism of acquiring resistance to HR+ breast cancer therapies. Hao et al have also demonstrated that Notch activation of the transcription of ERα target genes goes via a nuclear IKKα-dependent pathway (Hao et al., 2010). Therefore, Notch has emerged as a therapeutic target for the ERα negative breast cancer patient and in combination with anti-estrogen treatment for the ERα positive breast cancer patients. Thus, understanding of the mechanism of Notch action in the mammary gland is indispensable.

Several studies have been conducted on HR+ cell lines which acquired the resistance to the endocrine therapy by tamoxifen (Haughian et al., 2012, Lombardo et al.,). Haughian et al observed that when HR+ cell line T47D grows *in vivo* as a mammary xenograft without estrogen supplementation, specific luminobasal cell population, which is characterized by expression of CK5 and lack of hormone receptors, expands. Previously, this luminobasal population has been described as a minor ER- PR- CK5+ population that has the capacity to generate the majority of ER+ PR+ CK18+ CK5- cells and when HR+ breast cancers are treated with endocrine therapies that target ER, this population would escape such treatments and survive to repopulate the tumor (Horowitz et al., 2008). Expansion of this population has been attributed to Notch signaling since T47D cell line grown *in vivo* without estrogen supplementation did not have an expansion of the luminobasal population if at the same time Notch was inhibited.

Furthermore, pharmacological inhibition of Notch activation with gamma-secretase inhibitors (GSIs) in combination with tamoxifen has synergistic effects in ER+ breast cancer in vivo models (Rizzo et al., 2008, Hao et al., 2010)

These data implicated Notch signaling in ER target genes activation in breast cancer cell-lines which acquired resistance to endocrine therapy. Our data showed that upon abrogation of Notch signaling via RBP-Jκ deletion and γ-secretase inhibition a subpopulation of HR positive epithelial cells is losing PR. Since PR is an ER target gene, we suggest an *in vivo* mechanism through which Notch might co-regulate ERα dependent PR expression in adult mammary gland through RBP binding sites in the PR promoter acting as *cis* regulatory elements possibly through interaction of the RBP-Jκ with ER directly on the promoter.

This mechanism is not in line with the hypothesis that Notch suppression maintains HR responsiveness which might be due to the fact that studies were performed on the endocrine therapy resistant HR+ breast cancer cell lines while we studied normal mouse mammary epithelium. For this reason we tried to inhibit Notch signaling in endocrine therapy sensitive HR+ cell lines MCF7 and T47D to reduce PR expression and activate Notch signaling in the normal breast like cell line MCF10a to gain PR expression.

NOTCH SIGNALING IN THE HR+ BREAST CANCER CELL LINES

In vivo results are suggesting that Notch signaling is regulating PR expression in the HR+ cells. To investigate if the same effect Notch has in the HR+ breast cancer, we tried to inhibit Notch signaling in the HR+ breast cancer cell lines MCF-7 and T47D by γ-secretase inhibitor DAPT and by introduction of dominant negative form of Notch modulator Mastermind (MAML1). Although Notch inhibition was confirmed by loss of activated NICD1, DAPT treatment did not reduce PR on the protein level.

Quantitative RNA analysis showed that upon DAPT treatment, also PR transcription remained intact. Inhibition of Notch signaling by dominant negative form of MAML1 did not affect transcription of HEY1 or ER. However, PR expression was now significantly increased.

MCF10a is a cell line that represents normal population of basal human breast epithelial cells characterized by expression of p63. In this cell line we tried to induce expression of PR by expression of activated NICD1. As presented, Notch signaling was activated (increase of transcription of the HEY1 target gene), but PR expression was not affected. These results showed that PR expression cannot be activated solely by activation of Notch signaling but probably acts only as a co-activator together with ER.

P63 IN MOUSE MAMMARY STEM CELLS

p63 is expressed in the basal compartment of mammary epithelium. Notch activation in the primary basal cells in culture has an antagonistic effect on the p63 expression leading cells to change phenotype from basal to luminal (Yalcin Ozuysal et al., 2010).

Further to these results we hypothesized that, if down regulation of p63 leads cells to differentiation, then p63 should be responsible for the stem cell maintenance in the basal compartment of mouse mammary gland.

Hypothesis was tested on a $p63^{+/-}$ mouse because: a) complete knockout mouse is not viable b) p63 floxed mouse is available, however, available Cre constructs that are expressed in the basal compartment in the mammary gland are expressed also in the skin which would not develop normally without p63. Possibility of embryonic mammary bud transplantation was also excluded because mammary buds are not developed in homozygous mutants (Yang et al., 1999; Mills et al. 1999).

Therefore, we examined endogenous epithelium of the heterozygous p63 mutant and we performed serial transplantation of heterozygous epithelium in immunocompromised recipient mice. Endogenous $p63^{+/-}$ mammary epithelium showed significant delay in development of the mammary gland; however the epithelium managed to fill the entire mammary fat pad.

Serial transplantation assay additionally showed that growth of the $p63^{+/-}$ epithelium, in compare to the $p63^{+/+}$ epithelium transplanted contralaterally, is significantly affected already in second and even more strikingly in the third generation, suggesting that p63 has a role in the mouse mammary stem cell self-renewal and/or maintenance.

Recent in vivo study by Chakrabarti showed that overexpression of ΔNp63 isoform in MaSCs promotes MaSC activity while genetic ablation of even one allele reduces MaSC function in vivo. Also they demonstrated that ΔNp63 isoform regulates these phenotypes through Wnt signaling, probably by controlling the expression of frizzled receptor FZD7. Therefore, they suggested the ΔNp63-FZD7-Wnt axis as a driving force in MaSC maintenance. Analysis of the clinical samples of the triple negative cancer showed strong correlation between triple negative tumors and FZD7 (Chakrabarti et al., 2014) suggesting that MASC may be the cell of origin in a subset of TN tumors that are dependent on ΔNp63-FZD7-Wnt axis. Since this study confirmed our hypothesis that p63 promotes stem cells activity and set up a valid mechanism how p63 is regulating stem cells, we decided to discontinue this part of the project.

CONCLUSION

Several study showed that Notch signaling can elicit a cancer resistance to anti estrogen therapy by activating ER target genes (Rizzo et al., 2008, Hao et al., 2010). Our data suggest a mechanism by which Notch signaling via RBP-Jκ can act as a co-activator of PR expression together with ER. This is another confirmation that Notch inhibitors might play a crucial role in fighting cancer as a novel drug that can be used in combination with anti-estrogen drugs. In fact, clinical studies with this combination are already ongoing.

MATERIALS AND METHODS

MICE

The GFP transgenic mice, mTmG transgenic mice, Wnt4-EGFP-Cre transgenic mice, MMTV-Cre transgenic mice, transgenic Notch reporter mice, as well as mice with RBP floxed alleles and p63 floxed alleles were described elsewhere (Okabe et al., 1997; Muzumdar et al., 2007; Shan et al., 2010; Wagner et al., 2001; Duncan et al., 2005; Han et al., 2002; Mills et al., 2002). The mice were maintained and handled according to the Swiss guidelines for animal safety.

MAMMARY GLAND WHOLE MOUNT

Mammary glands were isolated and spread onto a glass slide. GFP and dTomato images were acquired on Leica MZ16F stereoscope with Leica DC300F camera. The glands were fixed in a 1:2 mixture of glacial acetic acid /100% ethanol, hydrated, stained overnight in 0.2% carmine (Sigma), dehydrated in graded solutions of ethanol, and cleared in 1:2 benzyl alcohol/benzyl benzoate (Sigma). Whole mount images were captured with Pixelink PL-A622 camera on a Leica MZFLIII stereoscope.

PREPARATION OF SINGLE EPITHELIAL CELLS FROM MOUSE MAMMARY GLAND

Preparation of single mammary epithelial cells is described in details in the manuscript for the book chapter “Analysis of mammary gland phenotypes by transplantation of the genetically marked mammary epithelium/epithelial cells” presented in Appendix B

FLOW CYTOMETRY AND CELL SORTING

After removal of lymph nodes, the mammary glands were isolated from 6, 12-weeks-old and p8,5 TNR mice and chopped manually with surgical blades. Single MMECs were prepared as described previously (Sleeman et al., 2006). Briefly, dead cells were excluded by DAPI staining (1:10000; Invitrogen A1310). Non-epithelial cells were excluded by using a cocktail of biotin labeled anti-CD31 (1:500) (eBioscience, 13-0319-82), anti-CD140a (1:500) eBioscience, 13-1401-82), anti TER119 (1:500)(eBioscience, 13-5921-82) and anti-CD45 (1:1000)(eBioscience, 13-0451-82) and APC conjugated streptavidin (0,2 μg/mL) (eBioscience, 17-4317-82), PE anti-mouse CD24 (0.5μg/ml; BD Pharmingen, 553262) was used to separate luminal and myoepithelial populations. BD FACSAria (I) Cell Sorting System (BD Biosciences) was used for sorting.

IMMUNOSTAINING OF MAMMARY GLANDS

For histological examination freshly isolated glands were fixed with 4% paraformaldehyde overnight at 4˚C. Sections were cut at 4μm. The following antibodies were used: anti ER (DAKO, M7047, 1D5 clone), anti-PR (1:800) (Neomarkers, RM-9102, SP2clone), anti p63 (1:100) (Neomarkers, MS1081, 4A4 clone), mouse anti GFP (1:200) (Santa Cruz, SC-9996), rabbit anti GFP (Invitrogen, A-11122), goat anti GFP (1:400)(AbCam, AB6673), anti Ki67 (1:100) (AbCam, AB16667), anti Caspase 3 (Cell Signaling, 9664S), anti RBP-Jκ (1:25) (Cell Signaling, 5313) and applied overnight at 4°C after

antigen retrieval in citrate buffer. Mouse-on-Mouse immunodetection Kit (Vector Laboratories) was used to block unspecific staining of mouse antibodies. Additional blocking was performed for ER staining with CAS-block reagent (Invitrogen, 008120). Pictures were acquired with Zeiss Axioplan 2-imaging fluorescence microscope with Axiocam MRm camera.

MICROARRAY ANALYSIS

RNA was isolated from 4 populations of cells sorted from 3 different groups of 6-weeks-old mice. Each group contained 18 animals. Affymetrix GeneChip technology was used to perform microarray.

Hierarchical analysis of the 4 populations was performed by Ward's minimum variance method. (https://stat.ethz.ch/R-manual/R-patched/library/stats/html/hclust.html)

CELL LINES AND NOTCH SIGNALING INHIBITION BY Γ-SECRETASE INHIBITOR DAPT

MCF-7 and T47D cell lines were obtained from the American Type Culture Collection. MCF-7 and T47D cells were maintained in DMEM supplemented with 10% FCS (or 10% charcoal-dextran stripped serum) and 1% penicillin/streptomycin/glutamine.

To inhibit Notch signaling cells were treated with 10 μM, 20 μM and 30 μM DAPT (Adipogen, CR1-0016) and with vehicle as a control for 48 hours.

VIRAL CONSTRUCTS AND VIRUS PRODUCTION

MSCV-dominant negative Mastermind retrovirus was kindly provided by Gian-Paolo Dotto.

Virus was produced in 293T cells plated on 10cm dish at 30-35% confluency. 2μg of viral vector and 2μg of amphotrophic packaging vector for retroviruses were transfected by using 3μl of Fugene (Roche) per μg of DNA. Following change of medium after 24 hours, virus was collected at 48 and 72 hours. Titration was done on 293T or primary mouse mammary epithelial cells by using different dilutions of virus and comparing the GFP expression under fluorescent microscope.

WESTERN BLOT

Cell lines were lysed in RIPA buffer (10 mM Tris-Cl (pH 8.0), 1 mM EDTA, 0.5 mM EGTA, 1% Triton X-100, 0.1% sodium deoxycholate, 0.1% SDS, 140 mM NaCl). Before use protease (Protease inhibitor cocktail tablets (Roche, Ref. No. 11873580001), 1mM Phenylmethylsulfonyl fluoride (PMSF), 10 μg/mL Aprotinin) and phosphatase inhibitors (1mM Sodium orthovanadate) were added.

Total cell lysate (40 μg per sample) was separated by SDS/PAGE on 12% polyacrilamide gel (80 V for stacking gel and 120 V for resolving gel) in 1x running buffer (25 mM Tris, 192 mM glycine,

0.1% SDS, pH 8.3) and transferred to nitrocellulose membrane (200 mA, 60 min) in 1x transfer buffer (25 mM Tris, 192 mM glycine, pH8.3), supplemented with 20% (v/v) methanol.

Immunoblotting of the membrane was performed with the following antibodies: anti PR (1:500) (Neomarkers, RM9102), anti ER (1:1000) (Santa Cruz, sc-543), anti-tubulin (1:10000) (Sigma, T6557), anti cleaved Notch1 (1:500) (Rockland immunochemicals Inc. 100-401-407) and anti-actin (1:10000) (Thermo Scientific, RB-9010). Antibodies were diluted in TBS buffer (50 mM Tris-Cl, 150 mM NaCl, pH 7.6) with 5% Bovine serum albumin and 0,1% Sodium azide and membranes were incubated on 4˚C o/n.

After overnight incubation, membranes were washed three times in TBS containing 0.05% Triton X-100 for 10 min each, the membrane was incubated with secondary antibody (anti-mouse-IgG), for 1 hour at RT. Secondary antibody was prepared in filtered TBS with 5% milk powder and 0.05% Tween. After incubation, membrane was subsequently washed three times as before. Proteins levels were finally revealed using enhanced chemiluminescent reagents according to the manufacturer's instructions. If needed, membranes were afterwards striped in 0.2 NaOH solution for 5 minutes and reblotted.

RNA AND cDNA PREPARATION AND QRT-PCR

Total RNA from breast cancer cell lines was extracted using RNeasy extraction kit (Qiagen).

Whole glands (lymph nodes removed) were used for total RNA extraction. The glands were homogenized in Trizol® (Invitrogen), the aqueous phase containing the RNA extracted with chloroform and processed according to the RNeasy® extraction kit (Qiagen).

RNA yield was measured at the spectrophotometer and 1µg of RNA from both cell lines and whole glands was reverse transcribed using MMLV reverse transcriptase (Invitrogen) and random hexamers (Roche), for 1h at 37ºC.

The resulting cDNAs were used for semiquantitative and quantitative PCR analysis using specific primers for the genes of interest.

SYBR Green PCR Core Reagent System (Qiagen) was used to perform semi-quantitative real time RT-PCRs (QRT.PCR) with Mastercycler realplex^2 (Eppendorf). The primers used for human and mouse samples are listed in the Table 1 and Table 2, respectively.

Table 1: *Primers used for human breast cancer cell lines MCF7 and T47D*

Gene	Forward primer	Reverse primer
GFP	GCACGACTTCTTCAAGTCCGCCATGCC	GCGGATCTTGAAGTTCACCTTGATGCC
ER	GCCATCAGGTGGATCAAAGT	GGAGATCTTCGACATGCTGC
PR	GTCAGTGGGCAGATCCTGTA	CGTAGCCCTTCCAAAGGAAT
Hey1	GGGAGGGGAACTATATTGAATTTT	ATTTGTGAATTTGAGATCCGTGT
36B4	CTTCCCACTTGCTGAAAAGG	CGACTCCTCCGACTCTTCCT

Table 2*: Primers used for total mouse mammary gland*

Gene	Forward primer	Reverse primer
SMA	ACGGGGTATTTGAGAGCGTA	GCTGTGAAGTCAGTGTCGATTT
p63	CCTTATGAGCCACCACAGGT	GCTGTCTTCATCTGCCTTCC
K14	GCCAACACTGAACTGGAGGT	CAAACTTGGTCCGGAAGTCA
GFP	GCACGACTTCTTCAAGTCCGCCATGCC	GCGGATCTTGAAGTTCACCTTGATGCC
Hey1	TGCACCAAAAGGAAAACACA	TGGTGCCTGTGAAACACAAC
ER	ACATGCCTATTGCTGGGTGT	AGCAAAATTAGCTGCCCTGA
PR	AAAGAGATGTCATGCCCAGT	CAATGGAAAAGCATTGCCTAA
FoxA1	TTGTCAATTTAACCATCACTTAAAGC	TTCCTCTTTGCCTTCTCAATG
WNT4	AGGAGTGCCAATACCAGTACC	TGTGAGAAGGCTACGCCATA
Casein α	CTTCAGAAGGTGAATCTCATGGG	CAGATTAGCAAGACTGGCAAGG
ELF5	GAGCATCAGACAGCCTGTGA	GCTGCCTCAATGAACTCCTC
36B4	GTGTGTCTGCAGATCGGGTA	CAGATGGATCAGCCAGGAAG

All the expression levels were normalized to 36B4 housekeeping gene in human and mouse. All statistical analysis was performed by two-tailed, paired Student's T-test.

TRANSPLANTATION OF MAMMARY EPITHELIUM

Transplantation of mammary gland is described in details in the manuscript for the book chapter "Analysis of mammary gland phenotypes by transplantation of the genetically marked mammary epithelium/epithelial cells" presented in Appendix B

QUANTIFICATION OF BRANCHING POINTS AND FAT PAD FILLING

Quantification of branching points was performed on images of mammary glands. For each gland, side-branches were counted in the complete area as of mammary gland. Branching points were statistically presented as a ratio of number of branching points in the transplanted mutant gland and number of branching points of contralaterally transplanted wild type gland.

Fat pad filling was quantified in the ImageJ software (Schneider et al., 2012) as a ratio of area covered with ducts and area of the entire fat pad.

Statistical analysis was performed by two-tailed, paired Student's T-test.

ADENO-CRE INTRADUCTAL INJECTION

RBP-Jκ$^{wt/wt}$ mTmG and RBP-Jκ$^{fl/fl}$ mTmG mice were anesthetized and prepared for the surgery as described in Appendix B.

Adeno-Cre virus was purchased from Vectorbiolabs (1045-HT). 107 PFU of the virus was mixed in 0,1% Trypan blue in PBS and injected into the main duct of the mouse mammary gland through cleaved nipple.

7 days after surgery mice were sacrificed and mammary glands extracted and analyzed.

BIOINFORMATICAL ANALYSIS

PR promoter regions were extracted from GeneBank database

Mouse: accession number NC_000075.6, from 8897707 to 8900479 nucleotide

Human: accession number NC_000011.10, from 2746 to 5746 nucleotide

Chimpanzee: accession number NC_006478.3, from 98978395 to 98975395 nucleotide

Pig: accession number NC_010451.3, from 36137511 to 36140511 nucleotide

Cat: accession number NC_018732.1, from 35295922 to 35298922 nucleotide

Rat: accession number NC_005107.4, from 7125658 to 7128658 nucleotide

Mouse and human promoter region sequence was analyzed by EMBOSS software (www.emboss.bioinfromatics.nl) using a short motifs search tool "*dreg*" to look for RBP-Jκ binding motifs.

Analysis of the conservation of the PR promoter region from different species was analyzed using Pro-Coffee tool for multiple alignment specifically designed to analyze homologous promoter regions (Erb et al., 2011).

CHROMATIN IMMUNOPRECIPITATION ASSAY

60 mg of mammary epithelium organoids was fixed with 1% formaldehyde, neutralized by the addition of 125 mM glycine. Cells were washed twice in ice-cold phosphate-buffered saline and homogenized in sodium dodecyl sulfate lysis buffer (1% sodium dodecyl sulfate, 10 mM EDTA, 50 mM Tris-HCl [pH 8.0]) containing protease inhibitors. Cross-linked DNA was sonicated to an average size

of 150-300 base pairs. The insoluble material was removed by centrifugation, and preclearing of the soluble chromatin was performed with a 50% slurry of protein G-Sepharose-salmon sperm DNA. Samples were incubated overnight at 4°C with 5 μg of antibody against RBP-Jκ (Cell signaling, 5313) and control (IgG) (Southern Biotechnology) separately. Immune complexes were collected with protein G-Sepharose and eluted. In parallel with the eluted immunoprecipitated samples, input templates were purified. Incubation at 65°C for 6 h was used to revert cross-linking. DNA was extracted from the samples using Phenol-chloroform extraction and ethanol precipitation. Extracted DNA was tested for binding sequences using primers from the Table 3. As a positive control primers for the RBP-Jκ binding site in the HES1 promoter were used and as a negative control primers for a fragment inside PR gene were used.

Table 3: *Primers used for total mouse mammary gland*

Binding site	Forward primer	Reverse primer
Binding site #1	TCAGGAGTATCGAGGTCATG	TGGTTGTTAACTAATGCCCAG
Binding site #2	TGCTCCTATAGGAGACTACC	AGGGAGAAGAGAATTCAAGGA
Binding site #3	GAATAACTGCAGGCTTCAGC	ACACCGTCATAAGCTGTCCA
Binding site #4	CTCCACAGTGTTCTCATGAC	CATGAGGTTCTCTTCAGTCC
Hey1	TGC CAA TCT GCG CAG CGA G	GAG GTG CGT GCA CAC TGA T
PR	AAAGAGATGTCATGCCCAGT	CAATGGAAAAGCATTGCCTAA

BIBLIOGRAPHY

Abd El-Rehim DM, Pander SE, Apish CE, Bell JA, Ram Paul RS, Blamey RW et al. (2004) Expression and co-expression of the members of the epidermal growth factor receptor (EGFR) family in invasive breast carcinoma. Br J Cancer 91, 1532-42.

Agrawal N, Frederick MJ, Pickering CR, Bettegowda C, Chang K, Li RJ et al. (2011) Exome sequencing of head and neck squamous cell carcinoma reveals inactivating mutations in NOTCH1. Science 333, 1154-7.

Artavanis-Tsakonas S, Muskavitch MA, and Yedvobnick B (1983) Molecular cloning of Notch, a locus affecting neurogenesis in Drosophila melanogaster. Proc Natl Acad Sci U S A 80, 1977-81.

Asselin-Labat ML, Sutherland KD, Barker H, Thomas R, Shackleton M, Forrest NC et al. (2007) Gata-3 is an essential regulator of mammary-gland morphogenesis and luminal-cell differentiation. Nat Cell Biol 9, 201-9.

Asselin-Labat ML, Sutherland KD, Vaillant F, Gyorki DE, Wu D, Holroyd S et al. (2011) Gata-3 negatively regulates the tumor-initiating capacity of mammary luminal progenitor cells and targets the putative tumor suppressor caspase-14. Mol Cell Biol 31, 4609-22.

Aster JC, Xu L, Karnell FG, Patriub V, Pui JC, and Pear WS (2000) Essential roles for ankyrin repeat and transactivation domains in induction of T-cell leukemia by notch1. Mol Cell Biol 20, 7505-15.

Balinsky BI (1950) On the prenatal growth of the mammary gland rudiment in the mouse. J Anat 84, 227-35.

Bate M, Rushton E, and Frasch M (1993) A dual requirement for neurogenic genes in Drosophila myogenesis. Dev Suppl 149-61.

Beleut M, Rajaram RD, Caikovski M, Ayyanan A, Germano D, Choi Y et al. (2010) Two distinct mechanisms underlie progesterone-induced proliferation in the mammary gland. Proc Natl Acad Sci U S A 107, 2989-94.

Bessho Y, Miyoshi G, Sakata R, and Kageyama R (2001) Hes7: a bHLH-type repressor gene regulated by Notch and expressed in the presomitic mesoderm. Genes Cells 6, 175-85.

Blaumueller CM, Qi H, Zagouras P, and Artavanis-Tsakonas S (1997) Intracellular cleavage of Notch leads to a heterodimeric receptor on the plasma membrane. Cell 90, 281-91.

Blaumueller CM, Qi H, Zagouras P, and Artavanis-Tsakonas S (1997) Intracellular cleavage of Notch leads to a heterodimeric receptor on the plasma membrane. Cell 90, 281-91.

Boggs K, Henderson B, and Reisman D (2009) RBP-J kappa binds to and represses transcription of the p53 tumor suppressor gene. Cell Biology International 33, 318-24.

Bolos V, Grego-Bessa J, and de la Pompa JL (2007) Notch signaling in development and cancer. Endocr Rev 28, 339-63.

Bouras T, Pal B, Vaillant F, Harburg G, Asselin-Labat ML, Oakes SR et al. (2008) Notch signaling regulates mammary stem cell function and luminal cell-fate commitment. Cell Stem Cell 3, 429-41.

Bozkulak EC and Weinmaster G (2009) Selective use of ADAM10 and ADAM17 in activation of Notch1 signaling. Mol Cell Biol 29, 5679-95.

Brisken C (2002) Hormonal control of alveolar development and its implications for breast carcinogenesis. J Mammary Gland Biol Neoplasia 7, 39-48.

Brisken C (2013) Progesterone signalling in breast cancer: a neglected hormone coming into the limelight. Nat Rev Cancer 13, 385-96.

Brisken C, Ayyannan A, Nguyen C, Heineman A, Reinhardt F, Tan J et al. (2002) IGF-2 is a mediator of prolactin-induced morphogenesis in the breast. Dev Cell 3, 877-87.

Brisken C, Heineman A, Chavarria T, Elenbaas B, Tan J, Dey SK et al. (2000) Essential function of Wnt-4 in mammary gland development downstream of progesterone signaling. Genes Dev 14, 650-4.

Brisken C, Kaur S, Chavarria TE, Binart N, Sutherland RL, Weinberg RA et al. (1999) Prolactin controls mammary gland development via direct and indirect mechanisms. Dev Biol 210, 96-106.

Brisken C, Park S, Vass T, Lydon JP, O'Malley BW, and Weinberg RA (1998) A paracrine role for the epithelial progesterone receptor in mammary gland development. Proc Natl Acad Sci U S A 95, 5076-81.

Brou C, Logeat F, Gupta N, Bessia C, LeBail O, Doedens JR et al. (2000) A novel proteolytic cleavage involved in Notch signaling: the role of the disintegrin-metalloprotease TACE. Mol Cell 5, 207-16.

Brou C, Logeat F, Lecourtois M, Vandekerckhove J, Kourilsky P, Schweisguth F et al. (1994) Inhibition of the DNA-binding activity of Drosophila suppressor of hairless and of its human homolog, KBF2/RBP-J kappa, by direct protein-protein interaction with Drosophila hairless. Genes Dev 8, 2491-503.

Buerger H, Otterbach F, Simon R, Poremba C, Diallo R, Decker T et al. (1999) Comparative genomic hybridization of ductal carcinoma in situ of the breast-evidence of multiple genetic pathways. J Pathol 187, 396-402.

Buono KD, Robinson GW, Martin C, Shi S, Stanley P, Tanigaki K et al. (2006) The canonical Notch/RBP-J signaling pathway controls the balance of cell lineages in mammary epithelium during pregnancy. Dev Biol 293, 565-80.

Burdon T, Sankaran L, Wall RJ, Spencer M, and Hennighausen L (1991) Expression of a whey acidic protein transgene during mammary development. Evidence for different mechanisms of regulation during pregnancy and lactation. J Biol Chem 266, 6909-14.

Candi E, Cipollone R, Rivetti di Val Cervo P, Gonfloni S, Melino G, and Knight R (2008) p63 in epithelial development. Cell Mol Life Sci 65, 3126-33.

Candi E, Rufini A, Terrinoni A, Dinsdale D, Ranalli M, Paradisi A et al. (2006) Differential roles of p63 isoforms in epidermal development: selective genetic complementation in p63 null mice. Cell Death Differ 13, 1037-47.

Carey LA, Perou CM, Livasy CA, Dressler LG, Cowan D, Conway K et al. (2006) Race, breast cancer subtypes, and survival in the Carolina Breast Cancer Study. JAMA 295, 2492-502.

Carroll DK, Carroll JS, Leong CO, Cheng F, Brown M, Mills AA et al. (2006) p63 regulates an adhesion programme and cell survival in epithelial cells. Nat Cell Biol 8, 551-61.

Chakrabarti R, Wei Y, Hwang J, Hang X, Andres Blanco M, Choudhury A et al. (2014) DeltaNp63 promotes stem cell activity in mammary gland development and basal-like breast cancer by enhancing Fzd7 expression and Wnt signalling. Nat Cell Biol 16, 1004-15, 1-13.

Ciarloni L, Mallepell S, and Brisken C (2007) Amphiregulin is an essential mediator of estrogen receptor alpha function in mammary gland development. Proc Natl Acad Sci U S A 104, 5455-60.

Clarke RB (2006) Ovarian steroids and the human breast: regulation of stem cells and cell proliferation. Maturitas 54, 327-34.

Clarke RB, Howell A, Potten CS, and Anderson E (1997) Dissociation between steroid receptor expression and cell proliferation in the human breast. Cancer Res 57, 4987-91.

Clarke RB, Spence K, Anderson E, Howell A, Okano H, and Potten CS (2005) A putative human breast stem cell population is enriched for steroid receptor-positive cells. Dev Biol 277, 443-56.

Cohen B, Shimizu M, Izrailit J, Ng NF, Buchman Y, Pan JG et al. (2010) Cyclin D1 is a direct target of JAG1-mediated Notch signaling in breast cancer. Breast Cancer Res Treat 123, 113-24.

Colaluca IN, Tosoni D, Nuciforo P, Senic-Matuglia F, Galimberti V, Viale G et al. (2008) NUMB controls p53 tumour suppressor activity. Nature 451, 76-80.

Corish P and Tyler-Smith C (1999) Attenuation of green fluorescent protein half-life in mammalian cells. Protein Eng 12, 1035-40.

Dabbs DJ, Chivukula M, Carter G, and Bhargava R (2006) Basal phenotype of ductal carcinoma in situ: recognition and immunohistologic profile. Mod Pathol 19, 1506-11.

Daniel CW, De Ome KB, Young JT, Blair PB, and Faulkin LJ, Jr. (1968) The in vivo life span of normal and preneoplastic mouse mammary glands: a serial transplantation study. Proc Natl Acad Sci U S A 61, 53-60.

Deugnier MA, Teuliere J, Faraldo MM, Thiery JP, and Glukhova MA (2002) The importance of being a myoepithelial cell. Breast Cancer Res 4, 224-30.

Di Marcotullio L, Ferretti E, Greco A, De Smaele E, Po A, Sico MA et al. (2006) Numb is a suppressor of Hedgehog signalling and targets Gli1 for Itch-dependent ubiquitination. Nat Cell Biol 8, 1415-23.

Dohn M, Zhang S, and Chen X (2001) p63alpha and DeltaNp63alpha can induce cell cycle arrest and apoptosis and differentially regulate p53 target genes. Oncogene 20, 3193-205.

Dontu G, Abdallah WM, Foley JM, Jackson KW, Clarke MF, Kawamura MJ et al. (2003) In vitro propagation and transcriptional profiling of human mammary stem/progenitor cells. Genes Dev 17, 1253-70.

Dontu G, Jackson KW, McNicholas E, Kawamura MJ, Abdallah WM, and Wicha MS (2004) Role of Notch signaling in cell-fate determination of human mammary stem/progenitor cells. Breast Cancer Res 6, R605-15.

Duarte A, Hirashima M, Benedito R, Trindade A, Diniz P, Bekman E et al. (2004) Dosage-sensitive requirement for mouse Dll4 in artery development. Genes Dev 18, 2474-8.

Duncan AW, Rattis FM, DiMascio LN, Congdon KL, Pazianos G, Zhao C et al. (2005) Integration of Notch and Wnt signaling in hematopoietic stem cell maintenance. Nat Immunol 6, 314-22.

Dupont S, Krust A, Gansmuller A, Dierich A, Chambon P, and Mark M (2000) Effect of single and compound knockouts of estrogen receptors alpha (ERalpha) and beta (ERbeta) on mouse reproductive phenotypes. Development 127, 4277-91.

Eblaghie MC, Song SJ, Kim JY, Akita K, Tickle C, and Jung HS (2004) Interactions between FGF and Wnt signals and Tbx3 gene expression in mammary gland initiation in mouse embryos. J Anat 205, 1-13.

Efstratiadis A, Szabolcs M, and Klinakis A (2007) Notch, Myc and breast cancer. Cell Cycle 6, 418-29.

Ellisen LW, Bird J, West DC, Soreng AL, Reynolds TC, Smith SD et al. (1991) TAN-1, the human homolog of the Drosophila notch gene, is broken by chromosomal translocations in T lymphoblastic neoplasms. Cell 66, 649-61.

Escot C, Theillet C, Lidereau R, Spyratos F, Champeme MH, Gest J et al. (1986) Genetic alteration of the c-myc protooncogene (MYC) in human primary breast carcinomas. Proc Natl Acad Sci U S A 83, 4834-8.

Faraldo MM, Taddei-De La Hosseraye I, Teuliere J, Deugnier MA, Moumen M, Thiery JP et al. (2006) [Mammary gland development: Role of basal myoepithelial cells]. J Soc Biol 200, 193-8.

Faraldo MM, Teuliere J, Deugnier MA, Taddei-De La Hosseraye I, Thiery JP, and Glukhova MA (2005) Myoepithelial cells in the control of mammary development and tumorigenesis: data from genetically modified mice. J Mammary Gland Biol Neoplasia 10, 211-9.

Filipovic A, Gronau JH, Green AR, Wang J, Vallath S, Shao D et al. (2011) Biological and clinical implications of nicastrin expression in invasive breast cancer. Breast Cancer Res Treat 125, 43-53.

Fischer A, Steidl C, Wagner TU, Lang E, Jakob PM, Friedl P et al. (2007) Combined loss of Hey1 and HeyL causes congenital heart defects because of impaired epithelial to mesenchymal transition. Circ Res 100, 856-63.

Fisher B, Jeong JH, Anderson S, Bryant J, Fisher ER, and Wolmark N (2002) Twenty-five-year follow-up of a randomized trial comparing radical mastectomy, total mastectomy, and total mastectomy followed by irradiation. N Engl J Med 347, 567-75.

Fleming RJ (1998) Structural conservation of Notch receptors and ligands. Semin Cell Dev Biol 9, 599-607.

Foley J, Dann P, Hong J, Cosgrove J, Dreyer B, Rimm D et al. (2001) Parathyroid hormone-related protein maintains mammary epithelial fate and triggers nipple skin differentiation during embryonic breast development. Development 128, 513-25.

Forster N, Saladi SV, van Bragt M, Sfondouris ME, Jones FE, Li Z et al. (2014) Basal cell signaling by p63 controls luminal progenitor function and lactation via NRG1. Dev Cell 28, 147-60.

Fre S, Hannezo E, Sale S, Huyghe M, Lafkas D, Kissel H et al. (2011) Notch lineages and activity in intestinal stem cells determined by a new set of knock-in mice. PLoS One 6, e25785.

Fre S, Huyghe M, Mourikis P, Robine S, Louvard D, and Artavanis-Tsakonas S (2005) Notch signals control the fate of immature progenitor cells in the intestine. Nature 435, 964-8.

Fryer CJ, White JB, and Jones KA (2004) Mastermind recruits CycC:CDK8 to phosphorylate the Notch ICD and coordinate activation with turnover. Mol Cell 16, 509-20.

Gallahan D, Jhappan C, Robinson G, Hennighausen L, Sharp R, Kordon E et al. (1996) Expression of a truncated Int3 gene in developing secretory mammary epithelium specifically retards lobular differentiation resulting in tumorigenesis. Cancer Res 56, 1775-85.

Gessler M, Knobeloch KP, Helisch A, Amann K, Schumacher N, Rohde E et al. (2002) Mouse gridlock: no aortic coarctation or deficiency, but fatal cardiac defects in Hey2 -/- mice. Curr Biol 12, 1601-4.

Ginestier C, Hur MH, Charafe-Jauffret E, Monville F, Dutcher J, Brown M et al. (2007) ALDH1 is a marker of normal and malignant human mammary stem cells and a predictor of poor clinical outcome. Cell Stem Cell 1, 555-67.

Goodell MA, Rosenzweig M, Kim H, Marks DF, DeMaria M, Paradis G et al. (1997) Dye efflux studies suggest that hematopoietic stem cells expressing low or undetectable levels of CD34 antigen exist in multiple species. Nat Med 3, 1337-45.

Grego-Bessa J, Luna-Zurita L, del Monte G, Bolos V, Melgar P, Arandilla A et al. (2007) Notch signaling is essential for ventricular chamber development. Dev Cell 12, 415-29.

Guo M, Jan LY, and Jan YN (1996) Control of daughter cell fates during asymmetric division: interaction of Numb and Notch. Neuron 17, 27-41.

Guo W, Keckesova Z, Donaher JL, Shibue T, Tischler V, Reinhardt F et al. (2012) Slug and Sox9 cooperatively determine the mammary stem cell state. Cell 148, 1015-28.

Han H, Tanigaki K, Yamamoto N, Kuroda K, Yoshimoto M, Nakahata T et al. (2002) Inducible gene knockout of transcription factor recombination signal binding protein-J reveals its essential role in T versus B lineage decision. Int Immunol 14, 637-45.

Hanahan D and Weinberg RA (2011) Hallmarks of cancer: the next generation. Cell 144, 646-74.

Hao L, Rizzo P, Osipo C, Pannuti A, Wyatt D, Cheung LWK et al. (2010) Notch-1 activates estrogen receptor-alpha-dependent transcription via IKK alpha in breast cancer cells. Oncogene 29, 201-13.

Harrison H, Simoes BM, Rogerson L, Howell SJ, Landberg G, and Clarke RB (2013) Oestrogen increases the activity of oestrogen receptor negative breast cancer stem cells through paracrine EGFR and Notch signalling. Breast Cancer Res 15, R21.

Haughian JM, Pinto MP, Harrell JC, Bliesner BS, Joensuu KM, Dye WW et al. (2012) Maintenance of hormone responsiveness in luminal breast cancers by suppression of Notch. Proc Natl Acad Sci U S A 109, 2742-7.

Hayward P, Brennan K, Sanders P, Balayo T, DasGupta R, Perrimon N et al. (2005) Notch modulates Wnt signalling by associating with Armadillo/beta-catenin and regulating its transcriptional activity. Development 132, 1819-30.

Heckman BM, Chakravarty G, Vargo-Gogola T, Gonzales-Rimbau M, Hadsell DL, Lee AV et al. (2007) Crosstalk between the p190-B RhoGAP and IGF signaling pathways is required for embryonic mammary bud development. Dev Biol 309, 137-49.

Heitzler P and Simpson P (1991) The choice of cell fate in the epidermis of Drosophila. Cell 64, 1083-92.

Helton ES, Zhu J, and Chen X (2006) The unique NH2-terminally deleted (DeltaN) residues, the PXXP motif, and the PPXY motif are required for the transcriptional activity of the DeltaN variant of p63. J Biol Chem 281, 2533-42.

Hens JR, Dann P, Zhang JP, Harris S, Robinson GW, and Wysolmerski J (2007) BMP4 and PTHrP interact to stimulate ductal outgrowth during embryonic mammary development and to inhibit hair follicle induction. Development 134, 1221-30.

Hilton HN, Graham JD, Kantimm S, Santucci N, Cloosterman D, Huschtscha LI et al. (2012) Progesterone and estrogen receptors segregate into different cell subpopulations in the normal human breast. Mol Cell Endocrinol 361, 191-201.

Hitoshi S, Alexson T, Tropepe V, Donoviel D, Elia AJ, Nye JS et al. (2002) Notch pathway molecules are essential for the maintenance, but not the generation, of mammalian neural stem cells. Genes Dev 16, 846-58.

Hori K, Cholewa-Waclaw J, Nakada Y, Glasgow SM, Masui T, Henke RM et al. (2008) A nonclassical bHLH Rbpj transcription factor complex is required for specification of GABAergic neurons independent of Notch signaling. Genes Dev 22, 166-78.

Horwitzt KB, Dye WW, Harrell JC, Kabos P, and Sartorius CA (2008) Rare steroid receptor-negative basal-like tumorigenic cells in luminal subtype human breast cancer xenografts. Proc Natl Acad Sci U S A 105, 5774-9.

Hu C, Dievart A, Lupien M, Calvo E, Tremblay G, and Jolicoeur P (2006) Overexpression of activated murine Notch1 and Notch3 in transgenic mice blocks mammary gland development and induces mammary tumors. Am J Pathol 168, 973-90.

Iso T, Hamamori Y, and Kedes L (2003) Notch signaling in vascular development. Arterioscler Thromb Vasc Biol 23, 543-53.

Iso T, Kedes L, and Hamamori Y (2003) HES and HERP families: multiple effectors of the Notch signaling pathway. J Cell Physiol 194, 237-55.

Itaranta P, Chi L, Seppanen T, Niku M, Tuukkanen J, Peltoketo H et al. (2006) Wnt-4 signaling is involved in the control of smooth muscle cell fate via Bmp-4 in the medullary stroma of the developing kidney. Dev Biol 293, 473-83.

Itoh M, Kim CH, Palardy G, Oda T, Jiang YJ, Maust D et al. (2003) Mind bomb is a ubiquitin ligase that is essential for efficient activation of Notch signaling by Delta. Dev Cell 4, 67-82.

Izon DJ, Aster JC, He Y, Weng A, Karnell FG, Patriub V et al. (2002) Deltex1 redirects lymphoid progenitors to the B cell lineage by antagonizing Notch1. Immunity 16, 231-43.

Jatoi I and Miller AB (2003) Why is breast-cancer mortality declining? Lancet Oncol 4, 251-4.

Jemal A, Murray T, Samuels A, Ghafoor A, Ward E, and Thun MJ (2003) Cancer statistics, 2003. CA Cancer J Clin 53, 5-26.

Jenni R, Oechslin E, Schneider J, Attenhofer Jost C, and Kaufmann PA (2001) Echocardiographic and pathoanatomical characteristics of isolated left ventricular non-compaction: a step towards classification as a distinct cardiomyopathy. Heart 86, 666-71.

Jhappan C, Gallahan D, Stahle C, Chu E, Smith GH, Merlino G et al. (1992) Expression of an activated Notch-related int-3 transgene interferes with cell differentiation and induces neoplastic transformation in mammary and salivary glands. Genes Dev 6, 345-55.

Jones C, Ford E, Gillett C, Ryder K, Merrett S, Reis-Filho JS et al. (2004) Molecular cytogenetic identification of subgroups of grade III invasive ductal breast carcinomas with different clinical outcomes. Clin Cancer Res 10, 5988-97.

Kageyama R and Ohtsuka T (1999) The Notch-Hes pathway in mammalian neural development. Cell Res 9, 179-88.

Kannabiran C, Zeng XY, and Vales LD (1997) The mammalian transcriptional repressor REP (CBF1) regulates interleukin-6 gene expression. Mol Cell Biol 17, 1-9.

Kastner P, Krust A, Turcotte B, Stropp U, Tora L, Gronemeyer H et al. (1990) Two distinct estrogen-regulated promoters generate transcripts encoding the two functionally different human progesterone receptor forms A and B. EMBO J 9, 1603-14.

Kiaris H, Politi K, Grimm LM, Szabolcs M, Fisher P, Efstratiadis A et al. (2004) Modulation of notch signaling elicits signature tumors and inhibits hras1-induced oncogenesis in the mouse mammary epithelium. Am J Pathol 165, 695-705.

Kidd S, Kelley MR, and Young MW (1986) Sequence of the notch locus of Drosophila melanogaster: relationship of the encoded protein to mammalian clotting and growth factors. Mol Cell Biol 6, 3094-108.

Kimble J, Henderson S, and Crittenden S (1998) Notch/LIN-12 signaling: transduction by regulated protein slicing. Trends Biochem Sci 23, 353-7.

Klinakis A, Lobry C, Abdel-Wahab O, Oh P, Haeno H, Buonamici S et al. (2011) A novel tumour-suppressor function for the Notch pathway in myeloid leukaemia. Nature 473, 230-3.

Krebs LT, Shutter JR, Tanigaki K, Honjo T, Stark KL, and Gridley T (2004) Haploinsufficient lethality and formation of arteriovenous malformations in Notch pathway mutants. Genes Dev 18, 2469-73.

Krebs LT, Xue Y, Norton CR, Shutter JR, Maguire M, Sundberg JP et al. (2000) Notch signaling is essential for vascular morphogenesis in mice. Genes Dev 14, 1343-52.

Kreuzaler PA, Staniszewska AD, Li W, Omidvar N, Kedjouar B, Turkson J et al. (2011) Stat3 controls lysosomal-mediated cell death in vivo. Nat Cell Biol 13, 303-9.

Kritikou EA, Sharkey A, Abell K, Came PJ, Anderson E, Clarkson RW et al. (2003) A dual, non-redundant, role for LIF as a regulator of development and STAT3-mediated cell death in mammary gland. Development 130, 3459-68.

Kurooka H and Honjo T (2000) Functional interaction between the mouse notch1 intracellular region and histone acetyltransferases PCAF and GCN5. J Biol Chem 275, 17211-20.

Lafkas D, Rodilla V, Huyghe M, Mourao L, Kiaris H, and Fre S (2013) Notch3 marks clonogenic mammary luminal progenitor cells in vivo. J Cell Biol 203, 47-56.

Lai EC (2002) Protein degradation: four E3s for the notch pathway. Curr Biol 12, R74-8.

LaMarca HL and Rosen JM (2008) Minireview: hormones and mammary cell fate--what will I become when I grow up? Endocrinology 149, 4317-21.

Landua JD, Visbal AP, and Lewis MT (2009) Methods for preparing fluorescent and neutral red-stained whole mounts of mouse mammary glands. J Mammary Gland Biol Neoplasia 14, 411-5.

Lathion S, Schaper J, Beard P, and Raj K (2003) Notch1 can contribute to viral-induced transformation of primary human keratinocytes. Cancer Res 63, 8687-94.

Lee CW, Raskett CM, Prudovsky I, and Altieri DC (2008) Molecular dependence of estrogen receptor-negative breast cancer on a notch-survivin signaling axis. Cancer Res 68, 5273-81.

Lee CW, Simin K, Liu Q, Plescia J, Guha M, Khan A et al. (2008) A functional Notch-survivin gene signature in basal breast cancer. Breast Cancer Res 10, R97.

Lee EY, Lee WH, Kaetzel CS, Parry G, and Bissell MJ (1985) Interaction of mouse mammary epithelial cells with collagen substrata: regulation of casein gene expression and secretion. Proc Natl Acad Sci U S A 82, 1419-23.

Leimeister C, Externbrink A, Klamt B, and Gessler M (1999) Hey genes: a novel subfamily of hairy- and Enhancer of split related genes specifically expressed during mouse embryogenesis. Mech Dev 85, 173-7.

Leimeister C, Schumacher N, Steidl C, and Gessler M (2000) Analysis of HeyL expression in wild-type and Notch pathway mutant mouse embryos. Mech Dev 98, 175-8.

Li M, Liu X, Robinson G, Bar-Peled U, Wagner KU, Young WS et al. (1997) Mammary-derived signals activate programmed cell death during the first stage of mammary gland involution. Proc Natl Acad Sci U S A 94, 3425-30.

Li W, Ferguson BJ, Khaled WT, Tevendale M, Stingl J, Poli V et al. (2009) PML depletion disrupts normal mammary gland development and skews the composition of the mammary luminal cell progenitor pool. Proc Natl Acad Sci U S A 106, 4725-30.

Lieber T, Kidd S, and Young MW (2002) kuzbanian-mediated cleavage of Drosophila Notch. Genes Dev 16, 209-21.

Lin CY, Strom A, Vega VB, Kong SL, Yeo AL, Thomsen JS et al. (2004) Discovery of estrogen receptor alpha target genes and response elements in breast tumor cells. Genome Biol 5, R66.

Lin YL, Sengupta S, Gurdziel K, Bell GW, Jacks T, and Flores ER (2009) p63 and p73 transcriptionally regulate genes involved in DNA repair. PLoS Genet 5, e1000680.

Lincoln J, Alfieri CM, and Yutzey KE (2004) Development of heart valve leaflets and supporting apparatus in chicken and mouse embryos. Dev Dyn 230, 239-50.

Ling H, Sylvestre JR, and Jolicoeur P (2010) Notch1-induced mammary tumor development is cyclin D1-dependent and correlates with expansion of pre-malignant multipotent duct-limited progenitors. Oncogene 29, 4543-54.

Livasy CA, Karaca G, Nanda R, Tretiakova MS, Olopade OI, Moore DT et al. (2006) Phenotypic evaluation of the basal-like subtype of invasive breast carcinoma. Mod Pathol 19, 264-71.

Lobry C, Oh P, Mansour MR, Look AT, and Aifantis I (2014) Notch signaling: switching an oncogene to a tumor suppressor. Blood 123, 2451-9.

Logeat F, Bessia C, Brou C, LeBail O, Jarriault S, Seidah NG et al. (1998) The Notch1 receptor is cleaved constitutively by a furin-like convertase. Proc Natl Acad Sci U S A 95, 8108-12.

Lombardo Y, Faronato M, Filipovic A, Vircillo V, Magnani L, and Coombes RC (2014) Nicastrin and Notch4 drive endocrine therapy resistance and epithelial to mesenchymal transition in MCF7 breast cancer cells. Breast Cancer Res 16, R62.

Lutolf S, Radtke F, Aguet M, Suter U, and Taylor V (2002) Notch1 is required for neuronal and glial differentiation in the cerebellum. Development 129, 373-85.

Lydon JP, DeMayo FJ, Funk CR, Mani SK, Hughes AR, Montgomery CA, Jr. et al. (1995) Mice lacking progesterone receptor exhibit pleiotropic reproductive abnormalities. Genes Dev 9, 2266-78.

Lyons WR, Li CH, and Johnson RE (1958) The hormonal control of mammary growth and lactation. Recent Prog Horm Res 14, 219-48; discussion 48-54.

Ma XJ, Salunga R, Tuggle JT, Gaudet J, Enright E, McQuary P et al. (2003) Gene expression profiles of human breast cancer progression. Proc Natl Acad Sci U S A 100, 5974-9.

Maier MM and Gessler M (2000) Comparative analysis of the human and mouse Hey1 promoter: Hey genes are new Notch target genes. Biochem Biophys Res Commun 275, 652-60.

Maillard I, Weng AP, Carpenter AC, Rodriguez CG, Sai H, Xu L et al. (2004) Mastermind critically regulates Notch-mediated lymphoid cell fate decisions. Blood 104, 1696-702.

Mailleux AA, Spencer-Dene B, Dillon C, Ndiaye D, Savona-Baron C, Itoh N et al. (2002) Role of FGF10/FGFR2b signaling during mammary gland development in the mouse embryo. Development 129, 53-60.

Mallepell S, Krust A, Chambon P, and Brisken C (2006) Paracrine signaling through the epithelial estrogen receptor alpha is required for proliferation and morphogenesis in the mammary gland. Proc Natl Acad Sci U S A 103, 2196-201.

Mandel H, Shemer R, Borochowitz ZU, Okopnik M, Knopf C, Indelman M et al. (2008) SERKAL syndrome: an autosomal-recessive disorder caused by a loss-of-function mutation in WNT4. Am J Hum Genet 82, 39-47.

Mani SA, Guo W, Liao MJ, Eaton EN, Ayyanan A, Zhou AY et al. (2008) The epithelial-mesenchymal transition generates cells with properties of stem cells. Cell 133, 704-15.

McGill MA, Dho SE, Weinmaster G, and McGlade CJ (2009) Numb regulates post-endocytic trafficking and degradation of Notch1. J Biol Chem 284, 26427-38.

McGill MA and McGlade CJ (2003) Mammalian numb proteins promote Notch1 receptor ubiquitination and degradation of the Notch1 intracellular domain. J Biol Chem 278, 23196-203.

Medici D, Hay ED, and Olsen BR (2008) Snail and Slug promote epithelial-mesenchymal transition through beta-catenin-T-cell factor-4-dependent expression of transforming growth factor-beta3. Mol Biol Cell 19, 4875-87.

Meurette O, Stylianou S, Rock R, Collu GM, Gilmore AP, and Brennan K (2009) Notch activation induces Akt signaling via an autocrine loop to prevent apoptosis in breast epithelial cells. Cancer Res 69, 5015-22.

Micchelli CA, Esler WP, Kimberly WT, Jack C, Berezovska O, Kornilova A et al. (2003) Gamma-secretase/presenilin inhibitors for Alzheimer's disease phenocopy Notch mutations in Drosophila. FASEB J 17, 79-81.

Mikaelian I, Hovick M, Silva KA, Burzenski LM, Shultz LD, Ackert-Bicknell CL et al. (2006) Expression of terminal differentiation proteins defines stages of mouse mammary gland development. Vet Pathol 43, 36-49.

Mills AA, Qi Y, and Bradley A (2002) Conditional inactivation of p63 by Cre-mediated excision. Genesis 32, 138-41.

Mills AA, Qi Y, and Bradley A (2002) Conditional inactivation of p63 by Cre-mediated excision. Genesis 32, 138-41.

Mills AA, Zheng B, Wang XJ, Vogel H, Roop DR, and Bradley A (1999) p63 is a p53 homologue required for limb and epidermal morphogenesis. Nature 398, 708-13.

Mizutani K, Yoon K, Dang L, Tokunaga A, and Gaiano N (2007) Differential Notch signalling distinguishes neural stem cells from intermediate progenitors. Nature 449, 351-5.

Mombaerts P, Iacomini J, Johnson RS, Herrup K, Tonegawa S, and Papaioannou VE (1992) RAG-1-deficient mice have no mature B and T lymphocytes. Cell 68, 869-77.

Monks J, Smith-Steinhart C, Kruk ER, Fadok VA, and Henson PM (2008) Epithelial cells remove apoptotic epithelial cells during post-lactation involution of the mouse mammary gland. Biol Reprod 78, 586-94.

Morel AP, Lievre M, Thomas C, Hinkal G, Ansieau S, and Puisieux A (2008) Generation of breast cancer stem cells through epithelial-mesenchymal transition. PLoS One 3, e2888.

Moyano JV, Evans JR, Chen F, Lu M, Werner ME, Yehiely F et al. (2006) AlphaB-crystallin is a novel oncoprotein that predicts poor clinical outcome in breast cancer. J Clin Invest 116, 261-70.

Muzumdar MD, Tasic B, Miyamichi K, Li L, and Luo L (2007) A global double-fluorescent Cre reporter mouse. Genesis 45, 593-605.

Nahta R and Esteva FJ (2007) Trastuzumab: triumphs and tribulations. Oncogene 26, 3637-43.

Nam Y, Sliz P, Song L, Aster JC, and Blacklow SC (2006) Structural basis for cooperativity in recruitment of MAML coactivators to Notch transcription complexes. Cell 124, 973-83.

Nandi S (1958) Endocrine control of mammarygland development and function in the C3H/ He Crgl mouse. J Natl Cancer Inst 21, 1039-63.

Nardulli AM, Greene GL, O'Malley BW, and Katzenellenbogen BS (1988) Regulation of progesterone receptor messenger ribonucleic acid and protein levels in MCF-7 cells by estradiol: analysis of estrogen's effect on progesterone receptor synthesis and degradation. Endocrinology 122, 935-44.

Nichols JT, Miyamoto A, and Weinmaster G (2007) Notch signaling--constantly on the move. Traffic 8, 959-69.

Nichols JT, Miyamoto A, and Weinmaster G (2007) Notch signaling--constantly on the move. Traffic 8, 959-69.

Nicholson DW, Ali A, Thornberry NA, Vaillancourt JP, Ding CK, Gallant M et al. (1995) Identification and inhibition of the ICE/CED-3 protease necessary for mammalian apoptosis. Nature 376, 37-43.

Nickoloff BJ, Qin JZ, Chaturvedi V, Denning MF, Bonish B, and Miele L (2002) Jagged-1 mediated activation of notch signaling induces complete maturation of human keratinocytes through NF-kappaB and PPARgamma. Cell Death Differ 9, 842-55.

Nielsen M, Thomsen JL, Primdahl S, Dyreborg U, and Andersen JA (1987) Breast cancer and atypia among young and middle-aged women: a study of 110 medicolegal autopsies. Br J Cancer 56, 814-9.

Nielsen TO, Hsu FD, Jensen K, Cheang M, Karaca G, Hu Z et al. (2004) Immunohistochemical and clinical characterization of the basal-like subtype of invasive breast carcinoma. Clin Cancer Res 10, 5367-74.

Nilsson S, Makela S, Treuter E, Tujague M, Thomsen J, Andersson G et al. (2001) Mechanisms of estrogen action. Physiol Rev 81, 1535-65.

Novak A, Guo C, Yang W, Nagy A, and Lobe CG (2000) Z/EG, a double reporter mouse line that expresses enhanced green fluorescent protein upon Cre-mediated excision. Genesis 28, 147-55.

Nylander K, Vojtesek B, Nenutil R, Lindgren B, Roos G, Zhanxiang W et al. (2002) Differential expression of p63 isoforms in normal tissues and neoplastic cells. J Pathol 198, 417-27.

Oakes SR, Naylor MJ, Asselin-Labat ML, Blazek KD, Gardiner-Garden M, Hilton HN et al. (2008) The Ets transcription factor Elf5 specifies mammary alveolar cell fate. Genes Dev 22, 581-6.

Oftedal OT (2002) The origin of lactation as a water source for parchment-shelled eggs. J Mammary Gland Biol Neoplasia 7, 253-66.

Ohlstein B and Spradling A (2007) Multipotent Drosophila intestinal stem cells specify daughter cell fates by differential notch signaling. Science 315, 988-92.

Ohtsuka T, Ishibashi M, Gradwohl G, Nakanishi S, Guillemot F, and Kageyama R (1999) Hes1 and Hes5 as notch effectors in mammalian neuronal differentiation. EMBO J 18, 2196-207.

Okabe M, Ikawa M, Kominami K, Nakanishi T, and Nishimune Y (1997) 'Green mice' as a source of ubiquitous green cells. FEBS Lett 407, 313-9.

O'Neill CF, Urs S, Cinelli C, Lincoln A, Nadeau RJ, Leon R et al. (2007) Notch2 signaling induces apoptosis and inhibits human MDA-MB-231 xenograft growth. Am J Pathol 171, 1023-36.

Ong CT, Cheng HT, Chang LW, Ohtsuka T, Kageyama R, Stormo GD et al. (2006) Target selectivity of vertebrate notch proteins. Collaboration between discrete domains and CSL-binding site architecture determines activation probability. J Biol Chem 281, 5106-19.

Oswald F, Kostezka U, Astrahantseff K, Bourteele S, Dillinger K, Zechner U et al. (2002) SHARP is a novel component of the Notch/RBP-Jkappa signalling pathway. EMBO J 21, 5417-26.

Oswald F, Tauber B, Dobner T, Bourteele S, Kostezka U, Adler G et al. (2001) p300 acts as a transcriptional coactivator for mammalian Notch-1. Mol Cell Biol 21, 7761-74.

Panin VM, Papayannopoulos V, Wilson R, and Irvine KD (1997) Fringe modulates Notch-ligand interactions. Nature 387, 908-12.

Parks AL, Klueg KM, Stout JR, and Muskavitch MA (2000) Ligand endocytosis drives receptor dissociation and activation in the Notch pathway. Development 127, 1373-85.

Parr C, Watkins G, and Jiang WG (2004) The possible correlation of Notch-1 and Notch-2 with clinical outcome and tumour clinicopathological parameters in human breast cancer. Int J Mol Med 14, 779-86.

Pear WS and Aster JC (2004) T cell acute lymphoblastic leukemia/lymphoma: a human cancer commonly associated with aberrant NOTCH1 signaling. Curr Opin Hematol 11, 426-33.

Pece S and Gutkind JS (2000) Signaling from E-cadherins to the MAPK pathway by the recruitment and activation of epidermal growth factor receptors upon cell-cell contact formation. J Biol Chem 275, 41227-33.

Perou CM, Sorlie T, Eisen MB, van de Rijn M, Jeffrey SS, Rees CA et al. (2000) Molecular portraits of human breast tumours. Nature 406, 747-52.

Petz LN and Nardulli AM (2000) Sp1 binding sites and an estrogen response element half-site are involved in regulation of the human progesterone receptor A promoter. Mol Endocrinol 14, 972-85.

Pintar A, De Biasio A, Popovic M, Ivanova N, and Pongor S (2007) The intracellular region of Notch ligands: does the tail make the difference? Biol Direct 2, 19.

Portanova P, Notaro A, Pellerito O, Sabella S, Giuliano M, and Calvaruso G (2013) Notch inhibition restores TRAIL-mediated apoptosis via AP1-dependent upregulation of DR4 and DR5 TRAIL receptors in MDA-MB-231 breast cancer cells. Int J Oncol 43, 121-30.

Poulson DF (1937) Chromosomal Deficiencies and the Embryonic Development of Drosophila Melanogaster. Proc Natl Acad Sci U S A 23, 133-7.

Pozzi S, Boergesen M, Sinha S, Mandrup S, and Mantovani R (2009) Peroxisome proliferator-activated receptor-alpha is a functional target of p63 in adult human keratinocytes. J Invest Dermatol 129, 2376-85.

Pritchard K (2005) Endocrinology and hormone therapy in breast cancer: endocrine therapy in premenopausal women. Breast Cancer Res 7, 70-6.

Raafat A, Goldhar AS, Klauzinska M, Xu K, Amirjazil I, McCurdy D et al. (2011) Expression of Notch receptors, ligands, and target genes during development of the mouse mammary gland. J Cell Physiol 226, 1940-52.

Raafat A, Zoltan-Jones A, Strizzi L, Bargo S, Kimura K, Salomon D et al. (2007) Kit and PDGFR-alpha activities are necessary for Notch4/Int3-induced tumorigenesis. Oncogene 26, 662-72.

Rajaram RD, Buric D, Caikovski M, Ayyanan A, Rougemont J, Shan J et al. (2015) Progesterone and Wnt4 control mammary stem cells via myoepithelial crosstalk. EMBO J

Rakha EA, Reis-Filho JS, Baehner F, Dabbs DJ, Decker T, Eusebi V et al. (2010) Breast cancer prognostic classification in the molecular era: the role of histological grade. Breast Cancer Res 12, 207.

Rand MD, Grimm LM, Artavanis-Tsakonas S, Patriub V, Blacklow SC, Sklar J et al. (2000) Calcium depletion dissociates and activates heterodimeric notch receptors. Mol Cell Biol 20, 1825-35.

Ranganathan P, Weaver KL, and Capobianco AJ (2011) Notch signalling in solid tumours: a little bit of everything but not all the time. Nat Rev Cancer 11, 338-51.

Rangarajan A, Talora C, Okuyama R, Nicolas M, Mammucari C, Oh H et al. (2001) Notch signaling is a direct determinant of keratinocyte growth arrest and entry into differentiation. EMBO J 20, 3427-36.

Raouf A, Zhao Y, To K, Stingl J, Delaney A, Barbara M et al. (2008) Transcriptome analysis of the normal human mammary cell commitment and differentiation process. Cell Stem Cell 3, 109-18.

Reedijk M, Odorcic S, Chang L, Zhang H, Miller N, McCready DR et al. (2005) High-level coexpression of JAG1 and NOTCH1 is observed in human breast cancer and is associated with poor overall survival. Cancer Res 65, 8530-7.

Reedijk M, Pinnaduwage D, Dickson BC, Mulligan AM, Zhang H, Bull SB et al. (2008) JAG1 expression is associated with a basal phenotype and recurrence in lymph node-negative breast cancer. Breast Cancer Res Treat 111, 439-48.

Regan JL, Kendrick H, Magnay FA, Vafaizadeh V, Groner B, and Smalley MJ (2012) c-Kit is required for growth and survival of the cells of origin of Brca1-mutation-associated breast cancer. Oncogene 31, 869-83.

Reis-Filho JS, Torio B, Albergaria A, and Schmitt FC (2002) p63 expression in normal skin and usual cutaneous carcinomas. J Cutan Pathol 29, 517-23.

Richert MM, Schwertfeger KL, Ryder JW, and Anderson SM (2000) An atlas of mouse mammary gland development. J Mammary Gland Biol Neoplasia 5, 227-41.

Rizzo P, Miao H, D'Souza G, Osipo C, Song LL, Yun J et al. (2008) Cross-talk between notch and the estrogen receptor in breast cancer suggests novel therapeutic approaches. Cancer Res 68, 5226-35.

Robinson DR, Kalyana-Sundaram S, Wu YM, Shankar S, Cao XH, Ateeq B et al. (2011) Functionally recurrent rearrangements of the MAST kinase and Notch gene families in breast cancer. Nat Med 17, 1646-U163.

Robinson GW (2007) Cooperation of signalling pathways in embryonic mammary gland development. Nat Rev Genet 8, 963-72.

Robinson GW, Karpf AB, and Kratochwil K (1999) Regulation of mammary gland development by tissue interaction. J Mammary Gland Biol Neoplasia 4, 9-19.

Romano RA, Smalley K, Magraw C, Serna VA, Kurita T, Raghavan S et al. (2012) DeltaNp63 knockout mice reveal its indispensable role as a master regulator of epithelial development and differentiation. Development 139, 772-82.

Rouzier R, Perou CM, Symmans WF, Ibrahim N, Cristofanilli M, Anderson K et al. (2005) Breast cancer molecular subtypes respond differently to preoperative chemotherapy. Clin Cancer Res 11, 5678-85.

Russell TD, Fischer A, Beeman NE, Freed EF, Neville MC, and Schaack J (2003) Transduction of the mammary epithelium with adenovirus vectors in vivo. J Virol 77, 5801-9.

Rustighi A, Tiberi L, Soldano A, Napoli M, Nuciforo P, Rosato A et al. (2009) The prolyl-isomerase Pin1 is a Notch1 target that enhances Notch1 activation in cancer. Nat Cell Biol 11, 133-42.

Sakakura T, Kusano I, Kusakabe M, Inaguma Y, and Nishizuka Y (1987) Biology of mammary fat pad in fetal mouse: capacity to support development of various fetal epithelia in vivo. Development 100, 421-30.

Sale S, Lafkas D, and Artavanis-Tsakonas S (2013) Notch2 genetic fate mapping reveals two previously unrecognized mammary epithelial lineages. Nat Cell Biol 15, 451-60.

Sanalkumar R, Dhanesh SB, and James J (2010) Non-canonical activation of Notch signaling/target genes in vertebrates. Cell Mol Life Sci 67, 2957-68.

Sansone P, Storci G, Giovannini C, Pandolfi S, Pianetti S, Taffurelli M et al. (2007) p66Shc/Notch-3 interplay controls self-renewal and hypoxia survival in human stem/progenitor cells of the mammary gland expanded in vitro as mammospheres. Stem Cells 25, 807-15.

Schneider CA, Rasband WS, and Eliceiri KW (2012) NIH Image to ImageJ: 25 years of image analysis. Nat Methods 9, 671-5.

Scholzen T and Gerdes J (2000) The Ki-67 protein: from the known and the unknown. J Cell Physiol 182, 311-22.

Schultz JR, Petz LN, and Nardulli AM (2003) Estrogen receptor alpha and Sp1 regulate progesterone receptor gene expression. Mol Cell Endocrinol 201, 165-75.

Scorilas A, Trangas T, Yotis J, Pateras C, and Talieri M (1999) Determination of c-myc amplification and overexpression in breast cancer patients: evaluation of its prognostic value against c-erbB-2, cathepsin-D and clinicopathological characteristics using univariate and multivariate analysis. Br J Cancer 81, 1385-91.

Seagroves TN, Lydon JP, Hovey RC, Vonderhaar BK, and Rosen JM (2000) C/EBPbeta (CCAAT/enhancer binding protein) controls cell fate determination during mammary gland development. Mol Endocrinol 14, 359-68.

Shackleton M, Vaillant F, Simpson KJ, Stingl J, Smyth GK, Asselin-Labat ML et al. (2006) Generation of a functional mammary gland from a single stem cell. Nature 439, 84-8.

Shan J, Jokela T, Skovorodkin I, and Vainio S (2010) Mapping of the fate of cell lineages generated from cells that express the Wnt4 gene by time-lapse during kidney development. Differentiation 79, 57-64.

Shehata M, Teschendorff A, Sharp G, Novcic N, Russell IA, Avril S et al. (2012) Phenotypic and functional characterisation of the luminal cell hierarchy of the mammary gland. Breast Cancer Res 14, R134.

Shien T, Tashiro T, Omatsu M, Masuda T, Furuta K, Sato N et al. (2005) Frequent overexpression of epidermal growth factor receptor (EGFR) in mammary high grade ductal carcinomas with myoepithelial differentiation. J Clin Pathol 58, 1299-304.

Shin BK, Lee Y, Lee JB, Kim HK, Lee JB, Cho SJ et al. (2008) Breast carcinomas expressing basal markers have poor clinical outcome regardless of estrogen receptor status. Oncol Rep 19, 617-25.

Shin HM, Minter LM, Cho OH, Gottipati S, Fauq AH, Golde TE et al. (2006) Notch1 augments NF-kappaB activity by facilitating its nuclear retention. EMBO J 25, 129-38.

Shyamala G (1999) Progesterone signaling and mammary gland morphogenesis. J Mammary Gland Biol Neoplasia 4, 89-104.

Silberstein GB (2001) Postnatal mammary gland morphogenesis. Microsc Res Tech 52, 155-62.

Slamon DJ, Clark GM, Wong SG, Levin WJ, Ullrich A, and McGuire WL (1987) Human breast cancer: correlation of relapse and survival with amplification of the HER-2/neu oncogene. Science 235, 177-82.

Sleeman KE, Kendrick H, Ashworth A, Isacke CM, and Smalley MJ (2006) CD24 staining of mouse mammary gland cells defines luminal epithelial, myoepithelial/basal and non-epithelial cells. Breast Cancer Res 8, R7.

Sleeman KE, Kendrick H, Robertson D, Isacke CM, Ashworth A, and Smalley MJ (2007) Dissociation of estrogen receptor expression and in vivo stem cell activity in the mammary gland. J Cell Biol 176, 19-26.

Smith GH, Gallahan D, Diella F, Jhappan C, Merlino G, and Callahan R (1995) Constitutive expression of a truncated INT3 gene in mouse mammary epithelium impairs differentiation and functional development. Cell Growth Differ 6, 563-77.

Song R, Koo BK, Yoon KJ, Yoon MJ, Yoo KW, Kim HT et al. (2006) Neuralized-2 regulates a Notch ligand in cooperation with Mind bomb-1. J Biol Chem 281, 36391-400.

Soriano JV, Uyttendaele H, Kitajewski J, and Montesano R (2000) Expression of an activated Notch4(int-3) oncoprotein disrupts morphogenesis and induces an invasive phenotype in mammary epithelial cells in vitro. Int J Cancer 86, 652-9.

Sorlie T, Perou CM, Tibshirani R, Aas T, Geisler S, Johnsen H et al. (2001) Gene expression patterns of breast carcinomas distinguish tumor subclasses with clinical implications. Proc Natl Acad Sci U S A 98, 10869-74.

Sorlie T, Tibshirani R, Parker J, Hastie T, Marron JS, Nobel A et al. (2003) Repeated observation of breast tumor subtypes in independent gene expression data sets. Proc Natl Acad Sci U S A 100, 8418-23.

Sotiriou C, Neo SY, McShane LM, Korn EL, Long PM, Jazaeri A et al. (2003) Breast cancer classification and prognosis based on gene expression profiles from a population-based study. Proc Natl Acad Sci U S A 100, 10393-8.

Stephenson NL and Avis JM (2012) Direct observation of proteolytic cleavage at the S2 site upon forced unfolding of the Notch negative regulatory region. Proc Natl Acad Sci U S A 109, E2757-65.

Sternlicht MD, Kedeshian P, Shao ZM, Safarians S, and Barsky SH (1997) The human myoepithelial cell is a natural tumor suppressor. Clin Cancer Res 3, 1949-58.

Stingl J, Eirew P, Ricketson I, Shackleton M, Vaillant F, Choi D et al. (2006) Purification and unique properties of mammary epithelial stem cells. Nature 439, 993-7.

Stockhausen MT, Sjolund J, and Axelson H (2005) Regulation of the Notch target gene Hes-1 by TGFalpha induced Ras/MAPK signaling in human neuroblastoma cells. Exp Cell Res 310, 218-28.

Strange R, Li F, Saurer S, Burkhardt A, and Friis RR (1992) Apoptotic cell death and tissue remodelling during mouse mammary gland involution. Development 115, 49-58.

Stransky N, Egloff AM, Tward AD, Kostic AD, Cibulskis K, Sivachenko A et al. (2011) The mutational landscape of head and neck squamous cell carcinoma. Science 333, 1157-60.

Strochlic L, Falk J, Goillot E, Sigoillot S, Bourgeois F, Delers P et al. (2012) Wnt4 participates in the formation of vertebrate neuromuscular junction. PLoS One 7, e29976.

Stylianou S, Clarke RB, and Brennan K (2006) Aberrant activation of notch signaling in human breast cancer. Cancer Res 66, 1517-25.

Su X, Paris M, Gi YJ, Tsai KY, Cho MS, Lin YL et al. (2009) TAp63 prevents premature aging by promoting adult stem cell maintenance. Cell Stem Cell 5, 64-75.

Sun X and Artavanis-Tsakonas S (1996) The intracellular deletions of Delta and Serrate define dominant negative forms of the Drosophila Notch ligands. Development 122, 2465-74.

Teuliere J, Faraldo MM, Deugnier MA, Shtutman M, Ben-Ze'ev A, Thiery JP et al. (2005) Targeted activation of beta-catenin signaling in basal mammary epithelial cells affects mammary development and leads to hyperplasia. Development 132, 267-77.

Tiffen PG, Omidvar N, Marquez-Almuina N, Croston D, Watson CJ, and Clarkson RW (2008) A dual role for oncostatin M signaling in the differentiation and death of mammary epithelial cells in vivo. Mol Endocrinol 22, 2677-88.

Timmerman LA, Grego-Bessa J, Raya A, Bertran E, Perez-Pomares JM, Diez J et al. (2004) Notch promotes epithelial-mesenchymal transition during cardiac development and oncogenic transformation. Genes Dev 18, 99-115.

Tobias JS (2004) Recent advances in endocrine therapy for postmenopausal women with early breast cancer: implications for treatment and prevention. Ann Oncol 15, 1738-47.

Uyttendaele H, Ho J, Rossant J, and Kitajewski J (2001) Vascular patterning defects associated with expression of activated Notch4 in embryonic endothelium. Proc Natl Acad Sci U S A 98, 5643-8.

Uyttendaele H, Soriano JV, Montesano R, and Kitajewski J (1998) Notch4 and Wnt-1 proteins function to regulate branching morphogenesis of mammary epithelial cells in an opposing fashion. Dev Biol 196, 204-17.

van Genderen C, Okamura RM, Farinas I, Quo RG, Parslow TG, Bruhn L et al. (1994) Development of several organs that require inductive epithelial-mesenchymal interactions is impaired in LEF-1-deficient mice. Genes Dev 8, 2691-703.

Van Keymeulen A, Rocha AS, Ousset M, Beck B, Bouvencourt G, Rock J et al. (2011) Distinct stem cells contribute to mammary gland development and maintenance. Nature 479, 189-93.

van Tetering G, van Diest P, Verlaan I, van der Wall E, Kopan R, and Vooijs M (2009) Metalloprotease ADAM10 is required for Notch1 site 2 cleavage. J Biol Chem 284, 31018-27.

Veltmaat JM, Mailleux AA, Thiery JP, and Bellusci S (2003) Mouse embryonic mammogenesis as a model for the molecular regulation of pattern formation. Differentiation 71, 1-17.

Veltmaat JM, Van Veelen W, Thiery JP, and Bellusci S (2004) Identification of the mammary line in mouse by Wnt10b expression. Dev Dyn 229, 349-56.

Visvader JE and Stingl J (2014) Mammary stem cells and the differentiation hierarchy: current status and perspectives. Genes Dev 28, 1143-58.

Wagner KU, McAllister K, Ward T, Davis B, Wiseman R, and Hennighausen L (2001) Spatial and temporal expression of the Cre gene under the control of the MMTV-LTR in different lines of transgenic mice. Transgenic Res 10, 545-53.

Wallberg AE, Pedersen K, Lendahl U, and Roeder RG (2002) p300 and PCAF act cooperatively to mediate transcriptional activation from chromatin templates by notch intracellular domains in vitro. Mol Cell Biol 22, 7812-9.

Wang HU, Chen ZF, and Anderson DJ (1998) Molecular distinction and angiogenic interaction between embryonic arteries and veins revealed by ephrin-B2 and its receptor Eph-B4. Cell 93, 741-53.

Welm BE, Tepera SB, Venezia T, Graubert TA, Rosen JM, and Goodell MA (2002) Sca-1(pos) cells in the mouse mammary gland represent an enriched progenitor cell population. Dev Biol 245, 42-56.

Weng AP, Ferrando AA, Lee W, Morris JPt, Silverman LB, Sanchez-Irizarry C et al. (2004) Activating mutations of NOTCH1 in human T cell acute lymphoblastic leukemia. Science 306, 269-71.

Weng AP, Nam Y, Wolfe MS, Pear WS, Griffin JD, Blacklow SC et al. (2003) Growth suppression of pre-T acute lymphoblastic leukemia cells by inhibition of notch signaling. Mol Cell Biol 23, 655-64.

Westfall MD and Pietenpol JA (2004) p63: Molecular complexity in development and cancer. Carcinogenesis 25, 857-64.

Wharton KA, Johansen KM, Xu T, and Artavanis-Tsakonas S (1985) Nucleotide sequence from the neurogenic locus notch implies a gene product that shares homology with proteins containing EGF-like repeats. Cell 43, 567-81.

Widelitz RB, Veltmaat JM, Mayer JA, Foley J, and Chuong CM (2007) Mammary glands and feathers: comparing two skin appendages which help define novel classes during vertebrate evolution. Semin Cell Dev Biol 18, 255-66.

Williams SE, Beronja S, Pasolli HA, and Fuchs E (2011) Asymmetric cell divisions promote Notch-dependent epidermal differentiation. Nature 470, 353-8.

Wu L, Aster JC, Blacklow SC, Lake R, Artavanis-Tsakonas S, and Griffin JD (2000) MAML1, a human homologue of Drosophila mastermind, is a transcriptional co-activator for NOTCH receptors. Nat Genet 26, 484-9.

Wysolmerski JJ, Philbrick WM, Dunbar ME, Lanske B, Kronenberg H, and Broadus AE (1998) Rescue of the parathyroid hormone-related protein knockout mouse demonstrates that parathyroid hormone-related protein is essential for mammary gland development. Development 125, 1285-94.

Yalcin-Ozuysal O, Fiche M, Guitierrez M, Wagner KU, Raffoul W, and Brisken C (2010) Antagonistic roles of Notch and p63 in controlling mammary epithelial cell fates. Cell Death Differ 17, 1600-12.

Yamamoto N, Yamamoto S, Inagaki F, Kawaichi M, Fukamizu A, Kishi N et al. (2001) Role of Deltex-1 as a transcriptional regulator downstream of the Notch receptor. J Biol Chem 276, 45031-40.

Yang A, Kaghad M, Wang Y, Gillett E, Fleming MD, Dotsch V et al. (1998) p63, a p53 homolog at 3q27-29, encodes multiple products with transactivating, death-inducing, and dominant-negative activities. Mol Cell 2, 305-16.

Yang A, Schweitzer R, Sun D, Kaghad M, Walker N, Bronson RT et al. (1999) p63 is essential for regenerative proliferation in limb, craniofacial and epithelial development. Nature 398, 714-8.

Yang LT, Nichols JT, Yao C, Manilay JO, Robey EA, and Weinmaster G (2005) Fringe glycosyltransferases differentially modulate Notch1 proteolysis induced by Delta1 and Jagged1. Mol Biol Cell 16, 927-42.

Yang X, Klein R, Tian X, Cheng HT, Kopan R, and Shen J (2004) Notch activation induces apoptosis in neural progenitor cells through a p53-dependent pathway. Dev Biol 269, 81-94.

Yoon K, Nery S, Rutlin ML, Radtke F, Fishell G, and Gaiano N (2004) Fibroblast growth factor receptor signaling promotes radial glial identity and interacts with Notch1 signaling in telencephalic progenitors. J Neurosci 24, 9497-506.

Yun K, Fischman S, Johnson J, Hrabe de Angelis M, Weinmaster G, and Rubenstein JL (2002) Modulation of the notch signaling by Mash1 and Dlx1/2 regulates sequential specification and differentiation of progenitor cell types in the subcortical telencephalon. Development 129, 5029-40.

Zeps N, Bentel JM, Papadimitriou JM, D'Antuono MF, and Dawkins HJ (1998) Estrogen receptor-negative epithelial cells in mouse mammary gland development and growth. Differentiation 62, 221-6.

Zheng X, Linke S, Dias JM, Zheng X, Gradin K, Wallis TP et al. (2008) Interaction with factor inhibiting HIF-1 defines an additional mode of cross-coupling between the Notch and hypoxia signaling pathways. Proc Natl Acad Sci U S A 105, 3368-73.

Zhou J, Chehab R, Tkalcevic J, Naylor MJ, Harris J, Wilson TJ et al. (2005) Elf5 is essential for early embryogenesis and mammary gland development during pregnancy and lactation. EMBO J 24, 635-44.

Zweifel ME, Leahy DJ, Hughson FM, and Barrick D (2003) Structure and stability of the ankyrin domain of the Drosophila Notch receptor. Protein Sci 12, 2622-32.

ANNEXÉ A: **MANUSCRIPTS**

Analysis of mammary gland phenotypes by transplantation of the genetically marked mammary epithelium/epithelial cells

Duje Buric[1], Cathrin Brisken[1]

[1]Ecole polytechnique fédérale de Lausanne (EPFL), ISREC - Swiss institute for experimental cancer research, SV2832 Station 19, CH-1015 Lausanne, Switzerland

Book chapter for an edition on **Mammary Gland Development**, to be published in the laboratory protocol book series **Methods in Molecular Biology**, published by Springer.

Introduction

The mouse mammary gland is a very attractive experimental system. Most of its development occurs after birth making it easy to study. As mammary glands are skin appendages that can be found on the back of the skin, they are readily accessible by surgery. The glands are paired organs and contra lateral glands can to the best of our current knowledge be directly compared.

The mammary gland's major components are a mammary fat pad and an epithelial structure that invades it. During embryonic development, a mammary bud forms from a placode in hte ventral skin around E12.5 that grows into a a small ductal system into the underlying specialized fatty stroma by E18,5. During the first 3 weeks of life (prepubertal stage), the rudimentary ductal system grows isometrically with the rest of the body. During puberty, between 3 and 8 weeks of age, the ductal system expands and invades the fat pad, driven by ovarian estrogens. With the onset of adulthood at around 8 weeks of age, regular cycles of ovarian estrogens and progesterone secretions, i.e. oestrous cycles, are established. Now, the ductal epithelial tree becomes more complex through a process called side branching driven by progesterone ***(1)***. When pregnancy occurs, progesterone levels increase further and the oestrous cycles are suppressed. Side branching is enhanced until the last third of pregnancy when under the influence of prolactin, extensive aleveologenesis occurs; little saccular outpouchings sprout from the ducts, which will produce milk.

DeOme first showed that it is possible to surgically remove the endogenous ductal tree from prepubertal females leaving behind approximately half the tissue as "cleared" fat pad, in which an epithelium fragment from another mouse can be engrafted ***(2)***, it will grow out to form a new ductal tree that behaves like the endogenous epithelium without establishing a link to the nipple. Even dissociated mammary epithelial cells, injected into the "cleared" fat pad were able to do so ***(3)***. Initially, the approach was used to characterize the properties of hyperplastic and malignant lesions in different mouse strains. ***(4-8),*** Subsequent reports showed the engraftment efficiency and the growth potential of normal mammary tissue and established that mammary epithelium can serially engraft ***(9-13)***.

With the advent of targeted gene deletion in the mouse germ line the transplantation of mammary epithelium was used to reveal mammary phenotypes secondary to systemic effects of the genetic change and to show discern epithelial intrinsic phenotypes ***(14-16)***. Additionally, the transplantation approach can be used to rescue epithelium from mouse mutants that are lethal by engrafting embryonic mammary buds into wild type mice as early as e 12.5 **(*17, 18*)**. More recently, engraftment of single cells in limiting dilutions ***(19)*** or of a specific single cells population obtained by fluorescence-activated cell sorting ***(20, 21)*** became a standard tool in mammary stem cell research.

A potential problem of the fat pad clearing approach is that endogenous epithelium may not be completely removed and compete with the graft. When the engrafted gland is analyzed prior to pregnancy and or up to mid pregnancy the implanted graft can readily be distinguished form endogenous epithelium because of its radial versus the uni directional growth pattern of the endogenous ductal system (Fig. 1). However, the ductal growths pattern can be impossible to discern when the fat pad is filled with mammary epithelium during late pregnancy. To unequivocally distinguish engrafted from endogenous epithelium the use of a marker is advisable. Initially, we recurred to using donor mice systemically expressing LacZ ***(22)*** which required a 5-bromo-4-chloro-3-indolyl-β-D-galactopyranoside (X-gal) staining followed by carmine alum counterstaining and whole mounting of the glands (***14)***. Nowadays, the availability of mice expressing different fluorescent proteins ***(23, 24)*** in the mammary gland has made the discrimination of epithelial from adipose tissue by fluorescent stereomicroscopy more convenient and applicable to live tissue ***(14, 15)***. The genetic markers are also useful for normalizing gene expression to the transplant outgrowth when contralateral glands are processed for Western blotting or quantitative RT-PCR experiments.

In this chapter, we will describe the preparation of the graft material, whether it is a piece of epithelium or a suspension of single cells, the preparation of the recipient animals, the engraftment into the cleared fat pad, and the analysis of the epithelial outgrowth.

As engrafting material we use either pieces of epithelium excised directly from the mammary gland of the donor mouse or suspensions of single cells. To obtain single cells from the mammary gland epithelium, we use a shortened and slightly modified version of the protocol from Matthew J. Smalley ***(25)*** where mammary glands are minced and treated with collagenase A and trypsin, washed with red blood cell lysis buffer and at the end shortly digested with trypsin and Dnase-1. For injection of single cells, we are using Matrigel as a medium for the engraftment. This was shown to increase the success rate possibly by preventing cell dispersal from the injection site ***(26)***. To obtain as much material as possible for the preparation of the suspension of single cells we isolate 4 out of 5 pairs of mammary glands in the mouse (Fig. 2). Cervical pair of mammary glands is usually not collected because of its position where it is hardly both accessible and distinguishable from the salivary gland.

Materials:

Media and Buffers:

1. Phosphate-buffered saline (PBS): 1.0% w/v sodium chloride, 0.025% w/v potassium chloride, 0.025% w/v disodium hydrogen orthophosphate and 0.1437% w/v potassium dihydrogen orthophosphate (prepared in the laboratory, filtered and autoclaved)
2. PBS/10% FCS medium: Phosphate-buffered saline plus 10% v/v heat-inactivated filtered fetal calf serum (FCS) (Invitrogen).
3. Leibowitz L15 medium with L-glutamine (L15) with no additives (Invitrogen, Paisley, UK).
4. Trypsin solution 1: 15 mg/mL trypsin from bovine pancreas (Sigma) is in serum-free L15. Stored at –20◦C in 1 mL aliquots (see ***Note 1***).
5. Collagenase A solution: 100 mg/mL Collagenase A (Roche) in PBS. Stored at –20◦C in 1,2 mL aliquots (see ***Note 2***).
6. Digestion solution: 1,2 mL of Collagenase A solution, 1mL of Trypsin solution 1, 37,8 mL of L15 medium with L-glutamine.
7. Trypsin solution 2: 0.25% trypsin, 0.02% EDTA in Hank’s balanced salt solution (Sigma)

8. DNAse-1 solution (5 μg/mL): 5 μg/mL bovine pancreatic DNase I (Roche) in serum-free L15. Store at –20◦C in 5-mL aliquots.

9. Matrigel solution: Falcon matrigel basement membrane matrix (BD Biosciences) is mixed with sterile PBS in the 1:8 ratio.

Preparation of donor tissue:

1. For tissue collection: Neoprene cork dissection board wrapped in aluminium foil and autoclaved, 70% ethanol in spray bottle to disinfect the animals, dissection tools (dissection needles for fixing the donor (dead) animal to the board, round-nosed scissors and two pairs of forceps), 100 mL beaker containing 70% ethanol for instruments sterilization and 15-mL Falcon tube containing sterile PBS for the tissue collection (kept on ice).

2. For preparation of tissue fragments: 2 sterile 10 cm Petri dishes containing 10 mL sterile PBS (see ***Note 3***), two pairs of forceps, round-nosed scissors, angled scissors (Vanna Scissors, angled-on-flat blades, 0.1-mm tip; World Precision Instruments), 5/45 jewelers' forceps (Agar scientific), clips for stitching, paper tissues and fluorescent dissection stereo-microscope (Leica).

3. For preparation of single cells: small beaker containing 70% ethanol for sterilizing tools, 50-mL Falcon tube containing sterile PBS for collection of mammary glands, scale to weigh the isolated tissue, 40 mL of digestion solution per batch of glands, red blood cell lysis buffer (Sigma), 2 mL per batch of glands of trypsin solution 2 and 5 mL per batch of glands of Dnase 1 solution, 40-μM cell strainers (BD Biosciences), Matrigel solution and two #22 scalpels.

For surgery:

Anaesthesia is performed according to the guidance of the Federal Veterinary Office of Switzerland. To minimize side-effects, it is advised to use isoflurane anaesthesia (5% of isoflurane in the atmosphere for the induction period until the mouse becomes ataxic, and 2% of isoflurane during the maintenance period with oxygen supply at rate of 5L/min during induction and 1L/min during maintenance period) with addition of analgesics chosen in accord with local veterinary guidance (buprenorphine at rate of 0,1 mg per kg of mouse) (see ***Note 4***).

Heating pad to warm up animals during the surgery procedure, double-sided tape, Betadine standardized solution (Provet) for the sterilization of the surgery spot (see ***Note 5***), two pairs of forceps, round-nosed scissors, angled spring scissors (Vanna Scissors, angled-on-flat blades, 0.1-mm tip; World Precision Instruments), 5/45 jewelers' forceps (Agar scientific), battery operated cauterizer (Gemini cautery products), 100 μL Hamilton's syringe, clips for stitching, clip removing forceps (Austos), cotton pads, sterile physiological solution and analgesic (Buprenorphine) for postoperative treatment (chosen according to Federal Veterinary Office of Switzerland) (see ***Note 6***).

Preparation for subsequent analysis:

Fluorescent stereomicroscope (Leica M205 FA), Camera, dissection tools, histological glass slides, plastic clips, glass beaker (size depending on the number of samples) with 4% w/v paraformaldehyde in PBS, glass beaker with 70% ethanol, container with liquid nitrogen.

Methods

Dissection of the donor mice

1. Mice are sacrificed in the CO_2 chamber, fixed on their back with pins to the dissection board and the ventral side is thoroughly sprayed with 70% ethanol to disinfect the skin. A ventral incision is carefully made with round nosed scissors pulling up the skin with forceps to avoid puncturing the muscle wall and the incision is extended to the top of the rib cage. Two further incisions are made to generate a Y-shaped opening extending down the lower limbs and up the upper limbs (Fig. 3). The skin is carefully pulled back from the body wall with forceps to expose the abdominal and the thoracic mammary glands, which stay attached to the skin. Thoracic glands are carefully detached from the skin by scissors and forceps. The connection between the abdominal and the inguinal gland is carefully cut with scissors (Fig. 3). A small incision is made above the subiliacal lymph node; the node is isolated and removed using forceps. Fourth mammary gland is carefully removed by forceps and scissors and placed into the falcon tube with sterile PBS.

Preparation of the engraftment material

Pieces of the tissues

1. Mammary gland from the donor mice expressing fluorescent protein is placed into the 10 cm plastic dish filled with sterile PBS and observed under the dissection fluorescence stereo-microscope. Pieces of approximately $1mm^3$ in size are cut with jewelers' forceps and angled scissors, placed in another petri dish containing PBS, which is kept on ice until the surgery.

Single cells

1. Batch of collected mammary glands is transferred into the tissue culture hood and placed on the previously autoclaved dissection board using forceps. Excess PBS is aspirated by lifting the board. Mammary glands are finely chopped with #22 scalpels until they become fine semi liquid slurry (see ***Note 7***).
2. Tissue slurry is weighed and transferred into the 50 mL Falcon tubes, 2 g per tube.
3. 40 mL of digestion mix and placed on the rotator at 37°C for two hours (see ***Note 8 and 9***).
4. After incubation, check that solution is homogeneous and fragments are smaller than 1-2mm in size. Falcon tube is placed in the centrifuge and spun at 1300 rpm for 5 minutes. The pellet will be enriched for epithelial fragments. Supernatant containing digestion medium and layer of fat is transferred to a new falcon tube and spun down again at same speed and time (see ***Note 10***). Supernatant from the second falcon tube is removed by aspiration. The pellet from the first falcon tube is resuspended in 10 mL and from the second falcon tube in 5 mL of PBS/10% FCS, they are pooled in a 15 mL falcon tube and spun down again followed by aspiration of supernatant.
5. Pellet is resuspended in 5 mL of red blood cell lysis buffer and incubated for 5 min at room temperature. Suspension is again spun down at 1300 rpm for 5 min and supernatant is aspirated.
6. Pellet is washed with 5 mL of PBS/10% FCS and spun down. Supernatant is aspirated.
7. Pellet is resuspended in 2 mL of trypsin solution 2 and incubated for 2 min at 37°C. Following incubation 5 mL of Dnase 1 solution are added and suspension is incubated for another 5 min at 37°C.

8. To inactivate trypsin, 8 mL of PBS/10% FCS are added. Suspension is filtered through a 40-μM cell strainer, spun down and resuspended into minimal amount of PBS/10% FCS. Cells are counted.

9. Just before the engraftment, 50 000 cells are transferred into Eppendorf tube. They are spun down in the table top centrifuge at 10 000 rpm for 1 min at room temperature, resuspended in 10 μL matrigel solution and kept on ice.

Transplantation

Regarding the choice of host for the transplantation a few points need to be considered. First choice, whenever possible, is an isogenic recipient. In case of doubt, isogenicity can be checked by skin grafts between randomly selected mice ***(27)***. When a mutation of interest is in a mixed genetic background of two distinct strains, frequently 129SV/C57Bl6J F-1 hybrids generated by parents of either background are suitable hosts ***(28, 29)***. Not only will the F1 daughter accept any mixture of alleles from the two strains but in addition the experiment benefits from the hybrid vigor that results from crossing two inbred strains and makes the F1 generation particularly healthy. However, not all the strains show histocompatibility with either the F-1 hybrids or the hosts from the same strains, requiring extensive backcrossing. In particular, with the advent of conditional deletions many mouse strains now contain elements of more than two genetic backgrounds. These complexities require the use of immune compromised mice.

A widely used model for transplantation experiments were *nude mice* in which *foxn1* gene is disrupted. As a result the mice are athymic and lack thymus-derived T-cells important in allograft rejection ***(30)***. However, nude females have abnormally low levels of circulating estrogens which may influence the growth of transplanted mammary epithelium (***31, 32)***.

Better recipients are mice lacking recombination activating genes 1 or 2 ($Rag1^{-/-}$) ***(33)*** or ($Rag2^{-/-}$) ***(34).*** The two genes are required for recognizing and cleaving signal specific sequences for somatic rearrangement of B and T cells receptors. As a result $Rag1^{-/-}$ and $Rag2^{-/-}$ mice have neither B nor T cells. Transplantation to these mice gives very good, reproducible results. However, with the recent

discoveries on the important role of immune cells in development and carcinogenesis of the mammary gland ***(35)*** show that results from this system need to be carefully interpreted.

Transplantation procedure

1. Mice are anesthetized in the incubation chamber with 5% isoflurane in the atmosphere and 5L/min of oxygen supply and then transferred on the heating pad (see ***Note 11***) at 37˚C with mask on the nose supplying 2% of isoflurane and 1L/min of oxygen. Buprenorphine at rate of 0,1 mg per kg bodyweight is administered subcutaneously for analgesia.

2. Mice are fixed on the heating pad with double-sided tape. The inguinal area is disinfected with Betadine standardized solution.

3. A ventral incision is made carefully with rounded nosed scissors and other two incisions perpendicularly to the ventral one on each side of the mouse finishing half way between nipple #4 and #5 trying not to puncture peritoneum (see ***Note 12***). Skin is carefully peeled off the peritoneum with forceps and abdominal gland is exposed (Fig.4).

4. To stop bleeding, the cauterizer is applied to blood vessel near junction by lymph node (Fig. 5.a) and blood vessel on the fat pad connection between 4th and 5th gland (Fig. 5.b) (see ***Note 13***).

5. Using angle spring scissors a cut is made at the peritoneal side of the subiliacal lymph node (Fig. 5.c) and the nipple side half of the gland containing rudimental ductal tree is excised leaving a cleared fat pad behind. The same procedure is applied to the contralateral side.

6. a) For the tissue fragment: Using only one side of the 5/45 jewelers' forceps a small pocket is made in the middle of the cleared fat pad (see ***Note 14***). Tissue piece is placed on the top of the pocket and gently pushed inside using one side of the 5/45 jewelers' forceps.

6. b) For the single cell injections: 50 000 cells in 10 μL of the matrigel solution are taken up with 100 μL Hamilton syringe. Suspension is carefully injected in the middle of the cleared fat pad (Fig. 6)

7. Mice are left on the heating pad while incisions are closed with metal clips (approx. 5 mm between each clip) (see ***Note 15***). 500 μL of physiological saline is injected into the mouse

intraperitoneally (see ***Note 16***) and tape, for fixing the mouse during surgery, is removed. Buprenorphine (0,1 mg per kg) is administered subcutaneously every 8 to 12 hours for 3 subsequent days.

8. Metal clips are removed with clip removing forceps 10 days after the surgery.

Phenotypic characterization

The timing of analysis of the transplanted glands is a parameter that has to be determined in light of the working hypothesis. As early as 3 days after surgery, limited growth can be observed in transplanted glands. As a rule of thumb, up to 21 days after surgery the terminal end buds can be seen and after 28-35 days the pubertal development in the recipient is over so the mammary gland should reach its adult stage ***(29)***. There is some variation depending on donor and host genetic backgrounds. To observe side-branching, mice should be examined at least 10 weeks after surgery. A phenotype related to alveologenesis can be observed between 14.5 and 18.5 days of pregnancy; lactation is best examined immediately after birth. As the milk cannot get out of the engrafted epithelium because there is no connection to the nipple, involution will start within a day after birth giving.

Mice are sacrificed in the CO_2 chamber, fixed on their back to the dissection board with four pins through their paws and the ventral side is sprayed with 70% ethanol to disinfect the skin. Y-shaped incision is made and mammary gland is isolated from the mouse as described above.

For analysis of fluorescent epithelial grafts:

1. Mammary gland is placed between the two glass slides and slides are held together with two plastic clips (see ***Note 17***).

2. Mammary gland between the two slides is observed under the fluorescent microscope and photographed for the analysis (see ***Note 18***).

3. For subsequent histological analysis mammary glands are placed into the plastic cassettes and placed into the PFA solution and left o/n at 4°C. Next day they are washed in PBS and

transferred to a beaker containing 70% ethanol. After this, the histological procedures can be performed at any time.

Whole mounting:

4. For the whole mount analysis the dissected mammary gland is spread on the glass slide and left to dry for several hours before fixation.

5. For any analysis requiring protein, RNA or DNA extraction mammary glands are placed into the Eppendorf tubes, flash-frozen in the liquid nitrogen and stored at -80°C (see ***Note 19***).

Notes

1. To avoid weighing of the trypsin, which is a very light charged powder that easily sticks to metal surface, the best way to prepare the solution is to add 16,7 mL of L15 medium directly into the original packaging and to vortex immediately. Trypsin dissolves easily and is instantly ready to use or to aliquot.

2. Collagenase A does not readily dissolve in PBS. Hence, it is recommended to prepare aliquots in advance. Briefly, add 25 mL of PBS directly to original packaging and mix it on the horizontal orbital shaker for several hours at 4°C until dissolved.

3. Usually, in the transplantation experiment mammary epithelium from a genetically modified mouse and control wild type mice are engrafted. The experimental, genetically modified is engrafted on one side, and the wild type placed contra laterally. In these cases, it is recommended to use 2 cm tissue culture dishes or 6-well plates to prepare the epithelial fragments for transplantation.

4. We use Isoflurane gas anaesthesia because it is well tolerated, we observe few side-effects and recovery time is short facilitating post-operative care. Alternatively, injectable anaesthesia (Xylazine 10 – 15 mg/kg bodyweight + Ketamine 80 – 100 mg/kg bodyweight) can be used, however, recovery time is much longer. We have noticed that *RAG 1*$^{-/-}$ mice are particularly sensitive to the injectable anaesthesia. Therefore, for any strain the dose has to be adjusted. Injectable anaesthesia does not require additional analgesia during the surgery.

5. In accord to Federal Veterinary Office of Switzerland guidance we use Betadine standardized solution to disinfect the mouse skin. 70% ethanol is to be avoided because evaporation of ethanol may lead to cooling down of the mouse and may increase mortality. Cotton is soaked with Betadine solution and rubbed into the mouse skin against the direction of the hair growth to optimize skin sterilization.

6. Buprenorphine at dose of 0,1 mg per kg body weight is used during surgery and for postoperative analgesia and the same dose is given daily for three days after surgery. Alternatively, paracetamol can be provided in the drinking water at 1mg/mL

7. To mince the mammary gland tissue, two #22 scalpels are taped together side by side. If different experimental groups of mice are used for the same experiment it is advisable to mince the glands in the most similar way possible, meaning for the same amount of time. Usually around 3 minutes are adequate for up to 2 mice (4 glands per mouse), count an extra 30 seconds for each additional mouse (maximum 5 mice per batch). While cutting/mincing the tissue bring it together with scalpels to the center of the board from time to time.

8. 20 mL of the digestion mix is optimal for 1 g of tissue.

9. It is advisable to gently shake the falcon tubes with the digestion mix every 15 minutes during collagenase A/trypsin digestion to ensure homogeneous digestion.

10. Shake the transferred supernatant vigorously to release the leftover organoids from the fat on the top.

11. If the heating pad does not have a precise electronic regulator, place a thermometer on it in order to have constant insight in the temperature. Slightest increase can cause dehydration of mouse and can lead to death.

12. In case the peritoneum is punctured, it is possible to stitch it with absorbable suture, placing a stitch every 1mm.

13. Cauterization has to be very gentle and careful, otherwise fat pad can get damaged and necrosis can prevent the graft taking.

14. It is extremely important that the pocket is well-centered in the middle of the fat pad and that the fragment is not placed underneath it. Outside the fat pad the graft will not grow.

15. When stitching the two perpendicular incisions, it is important to remove the tape fixing lower limbs of the mouse so that the stitches are made in a physiological position to avoid interfering with the mobility of the animal after surgery.

16. Sterile physiological solution is injected to accelerate recovery because surgery leads to dehydratation.

17. Mammary gland should be as dry as possible to avoid that it slips between the slides. Extra liquid can give rise to a false border that may cause problems with subsequent analyses, such as determining the extent of fat pad filling, as the size of fat pad may be overestimated..

18. EGFP transgenic mice ***(23)*** proposed in this chapter have a high intensity fluorescence signal in the epithelium and a very low one in the stroma. This renders it difficult to appreciate the fat pad borders and epithelium concomitantly in the GFP channel. In the DsRed channel, stroma has higher autofluorescence making it convenient to take the picture of the fat pad in red and epithelium in green.

19. To preserve RNA quality, mammary glands have to be isolated from live anesthetized mice.

Figure legends

Figures:

Figure 1. Difference in growth pattern between engrafted and endogenous mammary epithelium

Scheme of radial epithelial growth pattern in transplanted mammary gland (a.) and uni-directional growth pattern in the endogenous mammary gland (b.)

Figure 2. Anatomic location of mouse mammary glands:

Scheme showing a female mouse on its back. The position of the mammary glands are depicted with the thin lines, nipples are represented by black dots. a) cervical, b) first thoracic, c) second thoracic, d) abdominal, e) inguinal.

Figure 3. Surgical field for dissection of the donor mouse:

Scheme of a female mouse on its back. The incision lines are shown by dashed lines, order of incisions follows the numbering.

Figure 4. Surgical field for skin incision in the recipient mouse:

Scheme of a female mouse on its back showing the incisions positions with dashed lines. Numbers indicate order of incisions.

Figure 5. Surgical field for fat pad clearing in the recipient mouse:

Scheme of inguinal area with abdominal and inguinal gland (mammary gland is depicted with thin line and blood vessels with dotted line): a) arrow indicates where the blood vessels near the junction by the lymph node have to be cauterized. b) dotted line shows a connection between abdominal and inguinal gland that has to be cauterized. c) dashed line shows the position of the incision required to clear the fat pad.

Figure 6. Cell injection into cleared fat pad of the recipient mouse:

a) Scheme of inguinal area with fat pad after clearing being injected with cell suspension.

b) Schematic cross-section of inguinal fat pad; dashed line represents part of needle inside the fat pad.

References

1. Knight CH and Peaker M (1982) Development of the mammary gland. J Reprod Fertil 65, 521-36.

2. Faulkin LJ and DeOme KB (1958) The Effect of estradiol and cortisol on the transplantability and subsequent fate of normal, hyperplastic, and tumorous mammary tissue of C3H Mice. Cancer Res 18, 51-56.

3. Daniel CW and Deome KB (1965) Growth of Mouse Mammary Glands in Vivo after Monolayer Culture. Science 149, 634-6.

4. Deome KB, Faulkin LJ, Jr., Bern HA, and Blair PB (1959) Development of mammary tumors from hyperplastic alveolar nodules transplanted into gland-free mammary fat pads of female C3H mice. Cancer Res 19, 515-20.

5. Hoshino K, Gardner WU, and Pawlikowski RA (1965) The incidence of cancer in quantitatively transplanted mammary glands and its relation to age and milk agent of the donor and host mice. Cancer Res 25, 1792-803.

6. Muhlbock O (1956) The hormonal genesis of mammary cancer. Adv Cancer Res 4, 371-91.

7. Prehn RT (1953) Tumors and hyperplastic nodules in transplanted mammary glands. J Natl Cancer Inst 13, 859-71.

8. Shimkin MB, Wyman RS, and Andervont HB (1946) Mammary tumors in mice following transplantation of mammary tissue. J Natl Cancer Inst 7, 77.

9. Hoshino K (1962) Morphogenesis and growth potentiality of mammary glands in mice. I. Transplantability and growth potentiality of mammary tissue of virgin mice. J Natl Cancer Inst 29, 835-51.

10. Hoshino K (1963) Morphogenesis and growth potentiality of mammary glands in mice. II. Quantitative transplantation of mammary glands of normal male mice. J Natl Cancer Inst 30, 585-91.

11. Hoshino K (1964) Regeneration and Growth of Quantitatively Transplanted Mammary Glands of Normal Female Mice. Anat Rec 150, 221-35.

12. Hoshino K (1967) Transplantability of mammary gland in brown fat pads of mice. Nature 213, 194-5.

13. Hoshino K and Gardner WU (1967) Transplantability and life span of mammary gland during serial transplantation in mice. Nature 213, 193-4.

14. Brisken C, Park S, Vass T, Lydon JP, O'Malley BW, and Weinberg RA (1998) A paracrine role for the epithelial progesterone receptor in mammary gland development. Proc Natl Acad Sci U S A 95, 5076-81.

15. Mallepell S, Krust A, Chambon P, and Brisken C (2006) Paracrine signaling through the epithelial estrogen receptor alpha is required for proliferation and morphogenesis in the mammary gland. Proc Natl Acad Sci U S A 103, 2196-201.

16. Ciarloni L, Mallepell S, and Brisken C (2007) Amphiregulin is an essential mediator of estrogen receptor alpha function in mammary gland development. Proc Natl Acad Sci U S A 104, 5455-60.

17. Brisken C, Heineman A, Chavarria T, Elenbaas B, Tan J, Dey SK et al. (2000) Essential function of Wnt-4 in mammary gland development downstream of progesterone signaling. Genes Dev 14, 650-4.

18. Heckman-Stoddard BM, Vargo-Gogola T, Herrick MP, Visbal AP, Lewis MT, Settleman J et al. (2011) P190A RhoGAP is required for mammary gland development. Dev Biol 360, 1-10.

19. Pond AC, Bin X, Batts T, Roarty K, Hilsenbeck S, and Rosen JM (2013) Fibroblast growth factor receptor signaling is essential for normal mammary gland development and stem cell function. Stem Cells 31, 178-89.

20. Shackleton M, Vaillant F, Simpson KJ, Stingl J, Smyth GK, Asselin-Labat ML et al. (2006) Generation of a functional mammary gland from a single stem cell. Nature 439, 84-8.

21. Sleeman KE, Kendrick H, Robertson D, Isacke CM, Ashworth A, and Smalley MJ (2007) Dissociation of estrogen receptor expression and in vivo stem cell activity in the mammary gland. J Cell Biol 176, 19-26.

22. Friedrich G and Soriano P (1991) Promoter traps in embryonic stem cells: a genetic screen to identify and mutate developmental genes in mice. Genes Dev 5, 1513-23.

23. Okabe M, Ikawa M, Kominami K, Nakanishi T, and Nishimune Y (1997) 'Green mice' as a source of ubiquitous green cells. FEBS Lett 407, 313-9.

24. Vintersten K, Monetti C, Gertsenstein M, Zhang P, Laszlo L, Biechele S et al. (2004) Mouse in red: red fluorescent protein expression in mouse ES cells, embryos, and adult animals. Genesis 40, 241-6.

25. Smalley MJ (2010) Isolation, culture and analysis of mouse mammary epithelial cells. Methods Mol Biol 633, 139-70.

26. LaMarca HL, Visbal AP, Creighton CJ, Liu H, Zhang Y, Behbod F et al. (2010) CCAAT/enhancer binding protein beta regulates stem cell activity and specifies luminal cell fate in the mammary gland. Stem Cells 28, 535-44.

27. Daniel CW, Deome KB, Young JT, Blair PB, and Faulkin LJ, Jr. (2009) The in vivo life span of normal and preneoplastic mouse mammary glands: a serial transplantation study. 1968. J Mammary Gland Biol Neoplasia 14, 355-62.

28. Faulkin LJ, Jr. and Deome KB (1960) Regulation of growth and spacing of gland elements in the mammary fat pad of the C3H mouse. J Natl Cancer Inst 24, 953-69.

29. Williams MF and Hoshino K (1970) Early histogenesis of transplanted mouse mammary glands. I. Within 21 days following isografting. Z Anat Entwicklungsgesch 132, 305-17.

30. Flanagan SP (1966) 'Nude', a new hairless gene with pleiotropic effects in the mouse. Genet Res 8, 295-309.

31. Seibert K, Shafie SM, Triche TJ, Whang-Peng JJ, O'Brien SJ, Toney JH et al. (1983) Clonal variation of MCF-7 breast cancer cells in vitro and in athymic nude mice. Cancer Res 43, 2223-39.

32. Soule HD and McGrath CM (1980) Estrogen responsive proliferation of clonal human breast carcinoma cells in athymic mice. Cancer Lett 10, 177-89.

33. Mombaerts P, Iacomini J, Johnson RS, Herrup K, Tonegawa S, and Papaioannou VE (1992) RAG-1-deficient mice have no mature B and T lymphocytes. Cell 68, 869-77.

34. Shinkai Y, Rathbun G, Lam KP, Oltz EM, Stewart V, Mendelsohn M et al. (1992) RAG-2-deficient mice lack mature lymphocytes owing to inability to initiate V(D)J rearrangement. Cell 68, 855-67.

35. Reed JR and Schwertfeger KL (2010) Immune cell location and function during post-natal mammary gland development. J Mammary Gland Biol Neoplasia 15, 329-39.

Figures

Figure 1.

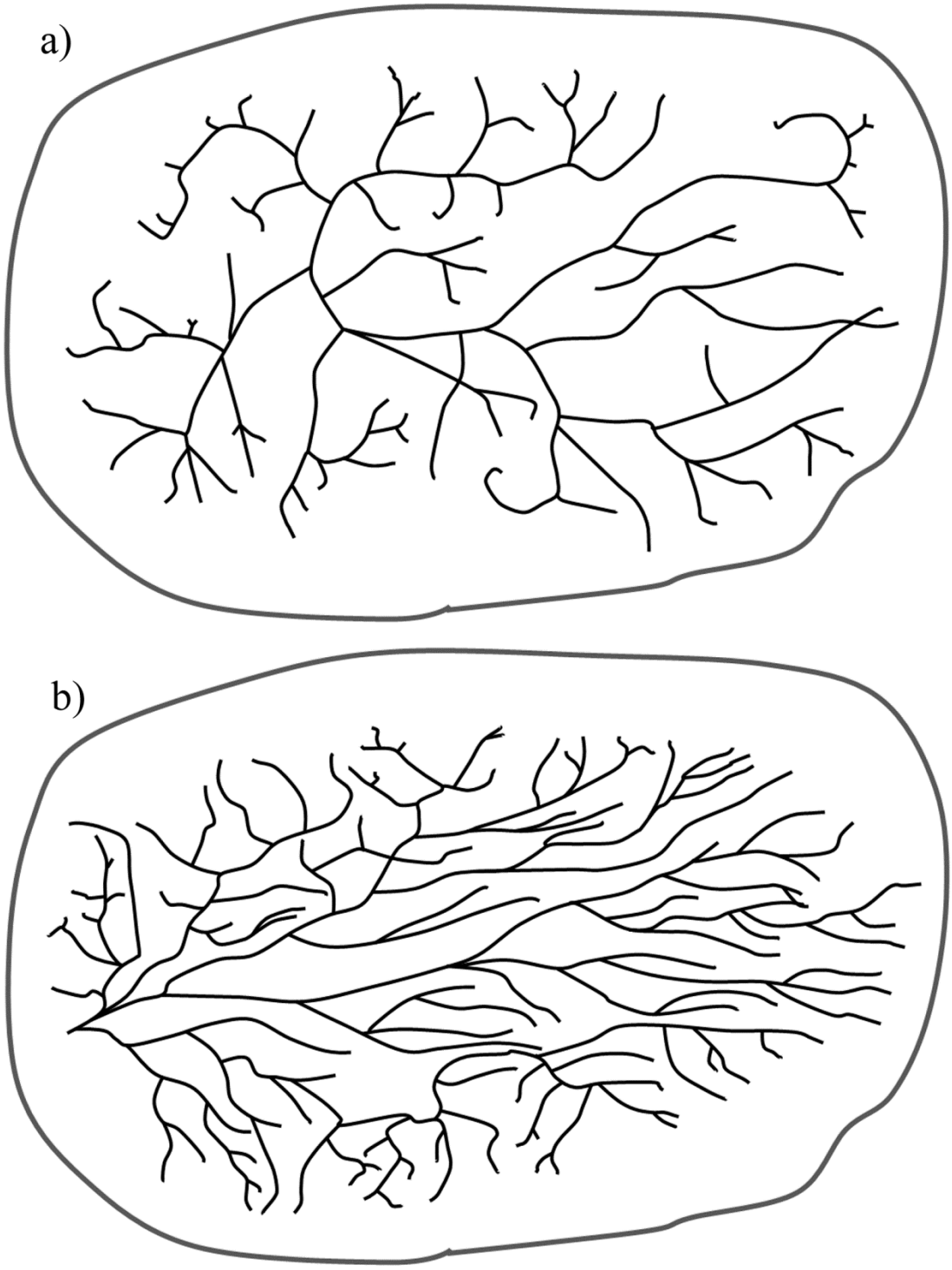

Figure 2.

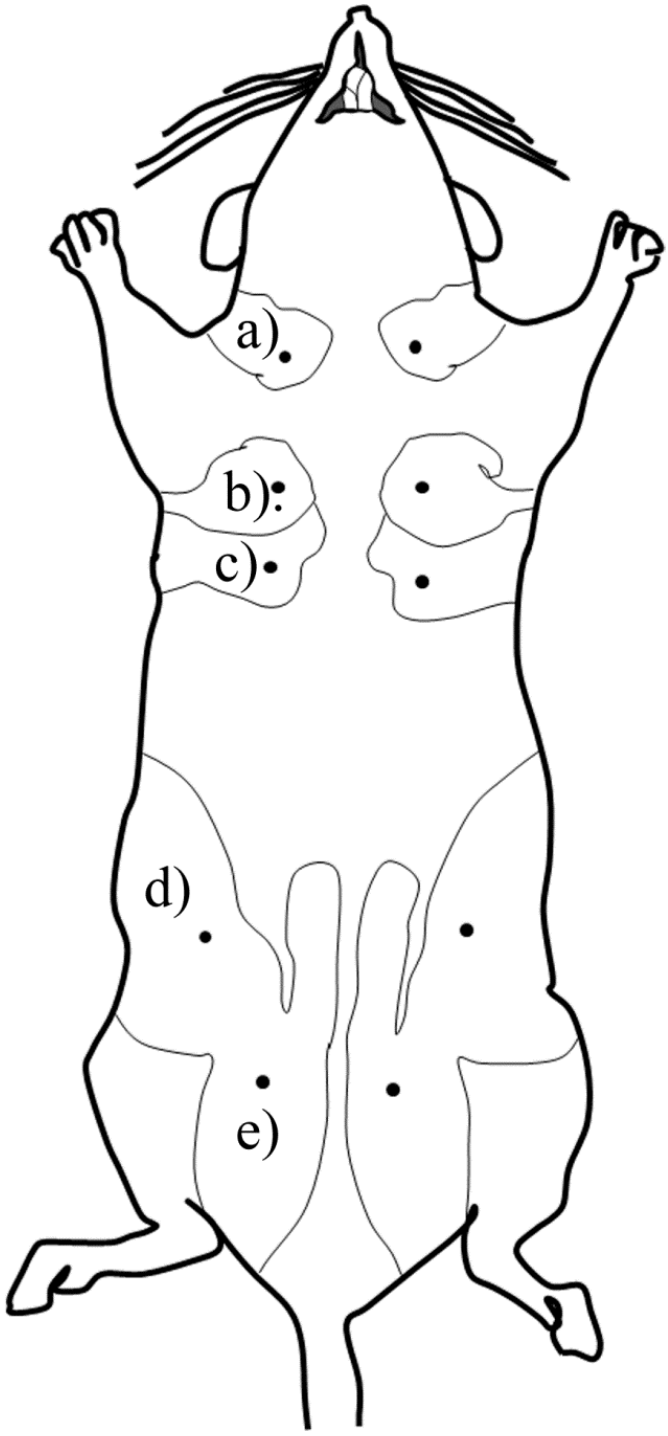

Figure 3.

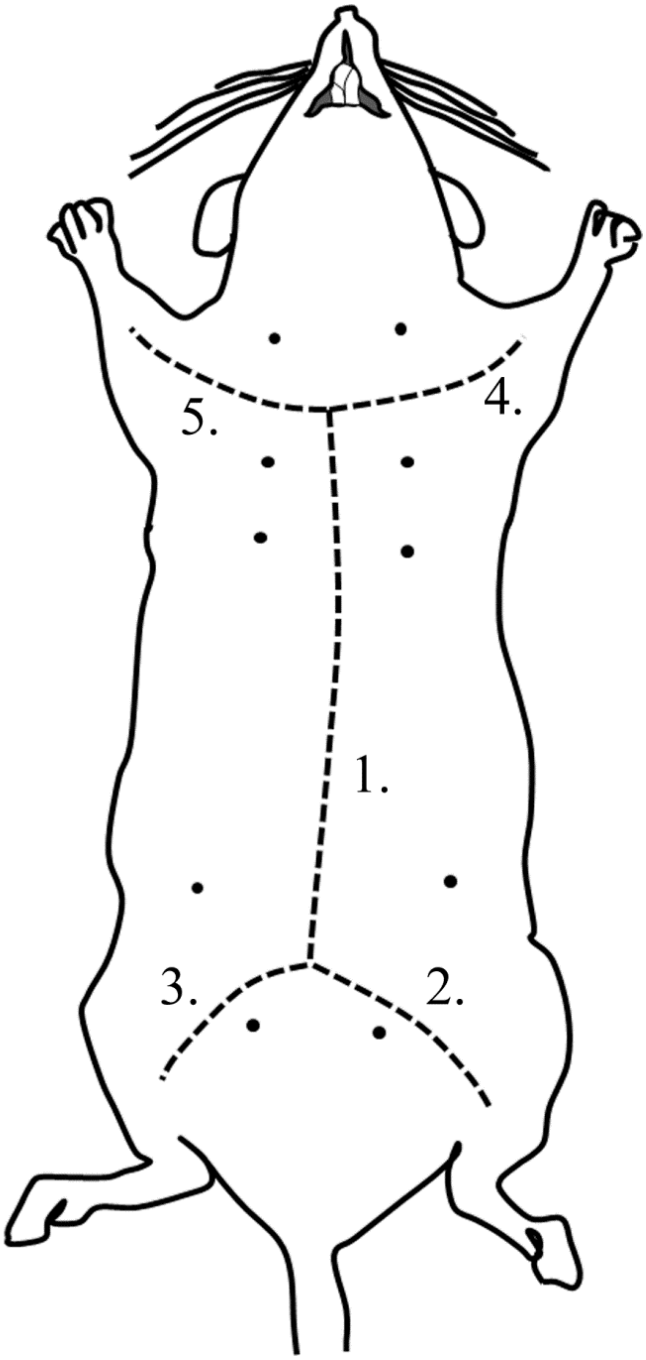

Figure 4.

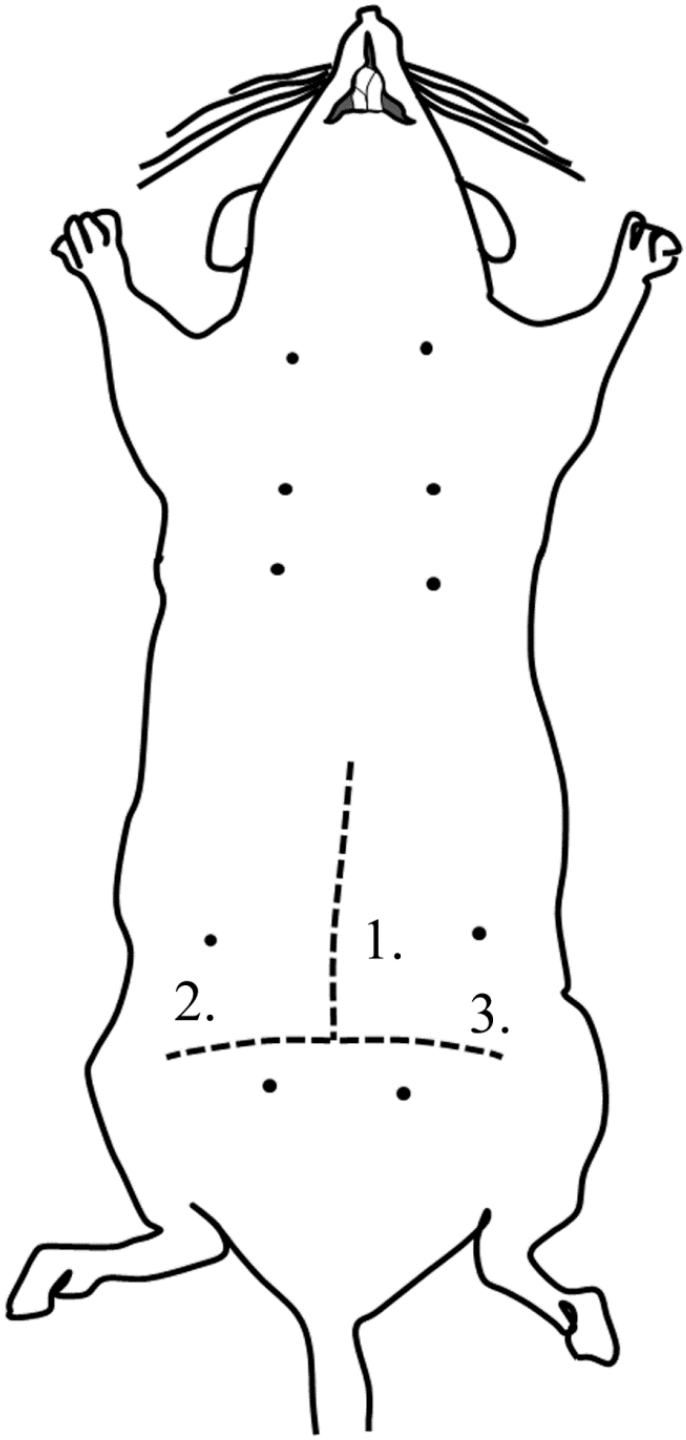

Figure 5.

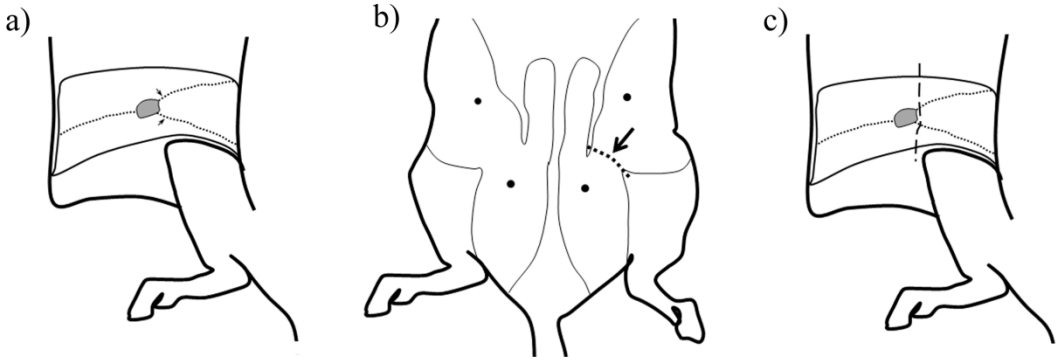

Figure 6.

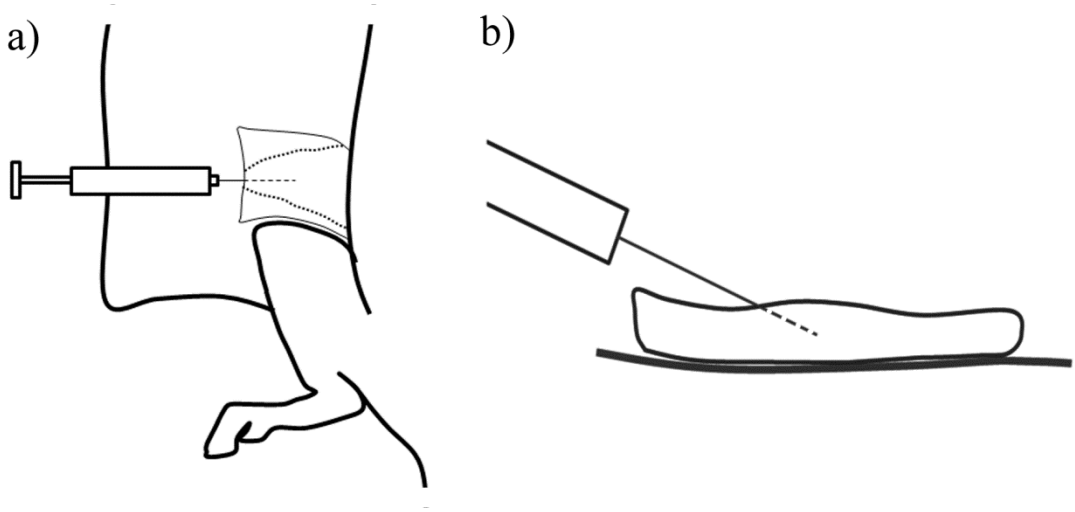

Published online: January 20, 2015

Article

TRANSPARENT PROCESS

THE EMBO JOURNAL

Progesterone and Wnt4 control mammary stem cells via myoepithelial crosstalk

Renuga Devi Rajaram[1,†], Duje Buric[1], Marian Caikovski[1], Ayyakkannu Ayyanan[1], Jacques Rougemont[2], Jingdong Shan[3], Seppo J Vainio[3], Ozden Yalcin-Ozuysal[4] & Cathrin Brisken[1,*]

Abstract

Ovarian hormones increase breast cancer risk by poorly understood mechanisms. We assess the role of progesterone on global stem cell function by serially transplanting mouse mammary epithelia. Progesterone receptor (PR) deletion severely reduces the regeneration capacity of the mammary epithelium. The PR target, receptor activator of Nf-κB ligand (RANKL), is not required for this function, and the deletion of Wnt4 reduces the mammary regeneration capacity even more than PR ablation. A fluorescent reporter reveals so far undetected perinatal Wnt4 expression that is independent of hormone signaling. Pubertal and adult Wnt4 expression is specific to PR$^+$ luminal cells and requires intact PR signaling. Conditional deletion of Wnt4 reveals that this early, previously unappreciated, Wnt4 expression is functionally important. We provide genetic evidence that canonical Wnt signaling in the myoepithelium required PR and Wnt4, whereas the canonical Wnt signaling activities observed in the embryonic mammary bud and in the stroma around terminal end buds are independent of Wnt4. Thus, progesterone and Wnt4 control stem cell function through a luminal–myoepithelial crosstalk with Wnt4 acting independent of PR perinatally.

Keywords canonical Wnt signaling; hormones; mammary stem cells; myoepithelium; paracrine

Subject Categories Development & Differentiation; Signal Transduction; Stem Cells

DOI 10.15252/embj.201490434 | Received 30 October 2014 | Revised 21 December 2014 | Accepted 23 December 2014

Introduction

The two key ovarian hormones, 17-β-estradiol (E2) and progesterone, regulate postnatal mammary gland development but also promote carcinogenesis in this organ. They act via nuclear receptors, the estrogen receptor α (ER) and the progesterone receptor (PR), respectively, which are expressed in between 30 and 50% of the mammary epithelial cells in the inner, luminal layer (Clarke *et al*, 1997). It was proposed that they impinge on ER-/PR-negative mammary stem cells by paracrine mechanisms (Tanos & Brisken, 2008). Experimental evidence for this model was provided with fluorescence-activated cell sorting (FACS)-based approaches (Asselin-Labat *et al*, 2010; Joshi *et al*, 2010). The single-cell-based methods have been used to characterize mammary epithelial cell populations and to establish a cellular hierarchy within the mammary epithelium. Among dissociated CD24$^+$ mouse mammary epithelial cells, the cell populations with high surface expression of integrin β1 (CD29^{hi}) or integrin α6 (CD49f^{hi}) were enriched for cells with the ability to establish new milk ducts in mammary fat pads surgically cleared of their endogenous epithelium and were hence considered bipotent mammary stem cells able to give rise to both luminal and basal/myoepithelial cell lineage (Shackleton *et al*, 2006; Stingl *et al*, 2006). These cells express basal/myoepithelial markers such as cytokeratin 5 and 14, smooth muscle actin, and laminin (Shackleton *et al*, 2006; Stingl *et al*, 2006) and their numbers increase during pregnancy and after stimulation with E2 and progesterone (Asselin-Labat *et al*, 2010; Joshi *et al*, 2010) and decrease upon ovariectomy or anti-estrogen treatment (Asselin-Labat *et al*, 2010).

However, the physiological relevance of the dramatic expansion of these bipotent stem cells in response to hormones (Asselin-Labat *et al*, 2010; Joshi *et al*, 2010) is questioned by lineage-tracing experiments showing that postnatal mammary gland development is largely driven by luminal and basal/myoepithelial lineage-restricted stem cells (Taddei *et al*, 2008; Zeng & Nusse, 2010; Van Keymeulen *et al*, 2011; Rios *et al*, 2014). The lineage-restricted stem cells are not amenable to study by the single stem cell assays where the normal stem cell niche and its microenvironment are disrupted.

Recurrent peaks in serum progesterone levels are linked to menstrual cycles which are an important risk factor for breast carcinogenesis (Brisken, 2013). Moreover, most cell proliferation occurs in the luminal compartment and breast cancers arise from luminal and/or luminal progenitor cells (Molyneux *et al*, 2010). This begs the question how important progesterone is to mammary stem cell

1 Ecole Polytechnique Fédérale de Lausanne (EPFL), ISREC - Swiss Institute for Experimental Cancer Research, Lausanne, Switzerland
2 Swiss Institute of Bioinformatics, Bioinformatics and Biostatistics Core Facility, Ecole polytechnique fédérale de Lausanne (EPFL), Lausanne, Switzerland
3 Faculty of Biochemisty and Molecular Medicine (FBMM), Biocenter Oulu and Infotech Oulu, Oulu Center for Cell Matrix Research, University of Oulu, Oulu, Finland
4 Department of Molecular Biology and Genetics, Izmir Institute of Technology, Izmir, Turkey
*Corresponding author. Tel +41 21 693 07 81; +41 21 693 07 62; Fax +41 21 693 07 40; E-mail: cathrin.brisken@epfl.ch
†Present address: Department of Pharmacology and Toxicology, University of Lausanne, Lausanne, Switzerland

function in the intact tissue context and through which signaling pathways it impinges on different types of mammary stem cells, that is, bipotential, luminal restricted, and basal restricted.

Mammary epithelium was shown to serially engraft cleared mammary fat pads for up to seven cycles (Daniel, 1973). This assay, which is based on the engraftment of an intact piece of mammary epithelium, preserves the epithelial architecture with its associated extracellular matrix, fibroblasts, and immune cells. It is currently the only way to assay comprehensively the mammary regeneration potential reflective of multiple types of stem and progenitor cells. We combine this assay with different genetic mutant strain to define the relative contributions of progesterone signaling and its downstream mediators RANKL and Wnt4 to the regenerative potential of the mammary epithelium.

Results

PR signaling for mammary epithelial self-renewal

To assess the role of PR signaling in mammary stem cell control, we serially engrafted pieces of intact mammary epithelium from the $PR^{-/-}$ and wild-type (WT) littermates into contralateral mammary fat pads surgically cleared of their endogenous epithelium (Fig 1A). This approach rather than injection of limiting dilutions of dissociated cell populations was chosen so that the physiological interactions between the stem/progenitor cells and their microenvironment in the mammary epithelium niche would be preserved and the function of all types of stem cells, the bipotential, the luminal-restricted, and the basal-restricted stem cells, could be evaluated. To unequivocally distinguish the engrafted cells from the endogenous epithelium that may inadvertently be left after surgery, we used donors that ubiquitously express the enhanced green fluorescent protein (EGFP) (Okabe *et al*, 1997). To ensure that comparable amounts of mutant (*MT*) and *WT* donor tissue with comparable amounts of epithelium were engrafted, we dissected pinhead-sized fragments from the inguinal glands near the lymph node on the side proximal to the teat. Eight to 12 weeks after grafting, recipients were sacrificed and the extent of outgrowth in the engrafted mammary glands was determined. Pieces of mammary tissue resulting from the contralateral $PR^{-/-}$ and *WT* grafts were dissected and retransplanted (Fig 1A). The *WT* epithelium completely reconstituted most of the fat pads over 4 serial transplant cycles, as expected, but the $PR^{-/-}$ epithelium ceased to reconstitute the mammary gland by the 3rd cycle (Fig 1B, C, and H).

Paracrine mediators of PR signaling in mammary epithelial self-renewal

The TNF-α family member, RANKL, was previously implicated in the paracrine control of mammary stem cells by hormones on the basis of use of dissociated individual stem cell assays (Asselin-Labat *et al*, 2010). To determine the functional importance of RANKL in epithelial self-renewal, we serially engrafted intact mammary epithelium derived from the $RANKL^{-/-}$ and the $RANKL^{+/+}$ mice into cleared contralateral mammary fat pads. *WT* epithelium fully reconstituted fat pads in most hosts over 4 serial transplants and grew as expected (Fig 1D and E). Unexpectedly, $RANKL^{-/-}$ epithelia had the same regeneration capacity (Fig 1D and E). The only significant difference was that the *MT* grafts generated fewer side branches (Fig 1D and insets), consistent with the reported proproliferative activity of RANKL and its role in side branching (Beleut *et al*, 2010).

We tested the role of Wnt4 since evidence has accumulated that Wnt signaling is important for mammary stem cell function (Cai *et al*, 2014; Kessenbrock *et al*, 2013; Liu *et al*, 2004; van Amerongen *et al*, 2012; Wang *et al*, 2014; Zeng & Nusse, 2010) and Wnt4 is a key paracrine mediator of progesterone action (Brisken *et al*, 2000). As $Wnt4^{-/-}$ mice die at birth (Vainio *et al*, 1999), intact mammary epithelial buds from E12.5/E13.5 embryos were used for the initial engraftment. It has been reported that embryonic epithelia have more stem cells than postnatal epithelia (Spike *et al*, 2012). Notwithstanding, we noticed that epithelial tissue isolated from the $Wnt4^{+/+}$ and the $Wnt4^{+/-}$ embryos reconstituted completely the mammary gland to the same extent as the *WT* epithelia from postnatal mammary glands through three transplantation cycles (Fig 1C, E, and G). However, the $Wnt4^{-/-}$ epithelium only established 50% of the fat pad in the first cycle and was reduced to 10% by the third cycle (Fig 1F and G). The much more significant impairment of reconstitution capacity of the $Wnt4^{-/-}$ versus the $PR^{-/-}$ grafts compared to their respective contralateral controls (Fig 1H) points to a key role for Wnt4 in the maintenance of the mammary stem cell function and indicates that PR is not exclusively controlling Wnt4 expression. RANKL

Figure 1. PR, RANKL, and Wnt4 and their role in the regenerative capacity of the mammary gland.

A Experimental scheme. Mammary tissue fragments dissected from wild-type (WT) or mutant (MT) donor mice were engrafted to contralateral mammary fat pads of $RAG1^{-/-}$ recipient mice surgically divested of the endogenous epithelium. Between 8 and 12 weeks later, the engrafted glands were assessed by fluorescent stereomicroscopy and new fragments were dissected for serial engraftment.

B, C Serial transplantations of $PR^{+/+}$ and $PR^{-/-}$ mammary epithelia. (B) Fluorescence stereo micrographs of third-generation mammary outgrowths derived from 8-week-old $PR^{+/+}$; *EGFP* and $PR^{-/-}$; *EGFP* donor mice. (C) Table summarizing 3 independent serial transplant experiments with $PR^{+/+}$; *EGFP* and $PR^{-/-}$; *EGFP*. Each engrafted gland is represented by a micrograph; black sectors represent area of fat pad filled by engrafted epithelium. Scale bar: 200 μm.

D, E Serial transplantation of $RANKL^{+/+}$ and $RANKL^{-/-}$ mammary epithelia. (D) Fluorescence stereo micrographs of third-generation mammary outgrowths derived from 5-week-old $RANKL^{+/+}$; *EGFP* and $RANKL^{-/-}$; *EGFP* donor mice. Insets: higher magnification showing side branches present in the WT control (arrowheads) absent from $RANKL^{-/-}$; *EGFP* epithelium. (E) Table summarizing three independent serial transplant experiments with $RANKL^{+/+}$; *EGFP* and $RANKL^{-/-}$; *EGFP* donor mice. Scale bar: 200 μm.

F, G Serial transplantation of $Wnt4^{+/+}$ and $Wnt4^{-/-}$ mammary epithelia. (F) Fluorescence stereo micrographs of third-generation mammary outgrowths derived from mammary buds of E12.5 and E13.5 $Wnt4^{+/+}$; *EGFP* and $Wnt4^{-/-}$; *EGFP* embryos. Scale bar: 200 μm. (G) Table summarizing three independent serial transplant experiments with $Wnt4^{+/+}$; *EGFP* donor mice. Scale bar: 200 μm.

H Box plot showing the difference between percentage of reconstitution between WT and MT contralateral grafts in each transplant generation. *P* values were determined by Mann–Whitney *U*-test.

Published online: January 20, 2015

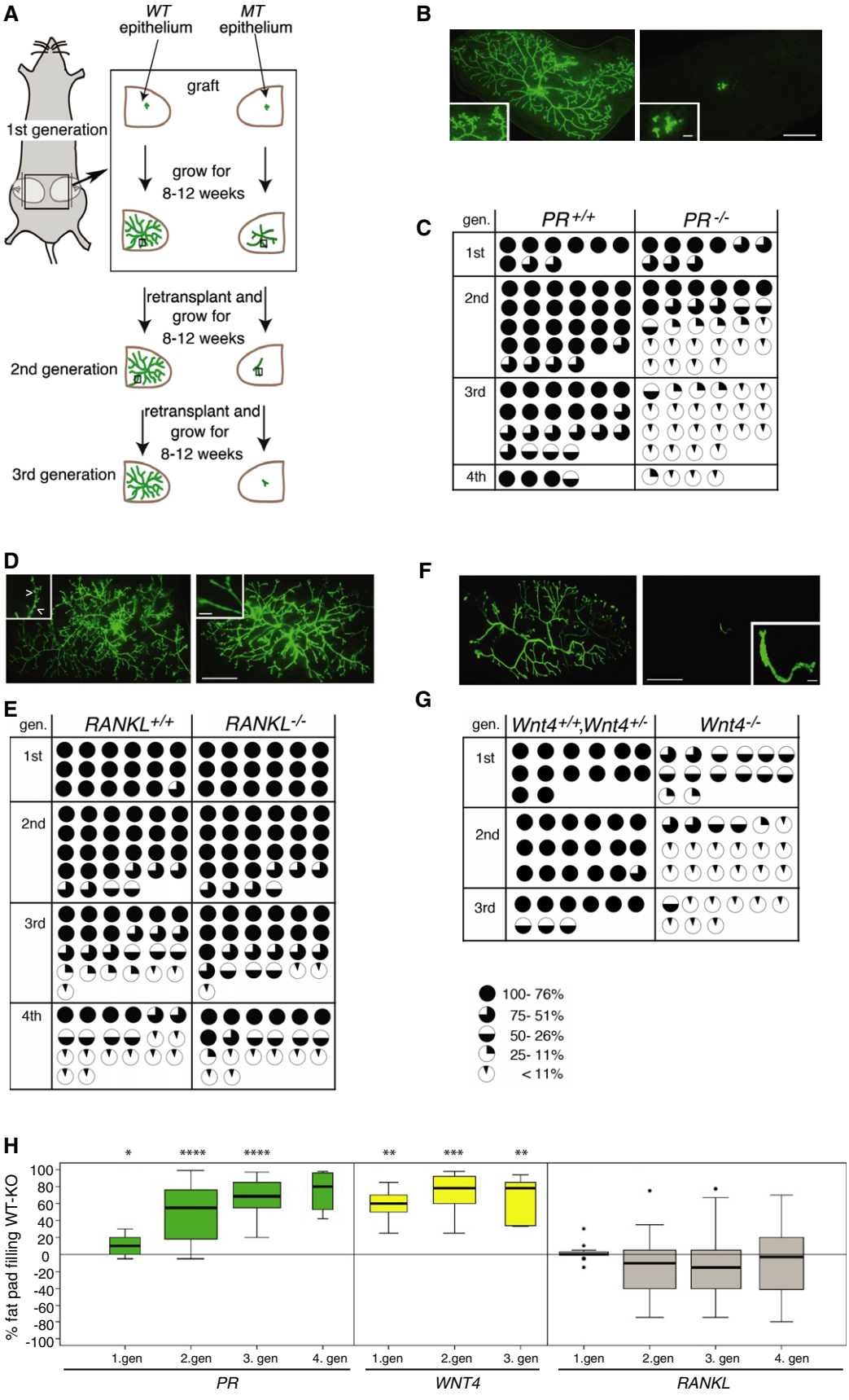

Figure 1.

does not appear to be essential in the control of the mammary stem cells under physiological conditions.

Control of Wnt4 expression

Previous studies suggested that Wnt4 is expressed only concomitant with high progesterone secretion in the adult and pregnant mammary gland (Gavin & McMahon, 1992; Weber-Hall *et al*, 1994). The finding that deletion of Wnt4 affected mammary regeneration potential more severely than abrogation of PR signaling suggested that Wnt4 may have PR-independent functions in stem cell stimulation. To detect Wnt4 expression at low levels, we crossed mice which express Cre from the Wnt4 locus (*Wnt4::Cre)* (Shan *et al*, 2009) to the *mT/mG* dual Cre reporter strain in which ubiquitous tomato expression is replaced by membrane EGFP upon Cre activation (Muzumdar *et al*, 2007). We failed to detect expression in embryos (E12.5 and E18.5) and were unable to detect EGFP in the mammary glands of newborn or 3-day-old double transgenic mice (*Wnt4::GFP)*. EGFP expression was detected on postnatal day 5 by fluorescence stereomicroscopy (Fig 2A) prior to the onset of ovarian function. Immunofluorescence of histological sections revealed EGFP expression in scattered mammary epithelial cells on day 5 (Fig 2B) and day 10 (Fig 2C). PR expression was not detected at these stages (Fig 2B and C). Consistent with Wnt4 being a PR target, the double immunofluorescence for histological sections from postnatal double transgenic mice (*Wnt4::EGFP)* suggested that EGFP expression is restricted to PR^+ luminal cells in the glands of pubertal mice (Fig 2D), adult (Fig 2E and inset), and pregnant females (Fig 2F and inset). To assess whether myoepithelial cells may express EGFP, we performed triple immunofluorescence for EGFP, PR, and the myoepithelial marker p63. In mammary epithelia from 5-day-old *Wnt4::EGFP* females ($n = 7$), rare double positive cells were detected, and in most sections, cells expressed either p63 or EGFP (Fig 2G). In 4- (Fig 2H) and 8-week-old (Fig 2I) females, p63 and EGFP staining labeled distinct cells. Thus, Wnt4 is expressed almost exclusively in luminal cells. The Wnt4 expressing cells appear to be terminally differentiated as no clonal clusters of $EGFP^+$ cells are observed.

To assess whether trace amounts of estrogens and progesterone of maternal origin could account for this perinatal Wnt4 expression, we analyzed d15 mammary glands from the *Wnt4::EGFP* mice on *WT*, $ER\alpha^{-/-}$, and $PR^{-/-}$ genetic backgrounds by epifluorescence stereomicroscopy. At this stage, ductal outgrowth was comparable by red fluorescence (Fig 2J–L). Neither *ERα* nor *PR* deletion altered *Wnt4::EGFP* expression (Fig 2M–O) indicating that perinatal Wnt4 expression is largely independent of ERα and PR signaling.

To determine the respective roles of the two major ovarian hormones in control of Wnt4 expression, we pooled epithelial-enriched organoids freshly isolated from mammary glands of pubertal and adult females ($n = 3$) and stimulated them for 6 h *ex vivo* (Fig 2P) (Ayyanan *et al*, 2011). Progesterone induced *Wnt4* mRNA expression in pubertal and adult organoids to 8.7- and 4.5-fold, respectively, whereas E2 elicited a 1.6-fold induction of *Wnt4* mRNA in the pubertal organoids only (Fig 2Q). To assess the physiological importance of PR signaling for pubertal Wnt4 expression, we grafted *Wnt4::GFP* epithelium derived from donors either $PR^{-/-}$ or *PRWT* to contralateral cleared fat pads of 3-week-old hosts. The engrafted glands were analyzed 3 weeks later when the recipients were pubertal. Epifluorescence stereomicroscopy for dTomato revealing unrecombined cells confirmed the presence of ductal outgrowth of *PRWT* and $PR^{-/-}$ grafts (Fig 2R and S). EGFP expression was readily detected in the *PRWT* graft (Fig 2T) but completely absent from some of the $PR^{-/-}$ grafts (Fig 2U). Double epifluorescence stereomicroscopy on a *PRWT* control graft reveals that EGFP is strongly enriched in the TEBs (Fig 2V and X), and in the contralateral $PR^{-/-}$ grafts, some EGFP expression is observed at the origin of the outgrowth (Fig 2W). These findings are consistent with perinatal ER-/PR-independent Wnt4 expression and indicate that pubertal Wnt4 induction is mediated by PR signaling.

Consequences of Wnt4 ablation on cell proliferation

The observation that Wnt4 deletion impaired the regenerative capacity of the mammary epithelium more severely than PR deletion did, pointed to a role of Wnt4 before puberty. The fat pad grafting approach used to determine Wnt4 function (Brisken *et al*, 2000) assesses gene function from puberty onward because the donor epithelium is placed into a 3-week-old host. To determine the role of Wnt4 perinatally and at the onset of puberty, we conditionally

Figure 2. Control of Wnt4 expression.

A Epifluorescence stereo micrograph of inguinal mammary gland from a 5-day-old *Wnt4::Cre; mT/mG* female ($n = 7$). Scale bars: 0.5 mm and 0.1 mm (inset).

B, C Histological sections of mammary glands from a 5-day-old (B; $n = 7$) and a 10-day-old (C; $n = 5$) *Wnt4::Cre; mT/mG* female stained by double immunofluorescence for EGFP (green) and PR (magenta, not detected), counterstained with DAPI (blue). Scale bar: 50 mm.

D–F EGFP (green) and PR (magenta) co-immunofluorescence counterstained with DAPI (blue) on histological sections from *mT/mG; Wnt4::Cre* mammary glands at different developmental stages. (D) TEB of a 4-week-old female ($n = 4$); scale bar: 30 μm. (E) Ducts of an 8-week-old female ($n = 3$); scale bar: 100 μm; inset, scale bar: 20 μm. (F) Duct of a female at day 10.5 of pregnancy ($n = 3$); scale bar: 150 μm; inset, scale bar: 30 μm.

G–I EGFP (green), PR (magenta), and p63 (white) triple co-immunofluorescence counterstained with DAPI (blue) on histological sections from *mT/mG; Wnt4::Cre* mammary glands at different developmental stages. (G) Ducts of 5-day-old female ($n = 3$). (H) TEB of a 4-week-old female ($n = 3$). (I) Duct of an 8-week-old female ($n = 3$). Scale bars: 30 μm.

J–O Epifluorescence stereo micrographs of mammary glands harvested from 15-day-old *Wnt4::GFP* females either WT ($n = 18$) (J, M), $ER\alpha^{-/-}$ ($n = 4$) (K, N), or $PR^{-/-}$ ($n = 3$) (L, O). dTomato expression (J–L); EGFP expression (M–O) is not abrogated in $ER\alpha^{-/-}$ nor $PR^{-/-}$ epithelia. Arrowheads mark the main duct originating from the nipple. Scale bar: 50 μm.

P Scheme of *ex vivo* hormone stimulation of mammary organoids.

Q Bar plots showing relative *PR* and *Wnt4* mRNA expression normalized to *CK18* mRNA in mammary organoids from 5 pubertal (6 weeks old) and 3 adult (11 weeks old) mice exposed for 6 h to vehicle (C), 17β-estradiol (20 nmol) (E2), or R5020 (20 nmol) (P). Bars represent the mean ± SD of 3 independent experiments.

R–X Epifluorescence stereo micrographs of contralateral mammary glands that were engrafted with *Wnt4::GFP* epithelium from 8-week-old females, either *PRWT* (R, T, V, X) or $PR^{-/-}$ (S, U, W). dTomato expression (R, S); EGFP expression (T, U) double epifluorescence (V, W, X) on contralateral engrafted glands 3 weeks after surgery when recipients were 6 weeks old. Representative result from three independent experiments. Arrowheads point to TEBs (V, X) or to origin of growth (W). Scale bar (R–W): 5 mm, (X): 1 mm.

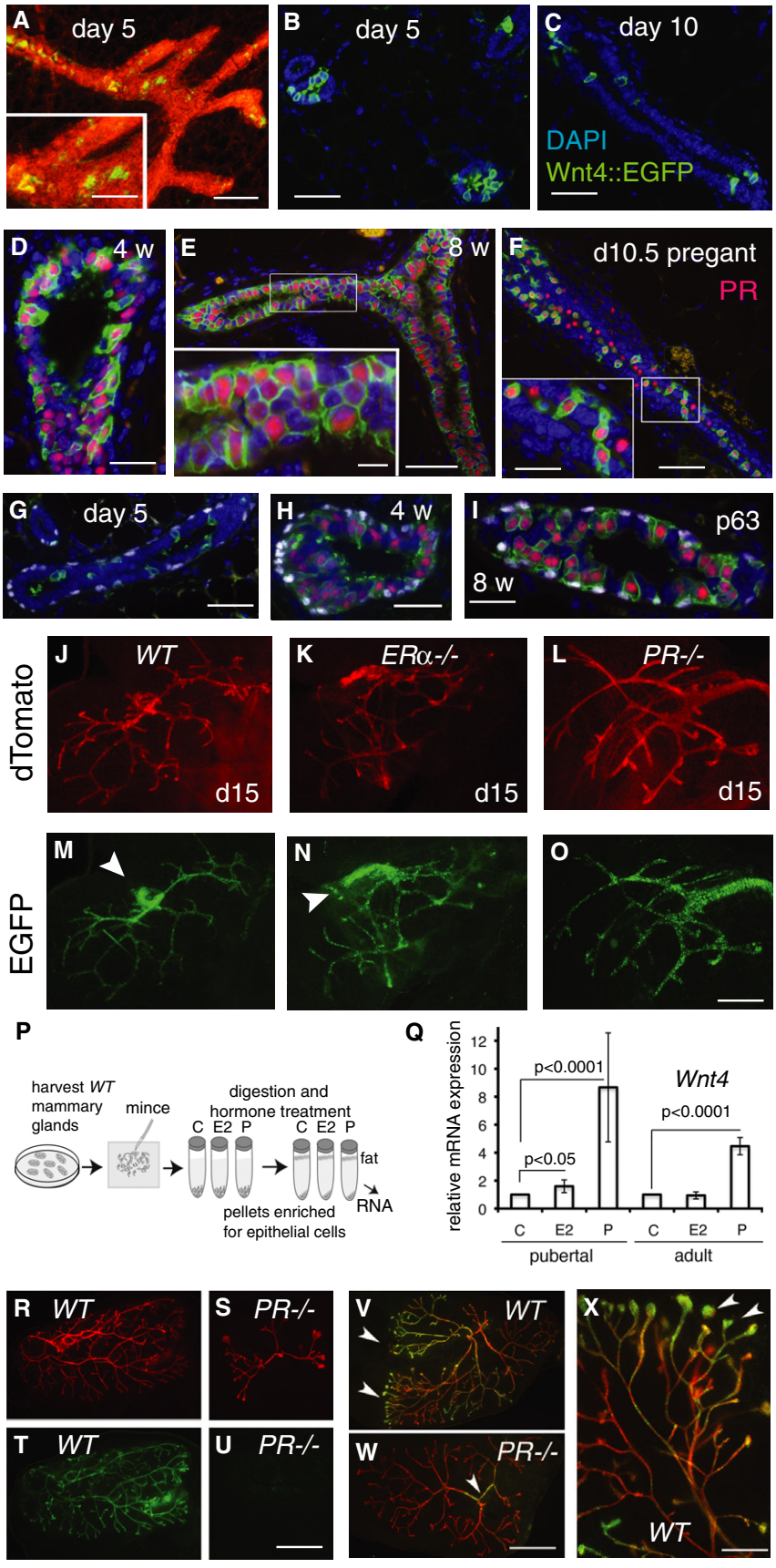
A day 5
B day 5
C day 10
DAPI
Wnt4::EGFP
D 4 w
E 8 w
F d10.5 pregant
PR
G day 5
H 4 w
I p63
8 w
dTomato
J WT
d15
K ERα-/-
d15
L PR-/-
d15
EGFP
M
N
O
P
harvest WT mammary glands
mince
digestion and hormone treatment
C E2 P
C E2 P
fat
RNA
pellets enriched for epithelial cells
Q
relative mRNA expression
Wnt4
p<0.0001
p<0.05
p<0.0001
C E2 P C E2 P
pubertal
adult
R WT
S PR-/-
V WT
X
T WT
U PR-/-
W PR-/-
WT

Figure 2.

deleted Wnt4 in the mammary epithelium by crossing mice with two conditional Wnt4 alleles ($Wnt4^{fl/fl}$) (Shan *et al*, 2010) to mice that express Cre in the mammary epithelium under the control of the MMTV-LTR (A-strain) (Wagner *et al*, 2001). To identify cells in which Cre-mediated recombination had occurred, the mice were crossed to the *mT/mG* dual Cre reporter strain (Muzumdar *et al*, 2007). Analysis of *MMTV::Cre; mT/mG* double transgenic females revealed widespread EGFP expression at postnatal day 10 both by stereo microscopy and (Fig 3A–E) immunofluorescence for EGFP (Fig 3F). In the *Wnt4* depleted *(MT)* mammary glands, a 10% decrease in the number of branching points was observed compared to control littermates around day 10 (Fig 3G and H). In pubertal *MT* glands, the number of terminal end buds (TEBs) had decreased to 54% of the controls (Fig 3I and J). Similarly, the area of fat pad filled by ducts was 60% of that measured in littermates (Fig 3I and K). Cell proliferation, as assessed by BrdU incorporation, was reduced to 65% of that in the *WT* counterparts in TEBs of Wnt4 mutants (Fig 3M). The proliferative index of about 6% in the subtending ducts was not affected in the Wnt4-deficient glands (Fig 3L). Thus, Wnt4 is required for perinatal and pubertal ductal expansion.

Activation of myoepithelial cells through canonical Wnt signaling

Wnt4 can activate its signaling, both canonical and non-canonical Wnt signaling (Lyons *et al*, 2004; Heinonen *et al*, 2011). Canonical Wnt signaling activity can be assessed *in vivo* using the *Axin2::LacZ* reporter mouse strain (Leung *et al*, 2002; Lustig *et al*, 2002) and was reported in a subset of $CD29f^{hi}$ or $CD49^{hi}$ breast stem cells

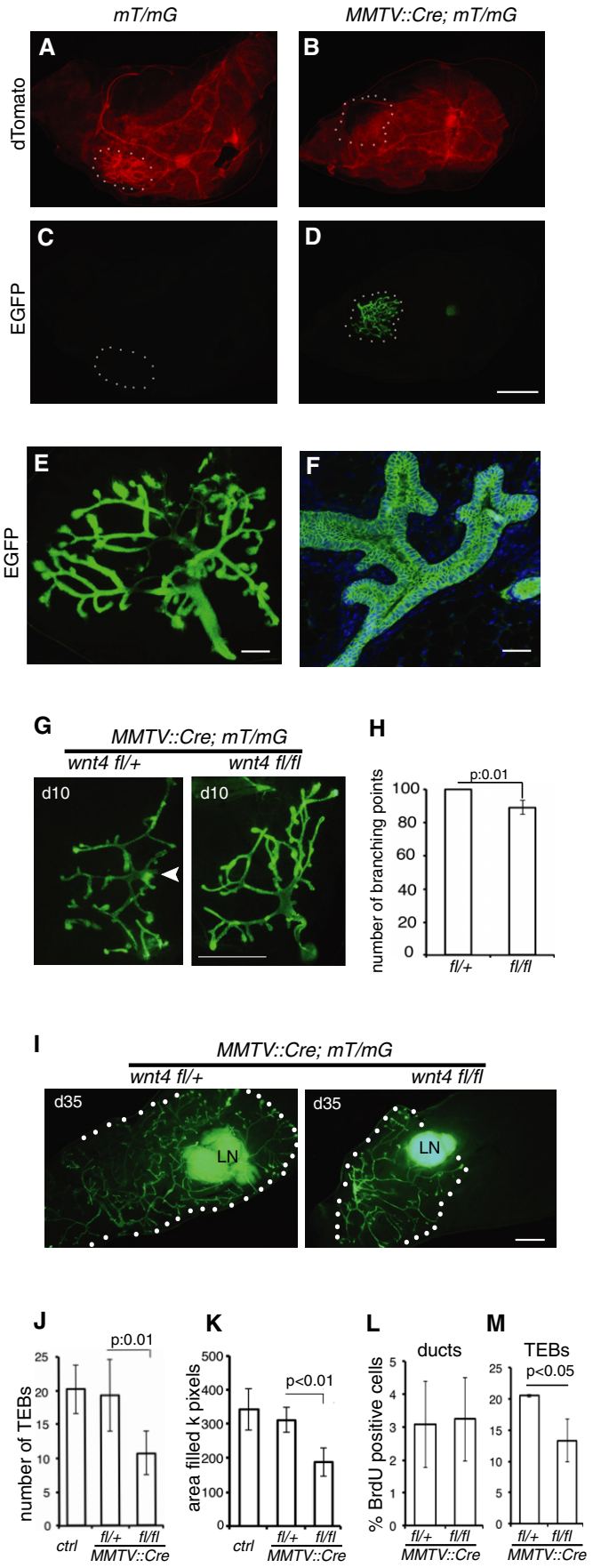

Figure 3. Conditional deletion of Wnt4 in the mammary epithelium and its consequences.

A–D Representative epifluorescence stereo micrographs of inguinal mammary glands from a 10-day-old *mT/mG* (A, C) and *MMTV::Cre; mT/mG* (B, D) female (n = 7). Scale bar: 1 mm.

E Higher magnification of inguinal mammary gland from a 10-day-old *MMTV::Cre; mT/mG* female. Scale bar: 0.2 mm.

F Immunofluorescence for EGFP (green) on a mammary gland section from a 10-day-old *MMTV::Cre; mT/mG* female counterstained with DAPI (blue) (n = 7). Scale bar: 30 μm.

G Epifluorescence stereo micrographs of mammary glands from 10-day-old littermates either *MMTV::Cre; mT/mG* $Wnt4^{fl/+}$ or *MMTV::Cre; mT/mG;* $Wnt4^{fl/fl}$. Scale bar: 1 mm. Arrowhead marks the main duct originating from the nipple.

H Bar plot showing ratio of branching points in prepubertal Cre^{+};$Wnt4^{fl/fl}$ (n = 12) relative to Cre^{+};$Wnt4^{fl/+}$ littermates (n = 10). Two-tailed, paired Student's t-test was used to calculate statistical significance.

I Fluorescence stereo micrographs of mammary glands from 35-day-old littermates either *MMTV::Cre; mT/m; Wnt4*$^{fl/+}$ or *MMTV::Cre; mT/m;*$Wnt4^{fl/fl}$. Note ductal elongation is delayed in *Wnt4*-deficient mammary epithelium compared to $Wnt4^{fl/+}$ control. LN: lymph node. Scale bar: 4 mm.

J, K Bar plots showing number of terminal end buds (TEBs) (J) and area of mammary fat pad filled by the ductal system (K). Ctrl ($Wnt4^{fl/wt}$ or $Wnt4^{fl/fl}$; Cre^{-}): n = 6, *fl/+*; Cre^{+}: n = 4, and *fl/fl*; Cre^{+}: n = 7). Data are presented as the mean ± SD. Two-tailed Student's t-test was used to calculate statistical significance.

L, M Bar plots showing BrdU incorporation index in inguinal mammary glands of 4-week-old $Wnt4^{fl/+}$; Cre^{+} (n = 3) or $Wnt4^{fl/fl}$; Cre^{+} (n = 4) in the ducts (L) and in the TEBs (M). Data are presented as the mean ± SD. Two-tailed Student's t-test was used to calculate statistical significance.

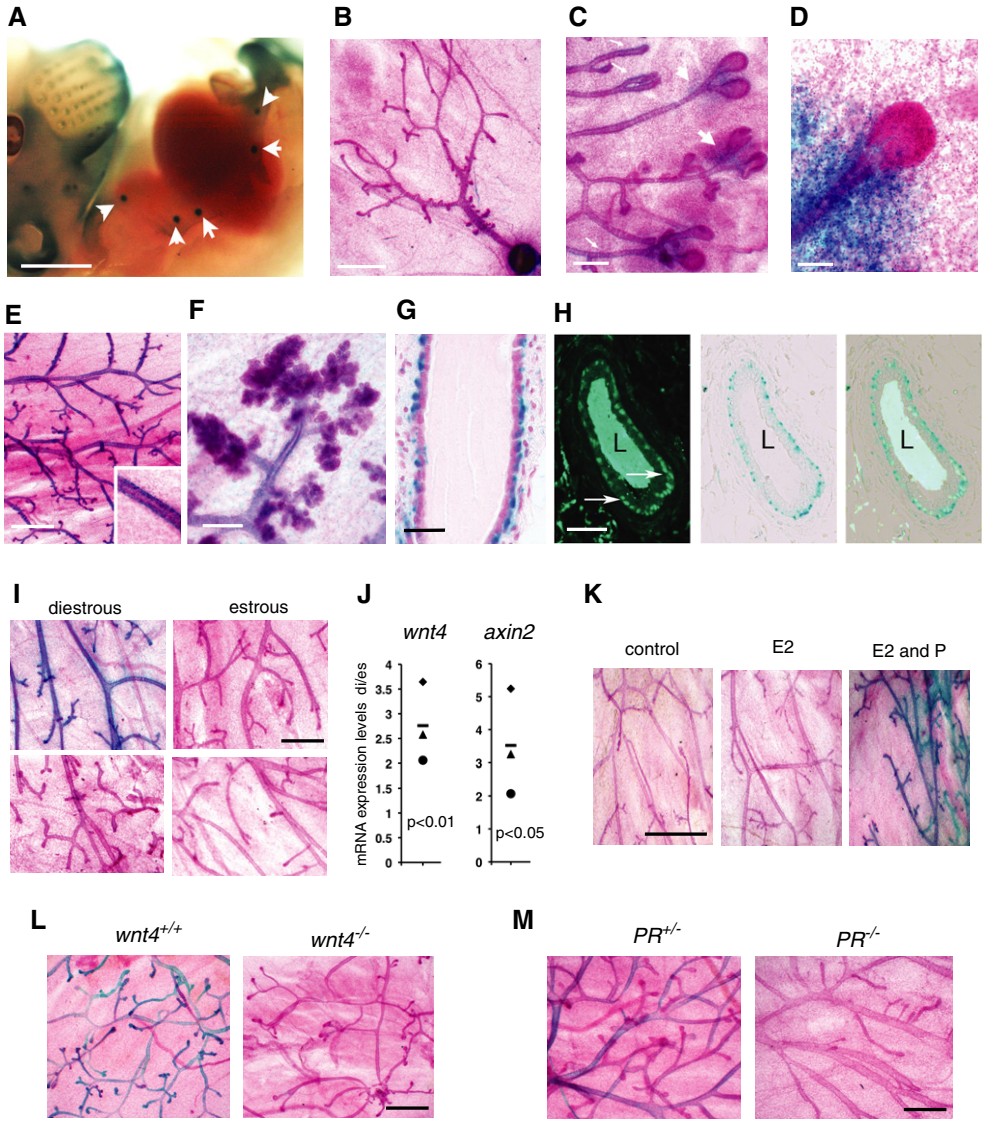

Figure 4. Canonical Wnt signaling activity during mammary gland development.

A Whole-mount micrograph of X-gal-stained *Axin2*$^{+/lacZ}$ in E12.5 embryo showing β-galactosidase expression in the mammary buds (arrows) (n = 8). Scale bar: 1 mm. Arrowheads mark mammary buds.

B–F Whole-mount micrographs of X-gal (blue)- and carmine alum (red)-stained mammary glands harvested from *Axin2*$^{+/lacZ}$ mice at distinct developmental stages. (B) At postnatal day 1, β-galactosidase activity detected in the nipple area (n = 6). Scale bar: 1 mm. (C, D) In 5-week-old mammary glands, reporter activity was detected around the ducts (small arrows) and in the neck region of the terminal end buds (TEBs) (large arrows) (C) (n = 8). Scale bars: 400 μm (C) and 100 μm (D). (E) At 8.5 day of pregnancy, reporter expression was detected in the ducts. Higher magnification (inset) suggests myoepithelial expression (n = 10). Scale bar: 1 mm. (F) Whole-mount at day 14.5 of pregnancy: reporter activity is limited to ducts (n = 5). Scale bar: 200 μm.

G Histological section of *Axin2::LacZ* mammary gland at day 8.5 of pregnancy counterstained with nuclear red; luminal epithelial cells show no detectable β-galactosidase activity but myoepithelial cells do. Scale bar: 200 μm.

H β-galactosidase activity (blue) colocalizes with the myoepithelial marker p63 (green) detected by immunofluorescence. Arrows point to myoepithelial cells. L, lumen. Scale bar: 100 μm.

I Representative whole-mount stereo micrographs of X-gal (blue)- and carmine alum (magenta)-stained mammary gland biopsies taken from 14-week-old *Axin2::LacZ* females collected at diestrus and estrus, respectively (n = 3). Scale bar: 200 μm.

J Relative *Wnt4* and *Axin2* mRNA expression in mammary glands from three mice in estrus versus diestrus assessed by semiquantitative qRT–PCR normalized to 18S rRNA. Two-tailed, paired Student's t-test was used to calculate statistical significance.

K Stereo micrographs of X-gal- and carmine alum-stained mammary glands from ovariectomized *Axin2::LacZ* females treated for 72 h with vehicle (n = 4) (left), 17-β-estradiol (E2) (n = 6) (center), 17-β-estradiol and progesterone (E2 and P) (n = 8) (right). Scale bar: 200 μm.

L, M Stereo micrographs of contralateral glands whole-mounted and X-gal stained after engraftment with mammary buds from *Axin2::LacZ* transgenic and *Wnt4*$^{+/+}$ or *Wnt4*$^{-/-}$ female E12.5 and E13.5 embryos (L) or *Axin2::LacZ* transgenic and either *PR*$^{+/-}$ or *PR*$^{-/-}$ 8-week-old females (M), at day 8.5 of pregnancy. β-galactosidase expression reflecting Axin2 transcription is readily detected in *PR*$^{+/-}$ as well as *Wnt4*$^{+/+}$ mammary epithelia but not in the *PR*$^{-/-}$ (n = 6) and *Wnt4*$^{-/-}$ counterparts (n = 6). Blue: X-gal staining; magenta: carmine alum counterstain. Scale bars: 200 μm.

(Zeng & Nusse, 2010; van Amerongen *et al*, 2012). We detected reporter activity in the mammary buds of E12.5/13.5 embryos (Fig 4A) consistent with previous reports based on an artificial Wnt signaling reporter (Chu *et al*, 2004). Perinatal β-galactosidase activity was confined to the nipple area (Fig 4B). Importantly, during puberty, LacZ expression was detected in the stroma surrounding the TEB necks (Fig 4C and D). In adulthood, β-galactosidase activity was readily detected in the ducts where it peaked on day 8.5 of pregnancy (Fig 4E). At day 14.5 of pregnancy, β-galactosidase activity was still detected in the ducts but not in the newly formed alveoli (Fig 4F). Histological sectioning suggested that X-gal staining mapped to the myoepithelial layer (Fig 4G); immunostaining with the myoepithelial marker p63 (Fig 4H) confirmed that LacZ is exclusively expressed in myoepithelial cells. Thus, canonical Wnt signaling in the postnatal mammary epithelium is confined to myoepithelial cells.

The peak in myoepithelial β-galactosidase activity during mid-pregnancy suggested that serum progesterone levels and hence Wnt4 expression may control canonical Wnt signaling activation. Indeed, when mammary glands in individual mice were analyzed, during progesterone-low estrous, they had lower β-galactosidase activity (Fig 4I) and lower *Wnt4* and *Axin2* mRNA levels than the glands analyzed during progesterone-high diestrous (Fig 4J); the fold differences varied between different animals (Fig 4I and J). To assess whether PR signaling induces canonical Wnt signaling, ovariectomized *Axin2::LacZ* females were treated with E2, to restore PR expression, and progesterone. Axin2 transcription reflected by β-galactosidase activity was induced by this combination but not by solvent or E2 alone (Fig 4K). Thus, progesterone stimulation results in increased transcription of Axin2, in the context of ER-dependent PR induction.

Multiple Wnts, some of which are secreted by mammary stromal cells, have been implicated in canonical Wnt signaling activation (Kessenbrock *et al*, 2013). To assess whether canonical Wnt signaling requires Wnt4 expression, we generated *Axin2::LacZ* transgenic mice in a $Wnt4^{-/-}$ background. In females engrafted with mammary buds from $Axin2::LacZ^{+}$ female embryos, β-galactosidase activity was readily detected in $Wnt4^{+/+}$ grafts at pregnancy day 8.5 but abrogated in the contralateral $Wnt4^{-/-}$ epithelia (Fig 4L). Similarly, it was decreased in $PR^{+/-}$ and abrogated in $PR^{-/-}$ epithelia (Fig 4M), indicating that both PR and Wnt4 are required for canonical Wnt signaling activation in the myoepithelium.

Our finding that Wnt4 expression is detected only from postnatal day 5 onward suggested that other family members, possibly Wnt10b, might be responsible for canonical Wnt signaling activation in the embryonic mammary bud. In line with this scenario, β-galactosidase activity was readily detected in the embryonic mammary buds of $Wnt4^{-/-}$*::axin2::LacZ* female E14.5 embryos (Fig 5A). To test whether the stromal Axin2 expression around TEB necks depends on epithelial Wnt4 expression, we generated *MMTV::Cre; axin2::LacZ* females either $Wnt4^{fl/fl}$ or $Wnt4^{fl/wt}$. Analysis of their mammary glands during puberty (6 weeks) showed that β-galactosidase activity was comparable between the two genotypes (Fig 5B). Thus, canonical Wnt signaling activation in the mammary bud and stroma is Wnt4 independent, whereas specifically in the myoepithelium, canonical Wnt signaling activation requires epithelial Wnt4 expression.

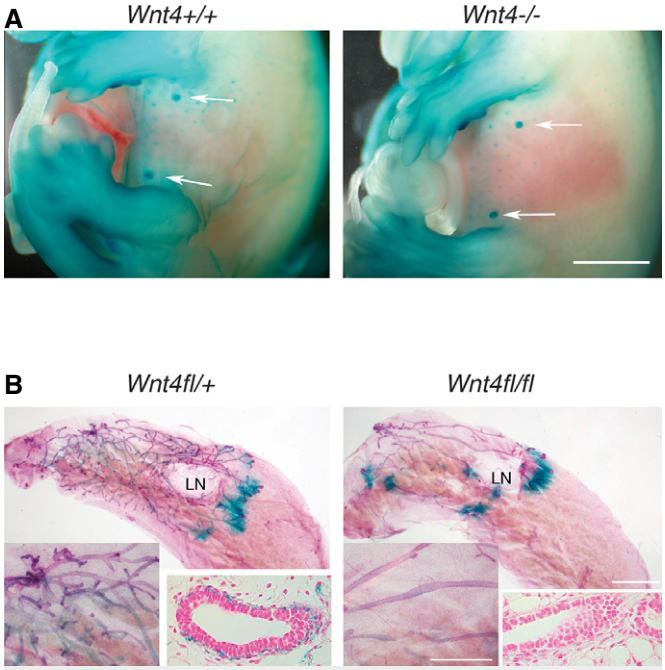

Figure 5. Wnt4-independent canonical Wnt signaling during mammary gland development.

A X-gal-stained whole-mounts of *Axin2::LacZ* embryos at E14.5 either $Wnt4^{+/+}$ *or* $Wnt4^{-/-}$ (n = 5 or 4, respectively). Arrows mark mammary buds. Scale bar: 5 mm.

B Whole-mount analysis of X-gal- and carmine alum-stained mammary glands harvested from 6-week-old littermates either $Wnt4^{fl/wt}$*;MMTV::Cre*$^{+}$*;* $Axin2^{+/lacZ}$ (n = 5) or $Wnt4^{fl/fl}$ *MMTV::Cre*$^{+}$*;*$Axin2^{+/lacZ}$ (n = 4). Left insets: higher magnification; right insets: histological section of the same gland. Note expression of reporter detected around the neck of TEBs in Wnt4-deficient and littermate control is comparable. LN, lymph node. Scale bars: 1 mm, and inset scale bar: 100 μm.

Discussion

Our data point to Wnt4 as a pivotal control factor of stem cell function for postnatal mammary gland development. We have uncovered a novel role for Wnt4 in perinatal development and puberty with progesterone as its major endocrine control factor. Progesterone, colloquially named 'pregnancy hormone,' appears as a primordial systemic factor in the postnatal mammary gland. It is the major proliferative stimulus to the adult mammary epithelium (Beleut *et al*, 2010) and controls the regenerative potential of the mammary gland by activating stem/progenitor cells throughout hormone-dependent development. Surprisingly, while hormone stimulation experiments had shown that estrogens induce Wnt4 expression (Brisken *et al*, 2000; Cai *et al*, 2014), we find that genetic deletion of PR signaling completely abrogated Wnt4 expression during puberty. Yet, the two ovarian hormones remain intertwined in Wnt4 control with ERα signaling acting indirectly as an upstream regulator of PR expression (Haslam & Shyamala, 1979) (Fig 6A).

We had previously analyzed Wnt4 function in the mammary gland by grafting $Wnt4^{-/-}$ embryonic buds to cleared fat pads of pubertal mice and therefore failed to discern the prepubertal function of Wnt4 uncovered through the use of the conditional Wnt4

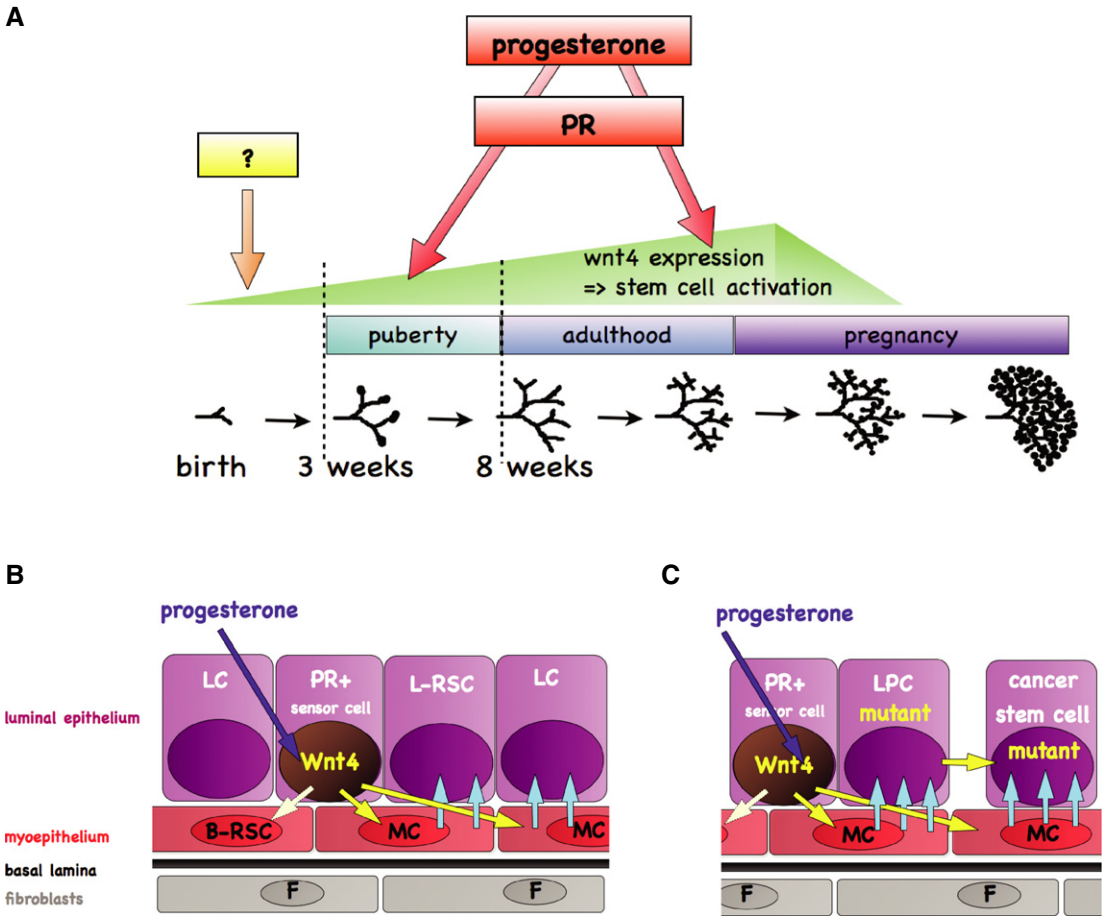

Figure 6. Models of hormonal stem cell control and Wnt4 action during mammary gland development.

A Control of mammary stem cell activity by Wnt4 during development. Schematic representation of mammary gland development (bottom) and control of mammary stem/progenitor cells by hormones (top). Model showing Wnt4 expression during mammary gland development. Wnt4 is important for stem cell activation throughout postnatal mammary gland development. Perinatal Wnt4 expression is independent of ER and PR, yet unknown factors control it. PR signaling is required for Wnt4 expression in puberty and adulthood. PR expression is induced by ER signaling.

B Model of Wnt4 action in the mammary epithelium. Progesterone stimulation results in Wnt4 induction in the PR^+ luminal cells (LC), the 'sensor cells.' The secreted Wnt4 acts on adjacent basal/myoepithelial cells (MC). In the myoepithelial cells, Wnt4 activates canonical Wnt signaling which induces changes in gene expression. This results in the secretion of factors and changes in the ECM (light blue arrows) that in turn impinge on stem cells (SC), luminal-restricted stem cells (L-RSC), and basal-restricted stem cells (B-RSC). Wnt4 may also act directly on stem cells that are found within the basal layer.

C Model for the tumorigenic effects of progesterone and Wnt4 in the mammary epithelium. Repeated activation of this intercellular signaling cascade downstream of PR signaling may promote tumorigenesis by expanding luminal progenitor cells with oncogenic mutations and by expanding the stem/progenitor cell compartment.

Data information: In (B, C), black: basal lamina, F: fibroblast, LC: luminal cell.

allele in the present work. The ability of $Wnt4^{-/-}$ epithelium to form alveoli, which was preserved in previous transplants (Brisken *et al*, 2000), was also observed upon serial transplantation when mice were impregnated in this study.

Our finding that RANKL is not important for stem cell potential is in apparent contradiction with previous results based on assays with dissociated cells (Asselin-Labat *et al*, 2010). Compared to the widely used single-cell-based assays in which a defined number of cells are injected, grafting of intact epithelial fragments does not allow one to determine the number or fraction of cells endowed with regenerative potential. The approach does not disentangle the role of different types of stem and progenitor cells and their relative contributions to the outgrowth cannot be defined. Yet, the method is robust and multiple repeats of the experiment combined with several rounds of transplantation give a semiquantitative appreciation of an intact regeneration potential in a physiological tissue context that is missed by the use of dissociated cells. In fact, to our knowledge, this is currently the only stem cell assay in which at least part of the microenvironment remains intact that is so important to stem cell function. When single cells are injected into a cleared fat pad, they need to survive and to adhere to the stroma, an environment they are not exposed to physiologically. Both of these biological activities require integrin signaling and control each other through direct cadherin-mediated cell–cell contacts. In the widely used FACS-based stem cell assays, mammary stem cells are selected for high expression of integrin β1 or α6 (Shackleton *et al*, 2006; Stingl *et al*, 2006). It is conceivable that the selected cells are not intrinsically better 'stem cells'

but that they have a strong advantage in adhering and surviving in the cleared fat pad, which is a *conditio sine qua non* for giving rise to *de novo* ducts. Alternatively, RANKL may be specifically required for the bipotential stem cells that are revealed under the challenging conditions of the single cell grafts. In the serial transplant approach, which is based on intact pieces of mammary tissue, the luminal- and the basal-restricted stem cells likely account for most of the cellular proliferation during development and a role of RANKL for the bipotent progenitors may not be discerned.

Our finding that Wnt4 secreted by PR^+ luminal cells activates canonical Wnt signaling exclusively in the neighboring basal/$p63^+$ cells, points to a scenario, in which the myoepithelial/basal cells are a central component of the microenvironment or 'niche' that controls different types of stem cells (Fig 6B). The myoepithelial/basal cells are ultimately under control of progesterone and Wnt4; hence, stem cell activity controlled through the microenvironment/niche is linked to reproductive needs. Whether the rare bipotent mammary stem cells that are found in the basal layer (Wang *et al*, 2014) are directly and/or indirectly activated by Wnt4 is not addressed by our experiments but will be an exciting line of future work.

The finding that the myoepithelial/basal cells are the prime target of Wnt4 bears on a long-standing conundrum. Wnt1 was long identified as an oncogene in the mouse mammary gland, and Wnt signaling is key for the development of the mammary gland. Yet, mutations in intracellular Wnt signaling components have not been found in breast carcinomas, which are of luminal origin. It is conceivable that Wnt signaling activation in the myoepithelial cells indirectly promotes tumorigenesis by inducing gene expression changes that result in the secretion of stimulatory signals and/or modulation of the extracellular matrix that result in the activation of luminal progenitor cells. Luminal progenitors with acquired oncogenic mutations could be expanded in response to Wnt4 stimulation of the myoepithelium (Fig 6C). In parallel, Wnt4, through its direct and/or indirect action on bipotent mammary stem cells, increases the number of stem cells. This in turn may result in an increased pool of luminal progenitors, which are more prone to oncogenic insults than more differentiated luminal cells.

These findings have clinical implications. The activation of the progesterone/Wnt4 pathway, which also operates in the human breast (Tanos *et al*, 2013; Pardo *et al*, 2014), may underlie the tumor promoting effects of recurrent menstrual cycles, oral contraception, and combined hormone replacement therapy with progestins. Selective progesterone receptor modulators and Wnt inhibitors, alone or together with RANKL inhibitors, may therefore be effective in breast cancer management, in particular, as preventive strategy in high-risk premenopausal women.

Materials and Methods

Animals

Axin2::LacZ (Lustig *et al*, 2002), *C57BL/6-Tg(Act-EGFP)* (Okabe *et al*, 1997), $ER\alpha^{-/-}$ (Dupont *et al*, 2000), *MMTV::Cre* (line A) (Wagner *et al*, 1997), *mT/mG* (Muzumdar *et al*, 2007), $PR^{-/-}$ (Lydon *et al*, 1995), $RAG1^{-/-}$ (Mombaerts *et al*, 1992), $RANKL^{-/-}$ (Wong *et al*, 1999), $Wnt4^{-/-}$ (Stark *et al*, 1994), $Wnt4^{Cre}$ (Shan *et al*, 2010), and $Wnt4^{fl/fl}$ mice (Shan *et al*, 2009) were kept on mixed genetic background 129SV/C57Bl6. All mice were maintained and handled according to the Swiss guidelines for animal safety. The ethic veterinary committee of canton of Vaud, Switzerland, approved all the animal experiments (Permit ID 1641.2 and 1641.3). To stage the estrus cycle, the vagina was flushed with 10 μl of PBS and vaginal secretions were collected, spread onto glass slides, and analyzed for different cell types (Caligioni, 2009). Mammary bud and mammary epithelial transplantations from 8-week-old donors were performed as described (Brisken *et al*, 2000). For serial transplantations, $EGFP^+$ mammary duct outgrowth was visualized by stereo epifluorescensce. Tissue fragments were prepared and retransplanted starting from at least three independent donors. Hormone treatments and BrdU injections were performed as described in Beleut *et al* (2010).

Mammary whole-mounts and image analysis

Mammary gland whole-mounting and (5-bromo-4-chloro-3-indolyl-beta-D-galacto-pyranoside) X-gal staining were performed as described (Brisken *et al*, 1998). Images were acquired either using a LEICA MZ FLIII stereomicroscope with PixeLINK (PL-A662) camera or LEICA M205FA/MZ16F fluorescent stereomicroscope with Leica DFC 340FX or Leica DC300F camera. Area of the fat pad filled by the mammary ducts was quantified by drawing a contour around the mammary ductal tips using Axiovision Rel 4.7 software. TEBs and branching points were quantified on images of whole-mounted mammary glands and on fluorescence stereo micrographs.

Immunostaining

Mammary glands were fixed in 4% paraformaldyde for 2 h at room temperature and embedded in paraffin. Five-micrometer sections were used for nuclear red and for immunohistochemical or immunofluorescence staining. Anti-p63 Molecular Probes 4A4 (1:100), anti-BrdU Oxford biotechnology, OBT0030, 1:300), anti-PR Thermo Fisher Scientific Pierce-MA1-411 (1:500), anti-GFP Molecular Probes A11122 (1:800). Images were acquired on LEICA DM 2000 microscope with a PixeLINK (PL-A662) camera or on Zeiss Axioplan 2-imaging fluorescence microscope with Axiocam MRm camera.

RNA extraction and semiquantitative RT–PCR

Mammary glands were homogenized in TRIzol (Invitrogen). Total RNA was isolated from fragments using RNeasy (Qiagen). cDNA was synthesized using random $p(dN)_6$ primers (Roche Diagnostics) and MMLV reverse transcriptase (Invitrogen). Semiquantitative real-time PCR analysis in triplicates was performed with SYBR Green PCR Core Reagents system (Qiagen)/PerfeCTa SYBR Green SuperMix for iQ™ (Quanta) on Realplex^2 (Eppendorf) or 7900HT Fast Real-Time PCR System (Applied Biosystems) qRT–PCR detection systems. All reactions were performed in triplicate. The following primers sequences were used: *Wnt4*, AGG AGT GCC AAT ACC AGT TCC, TGT GAG AAG GCT ACG CCA TA; *Axin-2*, GGC AGT GAT GGA GGA AAA TG, TGG GTG AGA GTT TGC ACT TG; *CK18*

(Schroeder & Lee, 1998); *18S rRNA*, GCA ATT ATT CCC CAT GAA CG, GGC CTC ACT AAA CCA TCC AA.

Statistics

Two-tailed, paired Student's *t*-test was used to calculate statistical significance; data are shown as means ± SD. Statistical analyses were carried out using Microsoft Excel. For serial transplantation, the extent of fat pad filling in percentage at each generation was compared by Wilcoxon signed rank test between contralateral outgrowths. The statistical software R was used for analysis. The statistical test used and *P*-values are indicated in each figure legend. $P < 0.05$ was considered to indicate statistical significance. $^{*}P < 0.05$, $^{**}P < 0.01$, $^{***}P < 0.001$.

Supplementary information for this article is available online: http://emboj.embopress.org

Acknowledgements

The authors would like to thank Drs. T. Tanos, A. Wilson, R. Jeitziner, and J. Dessimoz for advice and V. Simanis for critical reading of the manuscript; Drs. Y. Choi, J. Lydon, and T. Okabe for providing RANKL$^{+/-}$, PR$^{+/-}$, and C57BL/6-Tg(Act-EGFP) strains. This work was supported by funds from the Swiss National Center of Competence in Research (NCCR) in Molecular Oncology, SNF3100A0-112090, Oncosuisse, to C.B., a Marie Heim-Vögtlin fellowship from Swiss National Science Foundation (MHV - PMPDP3_129024) to R.D.R., and grants from the Academy of Finland (206038, 121647), Centre of Excellence Grant 2012–2017 of the Academy of Finland and FiDiPro (SQ) (251314), the Sigrid Jusélius Foundation, Novonordisk Fonden, and the European Union (LSHG-CT-2004-005085; HEALTH-F5-2008-223007 STAR-T REK, EURenOmics) to S.V.

Author contributions

RRD and CB designed experiments. MC, AA, and OYO performed experiments. RRD and DB performed experiments and analyzed data. JR and CB analyzed data. JS and SV provided mouse models. SV and CB contributed in writing the manuscript.

Conflict of interest

The authors declare that they have no conflict of interest.

References

van Amerongen R, Bowman AN, Nusse R (2012) Developmental stage and time dictate the fate of Wnt/beta-catenin-responsive stem cells in the mammary gland. *Cell Stem Cell* 11: 387 – 400

Asselin-Labat ML, Vaillant F, Sheridan JM, Pal B, Wu D, Simpson ER, Yasuda H, Smyth GK, Martin TJ, Lindeman GJ, Visvader JE (2010) Control of mammary stem cell function by steroid hormone signalling. *Nature* 465: 798 – 802

Ayyanan A, Laribi O, Schuepbach-Mallepell S, Schrick C, Gutierrez M, Tanos T, Lefebvre G, Rougemont J, Yalcin-Ozuysal O, Brisken C (2011) Perinatal exposure to bisphenol a increases adult mammary gland progesterone response and cell number. *Mol Endocrinol* 25: 1915 – 1923.

Beleut M, Rajaram RD, Caikovski M, Ayyanan A, Germano D, Choi Y, Schneider P, Brisken C (2010) Two distinct mechanisms underlie progesterone-induced proliferation in the mammary gland. *Proc Natl Acad Sci USA* 107: 2989 – 2994

Brisken C, Park S, Vass T, Lydon JP, O'Malley BW, Weinberg RA (1998) A paracrine role for the epithelial progesterone receptor in mammary gland development. *Proc Natl Acad Sci USA* 95: 5076 – 5081

Brisken C, Heineman A, Chavarria T, Elenbaas B, Tan J, Dey S, McMahon J, McMahon A, Weinberg R (2000) Essential function of Wnt-4 in mammary gland development downstream of progesterone signaling. *Genes Dev* 14: p650 – p654

Brisken C (2013) Progesterone signalling in breast cancer: a neglected hormone coming into the limelight. *Nat Rev Cancer* 13: 385 – 396

Cai C, Yu QC, Jiang W, Liu W, Song W, Yu H, Zhang L, Yang Y, Zeng YA (2014) R-spondin1 is a novel hormone mediator for mammary stem cell self-renewal. *Genes Dev* 28: 2205 – 2218.

Caligioni CS (2009) Assessing reproductive status/stages in mice. *Curr Prot Neurosci* 48: 4I:A.4I.1 – A.4I.8.

Chu EY, Hens J, Andl T, Kairo A, Yamaguchi TP, Brisken C, Glick A, Wysolmerski JJ, Millar SE (2004) Canonical WNT signaling promotes mammary placode development and is essential for initiation of mammary gland morphogenesis. *Development* 131: 4819 – 4829

Clarke RB, Howell A, Potten CS, Anderson E (1997) Dissociation between steroid receptor expression and cell proliferation in the human breast. *Cancer Res* 57: 4987 – 4991

Daniel CW (1973) Finite growth span of mouse mammary gland serially propagated in vivo. *Experientia* 29: 1422 – 1424.

Dupont S, Krust A, Gansmuller A, Dierich A, Chambon P, Mark M (2000) Effect of single and compound knockouts of estrogen receptors alpha (ERalpha) and beta (ERbeta) on mouse reproductive phenotypes. *Development* 127: 4277 – 4291

Gavin BJ, McMahon AP (1992) Differential regulation of the Wnt gene family during pregnancy and lactation suggests a role in postnatal development of the mammary gland. *Mol Cell Biol* 12: 2418 – 2423

Haslam SZ, Shyamala G (1979) Effect of oestradiol on progesterone receptors in normal mammary glands and its relationship with lactation. *Biochem J* 182: 127 – 131

Heinonen KM, Vanegas JR, Lew D, Krosl J, Perreault C (2011) Wnt4 enhances murine hematopoietic progenitor cell expansion through a planar cell polarity-like pathway. *PLoS One* 6: e19279

Joshi PA, Jackson HW, Beristain AG, Di Grappa MA, Mote PA, Clarke CL, Stingl J, Waterhouse PD, Khokha R (2010) Progesterone induces adult mammary stem cell expansion. *Nature* 465: 803 – 807

Kessenbrock K, Dijkgraaf GJ, Lawson DA, Littlepage LE, Shahi P, Pieper U, Werb Z (2013) A role for matrix metalloproteinases in regulating mammary stem cell function via the Wnt signaling pathway. *Cell Stem Cell* 13: 300 – 313

Leung JY, Kolligs FT, Wu R, Zhai Y, Kuick R, Hanash S, Cho KR, Fearon ER (2002) Activation of AXIN2 expression by beta-catenin-T cell factor. A feedback repressor pathway regulating Wnt signaling. *J Biol Chem* 277: 21657 – 21665

Liu BY, McDermott SP, Khwaja SS, Alexander CM (2004) The transforming activity of Wnt effectors correlates with their ability to induce the accumulation of mammary progenitor cells. *Proc Natl Acad Sci USA* 101: 4158 – 4163

Lustig B, Jerchow B, Sachs M, Weiler S, Pietsch T, Karsten U, van de Wetering M, Clevers H, Schlag PM, Birchmeier W, Behrens J (2002) Negative feedback loop of Wnt signaling through upregulation of conductin/axin2 in colorectal and liver tumors. *Mol Cell Biol* 22: 1184 – 1193

Lydon J, De MF, Funk C, Mani S, Hughes A, Montgomery CJ, Shyamala G, Conneely O, O'Malley B (1995) Mice lacking progesterone receptor exhibit pleiotropic reproductive abnormalities. *Genes Dev* 9: p2266 – p2278

Lyons JP, Mueller UW, Ji H, Everett C, Fang X, Hsieh JC, Barth AM, McCrea PD (2004) Wnt-4 activates the canonical beta-catenin-mediated Wnt

pathway and binds Frizzled-6 CRD: functional implications of Wnt/beta-catenin activity in kidney epithelial cells. *Exp Cell Res* 298: 369 – 387

Molyneux G, Geyer FC, Magnay FA, McCarthy A, Kendrick H, Natrajan R, Mackay A, Grigoriadis A, Tutt A, Ashworth A, Reis-Filho JS, Smalley MJ (2010) BRCA1 basal-like breast cancers originate from luminal epithelial progenitors and not from basal stem cells. *Cell Stem Cell* 7: 403 – 417.

Mombaerts P, Iacomini J, Johnson R, Herrup K, Tonegawa S, Papaioannou V (1992) RAG-1-deficient mice have no mature B and T lymphocytes. *Cell* 68: p869 – p877

Muzumdar MD, Tasic B, Miyamichi K, Li L, Luo L (2007) A global double-fluorescent Cre reporter mouse. *Genesis* 45: 593 – 605

Okabe M, Ikawa M, Kominami K, Nakanishi T, Nishimune Y (1997) 'Green mice' as a source of ubiquitous green cells. *FEBS Lett* 407: 313 – 319

Pardo I, Lillemoe HA, Blosser RJ, Choi M, Sauder CA, Doxey DK, Mathieson T, Hancock BA, Baptiste D, Atale R, Hickenbotham M, Zhu J, Glasscock J, Storniolo AM, Zheng F, Doerge R, Liu Y, Badve S, Radovich M, Clare SE (2014) Next-generation transcriptome sequencing of the premenopausal breast epithelium using specimens from a normal human breast tissue bank. *Breast Cancer Res* 16: R26

Rios AC, Fu NY, Lindeman GJ, Visvader JE (2014) In situ identification of bipotent stem cells in the mammary gland. *Nature* 506: 322 – 327

Schroeder JA, Lee DC (1998) Dynamic expression and activation of ERBB receptors in the developing mouse mammary gland. *Cell Growth Differ* 9: 451 – 464

Shackleton M, Vaillant F, Simpson KJ, Stingl J, Smyth GK, Asselin-Labat ML, Wu L, Lindeman GJ, Visvader JE (2006) Generation of a functional mammary gland from a single stem cell. *Nature* 439: 84 – 88

Shan J, Jokela T, Peltoketo H, Vainio S (2009) Generation of an allele to inactivate Wnt4 gene function conditionally in the mouse. *Genesis* 47: 782 – 788

Shan J, Jokela T, Skovorodkin I, Vainio S (2010) Mapping of the fate of cell lineages generated from cells that express the Wnt4 gene by time-lapse during kidney development. *Differentiation* 79: 57 – 64

Spike BT, Engle DD, Lin JC, Cheung SK, La J, Wahl GM (2012) A mammary stem cell population identified and characterized in late embryogenesis reveals similarities to human breast cancer. *Cell Stem Cell* 10: 183 – 197.

Stark K, Vainio S, Vassileva G, McMahon A (1994) Epithelial transformation of metanephric mesenchyme in the developing kidney regulated by Wnt-4. *Nature* 372: 679 – 683

Stingl J, Eirew P, Ricketson I, Shackleton M, Vaillant F, Choi D, Li HI, Eaves CJ (2006) Purification and unique properties of mammary epithelial stem cells. *Nature* 439: 993 – 997

Taddei I, Deugnier MA, Faraldo MM, Petit V, Bouvard D, Medina D, Fassler R, Thiery JP, Glukhova MA (2008) Beta1 integrin deletion from the basal compartment of the mammary epithelium affects stem cells. *Nat Cell Biol* 10: 716 – 722

Tanos T, Brisken C (2008) What signals operate in the mammary niche? *Breast Dis* 29: 69 – 82

Tanos T, Sflomos G, Echeverria PC, Ayyanan A, Gutierrez M, Delaloye JF, Raffoul W, Fiche M, Dougall W, Schneider P, Yalcin-Ozuysal O, Brisken C (2013) Progesterone/RANKL is a major regulatory axis in the human breast. *Sci Transl Med* 5: 182ra155

Vainio S, Heikkila M, Kispert A, Chin N, McMahon AP (1999) Female development in mammals is regulated by Wnt-4 signalling. *Nature* 397: 405 – 409

Van Keymeulen A, Rocha AS, Ousset M, Beck B, Bouvencourt G, Rock J, Sharma N, Dekoninck S, Blanpain C (2011) Distinct stem cells contribute to mammary gland development and maintenance. *Nature* 479: 189 – 193

Wagner KU, Wall RJ, St-Onge L, Gruss P, Wynshaw-Boris A, Garrett L, Li M, Furth PA, Hennighausen L (1997) Cre-mediated gene deletion in the mammary gland. *Nucleic Acids Res* 25: 4323 – 4330

Wagner KU, McAllister K, Ward T, Davis B, Wiseman R, Hennighausen L (2001) Spatial and temporal expression of the Cre gene under the control of the MMTV-LTR in different lines of transgenic mice. *Transgenic Res* 10: 545 – 553

Wang D, Cai C, Dong X, Yu QC, Zhang XO, Yang L, Zeng YA (2014) Identification of multipotent mammary stem cells by protein C receptor expression. *Nature* 517: 81 – 84.

Weber-Hall SJ, Phippard DJ, Niemeyer CC, Dale TC (1994) Developmental and hormonal regulation of Wnt gene expression in the mouse mammary gland. *Differentiation* 57: 205 – 214

Wong BR, Besser D, Kim N, Arron JR, Vologodskaia M, Hanafusa H, Choi Y (1999) TRANCE, a TNF family member, activates Akt/PKB through a signaling complex involving TRAF6 and c-Src. *Mol Cell* 4: 1041 – 1049

Zeng YA, Nusse R (2010) Wnt proteins are self-renewal factors for mammary stem cells and promote their long-term expansion in culture. *Cell Stem Cell* 6: 568 – 577

Published online: January 20, 2015

CURRICULUM VITAE

DUJE BURIC, BSc/MSc.

Address:	Rue des Terreaux 8 CH-1003 Lausanne	**Date of Birth:**	March 6th 1985
		Nationality:	Croatian
E-mail:	duje.buric@epfl.ch	**Telephone:**	+41 78 820 18 66

EDUCATION

Present-2010	**Ecole Polytecnique Fédérale de Lausanne, School of Life Sciences, Swiss Institute for Experimental Cancer Research, Prof. Cathrin Brisken group** Assistant-doctorant Representative of PhD students in the doctoral programe committee	**Lausanne, Switzerland**
2009 - 2003	**University of Zagreb, Faculty of Science, Department of Biology – Molecular Biology.** Dipl.ing. - BSc/Masters degree equivalent (obtained in June 2009)	**Zagreb, Croatia**

SKILLS

Science	**General molecular biology methodology and techniques:** manipulation of bacterial, plant and animal cells, transformation, cloning, PCR, site-directed mutagenesis, gel electrophoresis (agarose, SDS PAGE), transfection, GST pull down assay, Western blotting, lectine blotting, protein purification, immunofluorescence, yeast two-hybrid screening, basic cytochemistry and histochemistry methods. **Animal experimentation**: Running of the independent mouse colony, dissection and tissue and organ isolation, mammary epithelium transplantation, intraductal injection, ovariectomy. **Histology and histochemistry:** tissue fixation, microtome, histochemical and immunohistochemical techniques, immunofluorescent stainings **Flow cytometry:** Preparation of single cells and analysis of the mammary epithelial cells populations (LSRII machine)
Bioinform.	Basic bioinformatic methods and tools: ENTREZ, SRS, BLAST, PSI-BLAST, PHI-BLAST.

PROFESSIONAL EXPERIENCE

2009-2007	**The Mediterranean Institute for Life Sciences (MedILS), Diploma student:** Investigation of ubiquitin-binding zinc finger domain in novel proteins**.** Supervision: Prof. Ivan Dikic.	**Split, Croatia**
April 2008	**Institute of Biochemistry II, Molecular Signalling group.** One month training. Supervision: Dr. Fumiyo Ikeda	**Frankfurt, Germany**
2006-2005	**Biochemistry Course, Molecular Biology Programme, University of Zagreb, Faculty of Science.** Teaching assistant.	**Zagreb, Croatia**
2005-2004	**General and Inorganic Chemistry, Molecular Biology Programme, University of Zagreb, Faculty of Science.** Teaching assistant	**Zagreb, Croatia**

SCOLARSHIPS

Sept. 2009 **UNESCO fellowship** for participation on 10th International Summer School on Biophysics "Supramolecular Structure and Function" Rovinj, Croatia

2009- 2007 **Research Scholarship** - Mediterranean Institute of Life Sciences

Sept. 2006 **IUPAB fellowship** for participation on 9th International Summer School on Biophysics "Supramolecular Structure and Function" Rovinj, Croatia

MEETINGS AND CONFERENCES

2014 June — **International Conference „From Solid state to Biophysics", Dubrovnik, Croatia**
Invited Speaker

2013 June — **Gordon Conference: Mammary Gland Biology, Stowe VT, USA**
Participant

2012 June — **Gordon Conference: Mammary Gland Biology, Barga, Italy**
Participant

2011 September — **The Notch Meeting V., Athens, Greece**
Participant

2011 July — **1st Life Science Symposium by Doctoral Students „Cancer and Infection", Lausanne, Switzerland**
Member of the Organizing Comittee and participant

2010 May — **EMBO meeting: Cellular Signaling & Molecular Medicine, Cavtat, Croatia**
Member of the Local Organizing Comittee and participant

2009 September — **10th Internationale School on Biophysics „Molecular Structure and Function", Rovinj, Croatia**
Member of the Local Organizing Comittee and participant

2008 June — **EMBO meeting: Cellular Signaling & Molecular Medicine, Cavtat, Croatia.**
Member of the Local Organizing Committee and participant

2007 August — **MedILS Summer School: „Creating Interdisciplinary Research Project Workshop", MedILS, Split, Croatia.**

2006 September — **9th International School on Biophysics „Molecular Structure and Function", Rovinj, Croatia**
Member of the Local Organizing Committee and participant

ADDITIONAL SKILLS AND ACTIVITIES

Languages English (fluent), Italian (good), French (good), Croatian (native)

IT Skills Tools: Microsoft Office Package, OpenOffice.org Package, Adobe Photoshop, ImageJ, FlowJO. OS: Microsoft Windows XP/Vista/7/8, MacOS

Organizing Annual PhD students retreat (2010-2014), International School on Biophysics (2006, 2009), EMBO meeting (2008, 2010), Life science syposium (2011)

Volounteership Fighting Against Drug Addiction and Drug Abuse League (2003-2004), UNICEF office for Croatia (2003-2013)

Other Driving license (B), Lincesed Standard and Latin dances instructor, Argentinean tango

REFERENCES

Prof. Cathrin Brisken
EPFL SV ISREC UPBRI
Station 19
+41 021 693 07 81
cathrin.brisken@epfl.ch

Prof. Ivan Dikic
Institut fur Biochemie 2
Goethe-Universitat – Frankfurt am Main
+49 69 6301 5652
ivan.dikic@biochem2.de

Prof. Fumiyo Ikeda
Institute of Molecular Biotechnology
Vienna
fumiyo.ikeda@imba.oeaw.ac.at